Attachment F

Phase I-VI Closure Design Calculations

SCS ENGINEERS

CLIENT	PROJECT	JOB NO.
Hillsborough County	Southeast County Landfill	9215600.13

SUBJECT	BY	DATE
Stormwater Composite Drain Capacity Calculations	KLS	12/7/2021
Phase I - VI Closure - 25% Slope	CHECKED	DATE
	RBC	12/15/2021

OBJECTIVE: Verify the composite drain can convey the estimated stormwater quantities from the sideslope geocomposite predicted from the HELP model analysis.

REFERENCES:

1. Attachment 1 - Driscoplex Pipe Properties
2. Attachment 2 - Soil Properties
3. Attachment 3 - Manning's Roughness and Discharge Coefficients
4. Attachment 4 - HELP Model Summary

PROCEDURE:

1. Calculate the flow of stormwater through the composite drain gravel using Darcy's Law.
2. Calculate the flow from the composite drain gravel into through the composite drain pipe perforations.
3. Calculate the flow through the composite drain pipe
4. Compare HELP Model Peak Daily Flow from the geocomposite to the capacity of the composite drain.

COMPOSITE DRAIN DETAIL:

The below cross section is a detail of the composite drain. See Phase I-VI Closure Design Drawings.

SCS ENGINEERS

SHEET 2 OF 3

CLIENT	PROJECT	JOB NO.	
Hillsborough County	Southeast County Landfill	9215600.13	
SUBJECT		BY	DATE
Stormwater Composite Drain Capacity Calculations		KLS	12/7/2021
Phase I - VI Closure - 25% Slope		CHECKED	DATE
		RBC	12/15/2021

The diminsions below are from the composite drain detail included in the Phase I-VI Closure Design Drawings.

KNOWN:						
	Diameter of composite drain =	1.00	feet			
	Composite Drain Area, A_{drain} =	0.79	ft^2			
	Nominal pipe diameter =	4.00	inches	SDR 17		
	Pipe area (ID) =	0.08	ft^2	3.938	inches	Refer to Attachment 1
	Pipe area (OD) =	0.11	ft^2	4.500	inches	Refer to Attachment 1
	Pipe perforations =	0.50	inch			
	Pipe slope =	2.00%				

Calculate the hydraulic capacity of the composite drain by calculating the flow through the drain gravel and composite drain pipe. Compare results to peak leachate generation predicted by the HELP Model.

Q_{drain} = Gravel Flow + Pipe Flow = $Q_{gravel} + Q_{pipe}$
Q_{drain} = total flow through toe drain
Q_{gravel} = flow through gravel
Q_{pipe} = flow through pipe

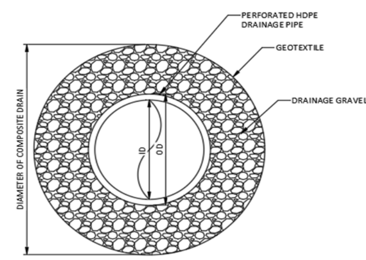

TYPICAL CROSS SECTION OF COMPOSITE DRAIN

1. Calculate flow through gravel using Darcy's Law.
Q_{gravel} = KiA

K = horizontal hydraulic conductivity =	10.00	cm/sec =	0.328	ft/sec	Refer to Attachment 2
i = hydraulic gradient =	2.00%	=	0.020	ft/ft	
A = cross section area = (A_{drain} - A_{pipeOD}) =	0.67	ft^2			
Q_{gravel} = flow through gravel =	4.43E-03	ft^3/sec			
=	0.27	ft^3/min			
Q_{gravel} =	**1.99**	**gal/min**			

2. Calculate flow into/through the composite drain pipe. Verify the perforations in the composite drain pipe are adequate for the peak flow anticipated based on the HELP Model.

Discharge equation, orifice flow rate = $Q_{orifice} = (C_d)(A_o)(2gh)^{0.5}$

C_d = coefficient of discharge =	0.61			Refer to Attachment 3, Table 17.5
D_o = diameter of orifice =	0.500	inch	0.042	feet
A_o = area of orifice = $((\pi)(D_o)^2)/4$ =	0.196	in^2	1.36E-03	ft^2
g = gravitational acceleration =	32.2	ft/sec^2		
h = static head =	0.066	inch	0.006	feet
$Q_{orifice} = (C_d)(A_o)(2gh)^{0.5}$ =	0.0005	ft^3/sec/orifice	0.22	gpm/orifice

Total length of toe drain pipe =	100	ft	Length from high point to dischage pipe (shortest drain)	
Number of perforations =	3.0	/ft	Perforation every 120 degrees	
Number of perforation rows =	3.0	/ft	Perforation at 4-inch intervals	
Number of perforations =	9.0	/ft		
Max flow =	0.004	ft^3/sec/ft	0.00	gpm/ft
Total flow into pipe through orifices =	0.45	ft^3/sec	**199.95**	**gal/min**

Q_{toe} = 199.95 gal/min > Q_{HELP} = 26.97 gal/min

FS = 7.41 = PASS

CLIENT Hillsborough County	PROJECT Southeast County Landfill	JOB NO. 9215600.13	
SUBJECT Stormwater Composite Drain Capacity Calculations Phase I - VI Closure - 25% Slope		BY KLS	DATE 12/7/2021
		CHECKED RBC	DATE 12/15/2021

3. Calculate the flow through the composite drain pipe using the Manning's equation and assuming a full flowing pipe.
$Q = 1.49/n * R^{2/3} * S^{1/2} * A$

n = Manning's roughness coefficient =	0.009		Refer to Attachment 3, Table 19A
A = cross section area of flow (inside) =	0.08	ft^2	Refer to Attachment 3
P_w = wetted perimeter = ID*π =	1.03	feet	Refer to Attachment 3
R = Hydraulic radius = A/P_w =	0.08	feet	Refer to Attachment 3
S = slope of pipe =	2.00%		

Q_{pipe} = flow through pipe = 0.37 ft^3/sec 167.82 gal/min

Q_{drain} = Gravel Flow + Pipe Flow = $Q_{gravel} + Q_{pipe}$
= 0.61 + 167.82

Q_{drain} = 168.4 gal/min Capacity of composite drain

Look at the maximum infiltration predicted in the HELP Model.

Peak flow/acre = Q_{max} =	5,191	cf/day/acre	Refer to Attachment 4
Area =	3	acres	Largest composite drain area approximately 2.3 acres
Peak flow = Q_{max} =	12,978	cf/day	
=	67.42	gal/min	

Q_{toe} = 168.43 gal/min > Q_{max} = 67.42 gal/min

FS = 2.5 = $\boxed{\text{PASS}}$

RESULT:

The composite drain is adequate to convey the predicted peak flow from the sideslope geocomposite, as predicted by the HELP Model.

SCS ENGINEERS

CLIENT	PROJECT	JOB NO.
Hillsborough County	Southeast County Landfill	9215600.13

SUBJECT	BY	DATE
Stormwater Composite Drain Capacity Calculations	KLS	12/7/2021
Phase I - VI Closure - 5% Slope	CHECKED	DATE
	RBC	12/15/2021

OBJECTIVE: Verify the composite drain can convey the estimated stormwater quantities from the sideslope geocomposite predicted from the HELP model analysis.

REFERENCES:

1. Attachment 1 - Driscoplex Pipe Properties
2. Attachment 2 - Soil Properties
3. Attachment 3 - Manning's Roughness and Discharge Coefficients
4. Attachment 4 - HELP Model Summary

PROCEDURE:

1. Calculate the flow of stormwater through the composite drain gravel using Darcy's Law.
2. Calculate the flow from the composite drain gravel into through the composite drain pipe perforations.
3. Calculate the flow through the composite drain pipe
4. Compare HELP Model Peak Daily Flow from the geocomposite to the capacity of the composite drain.

COMPOSITE DRAIN DETAIL:

The below cross section is a detail of the composite drain. See Phase I-VI Closure Design Drawings.

SCS ENGINEERS

SHEET 2 OF 3

CLIENT Hillsborough County	PROJECT Southeast County Landfill		JOB NO. 9215600.13
SUBJECT Stormwater Composite Drain Capacity Calculations Phase I - VI Closure - 5% Slope	BY KLS		DATE 12/7/2021
	CHECKED RBC		DATE 12/15/2021

The diminsions below are from the composite drain detail included in the Phase I-VI Closure Design Drawings.

KNOWN:

Diameter of composite drain =	1.00	feet				
Composite Drain Area, A_{drain} =	0.79	ft^2				
Nominal pipe diameter =	4.00	inches	SDR 17			
Pipe area (ID) =	0.08	ft^2	3.938	inches	Refer to Attachment 1
Pipe area (OD) =	0.11	ft^2	4.500	inches	Refer to Attachment 1
Pipe perforations =	0.50	inch				
Pipe slope =	2.00%					

Calculate the hydraulic capacity of the composite drain by calculating the flow through the drain gravel and composite drain pipe. Compare results to peak leachate generation predicted by the HELP Model.

Q_{drain} = Gravel Flow + Pipe Flow = $Q_{gravel} + Q_{pipe}$
Q_{drain} = total flow through toe drain
Q_{gravel} = flow through gravel
Q_{pipe} = flow through pipe

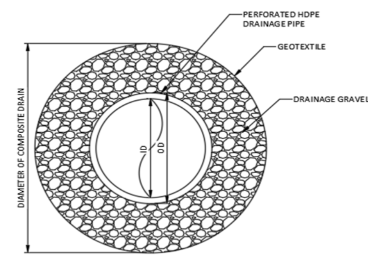

TYPICAL CROSS SECTION OF COMPOSITE DRAIN

1. Calculate flow through gravel using Darcy's Law.
Q_{gravel} = KiA

K = horizontal hydraulic conductivity =	10.00	cm/sec =	0.328	ft/sec	Refer to Attachment 2
i = hydraulic gradient =	2.00%	=	0.020	ft/ft	
A = cross section area = (A_{drain} - A_{pipeOD}) =	0.67	ft^2			
Q_{gravel} = flow through gravel =	4.43E-03	ft^3/sec			
=	0.27	ft^3/min			
Q_{gravel} =	**1.99**	**gal/min**			

2. Calculate flow into/through the composite drain pipe. Verify the perforations in the composite drain pipe are adequate for the peak flow anticipated based on the HELP Model.

Discharge equation, orifice flow rate = $Q_{orifice} = (C_d)(A_o)(2gh)^{0.5}$

C_d = coefficient of discharge =	0.61			Refer to Attachment 3, Table 17.5
D_o = diameter of orifice =	0.500	inch	0.042	feet
A_o = area of orifice = $((\pi)(D_o)^2)/4$ =	0.196	in^2	1.36E-03	ft^2
g = gravitational acceleration =	32.2	ft/sec^2		
h = static head =	0.066	inch	0.006	feet
$Q_{orifice} = (C_d)(A_o)(2gh)^{0.5}$ =	0.0005	ft^3/sec/orifice	0.22	gpm/orifice

Total length of toe drain pipe =	100	ft	Length from high point to discharge pipe (shortest drain)	
Number of perforations =	3.0	/ft	Perforation every 120 degrees	
Number of perforation rows =	3.0	/ft	Perforation at 4-inch intervals	
Number of perforations =	9.0	/ft		
Max flow =	0.004	ft^3/sec/ft	0.00	gpm/ft
Total flow into pipe through orifices =	0.45	ft^3/sec	**199.95**	**gal/min**

Q_{toe} = 199.95 gal/min > Q_{HELP} = 28.08 gal/min

FS = 7.12 = PASS

SCS ENGINEERS

SHEET 3 OF 3

CLIENT	PROJECT	JOB NO.
Hillsborough County	Southeast County Landfill	9215600.13

SUBJECT	BY	DATE
Stormwater Composite Drain Capacity Calculations	KLS	12/7/2021
Phase I - VI Closure - 5% Slope	CHECKED	DATE
	RBC	12/15/2021

3. Calculate the flow through the composite drain pipe using the Manning's equation and assuming a full flowing pipe.

$Q = 1.49/n * R^{2/3} * S^{1/2} * A$

n = Manning's roughness coefficient =	0.009		Refer to Attachment 3, Table 19A
A = cross section area of flow (inside) =	0.08	ft^2	Refer to Attachment 3
P_w = wetted perimeter = $ID*\pi$ =	1.03	feet	Refer to Attachment 3
R = Hydraulic radius = A/P_w =	0.08	feet	Refer to Attachment 3
S = slope of pipe =	2.00%		

Q_{pipe} = flow through pipe = 0.37 ft^3/sec 167.82 gal/min

Q_{drain} = Gravel Flow + Pipe Flow = $Q_{gravel} + Q_{pipe}$

= 0.61 + 167.82

Q_{drain} = 168.4 gal/min Capacity of composite drain

Look at the maximum infiltration predicted in the HELP Model.

Peak flow/acre = Q_{max} =	5,406	cf/day/acre	Refer to Attachment 4
Area =	3	acres	Largest composite drain area approximately 2.3 acres
Peak flow = Q_{max} =	13,515	cf/day	
=	70.21	gal/min	

Q_{toe} = 168.43 gal/min > Q_{max} = 70.21 gal/min

FS = 2.4 = PASS

RESULT:

The composite drain is adequate to convey the predicted peak flow from the sideslope geocomposite, as predicted by the HELP Model.

Attachment 1

Driscoplex Pipe Properties

Table 6 DriscoPlex® 4100 IPS Pipe Sizing System

Common Dimension Ratio's for DriscoPlex® 4100 IPS Pipe (Custom DR's available. Contact Performance Pipe)																
IPS		DR 21			DR 17			DR 13.5			DR 11			DR 9		
ASTM F714 PR		PR = 100 psi			PR = 125 psi			PR = 160 psi			PR = 200 psi			PR = 250 psi		
AWWA C906 PC		PC = 80 psi			PC = 100 psi			PC = 130 psi			PC = 160 psi			PC = 200 psi		
Pipe Size in.	OD, in.	Min. Wall, in.	Avg. ID, in.	Wgt. lbs/ft	Min. Wall, in.	Avg. ID, in.	Wgt. lbs/ft	Min. Wall, in.	Avg. ID, in.	Wgt. lbs/ft	Min. Wall, in.	Avg. ID, in.	Wgt. lbs/ft	Min. Wall, in.	Avg. ID, in.	Wgt. Lbs/ft
2	2.375				0.140	2.078	0.43	0.176	2.002	0.53	0.216	1.917	0.64	0.264	1.815	0.77
3	3.500				0.206	3.063	0.94	0.259	2.951	1.16	0.318	2.826	1.39	0.389	2.675	1.66
4	4.500	0.214	4.046	1.27	0.265	3.938	1.55	0.333	3.794	1.92	0.409	3.633	2.31	0.500	3.440	2.75
6	6.625	0.315	5.957	2.75	0.390	5.798	3.36	0.491	5.584	4.15	0.602	5.349	5.00	0.736	5.065	5.96
8	8.625	0.411	7.754	4.66	0.507	7.550	5.69	0.639	7.270	7.04	0.784	6.963	8.47	0.958	6.594	10.11
10	10.750	0.512	9.665	7.24	0.632	9.410	8.83	0.796	9.062	10.93	0.977	8.679	13.16	1.194	8.219	15.70
12	12.750	0.607	11.463	10.19	0.750	11.160	12.43	0.944	10.749	15.38	1.159	10.293	18.51	1.417	9.746	22.08
14	14.000	0.667	12.586	12.28	0.824	12.253	14.98	1.037	11.802	18.54	1.273	11.301	22.32	1.556	10.701	26.63
16	16.000	0.762	14.385	16.04	0.941	14.005	19.57	1.185	13.488	24.22	1.455	12.915	29.15	1.778	12.231	34.78
18	18.000	0.857	16.183	20.30	1.059	15.755	24.77	1.333	15.174	30.65	1.636	14.532	36.89	2.000	13.760	44.02
20	20.000	0.952	17.982	25.07	1.176	17.507	30.58	1.481	16.860	37.84	1.818	16.146	45.54	2.222	15.289	54.34
22	22.000	1.048	19.778	30.33	1.294	19.257	37.00	1.630	18.544	45.79	2.000	17.760	55.10	2.444	16.819	65.75
24	24.000	1.143	21.577	36.10	1.412	21.007	44.03	1.778	20.231	54.49	2.182	19.374	65.58	2.667	18.346	78.25
26	26.000	1.238	23.375	42.36	1.529	22.759	51.67	1.926	21.917	63.95	2.364	20.988	79.96	2.889	19.875	91.84
28	28.000	1.333	25.174	49.13	1.647	24.508	59.93	2.074	23.603	74.17	2.545	22.605	89.26	3.111	21.405	106.51
30	30.000	1.429	26.971	56.40	1.765	26.258	68.80	2.222	25.289	85.14	2.727	24.219	102.47	3.333	22.934	122.27
32	32.000	1.524	28.769	64.17	1.882	28.010	78.28	2.370	26.976	96.87	2.909	25.833	116.58			
34	34.000	1.619	30.568	72.44	2.000	29.760	88.37	2.519	28.660	109.36	3.091	27.447	131.61			
36	36.000	1.714	32.366	81.21	2.118	31.510	99.07	2.667	30.346	122.60	3.273	29.061	147.55			
42	42.000	2.000	37.760	110.54	2.471	36.761	134.84	3.111	35.405	166.88						
48	48.000	2.286	43.154	144.38	2.824	42.013	176.12									
54	54.000	2.571	48.549	182.73												

For pipe smaller than 2" see PP415, DriscoPlex® 5100 Water Service Pipe and Tubing.
Average inside diameter is calculated using Nominal OD and Minimum Wall plus 6% for use in estimating fluid flow. Actual ID will vary. When designing components to fit the pipe ID, refer to pipe dimensions and tolerances in the applicable pipe manufacturing specification.

Attachment 2

Soil Properties

Soil Mechanics in Engineering Practice

Third Edition

Karl Terzaghi
Late Professor of the Practice of Civil Engineering
Harvard University
Lecturer and Research Consultant in Civil Engineering
University of Illinois

Ralph B. Peck
Professor of Foundation Engineering, Emeritus
University of Illinois

Gholamreza Mesri
Professor of Civil Engineering
University of Illinois

A Wiley-Interscience Publication
JOHN WILEY & SONS, INC.
New York • Chichester • Brisbane • Toronto • Singapore

Table 14.1 Permeability and Drainage Characteristics of Soils*

Coefficient of Permeability k (m/s)	10^{0}	10^{-1}	10^{-2}	10^{-3}	10^{-4}	10^{-5}	10^{-6}	10^{-7}	10^{-8}	10^{-9}	10^{-10}	10^{-11}
Drainage				Good				Poor			Practically Impervious	
Soil types		Clean gravel		Clean sands, clean sand and gravel mixtures			Very fine sands, organic and inorganic silts, mixtures of sand silt and clay, glacial till, stratified clay deposits, etc.			"Impervious" soils, e.g., homogeneous clays below zone of weathering		
						"Impervious" soils modified by effects of vegetation and weathering						

* After Casagrande and Fadum (1940).

and arrangement of the pores together determine the porosity. In stiff clays and shales, as well as in rocks, macropores produced by fissures, joints, and cracks exert a major influence on the permeability.

14.3 Permeability of Granular Soils

The permeability of granular soils depends mainly on the cross-sectional areas of the pore channels. Since the average diameter of the pores in a soil at a given porosity increases in proportion to the average grain size, the permeability of granular soils might be expected to increase as the square of some characteristic grain size, designated as the *effective grain size*, D_e. Extensive investigations of filter sands by Hazen (1892) led to the equation

$$k(\text{m/s}) = C_e D_e^2 \qquad (14.6)$$

in which the parameter C_e includes the effects of the shape of the pore channels in the direction of flow and of the total volume of pores as determined by such properties as grain shape and gradation. The effective grain size best fitting Eq. 14.6 was found by Hazen to be the 10% size D_{10} (Article 5). The permeability data in Fig. 14.3 approximate a straight line with a slope equal to 2, consistent with Eq. 14.6. These data indicate an average value of $C_{10} = 10^{-2}$ when k is expressed in m/s and D_{10} in mm. According to the data in Fig. 14.3, Eq. 14.6 may underestimate or overestimate the permeability of granular soils by a factor of about 2.

Laboratory studies by Kenney et al. (1984) on the permeability of granular filters, using natural sands and

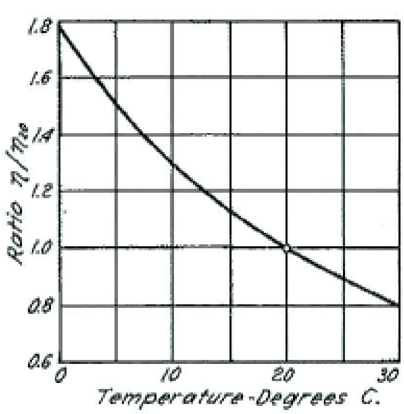

Figure 14.2 Relation between temperature and viscosity of water.

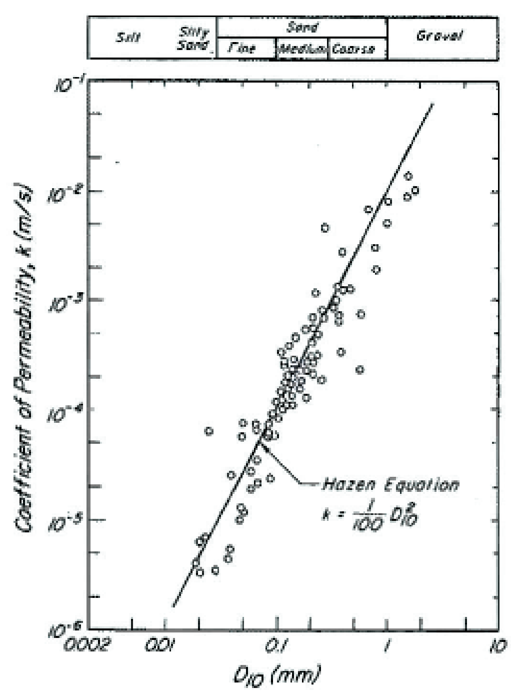

Figure 14.3 Hazen equation and data relating coefficient of permeability and effective grain size of granular soils (after Louden 1952).

Attachment 3

Manning's Roughness and Discharge Coefficients

Support

Civil Engineering Reference Manual
for the PE Exam

Eleventh Edition

Michael R. Lindeburg, PE

Professional Publications, Inc. • Belmont, CA

6. GOVERNING EQUATIONS FOR UNIFORM FLOW

Since water is incompressible, the continuity equation is

$$A_1 \mathrm{v}_1 = A_2 \mathrm{v}_2 \qquad 19.8$$

The most common equation used to calculate the flow velocity in open channels is the 1768 *Chezy equation*.[3]

$$\mathrm{v} = C\sqrt{RS} \qquad 19.9$$

Various methods for evaluating the *Chezy coefficient*, C, or "Chezy's C," have been proposed.[4] If the channel is small and very smooth, Chezy's own formula can be used. The friction factor, f, is dependent on the Reynolds number and can be found in the usual manner from the Moody diagram.

$$C = \sqrt{\frac{8g}{f}} \qquad 19.10$$

If the channel is large and the flow is fully turbulent, then the friction loss will not depend so much on the Reynolds number as on the channel roughness. The 1888 Manning formula is frequently used to evaluate the constant C.[5] Notice that the value of C depends only on the channel roughness and geometry. (The conversion constant 1.49 in Eq. 19.11(b) is reported as 1.486 by some authorities. 1.486 is the correct SI-to-English conversion, but it is doubtful whether this equation warrants four significant digits.)

$$C = \left(\frac{1.00}{n}\right) R^{1/6} \qquad \text{[SI]} \qquad 19.11(a)$$

$$C = \left(\frac{1.49}{n}\right) R^{1/6} \qquad \text{[U.S.]} \qquad 19.11(b)$$

n is the *Manning roughness coefficient* (*Manning constant*). Typical values of Manning's n are given in App. 19.A. Judgment is needed in selecting values since tabulated values often differ by as much as 30%. More important to recognize for sewer work is the layer of slime that often coats the sewer walls. Since the slime characteristics can change with location in the sewer, there can be variations in Manning's roughness coefficient along the sewer length.

Independent of these factors, the value of n also depends on the depth of flow, leading to a value (n_{full}) specifically intended for use with full flow. (It is seldom clear from tabulations such as App. 19.A whether the values are for full flow or general use.) The variation in n can be taken into consideration using *Camp's correction*, shown in App. 19.C. However, this degree of sophistication cannot be incorporated into an analysis problem unless a specific value of n is known for a specific depth of flow.

Combining Eqs. 19.9 and 19.11 produces the *Manning equation*, also known as the *Chezy-Manning equation*.

$$\mathrm{v} = \left(\frac{1.00}{n}\right) R^{2/3}\sqrt{S} \qquad \text{[SI]} \qquad 19.12(a)$$

$$\mathrm{v} = \left(\frac{1.49}{n}\right) R^{2/3}\sqrt{S} \qquad \text{[U.S.]} \qquad 19.12(b)$$

All of the coefficients and constants in the Manning equation may be combined into the *conveyance*, K.

$$\boxed{Q = \mathrm{v}A = \left(\frac{1.00}{n}\right) AR^{2/3}\sqrt{S}}$$
$$= K\sqrt{S} \qquad \text{[SI]} \qquad 19.13(a)$$

$$Q = \mathrm{v}A = \left(\frac{1.49}{n}\right) AR^{2/3}\sqrt{S}$$
$$= K\sqrt{S} \qquad \text{[U.S.]} \qquad 19.13(b)$$

Example 19.1

A rectangular channel on a 0.002 slope is constructed of finished concrete. The channel is 8 ft (2.4 m) wide. Water flows at a depth of 5 ft (1.5 m). What is the flow rate?

SI Solution

The hydraulic radius is

$$\boxed{R = \frac{A}{P}} = \frac{(2.4\ \text{m})(1.5\ \text{m})}{1.5\ \text{m} + 2.4\ \text{m} + 1.5\ \text{m}}$$
$$= 0.67\ \text{m}$$

From App. 19.A, the roughness coefficient for finished concrete is 0.012. The Manning coefficient is determined by Eq. 19.11(a).

$$C = \left(\frac{1.00}{n}\right) R^{1/6} = \left(\frac{1.00}{0.012}\right)(0.67\ \text{m})^{1/6}$$
$$= 77.9$$

The discharge is

$$Q = \mathrm{v}A = C\sqrt{RS}A$$
$$= \left(77.9\ \frac{\sqrt{\text{m}}}{\text{s}}\right)\left(\sqrt{(0.67\ \text{m})(0.002)}\right)(1.5\ \text{m})(2.4\ \text{m})$$
$$= 10.3\ \text{m}^3/\text{s}$$

Customary U.S. Solution

The hydraulic radius is

$$R = \frac{A}{P} = \frac{(8\ \text{ft})(5\ \text{ft})}{5\ \text{ft} + 8\ \text{ft} + 5\ \text{ft}}$$
$$= 2.22\ \text{ft}$$

[3] Pronounced "Shay′-zee." This equation does not appear to be dimensionally consistent. However, the coefficient C is not a pure number. Rather, it has units of (length)$^{1/2}$/time (i.e., (acceleration)$^{1/2}$).

[4] Other methods of evaluating C include the *Kutter equation* (also known as the *G.K. formula*) and the *Bazin formula*. These methods are interesting from a historical viewpoint, but both have been replaced by the Manning equation.

[5] This equation was originally proposed in 1868 by Gaukler and again in 1881 by Hagen, both working independently. For some reason, the Frenchman Flamant attributed the equation to an Irishman, R. Manning. In Europe and many other places, the Manning equation may be known as the *Strickler equation*.

APPENDIX 19.A
Manning's Roughness Coefficient[a,b]
(design use)

channel material	n
plastic (PVC and ABS)	0.009
clean, uncoated cast iron	0.013–0.015
clean, coated cast iron	0.012–0.014
dirty, tuberculated cast iron	0.015–0.035
riveted steel	0.015–0.017
lock-bar and welded steel pipe	0.012–0.013
galvanized iron	0.015–0.017
brass and glass	0.009–0.013
wood stave	
small diameter	0.011–0.012
large diameter	0.012–0.013
concrete	
average value used	0.013
typical commercial, ball and spigot rubber gasketed end connections	
– full (pressurized and wet)	0.010
– partially full	0.0085
with rough joints	0.016–0.017
dry mix, rough forms	0.015–0.016
wet mix, steel forms	0.012–0.014
very smooth, finished	0.011–0.012
vitrified sewer	0.013–0.015
common-clay drainage tile	0.012–0.014
asbestos	0.011
planed timber (flume)	0.012 (0.010–0.014)
canvas	0.012
unplaned timber (flume)	0.013 (0.011–0.015)
brick	0.016
rubble masonry	0.017
smooth earth	0.018
firm gravel	0.023
corrugated metal pipe (CMP)	0.024 (see App. 17.F)
natural channels, good condition	0.025
rip rap	0.035
natural channels with stones and weeds	0.035
very poor natural channels	0.060

[a]Compiled from various sources.
[b]Values outside these ranges have been observed, but these values are typical.

Figure 17.10 Discharge from a Tank

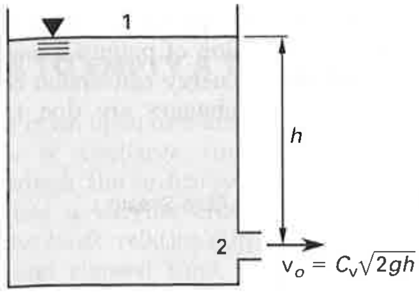

known as the ***velocity of approach***.) The only energy the fluid has is potential energy. At the jet, $p_2 = 0$. All of the potential energy difference $(z_1 - z_2)$ has been converted to kinetic energy. The theoretical velocity of the jet can be derived from the Bernoulli equation. Equation 17.66 is known as the equation for ***Torricelli's speed of efflux***.

$$v_t = \sqrt{2gh} \qquad 17.66$$

$$h = z_1 - z_2 \qquad 17.67$$

The actual jet velocity is affected by the orifice geometry. The *coefficient of velocity*, C_v, is an empirical factor that accounts for the friction and turbulence at the orifice. Typical values of C_v are given in Table 17.5.

$$v_o = C_v\sqrt{2gh} \qquad 17.68$$

$$C_v = \frac{\text{actual velocity}}{\text{theoretical velocity}} = \frac{v_o}{v_t} \qquad 17.69$$

The specific energy loss due to turbulence and friction at the orifice is calculated as a multiple of the jet's kinetic energy.

$$E_f = \left(\frac{1}{C_v^2} - 1\right)\frac{v_o^2}{2} = (1 - C_v^2)gh \qquad \text{[SI]} \qquad 17.70(a)$$

$$E_f = \left(\frac{1}{C_v^2} - 1\right)\frac{v_o^2}{2g_c} = (1 - C_v^2)h \times \frac{g}{g_c} \qquad \text{[U.S.]} \qquad 17.70(b)$$

The total head producing discharge (*effective head*) is the difference in elevations that would produce the same velocity from a frictionless orifice.

$$h_{\text{effective}} = C_v^2 h \qquad 17.71$$

The orifice guides quiescent water from the tank into the jet geometry. Unless the orifice is very smooth and the transition is gradual, momentum effects will continue to cause the jet to contract after it has passed through. The velocity calculated from Eq. 17.68 is usually assumed to be the velocity at the *vena contracta*, the section of smallest cross-sectional area. (See Fig. 17.11.)

Figure 17.11 *Vena Contracta of a Fluid Jet*

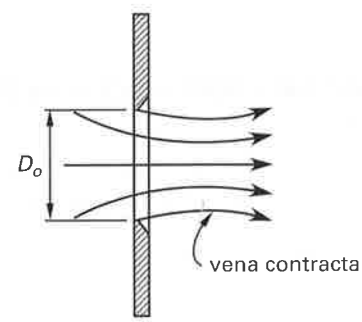

Table 17.5 *Approximate Orifice Coefficients, C, for Turbulent Water*

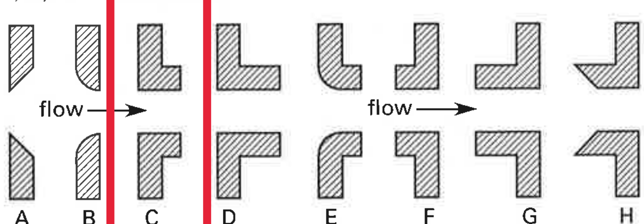

illustration	description	C_d	C_c	C_v
A	sharp-edged	0.62	0.63	0.98
B	round-edged	0.98	1.00	0.98
C	short tube* (fluid separates from walls)	0.61	1.00	0.61
D	sharp tube (no separation)	0.82	1.00	0.82
E	short tube with rounded entrance	0.97	0.99	0.98
F	reentrant tube, length less than one-half of pipe diameter	0.54	0.55	0.99
G	reentrant tube, length two to three pipe diameters	0.72	1.00	0.72
H	Borda	0.51	0.52	0.98
(none)	smooth, well-tapered nozzle	0.98	0.99	0.99

*A short tube has a length less than approximately three pipe diameters.

Attachment 4

HELP Model Summary

SCS ENGINEERS

SHEET 1 OF 2

CLIENT	PROJECT	JOB NO.
Hillsborough County	Southeast County Landfill	09215600.13

SUBJECT	BY	DATE
HELP Model Summary Final Landfill Closure	FCH	11/11/2021
Peak Daily Values	CHECKED	DATE
	KLS	11/16/2021

OBJECTIVE: To provide a quasi-two-dimensional hydrologic model of water movement across, into, through, and out of the landfill.
The program works to model the rainfall, runoff, infiltration, and other water pathways to evaluates the quantity of water building up on each layer of the final landfill closure system.

REFERENCES:
1. Attachment 1 - Top Slope (Min 330 Mil Composite) at 5% HELP Model Results
2. Attachment 2 - Side Slope (300 Mil Geocomposite) at 25% HELP Model Results
3. Attachment 3 - Geocomposite Transmissivity Data

PROCEDURE:
1. The layers of the landfill closure system is modeled within the HELP Model software and simulated to establish baseline for the water levels on each layer.
2. The site conditions - temperature, rainfall, evapotranspiration, etc., are input or simulated by NOAA weather data for the area.
3. The geocomposite properties are adjusted based on manufacturer's recommendations and results from the baseline simulation.
4. The water level on the geocomposite is evaluated.

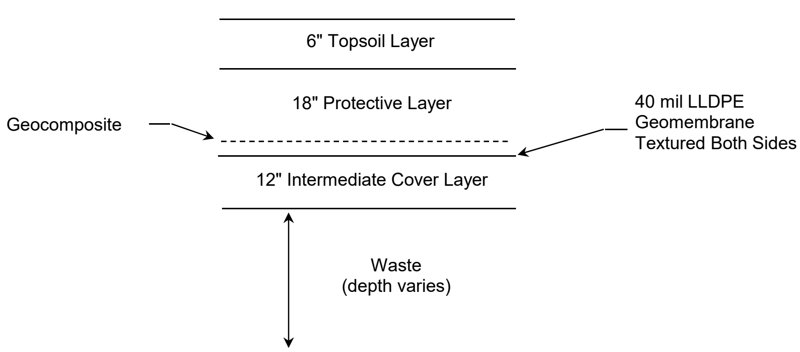

CLIENT	PROJECT	JOB NO.
Hillsborough County	Southeast County Landfill	09215600.13

SUBJECT	BY	DATE
HELP Model Summary Final Landfill Closure	FCH	11/11/2021
Peak Daily Values	CHECKED	DATE
	KLS	11/16/2021

PEAK DAILY VALUES:

Thickness of geocomposite at 100 hrs and loaded. Summary is on a per acre basis.

5% Top Slope Values; Soil K = 1E-4 cm/sec; Min. 330 Mil Composite				
Surface Length/Slope	Thickness at 100 hr (inches)	Max Head on Liner (inches)	Liquid Collected (ft^3/day)	Liquid Collected (gal/min)
L_{total} = 400 ft S = 5%	0.327	0.276	5,214	27.09

5% Top Slope Values; Soil K = 5E-4 cm/sec; Min. 330 Mil Composite				
Surface Length/Slope	Thickness at 100 hr (inches)	Max Head on Liner (inches)	Liquid Collected (ft^3/day)	Liquid Collected (gal/min)
L_{total} = 400 ft S = 5%	0.327	0.285	5,406	28.08

25% Side Slope Values; Soil K = 1E-4 cm/sec; 300 Mil Composite				
Surface Length/Slope	Thickness at 100 hr (inches)	Max Head on Liner (inches)	Liquid Collected (ft^3/day)	Liquid Collected (gal/min)
L_{total} = 120 ft S = 25%	0.297	0.066	5,179	26.90

25% Side Slope Values; Soil K = 5E-4 cm/sec; 300 Mil Composite				
Surface Length/Slope	Thickness at 100 hr (inches)	Max Head on Liner (inches)	Liquid Collected (ft^3/day)	Liquid Collected (gal/min)
L_{total} = 120 ft S = 25%	0.297	0.066	5,191	26.97

Result:

The HELP models indicate that the peak daily value of head on the closure liner does not exceed the depth of the respective top-of-crown or side slope drainage geocomposites after appropriate factors of safety have been applied to the geocomposite transmissivity (see Attachment 3 - Geocomposite Transmissivity Data). Both drainage geocomposites pass the design requirements for the upper and lower bounds of the hydraulic conductivity of the protective cover soil specified in the Technical Specifications.

SCS ENGINEERS

CLIENT	PROJECT	JOB NO.
Hillsborough County	Southeast County Landfill	09215600.13

SUBJECT	BY	DATE
Geocomposite Transmissivity/Hydraulic Conductivity Calculations Phase I - VI Closure	FCH	11/1/2021
	CHECKED	DATE
	KLS	11/16/2021

OBJECTIVE: To calculate the design hydraulic conductivity, design thickness, and porosity of the geocomposite selected for use in the final cover stormwater collection system at various loads using manufacturer's testing data. The calculations for the long-term transmissivity values of the geocomposite are based on 100-hour transmissivity values.

REFERENCES:

1. Attachment 1 - GRI Standard - GC8 Technical Release, April 17, 2001, Revised January 9, 2013
2. Attachment 2 - Test results for 100 hour transmissivity values.
3. Attachment 3 - Soil properties
4. Attachment 4 - Factor of Safety

PROCEDURE:

1. The design geocomposite hydraulic conductivities are calculated by adjusting manufacturer's transmissivity and thickness.
2. The geocomposite properties are adjusted based on the manufacturer's recommendations and GRI Standard - GC8 to determine geocomposite properties at various specific loads of interest.
3. Calculate 100-hour transmissivity, q_{100}, at the loads of interest using manufacturer's data.
4. Calculate geocomposite thickness at the loads of interest using manufacturer's data.
5. Calculate the geocomposite transmissivity after applying reduction factors.
6. Calculate the design transmissivity.
7. Calculate the design hydraulic conductivity from the design transmissivity and design thickness.

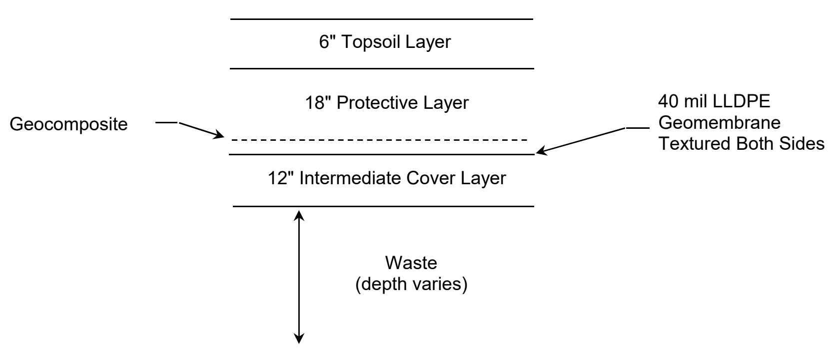

CLIENT	PROJECT	JOB NO.
Hillsborough County	Southeast County Landfill	09215600.13

SUBJECT	BY	DATE
Geocomposite Transmissivity/Hydraulic Conductivity Calculations	FCH	11/1/2021
Phase I - VI Closure	CHECKED	DATE
	KLS	11/16/2021

EQUATIONS:

Developed from Equations (1) and (2) pg GC8-3 - Refer to Attachment 1.

$$\theta_{allow} = (\theta_{ultimate})/RF_{IN}*RF_{CC}*RF_{BC}*RF_{CR}*FS)$$

Where:

θ_{allow} = Allowable transmissivity

$\theta_{ultimate}$ = Ultimate transmissivity (manufacturer's) under simulated conditions for 100 hours

RF_{IN} = Reduction Factor for elastic deformation, or intrusion of the adjacent geotextiles into the drainage channel. Since there is no long-term thickness data for material, use manufacturer provided Creep Reduction Factor at 100-hous for the design, as provided in Attachment 2

RF_{CC} = Reduction Factor for Chemical Clogging and/or precipitation of chemicals in the drainage core space

RF_{BC} = Reduction Factor for Biological Clogging in the drainage core space

RF_{CR} = Reduction Factor for Creep deformation of the drainage core and/or adjacent geotextile into the drainage channel

FS = Factor of Safety

$$RF_{CR} = \left[\frac{(t'/t) - (1 - n_{original})}{(t_{CR}/t) - (1 - n_{original})}\right]^3$$

Equation (6) pg GC8-7 - Attachment 1.

Where:

t' = Thickness at 100 hours

t = Virgin thickness

t_{CR} = Thickness at >>100 hours

$n_{original}$ = Original porosity

$= 1 - (\mu/\rho t)$

Equation (7) pg GC8-7 - Attachment 1.

μ = mass per unit area

ρ = density of formation

$$k = \frac{\theta_{allow}}{t'}$$

Developed from Equations (3) and (4) pg GC8-5 - Attachment 1.

Where:

k = Hydraulic conductivity, cm/sec

t' = Thickness at 100 hours

NOTES: RF_{IN} accounts for the geotextile encroaching on the geonet under a constant loading. A 100-hour transmissivity test accounts for intrusion. After the 100-hour seat time, the geotextile has already begun to intrude into the geonet, therefore, the transmissivity value reflects the intrusion. The transmissivity values for these calculations are all based on the 100-hour test, therefore, RF_{IN} = 1.0.

SCS ENGINEERS

CLIENT	PROJECT	JOB NO.
Hillsborough County	Southeast County Landfill	09215600.13

SUBJECT	BY	DATE
Geocomposite Transmissivity/Hydraulic Conductivity Calculations	FCH	11/1/2021
Phase I - VI Closure	CHECKED	DATE
	KLS	11/16/2021

OBJECTIVE: To determine the load on the final cover liner geocomposite under closed conditions.

KNOWN: Landfill closure cross-section.

Topsoil =	138.0	pcf	Refer to Attachment 2
Protective Cover =	138.0	pcf	Refer to Attachment 2

FINAL CLOSURE CONDITION - 54-INCH MAXIMUM DEPTH FINAL COVER:

Material	Material Density (pcf)	Depth of Material (ft)	Load (psf)		
Topsoil	138.0	0.5	69.0		
Protective Cover	138.0	5.0	690.0		
Total		5.5	759.0	<=	1,000

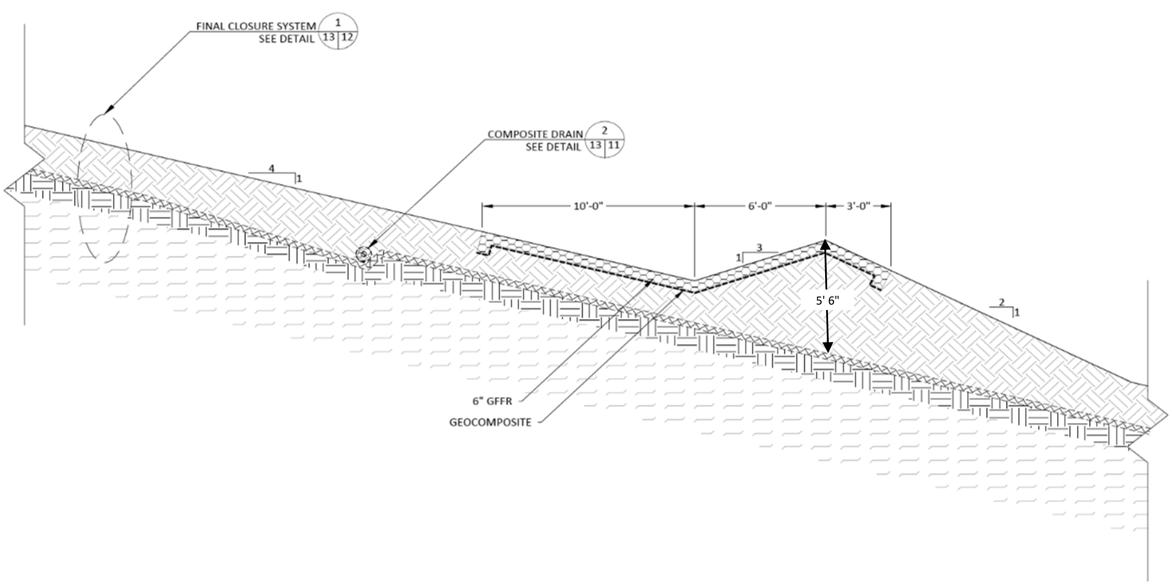

NOTES: Depth of material accounts for the thickness of soil along the side slope of the landfill.
The greater the depth of the soil, the larger the amount of loading the geocomposite could experience.
The depth of soil (5' 6") located at the berm is used to calculate the greatest load the geocomposite will experience.

CLIENT	PROJECT	JOB NO.
Hillsborough County	Southeast County Landfill	09215600.13

SUBJECT	BY	DATE
Geocomposite Transmissivity/Hydraulic Conductivity Calculations	FCH	11/1/2021
Phase I - VI Closure	CHECKED	DATE
	KLS	11/16/2021

PURPOSE: Calculate the design transmissivity, k, of a geocomposite under site specific boundary conditions for final closure loading conditions.

REFERENCES: From the AGRU technical department, the following Transmissivity (θ) and Creep values are known:

Plate/Sand/GC/Plate Manufacturer's 100 hour q_{100} Data Transmissivity	
@ 25% Gradient*	
Load (psf)	$q_{ultimate}$ (m^2/sec)
1,000	1.72E-03

* Value for 33% gradient was used for calculations. No data available for 1,000 psf at 25% gradient.

Refer to Attachment 3

Sand/GC/GM Creep	
@ 25% Gradient	
Load (psf)	RF_{CR}
1,000	1.01

Refer to Attachment 3

Plate/Sand/GC/Plate Manufacturer's 100 hour q_{100} Data Transmissivity	
@ 5% Gradient	
Load (psf)	$q_{ultimate}$ (m^2/sec)
1,000	3.30E-03

Refer to Technical Specifications which specify a minimum transmissivity and minimum thickness for top-of-crown geocomposite

Sand/GC/GM Creep at 100-hours	
@ 5% Gradient	
Load (psf)	RF_{CR}
1,000	1.01

Refer to Attachment 3

REDUCTION FACTORS:

RF - Intrusion, RF_{IN}
RF - Chemical Clogging, RF_{CC}
RF - Biological Clogging, RF_{BC}
RF - Creep, RF_{CR}
FS - Factor of Safety

Chemical Clogging RF_{CC} =	1.0	to	1.2	Refer to Attachment 1 pg GC8-9
Biological Clogging RF_{BC} =	1.2	to	3.5	Refer to Attachment 1 pg GC8-9

EQUATIONS:

$$\theta_{allow} = (\theta_{ultimate})/RF_{IN}*RF_{CC}*RF_{BC}*RF_{CR}*FS)$$

$$t' = (t)/(RF_{CR})$$

$$k = (\theta_{allow})/(t')$$

SCS ENGINEERS

CLIENT	PROJECT	JOB NO.
Hillsborough County	Southeast County Landfill	09215600.13

SUBJECT	BY	DATE
Geocomposite Transmissivity/Hydraulic Conductivity Calculations	FCH	11/1/2021
Phase I - VI Closure	CHECKED	DATE
	KLS	11/16/2021

FINAL CLOSURE CONDITION - 54-INCH MAXIMUM DEPTH FINAL COVER:

REDUCTION FACTORS:

RF_{IN} =	1.00	Refer to Calculation Page 2 Note	thickness, t =	300	mil
RF_{CC} =	1.00	Refer to Attachment 1 pg GC8-9		0.3	inches
RF_{BC} =	1.35	Refer to Attachment 1 pg GC8-9		0.762	cm
RF_{CR} =	1.01	Refer to Attachment 2			
FS =	2.00	Refer to Attachment 4			

@ 25% Gradient (Sideslopes)					
Load (psf)	$\theta_{Ultimate}$ (m^2/sec)	θ_{allow} (m^2/sec)	θ_{allow} (cm^2/sec)	*t' (cm)	k (cm/sec)
1,000	1.72E-03	6.31E-04	6.31	0.75446	8.36

Thickness at 100 hrs. **t' = 0.297 inches**

REDUCTION FACTORS:

RF_{IN} =	1.00	Refer to Calculation Page 2 Note	thickness, t =	330	mil
RF_{CC} =	1.00	Refer to Attachment 1 pg GC8-9		0.33	inches
RF_{BC} =	1.35	Refer to Attachment 1 pg GC8-9		0.8382	cm
RF_{CR} =	1.01	Refer to Attachment 2			
FS =	2.00	Refer to Attachment 4			

@ 5% Gradient (Top-of-crown)					
Load (psf)	$\theta_{Ultimate}$ (m^2/sec)	θ_{allow} (m^2/sec)	θ_{allow} (cm^2/sec)	*t' (cm)	k (cm/sec)
1,000	3.30E-03	1.21E-03	12.10	0.8299	14.58

Thickness at 100 hrs. **t' = 0.327 inches**

25% GRADIENT FOR VENEER STABILITY CALCULATIONS:

REDUCTION FACTORS:

FS[1] = 1.50

@ 25% Gradient for Veneer Stability					
Load (psf)	$\theta_{Ultimate}$ (m^2/sec) [2]	θ_{allow} (m^2/sec)	θ_{allow} (cm^2/sec)	*t' (cm)	k (cm/sec)
Load (psf)	1.72E-03	8.41E-04	8.41	0.75446	11.15

Thickness at 100 hrs. **t' = 0.297 inches**

"For θ_{allow} @ 25% gradient for Veneer Stability Calculation"

Notes for Veneer Stability Calculations:

1. Factor of safety adjusted from 2 to 1.5 as an additional factor of safety is applied in the veneer stability calculations.
2. A more conservative (33% gradient) θultimate value was used for 25% gradient.

Attachment 1

GRI Standard – GC8 Technical Release, Rev. 1: January 9, 2013

Geosynthetic Institute
475 Kedron Avenue
Folsom, PA 19033-1208 USA
TEL (610) 522-8440
FAX (610) 522-8441

Original: April 17, 2001
Rev. 1: January 9, 2013-Editorial

GRI Standard GC8*

Standard Guide for

Determination of the Allowable Flow Rate of a Drainage Geocomposite

1. Scope

1.1 This guide presents a methodology for determining the allowable flow rate of a candidate drainage geocomposite. The resulting value can be used directly in a hydraulics-related design to arrive at a site-specific factor of safety.

1.2 The procedure is to first determine the candidate drainage composite's flow rate for 100-hours under site-specific conditions, and then modify this value by means of creep reduction and clogging reduction factors.

1.3 For aggressive liquids, a "go-no go" chemical resistance procedure is suggested. This is a product-specific verification test for both drainage core and geotextile covering.

1.4 The type of drainage geocomposites under consideration necessarily consists of a drainage core whose purpose it is to convey liquid within its manufactured plane. The drainage core can be a geonet, 3-D mesh, built-up columns, single or double cuspations, etc.

1.5 The drainage core usually consists of a geotextile on its upper and/or lower surface. In some cases, the drainage core is used by itself. The guide addresses all of these variations.

1.6 The guide is also applicable to thick nonwoven geotextiles when they are utilized for their drainage capability.

*This GRI standard is developed by the Geosynthetic Research Institute through consultation and review by the member organizations. This specification will be reviewed at least every 2-years, or on an as-required basis. In this regard it is subject to change at any time. The most recent revision date is the effective version.

1.7 All types of polymers are under consideration in this guide.

1.8 The guide does not address the required (or design) flow rate to which a comparison is made for the final factor of safety value. This is clearly a site-specific issue.

2. Referenced Documents

2.1 ASTM Standards

D1987 – "Test Method for Biological Clogging of Geotextile or Soil/Geotextile Filters"

D2240 – "The Method for Rubber Property – Durometer Hardness"

D4716 – "Test Method for Constant Head Hydraulic Transmissivity (In Plane Flow) of Geotextiles and Geotextile Related Products"

D5322 – "Standard Practice for Immersion Procedures for Evaluating the Chemical Resistance of Geosynthetics to Liquids"

D6364 – "Test Method for Determining the Short-Term Compression Behavior of Geosynthetics"

D6388 – "Standard Practice for Tests to Evaluate the Chemical Resistance of Geonets to Liquids"

D6389 – "Standard Practice for Tests to Evaluate the Chemical Resistance of Geotextiles to Liquids"

2.2 GRI Standards

GS4 – Test Method for Time Dependent (Creep) Deformation Under Normal Pressure

2.3 Literature

Giroud, J.-P., Zhao, A. and Richardson, G. N. (2000), "Effect of Thickness Reduction on Geosynthetic Hydraulic Transmissivity," Geosynthetics International, Vol. 7, Nos. 4-6, pp. 433-452.

Koerner, R. M. (2012), Designing with Geosynthetics, 6th Edition, Xlibris Publishing Co., 914 pgs.

3. Summary of Guide

3.1 This guide presents the necessary procedure to be used in obtaining an allowable flow rate of a candidate drainage geocomposite. The resulting value is then compared to a required (or design) flow rate for a product-specific and site-specific factor of safety. The guide does not address the required (or design) flow rate value, nor the subsequent factor of safety value.

3.2 The procedures recommended in this guide use either ASTM or GRI test methods.

3.3 The guide is applicable to all types of drainage geocomposites regardless of their core configuration or geotextile type. It can also be used to evaluate thick nonwoven geotextiles.

4. Significance and Use

4.1 The guide is meant to establish uniform test methods and procedures in order for a designer to determine the allowable flow rate of a candidate drainage geocomposite for site-specific conditions.

4.2 The guide requires communication between the designer, testing organization and manufacturer in setting site-specific control variables such as product orientation, stress level, stress duration, type of permeating liquid and materials below/above the geocomposite test specimen.

4.3 The guide is useful to testing laboratories in that a prescribed guide is at hand to provide appropriate data for both designer and manufacturer clients.

5. Structure of the Guide

5.1 Basic Formulation – This guide is focused on determination of a "q_{allow}" value using the following formula:

$$\boxed{q_{allow} = q_{100}\left[\frac{1}{RF_{CR} \times RF_{CC} \times RF_{BC}}\right] \qquad (1)}$$

where

q_{allow} = allowable flow rate
q_{100} = initial flow rate determined under simulated conditions for 100-hour duration
RF_{CR} = reduction factor for creep to account for long-term behavior
RF_{CC} = reduction factor for chemical clogging
RF_{BC} = reduction factor for biological clogging

Note 1: By simulating site-specific conditions (except for load duration beyond 100 hours and chemical/biological clogging), additional reduction factors such as intrusion need not be explicitly accounted for.

Note 2: The value of q_{allow} is typically used to determine the product-specific and site-specific flow rate factor of safety as follows:

$$\boxed{FS = \frac{q_{allow}}{q_{reqd}} \qquad (2)}$$

The value of "q_{reqd}" is a design issue and is not addressed in this guide. Likewise, the numeric value of the factor-of-safety is not addressed in this guide. Suffice it to say that, depending on the duration and criticality of the situation, FS-values should be conservative unless experience allows otherwise.

5.2 Upon selecting the candidate drainage geocomposite product, one must obtain the 100-hour duration flow rate according to the ASTM D4716 transmissivity test. This establishes the base value to which drainage core creep beyond 100-hours and clogging from chemicals and biological matter must be accounted for.

> Note 3: It is recognized that the default duration listed in ASTM D4716 is 15-minutes. This guide purposely requires that the test conditions be maintained for 100-hours.

5.3 Reduction Factor for Creep – This is a long-term (typically 10,000 hours) compressive load test focused on the stability and/or deformation of the drainage core without the covering geotextiles. Stress orientation can be perpendicular or at an angle to the test specimen depending upon site-specific conditions.

5.4 Chemical and/or Biological Clogging – The issue of long term reduction factors to account for clogging within the core space is a site-specific issue. The issue is essentially impractical to simulate in the laboratory, hence a table is provided for consideration by the designer.

5.5 Chemical Resistance/Durability – This procedure results in a "go-no go" decision as to potential chemical reactions between the permeating liquid and the polymers comprising the drainage core and geotextiles. The issue will be addressed in this guide but is not a reduction factor, per se.

6. Determination of the Base Line Flow Rate (q_{100})

6.1 Using the ASTM D4716 transmissivity test with the conditions stated below (unless otherwise agreed upon by the parties involved), determine the 100-hour flow rate of the drainage geocomposite under consideration.

6.1.1 The test specimen shall be the entire geocomposite. If geotextiles are bonded to the drainage core, they shall not be removed and the entire geocomposite shall be tested as a unit. A minimum of three replicate samples in the site-specific orientation shall be tested and the results averaged for the reported value.

6.1.2 Specimen size shall be 300 × 300 mm (12 × 12 in.) within the stressed area.

6.1.3 The specimen orientation is to be agreed upon by the designer, testing laboratory and manufacturer. In this regard, it should be recognized that the specimen orientation during testing has to match the proposed installation orientation. Thus the site-specific design governs both the testing orientation and subsequent field installation orientation.

6.1.4 Specimen substratum shall be one of the following four options. The decision of which is made by the project designer, testing organization and manufacturer. The options are (i) rigid platen, (ii) foam, (iii) sand or (iv) site-specific soil or other material.

6.1.4.1 If a rigid platen is used the choices are usually wood, plastic or metal. The testing laboratory must identify the specifics of the material used.

6.1.4.2 If closed cell foam is used, it shall be 12 mm (0.5 in.) thick and a maximum durometer of 2.0 as measured in ASTM D2240, Type D.

6.1.4.3 If sand is used it shall be Ottawa test sand at a relative density of 85%, water content of 10% and compacted thickness of 25 mm (1.0 in.).

6.1.4.4 If site-specific soil or other material is used it must be carefully considered and agreed upon between the parties involved. Size, gradation, moisture content, density, etc., are all important considerations.

6.1.5 Specimen superstratum shall also be one of the four same options as mentioned in § 6.1.3 above. It need not be the same as the substratum.

6.1.6 The applied stress level is at the discretion of the designer, testing organization and manufacturer. Unless stated otherwise, the orientation shall be normal to the test specimen.

6.1.7 The duration of the loading shall be for 100 hours. A single site-specific data point is obtained at that time, i.e., it is not necessary to perform intermediate flow rate testing, unless otherwise specified by the various parties involved.

6.1.8 The hydraulic gradient at which the above data point is taken (or a range of hydraulic gradients) is at the discretion of the designer, testing organization and manufacturer.

6.1.9 The permeating liquid is to be tap water, unless agreed upon otherwise by the designer, testing organization, and manufacturer.

6.1.10 Calculations

$$\boxed{Q = kiA \qquad (3)}$$

$$Q = ki(Wt)$$

$$\boxed{Q/W = \theta i \qquad (4)}$$

$$q = \theta i \qquad (5)$$

where

Q = flow rate per unit time (m^3/sec)
k = permeability (m/sec)
i = hydraulic gradient (= H/L)
H = head loss across specimen (m)
L = length of specimen (m)
A = cross sectional area of specimen (m^2)
W = width of specimen (m)
t = thickness of specimen (m)
θ = transmissivity (m^3/sec-m or m^2/sec)
q = flow rate per unit width (m^2/sec)

The results can be presented as flow rate per unit width (Q/W), or as transmissivity (θ), as agreed upon by the parties involved.

7. Reduction Factor for Creep

7.1 Using the GRI GS4 test method or ASTM D6364 (mod.) for time dependent (creep) deformation, the candidate drainage core is placed under compressive stress and its decrease in thickness (deformation) is monitored over time.

> Note 4: This is not a flow rate test, although the test specimen can be immersed in a liquid to be agreed upon by the designer, testing organization, and manufacturer. However, it is usually a test conducted without liquid.

7.1.1 <u>The test specimen shall be the drainage core only</u>. If geotextiles are bonded to the drainage core they should be carefully removed. Alternatively, a sample of the drainage core can be obtained from the manufacturer before the geotextiles are attached. A minimum of three replicate tests shall be performed and the results averaged for the reported value.

7.1.2 Specimen size should be 150 × 150 mm (6.0 × 6.0 in.) and placed in a rigid box made from a steel base and sides. The steel load plate above the test specimen shall be used to transmit a constant stress over time. Deformation of the upper plate is measured by at least two dial gauges and the results averaged accordingly.

> Note 5: For high stress conditions requiring a large size and number of weights with respect to laboratory testing and safety, the specimen size can be reduced to 100 × 100 mm (4.0 × 4.0 in.).

7.1.3 Specimen substratum and superstratum shall be rigid platens. Alternatively, a 1.5 mm (60 mil) thick HDPE geomembrane can be placed against the drainage core with the steel plates as back-ups.

7.1.4 The test specimen shall be dry unless water or a simulated or site-specific leachate is agreed upon by the parties involved.

7.1.5 The normal stress magnitude(s) shall be the same as applied in the transmissivity test described in Section 6.0. Alternatively, it can be as agreed upon by the designer, testing organization, and manufacturer.

7.1.6 The load inclination shall be normal to the test specimen. If there exists a tendency for the core structure to deform laterally, separate tests at the agreed upon load inclinations shall also be performed at the discretion of the parties involved.

7.1.7 The dwell time shall be 10,000 hours. If, however, this is a confirmation test (or if a substantial data base exists on similar products of the same type), the dwell time can be reduced to 1000 hours. This decision must be made with agreement between the designer, testing organization, and manufacturer.

> Note 6: Alternative procedures to arrive at an acceptable value for the creep reduction factor based on shorter test times (e.g., the use of time-temperature superposition or stepped isothermal method) may be acceptable if agreed upon by the various parties involved.

7.1.8 The above process results in a set of creep curves similar to Figure 1(a). The curves are to be interpreted as shown in Figure 1(b). The reduction factor for creep of the core is interpreted according to the following formulas, after Giroud, Zhao and Richardson (2000).

$$RF_{CR} = \left[\frac{(t_{CO} / t_{original}) - (1 - n_{original})}{(t_{CR} / t_{original}) - (1 - n_{original})} \right]^3 \qquad (6)$$

where

RF_{CR}	=	reduction factor for creep
$t_{original}$	=	original thickness (m)
t_{CO}	=	thickness at 100-hours (m)
t_{CR}	=	thickness at >>100-hours, e.g., at 10,000 hours (m)
$n_{original}$	=	original porosity (see Equation 7)

$$n_{original} = 1 - \frac{\mu}{\rho t_{original}} \qquad (7)$$

where

μ	=	mass per unit area (kg/m^2)
ρ	=	density of the formulation (kg/m^3)

7.1.9 The above illustrated numeric procedure is <u>not applicable</u> to drainage geocomposites which include geotextiles. It is for the drainage core only.

<u>Example</u>: A HDPE geonet has the following properties: mass per unit area μ = 1216 g/m^2 (or 1.216 kg/m^2); density ρ = 950 kg/m^2 and original thickness of 8.55 mm.

Test specimens were evaluated according to ASTM D4716 for 100 hours and the average thickness decreased to 7.14 mm. A 10,000 hour creep test was then performed on a representative specimen according to GRI-GS4 and the resulting thickness further decreased to 6.30 mm. Thus Δy in Figure 1(b) is 7.14 – 6.30 = 0.84 mm. Determine the creep reduction factor "RF_{CR}".

<u>Solution</u>: The porosity n, is calculated according to Eq. (7) as follows

$$n_{original} = 1 - \frac{\mu}{\rho t_{original}}$$

$$= 1 - \frac{1.216}{(950)(0.00855)}$$

$$= 1 - 0.150$$

$$n_{original} = 0.850$$

The reduction factor for creep is calculated according to Eq. (6) as follows:

$$RF_{CR} = \left[\frac{(t_{CO} / t_{original}) - (1 - n_{original})}{(t_{CR} / t_{original}) - (1 - n_{original})} \right]^3$$

$$= \left[\frac{(7.14 / 8.55) - (1 - 0.850)}{(6.30 / 8.55) - (1 - 0.850)} \right]^3$$

$$= \left[\frac{0.835 - 0.150}{0.737 - 0.150} \right]^3$$

$$= \left[\frac{0.685}{0.587} \right]^3$$

$$RF_{CR} = 1.59$$

Note 7: Other calculation methods to arrive at the above numeric value of creep reduction factor may be considered if agreed upon by the various parties involved.

8. Reduction Factors for Core Clogging

There are two general types of core clogging that might occur over a long time period. They are chemical clogging and biological clogging. Both are site-specific and both are essentially impractical to simulate in the laboratory.

8.1 Chemical clogging within the drainage core space can occur with precipitates deposited from high alkalinity soils, typically calcium and magnesium. Other precipitates can also be envisioned such as fines from turbid liquids although this is less likely since the turbid liquid must typically pass through a geotextile filter. It is obviously a site-specific situation.

8.2 Biological clogging within the drainage core space can occur by the growth of biological organisms or by roots growing through the overlying soil and extending downward, through the geotextile filter, and into the drainage core. It is a site-specific situation and depends on the local, or anticipated, vegetation, cover soil, hydrology, etc.

8.3 Default tables for the above two potential clogging mechanisms (chemical and biological) are very subjective and by necessity broad in their upper and lower limits. The following table is offered as a guide.

Range of Clogging Reduction Factors (modified from Koerner, 1998)

Application	Chemical Clogging (RF_{CC})	Biological Clogging (RF_{BC})
Sport fields	1.0 to 1.2	1.1 to 1.3
Capillary breaks	1.0 to 1.2	1.1 to 1.3
Roof and plaza decks	1.0 to 1.2	1.1 to 1.3
Retaining walls, seeping rock and soil slopes	1.1 to 1.5	1.0 to 1.2
Drainage blankets	1.0 to 1.2	1.0 to 1.2
Landfill caps	1.0 to 1.2	1.2 to 3.5
Landfill leak detection	1.1 to 1.5	1.1 to 1.3
Landfill leachate collection	1.5 to 2.0	1.1 to 1.3

9. Polymer Degradation

9.1 Degradation of the materials from which the drainage geocomposite are made, with respect to the site-specific liquid being transmitted, is a polymer issue. Most geocomposite drainage cores are made from polyethylene, polypropylene, polyamide or polystyrene. Most geotextile filter/separators covering the drainage cores are made from polypropylene, polyester or polyethylene.

Note 8: It is completely inappropriate to strip the factory bonded geotextile off of the drainage core and then test one or the other component. The properties of both the geotextile and drainage core will be altered in the lamination process from their original values.

9.2 If polymer degradation testing is recommended, the drainage core and the geotextile should be tested separately in their as-received condition before lamination and bonding.

9.3 The incubation of the drainage cores and/or geotextile coupons is to be done according to the ASTM D5322 immersion procedure.

9.4 The testing of the incubated drainage cores is to be done according to ASTM D6388 which stipulates various test methods for evaluation of incubated geonets.

Note 9: For drainage cores other than geonets, e.g., columnar, cuspated, meshes, etc., it may be necessary to conduct additional tests than appear in ASTM D6388. These tests, and their procedures, should be discussed and agreed upon by the project designer, testing organization, and manufacturer.

9.5 The testing of the incubated geotextiles is to be done according to ASTM D6389 which stipulates various test methods for evaluation of incubated geotextiles.

Note 10: The information obtained in testing the drainage core (Section 9.4) and the geotextile (Section 9.5) result in a "go-no go" situation and not in a reduction factor, per se. If an adverse chemical reaction is indicated, one must select a different type of geocomposite material (drainage core and/or geotextile).

10. Summary

10.1 For a candidate drainage geocomposite, the 100-hour flow rate behavior under the site-specific set of variables, e.g., specimen orientation, stress level, hydraulic gradient, and permeating liquid is to be obtained per ASTM D4716 following procedures of Section 6.0.

10.2 A reduction factor for long term creep of the drainage core following Section 7.0 per GRI GS4 or ASTM D6364 (mod.) is then obtained. The result is usually a unique value for a given set of conditions.

10.3 A reduction factor for chemical and/or biological clogging, as discussed in Section 8.0 can be included. It is very much a site-specific situation at the discretion of the parties involved.

10.4 Polymer degradation to aggressive liquids is covered in separate immersion and test protocols, e.g., ASTM D5322 (immersion), ASTM D6388 (geonets) and ASTM D6389 (geotextiles) as discussed in Section 9.0. The procedure does not result in a reduction factor, rather in a "go-no go" decision with the product under consideration.

10.5 Other possible flow rate reductions and/or concerns such as flow in overlap regions, effect of high or low temperatures, etc., are site-specific and cannot readily be generalized in a guide such as this.

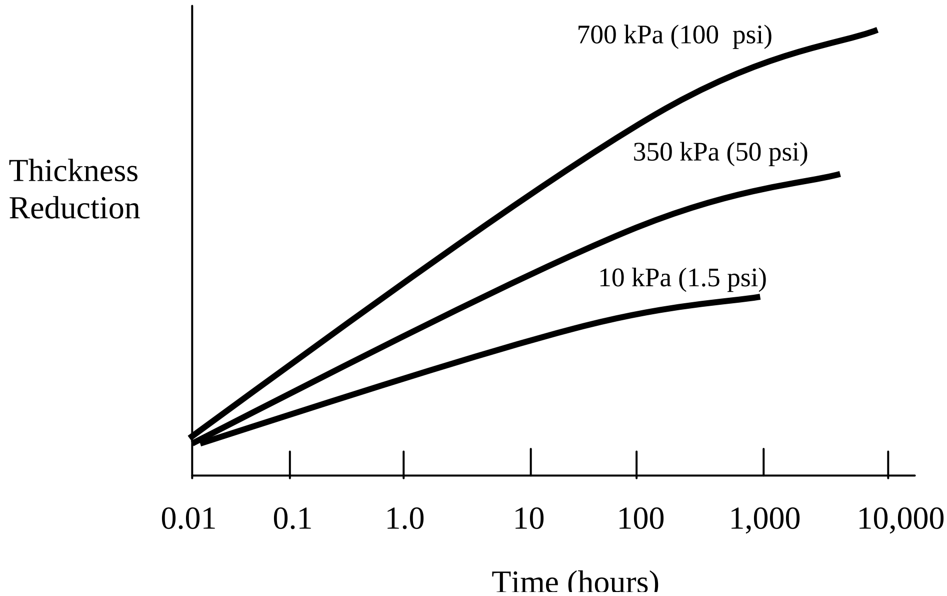

(a) Hypothetical data from creep testing illustrating effect of normal load magnitude

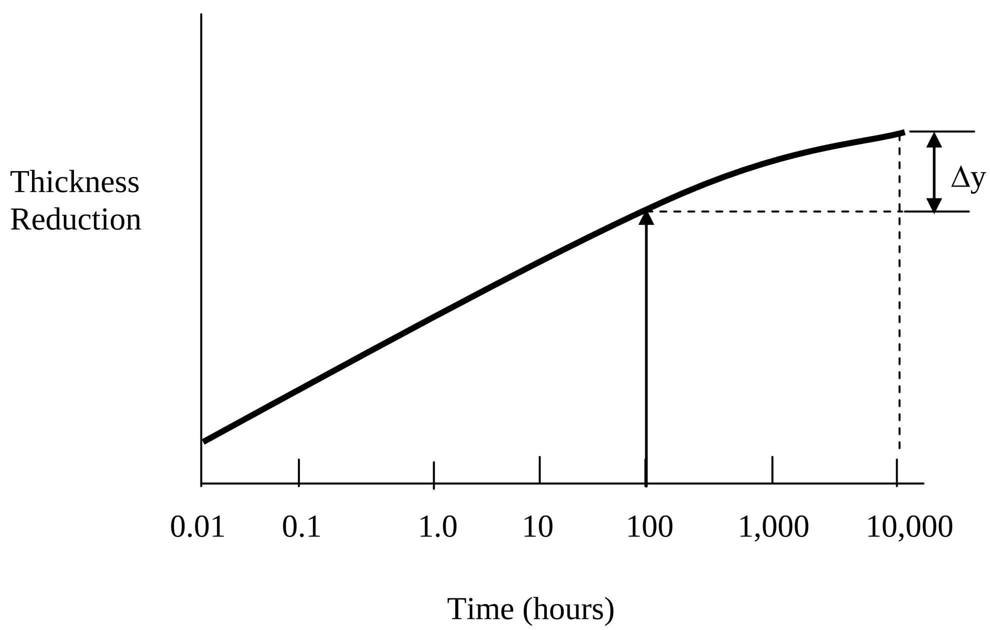

(b) Interpretation of project specific normal load curve to obtain creep reduction factor

Figure 1 – Hypothetical example of creep test data and data interpretation to obtain creep reduction factor

Attachment 2

Geocomposite Transmissivity Data

The Plastics Experts.

Geocomposite

300 MIL

AGRU America's Geocomposite Closure System is the traditional method for closures, which utilizes AGRU MicroSpike® or AGRU Smooth Liner® geomembrane, overlain by a geocomposite drainage layer, soil cover layer, and vegetative layer.

All information, recommendations and suggestions appearing in this literature concerning the use of our products are based upon tests and data believed to be reliable; however, it is the user's responsibility to determine the suitability for their own use of the products described herein. Since the actual use by others is beyond our control, no guarantee or warranty of any kind, expressed or implied, is made by AGRU America as to the effects of such use or the results to be obtained, nor does AGRU America assume any liability in connection herewith. Any statement made herein may not be absolutely complete since additional information may be necessary or desirable when particular or exceptional conditions or circumstances exist or because of applicable laws or government regulations. Nothing herein is to be construed as permission or as a recommendation to infringe any patent.

GEONET COMPONENT [1]

Property	Test Method	Frequency	Minimum Average Values
Thickness, mil (mm)	ASTM D5199	50,000 sf	300 (7.6)
Peak Tensile Strength MD, lbs./ in. (N/mm)	ASTM D5035/7179	50,000 sf	75 (13.3)
Density, g/cm^3	ASTM D792, Method B	50,000 sf	0.94
Carbon Black Content (%)	ASTM D4218	50,000 sf	2 - 3
Transmissivity[2], m^2/sec. (gal/min/ft)	ASTM D4716	500,000 sf	8×10^{-3} (38.6)

GEOTEXTILE COMPONENT [1]

Property	Test Method	Frequency	Minimum Average Values		
Mass per Unit Area, oz./sq. yd. (g/m^2)	ASTM D5261	100,000 sf	6.0 (203)	8.0 (271)	10.0 (339)
Grab Tensile Strength, lbs.(N)	ASTM D4632	100,000 sf	170 (757)	220 (979)	270 (1200)
Grab Elongation, %	ASTM D4632	100,000 sf	50	50	50
Trapezoidal Tear, lbs. (N)	ASTM D4533	100,000 sf	65 (289)	95 (423)	105 (467)
CBR Puncture , lbs (N)	ASTM D6241	500,000 sf	435 (1935)	600 (2670)	725 (3230)
Permittivity[3], $sec.^{-1}$	ASTM D4491	500,000 sf	1.5	1.3	1.1
Water Flow, [3] gpm./ ft^2 (l/min/m^2)	ASTM D4491	500,000 sf	110 (4479)	95 (3895)	80 (3280)
AOS, U.S. Sieve max (mm)[3]	ASTM D4751	500,000 sf	70 (0.212)	80 (0.180)	100 (0.150)

GEOCOMPOSITE

Property	Test Method	Frequency	Minimum Average Values		
Ply Adhesion, lbs./ in. (g/cm)	ASTM D7005	50,000 sf	1 (178)	1 (178)	1 (178)
Transmissivity [2], m^2/sec. (gal/min/ft)	ASTM D4716	500,000 sf - Double	9×10^{-4} (4.3)	9×10^{-4} (4.3)	7×10^{-4} (3.4)
	ASTM D4716	500,000 sf - Single	3×10^{-3} (14.5)	3×10^{-3} (14.5)	2×10^{-3} (9.6)

SUPPLY INFORMATION

Standard Roll Length[4]	at Fabric Weight	6-oz	8-oz	10-oz
Double Sided		160	150	140
Single Sided		180	180	170

Notes:
(1) Component properties are prior to lamination
(2) Geonet & Geocomposite . Transmissivity at 21°C, gradient of 0.1, load of 10,000 psf, seat time 15 min. between steel plates.
(3) At time of manufacture. Handling may change these properties.
(4) All roll widths are 14.5 feet. All roll lengths and widths have a tolerance of ±1%
(5) UV Resistance after 500 hours for the geotextile componet exhibits 70% strength retained via ASTM D4355

AGRU America, Inc.
500 Garrison Road
Georgetown, SC 29440 USA
(800) 373-2478 | Fax: (843) 546-0516
salesmkg@agruamerica.com
Revision Date: February 23, 2018 10:07 AM

agru
The Plastics Experts.

Geocomposite

330 MIL

AGRU America's Geocomposite Closure System is the traditional method for closures, which utilizes AGRU MicroSpike® or AGRU Smooth Liner® geomembrane, overlain by a geocomposite drainage layer, soil cover layer, and vegetative layer.

GEONET COMPONENT (1)

Property	Test Method	Frequency	Minimum Average Values
Thickness, mil (mm)	ASTM D5199	50,000 sf	330 (8.3)
Peak Tensile Strength MD, lbs./ in. (N/mm)	ASTM D5035/7179	50,000 sf	95 (16.5)
Density, g/cm^3	ASTM D792, Method B	50,000 sf	0.94
Carbon Black Content (%)	ASTM D4218	50,000 sf	2 - 3
Transmissivity(2), m^2/sec. (gal/min/ft)	ASTM D4716	500,000 sf	9×10^{-3} (43.4)

GEOTEXTILE COMPONENT (1)

Property	Test Method	Frequency	Minimum Average Values		
Mass per Unit Area, oz./sq. yd. (g/m^2)	ASTM D5261	100,000 sf	6.0 (203)	8.0 (271)	10.0 (339)
Grab Tensile Strength, lbs.(N)	ASTM D4632	100,000 sf	170 (757)	220 (979)	270 (1200)
Grab Elongation, %	ASTM D4632	100,000 sf	50	50	50
Trapezoidal Tear, lbs. (N)	ASTM D4533	100,000 sf	65 (289)	95 (423)	105 (467)
CBR Puncture , lbs (N)	ASTM D6241	500,000 sf	435 (1935)	600 (2670)	725 (3230)
Permittivity(3), $sec.^{-1}$	ASTM D4491	500,000 sf	1.5	1.3	1.1
Water Flow, (3) gpm./ ft^2 ($l/min/m^2$)	ASTM D4491	500,000 sf	110 (4479)	95 (3895)	80 (3280)
AOS, U.S. Sieve max (mm)(3)	ASTM D4751	500,000 sf	70 (0.212)	80 (0.180)	100 (0.150)

GEOCOMPOSITE

Property	Test Method	Frequency	Minimum Average Values		
Ply Adhesion, lbs./ in. (g/cm)	ASTM D7005	50,000 sf	1 (178)	1 (178)	1 (178)
Transmissivity (2), m^2/sec. (gal/min/ft)	ASTM D4716	500,000 sf - Double	9×10^{-4} (4.3)	9×10^{-4} (4.3)	7×10^{-4} (3.4)
	ASTM D4716	500,000 sf - Single	3×10^{-3} (14.5)	3×10^{-3} (14.5)	2×10^{-3} (9.6)

SUPPLY INFORMATION

Standard Roll Length(4)	at Fabric Weight	6-oz	8-oz	10-oz
Double Sided		140	130	120
Single Sided		160	160	150

Notes:
(1) Component properties are prior to lamination
(2) Geonet & Geocomposite . Transmissivity at 21°C, gradient of 0.1, load of 10,000 psf, seat time 15 min. between steel plates.
(3) At time of manufacture. Handling may change these properties.
(4) All roll widths are 14.5 feet. All roll lengths and widths have a tolerance of ±1%
(5) UV Resistance after 500 hours for the geotextile componet exhibits 70% strength retained via ASTM D4355

AGRU America, Inc.
500 Garrison Road
Georgetown, SC 29440 USA

(800) 373-2478 | Fax: (843) 546-0516
salesmkg@agruamerica.com
Revision Date: February 23, 2018 10:07 AM

Herron, Fauve

From: Bill Urchik <BUrchik@AgruAmerica.com>
Sent: Thursday, July 1, 2021 2:22 PM
To: Herron, Fauve
Subject: Typical Trans test results

Type	Load (psf)	Gradient	Seat Time (HR)			Trans Result
8-300-8	300	0.5	100	R&D	Plate/Sand/8-300-8/Plate	1.34E-03
8-300-8	1,000	0.1	100	N/A	Plate / Sand / 8-300-8 / Plate	2.68E-03
8-300-8	1,000	0.33	100	N/A	Plate / Sand / 8-300-8 / Plate	1.72E-03
8-330-8 Composite	1,044	0.1	100	N/A	Plate / Sand / 8-330-8 Composite / Plate	3.08E-03

Fauve,

Test data is very limited at low normal loads as typically 300/330mil composite are used for high normal load conditions in landfill cells. Please let me know if you have any questions.

Bill

Bill Urchik
Project Engineer NE USA/Canada
AGRU America, Inc.

Mobile: (716)704-9291
Office: (585) 418-5016
500 Garrison Road
Georgetown, SC 29440 USA
agruamerica.com

Beben, David

From: Mike Gnau <MGnau@AgruAmerica.com>
Sent: Monday, January 11, 2021 8:31 AM
To: Beben, David
Subject: FW: Marion County

Good morning, David.

Please see below as requested.

- 5% slope
  - 8/250/8 – 8.5×10^{-4} m^2/sec
  - 8/300/8 – 2.5×10^{-3} m^2/sec

Please let me know if you require additional information.

Mike

From: Beben, David [mailto:DBeben@scsengineers.com]
Sent: Friday, January 8, 2021 4:54 PM
To: Mike Gnau <MGnau@AgruAmerica.com>
Subject: RE: Marion County

Mike – sorry to keep bugging but do you have transmissivity values for the same conditions with a five percent slope?

- 33% slope
  - 8/250/8 – 4.5×10^{-4} m^2/sec
  - 8/300/8 – 1.2×10^{-3} m^2/sec
- 5% slope
  - 8/250/8 – 8.5×10^{-4} m^2/sec
  - 8/300/8 – 2.5×10^{-3} m^2/sec

From: Mike Gnau <MGnau@AgruAmerica.com>
Sent: Wednesday, January 6, 2021 3:33 PM
To: Beben, David <DBeben@scsengineers.com>
Cc: Radford, Mike <MRadford@scsengineers.com>; Chris Eichelberger <CEichelberger@AgruAmerica.com>
Subject: RE: Marion County

David,

Below are creep reduction factors as requested:

- 8/250/8 – 1.02
- 8/300/8 – 1.01

These are actually values for 1000 psf so they are conservative for 500 psf.

Please let me know if you require additional information.

Thank you,

Mike

Michael Gnau, P.E.
Regional Manager
AGRU America, Inc.

Mobile: (502) 797-9301
Fax: (843) 527-2738
500 Garrison Road
Georgetown, SC 29440
agruamerica.com

From: Beben, David [mailto:DBeben@scsengineers.com]
Sent: Wednesday, January 6, 2021 2:03 PM
To: Mike Gnau <MGnau@AgruAmerica.com>
Cc: Radford, Mike <MRadford@scsengineers.com>; Chris Eichelberger <CEichelberger@AgruAmerica.com>
Subject: RE: Marion County

Mike – what are the creep reduction factors you specify for the 250 and 300 mil geocomposites?

From: Mike Gnau <MGnau@AgruAmerica.com>
Sent: Tuesday, November 3, 2020 9:51 AM
To: Beben, David <DBeben@scsengineers.com>
Cc: Radford, Mike <MRadford@scsengineers.com>; Chris Eichelberger <CEichelberger@AgruAmerica.com>
Subject: RE: Marion County

Good morning, David.

Below are recommended transmissivity values based on the conditions outlined:

- 8/250/8 – 4.5 x 10^{-4} m^2/sec
- 8/300/8 – 1.2 x 10^{-3} m^2/sec

Attachment 3

Soil Properties

Soil Mechanics

T. William Lambe • Robert V. Whitman

Massachusetts Institute of Technology

1969

JOHN WILEY & SONS, New York • Chichester • Brisbane • Toronto • Singapore

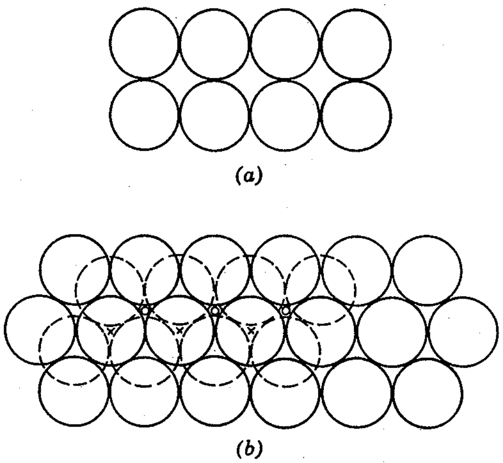

Fig. 3.2 Arrangements of uniform spheres. (*a*) Plan and elevation view: simple cubic packing. (*b*) Plan view: dense packing. Solid circles, first layer; dashed circles, second layer; ∘, location of sphere centers in third layer: face-centered cubic array; ×, location of sphere centers in third layer: close-packed hexagonal array. (From Deresiewicz, 1958.)

these simple packings can be computed from the geometry of the packings, and the results are given in Table 3.2.

This table also gives densities for some typical granular soils in both the "dense" and "loose" states. A variety of tests have been proposed to measure the maximum and

Table 3.2 Maximum and Minimum Densities for Granular Soils

Description	Void Ratio		Porosity (%)		Dry Unit Weight (pcf)	
	e_{max}	e_{min}	n_{max}	n_{min}	$\gamma_{d\,min}$	$\gamma_{d\,max}$
Uniform spheres	0.92	0.35	47.6	26.0	—	—
Standard Ottawa sand	0.80	0.50	44	33	92	110
Clean uniform sand	1.0	0.40	50	29	83	118
Uniform inorganic silt	1.1	0.40	52	29	80	118
Silty sand	0.90	0.30	47	23	87	127
Fine to coarse sand	0.95	0.20	49	17	85	138
Micaceous sand	1.2	0.40	55	29	76	120
Silty sand and gravel	0.85	0.14	46	12	89	146

138 pcf

B. K. Hough, *Basic Soils Engineering*. Copyright © 1957, The Ronald Press Company, New York.

minimum void ratios (Kolbuszewski, 1948). The test to determine the maximum density usually involves some form of vibration. The test to determine minimum density usually involves pouring oven-dried soil into a container. Unfortunately, the details of these tests have not been entirely standardized, and values of the maximum density and minimum density for a given granular soil depend on the procedure used to determine them. By using special measures, one can obtain densities greater than the so-called maximum density. Densities considerably less than the so-called minimum density can be obtained, especially with very fine sands and silts, by slowly sedimenting the soil into water or by fluffing the soil with just a little moisture present.

The smaller the range of particle sizes present (i.e., the more nearly uniform the soil), the smaller the particles, and the more angular the particles, the smaller the minimum density (i.e., the greater the opportunity for building a loose arrangement of particles). The greater the range of particle sizes present, the greater the maximum density (i.e., the voids among the larger particles can be filled with smaller particles).

A useful way to characterize the density of a natural granular soil is with *relative density* D_r, defined as

$$D_r = \frac{e_{max} - e}{e_{max} - e_{min}} \times 100\% = \frac{\gamma_{d\,max}}{\gamma_d} \times \frac{\gamma_d - \gamma_{d\,min}}{\gamma_{d\,max} - \gamma_{d\,min}} \times 100\% \tag{3.1}$$

where

e_{min} = void ratio of soil in densest condition
e_{max} = void ratio of soil in loosest condition
e = in-place void ratio
$\gamma_{d\,max}$ = dry unit weight of soil in densest condition
$\gamma_{d\,min}$ = dry unit weight of soil in loosest condition
γ_d = in-place dry unit weight

Table 3.3 characterizes the density of granular soils on the basis of relative density.

Table 3.3 Density Description

Relative Density (%)	Descriptive Term
0–15	Very loose
15–35	Loose
35–65	Medium
65–85	Dense
85–100	Very dense

Values of water content for natural granular soils vary from less than 0.1% for air-dry sands to more than 40% for saturated, loose sand.

Typical Values of Phase Relationships for Cohesive Soils

The range of values of phase relationships for cohesive soils is much larger than for granular soils. Saturated sodium montmorillonite at low confining pressure can exist at a void ratio of more than 25; saturated clays

Attachment 4

Factor of Safety

$$k_{LTIS} = \frac{k_{measured}}{\prod(RF)} = \frac{k_{measured}}{RF_{PC} \times RF_{CC} \times RF_{BC}} \tag{15}$$

where: k_{LTIS} = long-term-in-soil hydraulic conductivity of the granular material, i.e. hydraulic conductivity of the granular material located in the soil and subjected to conditions that can cause the development of clogging during the design life of the liquid collection layer; and $k_{measured}$ = hydraulic conductivity of a specimen of granular material representative of the granular material as installed, measured in a hydraulic conductivity test performed with water during a short period of time so that clogging does not develop.

1.7.4 *Factor of Safety*

In addition to the reduction factors described in Sections 1.7.2 and 1.7.3, a factor of safety, *FS*, is used in all calculations to take into account possible uncertainties, such as the fact that the measurement of hydraulic characteristics (i.e. hydraulic conductivity and hydraulic transmissivity) is generally delicate and prone to errors. Values such as 2 or 3, or sometimes greater values, are typically recommended for the factor of safety.

In the equations provided in the present paper, there are two ways of using a factor of safety. The factor of safety can be applied to the maximum liquid thickness, FS_T, or to the relevant hydraulic characteristic, FS_H, i.e. the hydraulic transmissivity in the case of a geosynthetic liquid collection layer or the hydraulic conductivity in the case of a granular liquid collection layer. The two ways (factor of safety on the maximum liquid thickness and factor of safety on the hydraulic characteristic) will be compared.

It is important to note that FS_T and FS_H are not partial factors of safety to be used simultaneously. They are two ways of expressing the factor of safety of the liquid collection layer.

1.7.5 *Use of Reduction Factors and Factor of Safety*

As indicated in Section 1.3, there are two design approaches: the thickness approach (described in Section 3) that consists of calculating the maximum liquid thickness, and the hydraulic characteristic approach (described in Section 4) that consists of calculating the required hydraulic conductivity of the liquid collection layer material or the hydraulic transmissivity of the liquid collection layer. Use of the reduction factors in these two approaches is described in Section 3 for the thickness approach and in Section 4 for the hydraulic characteristic approach.

1.8 Design Options

The flow capacity of a liquid collection layer depends on two sets of characteristics: the intrinsic characteristics of the liquid collection layer and the characteristics of the slope on which the liquid collection layer is installed. The intrinsic characteristics are the thickness of the liquid collection layer and the hydraulic conductivity of the liquid collection layer material (or the hydraulic transmissivity of the liquid collection layer, which is the product of the thickness and hydraulic conductivity). The characteristics

CLIENT	PROJECT	JOB NO.
Hillsborough County	Southeast County Landfill	09215600.13

SUBJECT	BY	DATE
Geotextile Calculations	FCH	11/12/2021
Phase I - VI Closure - 5% Slope	CHECKED	DATE
	KLS	11/18/2021

OBJECTIVE: Calculate if the geotextile specified within the project has sufficient drainage characteristics to allow liquid to pass through. The geotextile functions as a filter to prevent adjacent particles from washing through the geotextile. The following calculations determine acceptable parameters for the protective cover based on the proposed geotextile to demonstrate that retention criterion is met.

REFERENCES:

1. Attachment 1 - Geotextile Data
2. Attachment 2 - Landfill Design and Construction
3. Attachment 3 - Grain Size Distribution
4. Attachment 4 - Coefficient of Uniformity
5. Attachment 5 - Geotextile Thickness
6. Attachment 6 - Liquid Collection Systems
7. Attachment 7 - Darcy's Law
8. Attachment 8 - Transmissivity Calculations
9. Attachment 9 - Aggregates
10. Attachment 10 - CAT Tire Pressure
11. Attachment 11 - Designing with Geosynthetics

CLIENT	PROJECT	JOB NO.
Hillsborough County	Southeast County Landfill	09215600.13

SUBJECT	BY	DATE
Geotextile Calculations	FCH	11/12/2021
Phase I - VI Closure - 5% Slope	CHECKED	DATE
	KLS	11/18/2021

OBJECTIVE: Calculate if the geotextile specified within the project has sufficient drainage characteristics to allow liquid to pass through. The geotextile functions as a filter to prevent adjacent particles from washing through the geotextile. The following calculations determine acceptable parameters for the protective cover based on the proposed geotextile to demonstrate that retention criterion is met.

Material: 6-oz. non-woven geotextile

Specification AOS = Apparent opening size = 0.212 mm   Refer to Attachment 1

Calculate the linear coefficient of uniformity, C_u', from soil particle size distribution and compare to Giroud's retention criterion.

$C_u'_{\text{drainage layer}} = (d'_{100} / d'_0)^{1/2}$ Refer to Attachment 2, Eq. 1

$C_u'_{\text{drainage layer}}$ = linear coefficient of uniformity of the protective cover

d'_{100} = linear projection of the 100% passing of the protective cover particle size distribution

d'_0 = linear projection of the 0% passing of the soil particles size distribution

Table 1. Giroud's Retention Criterion for Geotextile Filters (for dense soil)   Refer to Attachment 2, Table 1

Linear coefficient of uniformity, C_u'	Retention Criterion (dense soil)
$1 < C_u'_{\text{protective cover}} < 3$	$AOS_{\text{geotextile}} < 2 \times C_u'_{\text{protective cover}} \times d'_{50}$
$C_u'_{\text{protective cover}} > 3$	$AOS_{\text{geotextile}} < (18/C_u'_{\text{protective cover}}) \times d'_{50}$

Note, the data provided below is for the protective cover soil that should be used.

The Geotextile Technical Specification requires the proposed material to be tested before placement to ensure the above stated retention criterion is met. Refer to Attachment 3 for Grain Size Distribution of material used.

Sieve No.	(mm)	% Passing
4	4.75	100%
30	0.595	95%
50	0.300	65%
70	0.210	20%
200	0.074	8%

Soil Densities					
Loose		Medium		Dense	
AOS < (9/C'u)(d'50)		AOS < (13.5/C'u)(d'$_{50}$)		AOS < (18/C'u)(d'$_{50}$)	
AOS	(9/C'u)(d'50)	AOS	(13.5/C'u)(d'50)	AOS	(18/C'u)(d'50)
0.212	0.782	0.212	1.173	0.212	1.564
OK		OK		OK	

6 oz nonwoven needlepunched geotextile is applicable for the retainage of the given soil when the relative density is loose, medium or dense.

d_{10} =	0.09
d_{30} =	0.25
d_{50} =	0.28
d_{60} =	0.29

Refer to Attachment 3

Since d_{10} >0.074 mm and d_{10} < 4.75 mm, soil is less than 10% fines and less than 90% gravel. The application is retention.

$$C_u'_{\text{drainage layer}} = \frac{d_{60}}{d_{10}} = 3.22$$

$C_u'_{\text{drainage layer}} > 3$ => Non-Uniformly Graded

Refer to Attachment 4

Therefore, the geotextile retention criterion should be as follows:

$AOS_{\text{geotextile}}$ = 1.564 mm $AOS_{\text{specification}}$ = 0.212 mm

$AOS_{\text{geotextile}}$ > $AOS_{\text{specification}}$

The retention criterion is met for the calculations provided.

CLIENT	PROJECT	JOB NO.
Hillsborough County	Southeast County Landfill	09215600.13

SUBJECT	BY	DATE
Geotextile Calculations	FCH	11/12/2021
Phase I - VI Closure - 5% Slope	CHECKED	DATE
	KLS	11/18/2021

PERMEABILITY:

The criterion for geotextile permeability with respect to the overlying protective cover soil layer extablished by Giroud is as follows.

$k_g > i_s \times k_s$ — Refer to Attachment 2, Eq. 3

k_g = geotextile hydraulic conductivity

i_s = hydraulic gradient in protective cover next to the geotextile

k_s = hydraulic conductivity of protective cover

Calculate the geotextile hydraulic conductivity.

$k_g = \Psi_{ult} \times t_g$ — Refer to Attachment 2, Eq. 6

k_g = geotextile hydraulic conductivity			
Ψ_g = geotextile permittivity =	1.5	sec^{-1}	Refer to Attachment 1
$t_{initial}$ = initial geotextile thickness =	80.00	mils	Refer to Attachment 5
=	0.203	cm	
$RF_{thickness}$ = Thickness Reduction Factor =	2.9		Refer to Attachment 6
t_g = geotextile thickness under load =	0.0701	cm	
i_s = protective cover hydraulic gradient =	1.00		Refer to Attachment 2
k_s = soil hydraulic conductivity =	0.0005	cm/sec	Refer to Technical Specifications Section 02220
$k_g = \Psi_g \times t_g$ =	0.105	cm/sec	
$i_s \times k_s$ =	0.0005	cm/sec	

k_g = 0.105 > $i_s \times k_s$ = 0.0005

The geotextile has a higher hydraulic conductivity than the overlying soil by of Factor of Safety of:

FS = 210.2

Evaluate the geotextile permeability with respect to expected peak flow rates using Darcy's Law and incorporating reduction factors for soil clogging, intrusion, creep reduction, chemical clogging, and biological clogging.

Establish the ultimate flow rate of the geotextile under the peak load.

$q_{ultimate} = k_g \times i_s \times A_g$ — Refer to Attachment 7

$q_{ultimate}$ = ultimate flow rate			
k_g = geotextile hydraulic conductivity =	0.105	cm/sec	
=	0.0034	ft/sec	
i_s = protective cover hydraulic gradient =	1.00		Refer to Attachment 2
Pg = Perimeter of geotextile (available flow area) =	4.00	in	For composite drain, depth equals pipe diameter
Pg = Perimeter of geotextile =	0.33	ft	
$Length_{pipe}$ =	109	ft	1 AC/400 feet slope length
A_g = area of geotextile available for flow =	36.30	ft^2	(A_g = Perimeter x Length)

$q_{ultimate} = k_g \times i_s \times A_g$ = 0.1 ft^3/sec

SCS ENGINEERS

CLIENT	PROJECT	JOB NO.
Hillsborough County	Southeast County Landfill	09215600.13

SUBJECT	BY	DATE
Geotextile Calculations	FCH	11/12/2021
Phase I - VI Closure - 5% Slope	CHECKED	DATE
	KLS	11/18/2021

Calculate the long-term maximum allowable flow rate (q_{allow}) for the specified geotextile.

$$q_{allow} = q_{ultimate}\left\{\frac{1}{RF_{SC} \times RF_{CR} \times RF_{IN} \times RF_{CC} \times RF_{BC}}\right\}$$

Refer to Attachment 8

q_{allow} = allowable flow rate			
$q_{ultimate}$ = ultimate flow rate	0.1	ft^3/sec	
RF_{SC} = reduction factor for soil clogging =	1.00		Refer to Attachment 8
RF_{CR} = reduction factor for creep reduction =	1.01		Refer to Attachment 8
RF_{IN} = reduction factor for intrusion =	1.00		Refer to Attachment 8
RF_{CC} = reduction factor for chemical clogging =	1.00		Refer to Attachment 8
RF_{BC} = reduction factor for biological clogging =	1.35		Refer to Attachment 8
ΣRF = product of reduction factors =	1.36		

q_{allow} = 0.09 ft^3/sec

Evaluate the factor of safety against insufficient permeability by comparing the q_{allow} with the peak predicted from the HELP model analyses:

$FS = q_{allow} / q_{peak}$

q_{allow} =	0.09	ft^3/sec
q_{peak} = HELP Model peak daily flow rate =	5,406	ft^3/day
=	0.06	ft^3/sec
$FS = q_{allow} / q_{peak}$ =	1.5	

Since FS > 1

The proposed geotextile for use safisfies the permeability criterion.

Establish if the specified geotextile requirements meet the minimum survivability requirements for construction stresses as suggested by Giroud (2000):

Table 3. Giroud's Geotextile Filter Survivability Requirements   Refer to Attachment 2

Property	ASTM Test Method	Recommended Value		Specification Value*	
Grab Strength	D4632	180	lbs	170	lbs
Tear Strength	D4533	50	lbs	65	lbs
Puncture Strength	D6241	80	lbs	435	lbs

* Refer to Attachment 1

The geotextile specification requirements meet the survivability requirements for construction stresses as suggested by Giroud (2000) or are calculated to meet an appropriate factor of safety.

SCS ENGINEERS

CLIENT	PROJECT	JOB NO.
Hillsborough County	Southeast County Landfill	09215600.13

SUBJECT	BY	DATE
Geotextile Calculations	FCH	11/12/2021
Phase I - VI Closure - 5% Slope	CHECKED	DATE
	KLS	11/18/2021

Calculate if the requirements of the geotextile specification meet the minimum grab resistance strength, tear resistance strength, and puncture strength requirements for construction stresses with acceptable factors of safety:

Construction stresses

d_a = average gravel diameter =	0.5	inches	Refer to Attachment 9
=	12.7	mm	
p' = applied construction pressure =	5,040	psf	Refer to Attachment 10
f(ε) = geotextile strain function =	0.33		Refer to Attachment 11
FS =	2.0		
$RF_{tensile}$ = cumulative grab tensile strength reduction factor =	1.5		
$RF_{puncture}$ = cumulative puncture resistance reduction factor =	2.0		

Establish the FS for grab tensile strength

$T_{required} = p'd_v^2\{f(\varepsilon)\}$ Refer to Attachment 11, Eq. 29

d_v = maximum void diameter = $0.33d_a$ =	0.0042	m	
Convert Pressure (kPa) =	psf*0.04788		
p' = applied construction pressure =	241.315	kPa	
f(ε) = geotextile strain function =	0.33		
$T_{required}$ =	0.0014	$kPa\text{-}m^2$	
=	0.32	lbs	

$T_{allow} = T_{ult} / RF_{tensile}$

T_{ult} = specified grab strength =	170.0	lbs	
$RF_{tensile}$ = cumulative grab tensile strength reduction factor =	1.5		Refer to Attachment 11
T_{allow} =	113.3	lbs	
FS = $T_{allow} / T_{required}$ =	356.8		Refer to Attachment 11

Since FS > 2 OK

Under the given conditions, the specified geotextile satisfies the grab tensile strength requirement.

Secondary check (using tire inflation pressure):

$T_{required} = p'd_v^2\{f(\varepsilon)\}$

Max. recommended pressure =	35.0	psi	
p' = tire inflation pressure =	5,040	psf	
	241.3	kPa	Refer to Attachment 10
$T_{required}$ =	0.0014	$kPa\text{-}m^2$	
=	0.32	lbs	

$T_{allow} = T_{ult} / RF_{tensile}$

T_{allow} =	113.3	lbs
FS = $T_{allow} / T_{required}$ =	356.8	

FS > 2 Ok

SCS ENGINEERS

		SHEET 6	OF 6
CLIENT Hillsborough County	PROJECT Southeast County Landfill	JOB NO. 09215600.13	
SUBJECT Geotextile Calculations Phase I - VI Closure - 5% Slope		BY FCH	DATE 11/12/2021
		CHECKED KLS	DATE 11/18/2021

Calculate the FS for puncture resistance force

$F_{required} = p'd_a^2S_1S_2S_3$ Refer to Attachment 11

p' = applied construction pressure =	241.315	kPa	
=	2.41E+05	Pa	
d_a = average gravel diameter =	12.70	mm	
=	0.01	m	
d_{probe} = diameter of probe used for ASTM D4833 =	8.0	mm	
S_1 = protusion factor = h_h / d_a =	1.00		Worst case scenario: $h_h=d_a$
S_2 = scale factor to adjust to ASTM D4833 = d_{probe} / d_a =	0.63		Refer to Attachment 11
S_3 = shape factor to adjust to ASTM D4833 = $1 - A_p / A_c$ =	0.70		
$F_{required}$ =	17.2	N	
=	3.9	lbs	

$F_{allow} = F_{ult} / RF_{puncture}$

F_{ult} = specified puncture strength =	435.0	lbs	
$RF_{puncture}$ = cumulative puncture resistance reduction factor =	2.0		
F_{allow} =	217.5	lbs	
FS = $F_{allow} / F_{required}$ =	56.4		Refer to Attachment 11

Since FS > 2 OK

Under the given conditions, the specified geotextile satisfies the puncture resistance force requirement.

Secondary check (using tire inflation pressure)

$F_{required} = p'd_a^2S_1S_2S_3$

p' = tire inflation pressure =	241.32	kPa
$F_{required}$ =	17.2	N
	3.9	lbs

$F_{allow} = F_{ult} / RF_{puncture}$

F_{ult} = specified puncture strength =	435.0	lbs
F_{allow} =	217.5	lbs
FS = $F_{allow} / F_{required}$ =	56.4	

FS > 2 Ok

Conclusion:

Analysis	Calculated FS
Hydraulic Conductivity	210.2
Permeability	1.5
Grap Tensile Resistence	356.8
Puncture Resistence	56.4

Based upon the results of the previous analysis, the geotextile will provide adequate flow from composite into the composite drains and protections for the underlying geomembrane liner.

Analysis of the specified geotextile was performed with consideration of the actual boundary conditions. Appropriate reduction factors were accounted for in the analyses. Particle sizes and other data were based on the materials presented in the project specifications.

CLIENT	PROJECT	JOB NO.
Hillsborough County	Southeast County Landfill	09215600.13

SUBJECT	BY	DATE
Geotextile Calculations	FCH	11/12/2021
Phase I - VI Closure - 25% Slope	CHECKED	DATE

OBJECTIVE: Calculate if the geotextile specified within the project has sufficient drainage characteristics to allow liquid to pass through. The geotextile functions as a filter to prevent adjacent particles from washing through the geotextile. The following calculations determine acceptable parameters for the protective cover based on the proposed geotextile to demonstrate that retention criterion is met.

REFERENCES:

1. Attachment 1 - Geotextile Data
2. Attachment 2 - Landfill Design and Construction
3. Attachment 3 - Grain Size Distribution
4. Attachment 4 - Coefficient of Uniformity
5. Attachment 5 - Geotextile Thickness
6. Attachment 6 - Liquid Collection Systems
7. Attachment 7 - Darcy's Law
8. Attachment 8 - Transmissivity Calculations
9. Attachment 9 - Aggregates
10. Attachment 10 - CAT Tire Pressure
11. Attachment 11 - Designing with Geosynthetics

CLIENT	PROJECT	JOB NO.
Hillsborough County	Southeast County Landfill	09215600.13

SUBJECT	BY	DATE
Geotextile Calculations	FCH	11/12/2021
Phase I - VI Closure - 25% Slope	CHECKED	DATE

OBJECTIVE: Calculate if the geotextile specified within the project has sufficient drainage characteristics to allow liquid to pass through. The geotextile functions as a filter to prevent adjacent particles from washing through the geotextile. The following calculations determine acceptable parameters for the protective cover based on the proposed geotextile to demonstrate that retention criterion is met.

Material: 6-oz. non-woven geotextile

Specification AOS = Apparent opening size = 0.212 mm — Refer to Attachment 1

Calculate the linear coefficient of uniformity, C_u', from soil particle size distribution and compare to Giroud's retention criterion.

$C_u'_{\text{drainage layer}} = (d'_{100} / d'_0)^{1/2}$ — Refer to Attachment 2, Eq. 1

$C_u'_{\text{drainage layer}}$ = linear coefficient of uniformity of the protective cover

d'_{100} = linear projection of the 100% passing of the protective cover particle size distribution

d'_0 = linear projection of the 0% passing of the soil particles size distribution

Table 1. Giroud's Retention Criterion for Geotextile Filters (for dense soil) — Refer to Attachment 2, Table 1

Linear coefficient of uniformity, C_u'	Retention Criterion (dense soil)
$1 < C_u'_{\text{protective cover}} < 3$	$AOS_{\text{geotextile}} < 2 \times C_u'_{\text{protective cover}} \times d'_{50}$
$C_u'_{\text{protective cover}} > 3$	$AOS_{\text{geotextile}} < (18/C_u'_{\text{protective cover}}) \times d'_{50}$

Note, the data provided below is for the protective cover soil that should be used.

The Geotextile Technical Specification requires the proposed material to be tested before placement to ensure the above stated retention criterion is met. Refer to Attachment 3 for Grain Size Distribution of material used.

Sieve No.	(mm)	% Passing
4	4.75	100%
30	0.595	95%
50	0.300	65%
70	0.210	20%
200	0.074	8%

Soil Densities					
Loose		Medium		Dense	
AOS < (9/C'u)(d'50)		AOS < (13.5/C'u)(d'_{50})		AOS < (18/C'u)(d'_{50})	
AOS	(9/C'u)(d'50)	AOS	(13.5/C'u)(d'50)	AOS	(18/C'u)(d'50)
0.212	0.902	0.212	1.353	0.212	1.804
OK		OK		OK	

6 oz nonwoven needlepunched geotextile is applicable for the retainage of the given soil when the relative density is loose, medium or dense.

d_{10} =	0.09
d_{30} =	0.25
d_{50} =	0.28
d_{60} =	0.29

Refer to Attachment 3

Since d_{10} >0.074 mm and d_{10} < 4.75 mm, soil is less than 10% fines and less than 90% gravel. The application is retention.

$$C_u'_{\text{drainage layer}} = \frac{d_{60}}{d_{10}} = 3.22$$

$C_u'_{\text{drainage layer}} > 3$ => Non-Uniformly Graded

Refer to Attachment 4

Therefore, the geotextile retention criterion should be as follows:

$AOS_{\text{geotextile}}$ = 1.564 mm $\qquad AOS_{\text{specification}}$ = 0.212 mm

$AOS_{\text{geotextile}} > AOS_{\text{specification}}$

The retention criterion is met for the calculations provided.

SCS ENGINEERS			
		SHEET 3	OF 6
CLIENT Hillsborough County	PROJECT Southeast County Landfill	JOB NO. 09215600.13	
SUBJECT Geotextile Calculations Phase I - VI Closure - 25% Slope		BY FCH	DATE 11/12/2021
		CHECKED 0	DATE 1/0/1900

PERMEABILITY:

The criterion for geotextile permeability with respect to the overlying protective cover soil layer extablished by Giroud is as follows.

$k_g > i_s \times k_s$ — Refer to Attachment 2, Eq. 3

k_g = geotextile hydraulic conductivity
i_s = hydraulic gradient in drainage soil next to the geotextile
k_s = hydraulic conductivity of protective cover

Calculate the geotextile hydraulic conductivity.

$k_g = \Psi_{ult} \times t_g$ — Refer to Attachment 2, Eq. 6

k_g = geotextile hydraulic conductivity			
Ψ_g = geotextile permittivity =	1.5	sec^{-1}	Refer to Attachment 1
$t_{initial}$ = initial geotextile thickness =	80.00	mils	Refer to Attachment 5
=	0.203	cm	
$RF_{thickness}$ = Thickness Reduction Factor =	2.9		Refer to Attachment 6
t_g = geotextile thickness under load =	0.0701	cm	
i_s = protective cover hydraulic gradient =	1.00		Refer to Attachment 2
k_s = soil hydraulic conductivity =	0.0005	cm/sec	Refer to Technical Specifications Section 02220
$k_g = \Psi_g \times t_g$ =	0.105	cm/sec	
$i_s \times k_s$ =	0.0005	cm/sec	

k_g = 0.105 > $i_s \times k_s$ = 0.0005

The geotextile has a higher hydraulic conductivity than the overlying soil by of Factor of Safety of:

FS = 210.2

Evaluate the geotextile permeability with respect to expected peak flow rates using Darcy's Law and incorporating reduction factors for soil clogging, intrusion, creep reduction, chemical clogging, and biological clogging.

Establish the ultimate flow rate of the geotextile under the peak load.

$q_{ultimate} = k_g \times i_s \times A_g$ — Refer to Attachment 7

$q_{ultimate}$ = ultimate flow rate			
k_g = geotextile hydraulic conductivity =	0.105	cm/sec	
=	0.0034	ft/sec	
i_s = protective cover hydraulic gradient =	1.00		Refer to Attachment 2
Pg = Perimeter of geotextile (available flow area) =	4.00	in	For composite drain, depth equals pipe diameter
Pg = Perimeter of geotextile =	0.33	ft	
$Length_{pipe}$ =	363	ft	1 AC/120 feet slope length
A_g = area of geotextile available for flow =	121.00	ft^2	(A_g = Perimeter x Length)

$q_{ultimate} = k_g \times i_s \times A_g$ = 0.4 ft^3/sec

CLIENT	PROJECT	JOB NO.
Hillsborough County	Southeast County Landfill	09215600.13

SUBJECT	BY	DATE
Geotextile Calculations	FCH	11/12/2021
Phase I - VI Closure - 25% Slope	CHECKED	DATE
	0	1/0/1900

Calculate the long-term maximum allowable flow rate (q_{allow}) for the specified geotextile.

$$q_{allow} = q_{ultimate} \left\{ \frac{1}{RF_{SC} \times RF_{CR} \times RF_{IN} \times RF_{CC} \times RF_{BC}} \right\}$$

Refer to Attachment 8

q_{allow} = allowable flow rate			
$q_{ultimate}$ = ultimate flow rate	0.4	ft^3/sec	
RF_{SC} = reduction factor for soil clogging =	1.00		Refer to Attachment 8
RF_{CR} = reduction factor for creep reduction =	1.01		Refer to Attachment 8
RF_{IN} = reduction factor for intrusion =	1.00		Refer to Attachment 8
RF_{CC} = reduction factor for chemical clogging =	1.00		Refer to Attachment 8
RF_{BC} = reduction factor for biological clogging =	1.35		Refer to Attachment 8
ΣRF = product of reduction factors =	1.36		

q_{allow} = 0.31 ft^3/sec

Evaluate the factor of safety against insufficient permeability by comparing the q_{allow} with the peak predicted from the HELP model analyses:

$FS = q_{allow} / q_{peak}$

q_{allow} =	0.31	ft^3/sec
q_{peak} = HELP Model peak daily flow rate =	5,191	ft^3/day
=	0.06	ft^3/sec
$FS = q_{allow} / q_{peak}$ =	5.1	

Since FS > 1

The proposed geotextile for use safisfies the permeability criterion.

Establish if the specified geotextile requirements meet the minimum survivability requirements for construction stresses as suggested by Giroud (2000):

Table 3. Giroud's Geotextile Filter Survivability Requirements — Refer to Attachment 2

Property	ASTM Test Method	Recommended Value		Specification Value*	
Grab Strength	D4632	180	lbs	170	lbs
Tear Strength	D4533	50	lbs	65	lbs
Puncture Strength	D6241	80	lbs	435	lbs

* Refer to Attachment 1

The geotextile specification requirements meet the survivability requirements for construction stresses as suggested by Giroud (2000) or are calculated to meet an appropriate factor of safety.

SCS ENGINEERS

SHEET 5 OF 6

CLIENT	PROJECT	JOB NO.	
Hillsborough County	Southeast County Landfill	09215600.13	
SUBJECT		BY	DATE
Geotextile Calculations		FCH	11/12/2021
Phase I - VI Closure - 25% Slope		CHECKED	DATE
		0	1/0/1900

Calculate if the requirements of the geotextile specification meet the minimum grab resistance strength, tear resistance strength, and puncture strength requirements for construction stresses with acceptable factors of safety:

Construction stresses

d_a = average gravel diameter =	0.5	inches	Refer to Attachment 9
=	12.7	mm	
p' = applied construction pressure =	5,040	psf	Refer to Attachment 10
f(ε) = geotextile strain function =	0.33		Refer to Attachment 11
FS =	2.0		
$RF_{tensile}$ = cumulative grab tensile strength reduction factor =	1.5		
$RF_{puncture}$ = cumulative puncture resistance reduction factor =	2.0		

Establish the FS for grab tensile strength

$T_{required} = p'd_v^2\{f(\varepsilon)\}$ Refer to Attachment 11, Eq. 29

d_v = maximum void diameter = $0.33d_a$ =	0.0042	m	
Convert Pressure (kPa) =	psf*0.04788		
p' = applied construction pressure =	241.315	kPa	
f(ε) = geotextile strain function =	0.33		
$T_{required}$ =	0.0014	$kPa\text{-}m^2$	
=	0.32	lbs	

$T_{allow} = T_{ult} / RF_{tensile}$

T_{ult} = specified grab strength =	170.0	lbs	
$RF_{tensile}$ = cumulative grab tensile strength reduction factor =	1.5		Refer to Attachment 11
T_{allow} =	113.3	lbs	
$FS = T_{allow} / T_{required}$ =	356.8		Refer to Attachment 11

Since FS > 2 OK

Under the given conditions, the specified geotextile satisfies the grab tensile strength requirement.

Secondary check (using tire inflation pressure):

$T_{required} = p'd_v^2\{f(\varepsilon)\}$

Max. recommended pressure =	35.0	psi	
p' = tire inflation pressure =	5,040	psf	
	241.3	kPa	Refer to Attachment 10
$T_{required}$ =	0.0014	$kPa\text{-}m^2$	
=	0.32	lbs	

$T_{allow} = T_{ult} / RF_{tensile}$

T_{allow} =	113.3	lbs
$FS = T_{allow} / T_{required}$ =	356.8	

FS > 2 Ok

CLIENT	PROJECT	JOB NO.
Hillsborough County	Southeast County Landfill	09215600.13

SUBJECT	BY	DATE
Geotextile Calculations	FCH	11/12/2021
Phase I - VI Closure - 25% Slope	CHECKED	DATE
	0	1/0/1900

Calculate the FS for puncture resistance force

$F_{required} = p'd_a^2S_1S_2S_3$ — Refer to Attachment 11

p' = applied construction pressure =	241.315	kPa	
=	2.41E+05	Pa	
d_a = average gravel diameter =	12.70	mm	
=	0.01	m	
d_{probe} = diameter of probe used for ASTM D4833 =	8.0	mm	
S_1 = protusion factor = h_h / d_a =	1.00		Worst case scenario: h_h=d_a
S_2 = scale factor to adjust to ASTM D4833 = d_{probe} / d_a =	0.63		Refer to Attachment 11
S_3 = shape factor to adjust to ASTM D4833 = 1 - A_p / A_c =	0.70		
$F_{required}$ =	17.2	N	
=	3.9	lbs	

$F_{allow} = F_{ult} / RF_{puncture}$

F_{ult} = specified puncture strength =	435.0	lbs	
$RF_{puncture}$ = cumulative puncture resistance reduction factor =	2.0		
F_{allow} =	217.5	lbs	
FS = F_{allow} / $F_{required}$ =	56.4		Refer to Attachment 11

Since FS > 2 OK

Under the given conditions, the specified geotextile satisfies the puncture resistance force requirement.

Secondary check (using tire inflation pressure)

$F_{required} = p'd_a^2S_1S_2S_3$

p' = tire inflation pressure =	241.32	kPa
$F_{required}$ =	17.2	N
	3.9	lbs

$F_{allow} = F_{ult} / RF_{puncture}$

F_{ult} = specified puncture strength =	435.0	lbs
F_{allow} =	217.5	lbs
FS = F_{allow} / $F_{required}$ =	56.4	

FS > 2 Ok

Conclusion:

Analysis	Calculated FS
Hydraulic Conductivity	210.2
Permeability	5.1
Grap Tensile Resistence	356.8
Puncture Resistence	56.4

Based upon the results of the previous analysis, the geotextile will provide adequate flow from composite into the composite drains and protections for the underlying geomembrane liner.

Analysis of the specified geotextile was performed with consideration of the actual boundary conditions. Appropriate reduction factors were accounted for in the analyses. Particle sizes and other data were based on the materials presented in the project specifications.

Attachment 1

Geotextile Data

agru
The Plastics Experts.

Geocomposite

300 MIL

AGRU America's Geocomposite Closure System is the traditional method for closures, which utilizes AGRU MicroSpike® or AGRU Smooth Liner® geomembrane, overlain by a geocomposite drainage layer, soil cover layer, and vegetative layer.

GEONET COMPONENT (1)

Property	Test Method	Frequency	Minimum Average Values
Thickness, mil (mm)	ASTM D5199	50,000 sf	300 (7.6)
Peak Tensile Strength MD, lbs./ in. (N/mm)	ASTM D5035/7179	50,000 sf	75 (13.3)
Density, g/cm³	ASTM D792, Method B	50,000 sf	0.94
Carbon Black Content (%)	ASTM D4218	50,000 sf	2 - 3
Transmissivity(2), m²/sec. (gal/min/ft)	ASTM D4716	500,000 sf	8 x 10^{-3} (38.6)

GEOTEXTILE COMPONENT (1)

Property	Test Method	Frequency	Minimum Average Values		
Mass per Unit Area, oz./sq. yd. (g/m²)	ASTM D5261	100,000 sf	6.0 (203)	8.0 (271)	10.0 (339)
Grab Tensile Strength, lbs.(N)	ASTM D4632	100,000 sf	170 (757)	220 (979)	270 (1200)
Grab Elongation, %	ASTM D4632	100,000 sf	50	50	50
Trapezoidal Tear, lbs. (N)	ASTM D4533	100,000 sf	65 (289)	95 (423)	105 (467)
CBR Puncture , lbs (N)	ASTM D6241	500,000 sf	435 (1935)	600 (2670)	725 (3230)
Permittivity(3), sec.$^{-1}$	ASTM D4491	500,000 sf	1.5	1.3	1.1
Water Flow, (3) gpm./ ft² (l/min/m²)	ASTM D4491	500,000 sf	110 (4479)	95 (3895)	80 (3280)
AOS, U.S. Sieve max (mm)(3)	ASTM D4751	500,000 sf	70 (0.212)	80 (0.180)	100 (0.150)

GEOCOMPOSITE

Property	Test Method	Frequency	Minimum Average Values		
Ply Adhesion, lbs./ in. (g/cm)	ASTM D7005	50,000 sf	1 (178)	1 (178)	1 (178)
Transmissivity (2), m²/sec. (gal/min/ft)	ASTM D4716	500,000 sf - Double	9 x 10^{-4} (4.3)	9 x 10^{-4} (4.3)	7 x 10^{-4} (3.4)
	ASTM D4716	500,000 sf - Single	3 x 10^{-3} (14.5)	3 x 10^{-3} (14.5)	2 x 10^{-3} (9.6)

SUPPLY INFORMATION

Standard Roll Length(4)	at Fabric Weight	6-oz	8-oz	10-oz
Double Sided		160	150	140
Single Sided		180	180	170

Notes:
(1) Component properties are prior to lamination
(2) Geonet & Geocomposite . Transmissivity at 21°C, gradient of 0.1, load of 10,000 psf, seat time 15 min. between steel plates.
(3) At time of manufacture. Handling may change these properties.
(4) All roll widths are 14.5 feet. All roll lengths and widths have a tolerance of ±1%
(5) UV Resistance after 500 hours for the geotextile componet exhibits 70% strength retained via ASTM D4355

AGRU America, Inc.
500 Garrison Road
Georgetown, SC 29440 USA

(800) 373-2478 | Fax: (843) 546-0516
salesmkg@agruamerica.com
Revision Date: February 23, 2018 10:07 AM

www.agruamerica.com

agru
The Plastics Experts.

Geocomposite

330 MIL

AGRU America's Geocomposite Closure System is the traditional method for closures, which utilizes AGRU MicroSpike® or AGRU Smooth Liner® geomembrane, overlain by a geocomposite drainage layer, soil cover layer, and vegetative layer.

GEONET COMPONENT (1)

Property	Test Method	Frequency	Minimum Average Values
Thickness, mil (mm)	ASTM D5199	50,000 sf	330 (8.3)
Peak Tensile Strength MD, lbs./ in. (N/mm)	ASTM D5035/7179	50,000 sf	95 (16.5)
Density, g/cm^3	ASTM D792, Method B	50,000 sf	0.94
Carbon Black Content (%)	ASTM D4218	50,000 sf	2 - 3
Transmissivity(2), m^2/sec. (gal/min/ft)	ASTM D4716	500,000 sf	9×10^{-3} (43.4)

GEOTEXTILE COMPONENT (1)

Property	Test Method	Frequency	Minimum Average Values		
Mass per Unit Area, oz./sq. yd. (g/m^2)	ASTM D5261	100,000 sf	6.0 (203)	8.0 (271)	10.0 (339)
Grab Tensile Strength, lbs.(N)	ASTM D4632	100,000 sf	170 (757)	220 (979)	270 (1200)
Grab Elongation, %	ASTM D4632	100,000 sf	50	50	50
Trapezoidal Tear, lbs. (N)	ASTM D4533	100,000 sf	65 (289)	95 (423)	105 (467)
CBR Puncture , lbs (N)	ASTM D6241	500,000 sf	435 (1935)	600 (2670)	725 (3230)
Permittivity(3), $sec.^{-1}$	ASTM D4491	500,000 sf	1.5	1.3	1.1
Water Flow, (3) gpm./ ft^2 (l/min/m^2)	ASTM D4491	500,000 sf	110 (4479)	95 (3895)	80 (3280)
AOS, U.S. Sieve max (mm)(3)	ASTM D4751	500,000 sf	70 (0.212)	80 (0.180)	100 (0.150)

GEOCOMPOSITE

Property	Test Method	Frequency	Minimum Average Values		
Ply Adhesion, lbs./ in. (g/cm)	ASTM D7005	50,000 sf	1 (178)	1 (178)	1 (178)
Transmissivity (2), m^2/sec. (gal/min/ft)	ASTM D4716	500,000 sf - Double	9×10^{-4} (4.3)	9×10^{-4} (4.3)	7×10^{-4} (3.4)
	ASTM D4716	500,000 sf - Single	3×10^{-3} (14.5)	3×10^{-3} (14.5)	2×10^{-3} (9.6)

SUPPLY INFORMATION

Standard Roll Length(4)	at Fabric Weight	6-oz	8-oz	10-oz
Double Sided		140	130	120
Single Sided		160	160	150

Notes:
(1) Component properties are prior to lamination
(2) Geonet & Geocomposite . Transmissivity at 21°C, gradient of 0.1, load of 10,000 psf, seat time 15 min. between steel plates.
(3) At time of manufacture. Handling may change these properties.
(4) All roll widths are 14.5 feet. All roll lengths and widths have a tolerance of ±1%
(5) UV Resistance after 500 hours for the geotextile componet exhibits 70% strength retained via ASTM D4355

AGRU America, Inc.
500 Garrison Road
Georgetown, SC 29440 USA

(800) 373-2478 | Fax: (843) 546-0516
salesmkg@agruamerica.com
Revision Date: February 23, 2018 10:07 AM

www.agruamerica.com

Attachment 2

Landfill Design and Construction

DESIGN EXAMPLE

GEOTEXTILE FILTER FOR A LANDFILL LEACHATE COLLECTION SYSTEM

Prepared by J.P. Giroud
GeoSyntec Consultants

DEFINITION OF THE DESIGN EXAMPLE

- Type of Structure: • Landfill leachate collection system
- Type of Application: • Geotextile filter is between the protective cover soil and the drainage medium (sand or geosyntheticsnet)
- Geosynthetic Function: Filtration
- Geosynthetic Properties: Apparent opening size (AOS), permittivity, and porosity

GIVEN DATA

- The cross section of a landfill lining system with a leachate collection system is given in Figure 1.
- The particle size distribution of the protective cover soil overlying the geotextile is given in Figure 2.
- The hydraulic conductivity of the protective cover soil is:

$k_s = 1 \times 10^{-5}$ m/s (1×10^{-3} cm/sec)

- A polyester needlepunched nonwoven geotextile filter is considered. This geotextile has the following properties:

  - Mass per unit area: 0.34 kg/m^2 (10 oz/yd^2)

  - Permittivity (measured under a compressive stress equal to the field overburden stress):

    $\psi_g = 0.3\ s^{-1}$

  - Thickness (measured under a compressive stress equal to the field overburden stress):

    $t_g = 2$ mm

  - Apparent opening size (AOS):

    $O_{95} = 150\ \mu m$ (U.S. Sieve No. 100)

  - Grab strength: 1020 N (230 lbs)

  - Tear strength: 555 N (125 lbs)

  - Puncture strength: 555 N (125 lbs)

  - Burst strength: 2,750 kPa (400 psi)

DESIGN

A geotextile filter should meet three geotextile filter criteria:

- retention criterion;
- permeability criterion; and
- porosity criterion.

In addition, survivability criteria should be met and boundary requirements dictated by the adjacent drainage material should be met.

Step 1. Retention Criterion

- Method Number 1

This method uses Giroud's retention criterion as follows:

- Trace a straight line as close as possible to the central portion of the particle size distribution curve of the soil (Figure 3).
- Read the values of d' and d'_{00} at the two extremities of this straight line.
- Calculate the linear coefficient of uniformity of the soil:

$$\boxed{C'_u = \sqrt{d'_{100} / d'_0} \qquad \text{(Equation 1)}}$$

  - Use Giroud's retention criterion given in Table 1. To use this criterion, it is necessary to know the linear coefficient of uniformity of the soil (calculated as indicated above) and the density of the soil, which the designer can estimate based on data pertinent to the project.

- Example

- First, determine the linear coefficient of uniformity. According to Figure 3:

  $d' = 0.007$ mm $\qquad d'_{00} = 17$ mm

  Hence:

  $$C'_u = \sqrt{17/0.007} = 49$$

- Then, use Giroud's retention criterion (Table 1).

  Using the linear coefficient of uniformity calculated above and considering that the protective cover soil in a landfill is dense (due to high overburden stress and assuming it has been properly compacted), Table 1 shows that the following criterion should be used:

  $$O_{95} < 18\ d_{50} / C'$$

  where: O_{95} = apparent opening size (AOS) of the filter; d_{50} = soil particle size such that 50% by weight of soil particles are smaller than d_{50}; and C' = linear coefficient of uniformity.

  With the value $C' = 49$ calculated in Step 1, the above equation becomes:

  $$O_{95} < 18\ d_{50} / 49$$

  According to Figure 2, $d_{50} = 0.47$ mm.

  Hence:

  $O_{95} < 0.17$ mm (U.S. Sieve No. 100)

  In other words, the apparent opening size (AOS) of the geotextile filter must be less than 0.17 mm (or the U.S. Sieve number used to express the geotextile filter AOS should be larger than 100). Many available nonwoven geotextiles meet this requirement.

- Method Number 2

If the retention criterion recommended by the Federal Highway Administration (FHWA) is used, the following should be done for Step 1:

- First calculate the coefficient of uniformity of the particle size distribution given in Figure 1:

$$\boxed{C_u = d_{60} / d_{10} \qquad \text{(Equation 2)}}$$

$$C_u = 1 \text{ mm} / 0.009 \text{ mm} = 111$$

- Then use the FHWA retention criterion given in Table 2.
For $C_u > 8$, the following criterion should be used:

$$O_{95} < d_{85} \quad (B = 1)$$

Hence:

$$O_{95} < 7 \text{ mm} \quad (0.275 \text{ in.})$$

In other words, according to this design method, the apparent opening size (AOS) of the geotextile filter must be less than 7 mm (0.275 in.), which is very large.

This geotextile opening size is very large and it is legitimate to fear that the overlying protective cover soil would not be retained if a geotextile filter with such large openings were used. Obtaining excessively large filter openings is a common problem when designing filters for soils with a large coefficient of uniformity. In geotechnical engineering, it is standard practice to eliminate particles coarser than 4.75 mm (U.S. Sieve No. 4) when designing filters. This practice is intended to compensate for the fact that classical filter criteria for granular filters are not applicable to soils with a large coefficient of uniformity. Similarly, the FHWA recommends that only particles smaller than 4.75 mm (U.S. Sieve No. 4) be considered when the FHWA geotextile retention criterion is used for soils having a large value of the coefficient of uniformity, C_u. If this were done with the particle size distribution curve shown in Figure 2, we would obtain the following new values for d_{100}, d_{85}, etc., as shown in Figure 5:

new $d_{100} = 4.75$ mm = actual d_{80}
new $d_{85} = 1.6$ mm = actual d_{68} (since $80\% \times 85\% = 68\%$)
new $d_{60} = 0.4$ mm = actual d_{48} (since $80\% \times 60\% = 48\%$)
new $d_{10} = 0.005$ mm = actual d_8 (since $80\% \times 10\% = 8\%$)

As a result:

new C_u = new d_{60}/new d_{10} = 0.4 / 0.005 = 80

According to Table 2, the FHWA criterion to use in this case is:

$O_{95} < d_{85}$ (using, of course, the new d_{85})

Hence:

$O_{95} < 1.6$ mm (U.S. Sieve No. 10)

In other words, according to this design method, the apparent opening size (AOS) of the geotextile filter must be less than 1.6 mm (or the U.S. Sieve number used to express the geotextile AOS should be no less than 10).

- Selected Method

The filter opening size value of 1.6 mm obtained with the second method, 1.6 mm, is very large and, in our judgment, may lead to soil piping. On the other hand, a filter with 1.6 mm openings is less likely to clog than a filter with 0.17 mm openings, as determined using the first method.

In the case of a filter used for a leachate collection system, clogging of the filter would only delay leachate collection, whereas piping would cause clogging of the leachate collection drainage layer (here, a geonet), which would severely impair leachate collection.

Therefore, the filter opening size obtained with the first method, 0.17 mm, should be selected.

<u>Step 2.</u> Permeability Criterion

- Method

The criterion established by Giroud is:

$$\boxed{k_g > i_s\, k_s \quad \text{(Equation 3)}}$$

where: k_g = geotextile hydraulic conductivity; i_s = hydraulic gradient in soil next to the geotextile filter; and k_s = soil hydraulic conductivity.

According to Giroud [1988], typical values of hydraulic gradients are as follows:

- $i_s \leq 1$ — for many cases of drainage under roads, embankments, soil layers on slopes, etc., when the main source of liquid is precipitation;
- $i_s = 1.5$ — in the case of drainage trenches, vertical drains behind walls, and leachate collection layers in waste disposal landfills;
- $i_s = 1.5$ to 2 — for toe drains in earth dams;
- $i_s = 3$ to 10 (or more) — in dam clay cores, depending on the core thickness; and
- $i_s \approx 10$ (or more) — in clay liners for liquid impoundments.

A factor of safety of 10 or more is recommended when lack of permeability of the filter could have catastrophic consequences, e.g., dams and soil layers on slopes. As a result, Equation 8 may range from $k_g > k_s$, when $i_s = 1$ and no safety factor is needed, to $k_g > 100\ k_s$ or more in the case if a very thin dam clay core.

Alternatively, the method recommended by the FHWA is as follows:

- For small gradients and stable soil:

$$k_g > k_s \text{(Equation 4)}$$

- For high gradients and erodible soils:

$$k_g > 10\ k_s \qquad \text{(Equation 5)}$$

The value of the soil hydraulic conductivity, k_g, to be used in Equations 3, 4, and 5 should be measured under a compressive stress equal to the one expected in the field. In many cases, the geotextile permittivity, ψ_g, is given. The geotextile hydraulic conductivity, k_g, can then be derived as follows:

$$\boxed{k_g = \psi_g\ t_g} \qquad \text{(Equation 6)}$$

where: t_g = geotextile thickness under the compressive stress expected in the field.

- Example

The hydraulic conductivity of the considered geotextile is given by Equation 6, using the values of $\psi_g = 0.3\ s^{-1}$ and $t_g = 2 \times 10^{-3}$ m provided in the "Given Data" Section:

$$k_g = 0.3 \times 2 \times 10^{-3} = 6 \times 10^{-4} \text{ m/s}$$

Then, Equation 3 can be used with $i_s = 1.5$, according to guidance provided after Equation 3, and $k_s = 1 \times 10^{-5}$ m/s provided in the "Given Data" Section:

$k_g > 1.5 \times 10^{-5}$ m/s (1.5×10^{-3} cm/s)

No factor of safety is necessary since lack of permeability of the filter would not have catastrophic consequences.

The method recommended by the FHWA would give a slightly different result. Since the gradient is small and assuming that the soil is not erodible, Equation 4 applies, hence:

$k > 1 \times 10^{-5}$ m/s (1×10^{-3} cm/s)

It appears that the considered geotextile filter, with its hydraulic conductivity of 6×10^{-4} m/s, satisfies the above requirements with a factor of safety of 40 (Giroud's criterion) or 40 (FHWA criterion).

<u>Step 3</u>. Porosity Criterion

- Method

To minimize the risk of clogging, the following criteria shall be met:

- Nonwoven geotextile: porosity > 30%
- Woven geotextile: percent open area > 4%

The porosity of a nonwoven geotextile can be calculated using the following equation:

$$n = 1 - \mu/(t_g \rho_f) \qquad \text{(Equation 7)}$$

where: n = geotextile porosity or planar porosity; μ = geotextile mass per unit area; t_g = geotextile thickness; and ρ_f = density of filaments. (Note: The value of n obtained using

Equation 7 must be multiplied by 100 to express the porosity of a nonwoven as a percentage or to obtain the percent open area of a woven.)

- Example

In this project, a needlepunched nonwoven geotextile is considered. Most needlepunched nonwoven geotextiles have a porosity of approximately 90%. Therefore, it is expected that the porosity requirement of 30% will easily be met. This is verified below.

The porosity of the considered nonwoven geotextile under the project overburden stress can be calculated using Equation 7, knowing that the density of polyester is 1380 kg/m^3:

$$n = 1 - 0.34/(2 \times 10^{-3} \times 1380)$$

$$n = 0.88 = 88\%$$

As expected, this value is greater than the required 30%.

<u>Step 4</u>. Survivability Requirements

- Method

The geotextile filter must withstand stresses due to construction activities. Survivability requirements that must be met by geotextiles used in drainage applications are given in Table 3.

- Example

The geotextile will be installed over the drainage medium (geonet or granular material) and covered with the protective cover soil. The protective cover soil will be compacted. Therefore the values indicated in the "Class A" column of Table 3 should be selected. The geotextile defined in the "Given Data" Section at the beginning of this design example meets all the above requirements.

Step 5. Boundary Requirements

More and more synthetic drainage materials such as geonets are used. If the geotextile filter is thick, compressible, and compliant, it may partially penetrate into the channels of the synthetic drainage layer, thereby decreasing its hydraulic transmissivity. This effect is particularly marked with needlepunched nonwoven geotextiles in contact with geonets. It is therefore important to conduct hydraulic transmissivity tests of the synthetic drainage layer with the considered geotextile in contact with it.

CONCLUSIONS

The selected geotextile filter must meet the following design and survivability requirements which were determined in this design example.

- Design Requirements

- Apparent opening size:

  $O_{95} <$ 0.17 mm (U.S. Sieve No. 100)

- Hydraulic conductivity:

  $k_g > 1 \times 10^{-5}$ m/s (1×10^{-3} cm/sec)

- Porosity:

  - nonwovens: porosity > 30%
  - wovens: percent open area > 4%

- Survivability Requirements

  - Grab strength: 800 N (180 lbs)
  - Tear strength: 220 N (50 lbs)
  - Puncture strength: 360 N (80 lbs)
  - Burst strength: 2000 kPa (290 psi)

The geotextile filter considered in the "Given Data" Section at the beginning of this design example meets all the above requirements. In addition, hydraulic transmissivity tests should be conducted on a specimen including the considered synthetic drainage layer and geotextile filter, as well as the adjacent soil, to verify that the synthetic drainage layer has the required hydraulic transmissivity with these boundary conditions. The hydraulic transmissivity test must be conducted under a compressive stress at least equal to the expected field compressive stress.

REFERENCES

FHWA, "*Geotextile Engineering Manual*", DTFH61-83-C-00150, Federal Highway Administration, Washington, D.C., Mar 1985, 917 p.

Giroud, J.P., "Filter Criteria for Geotextiles", *Proceedings, Second International Conference on Geotextiles*, Vol. 1, Las Vegas, NV, August 1982, pp. 103-108. Reproduced in Giroud, J.P., "*Geotextiles and Geomembranes. Definitions, Properties and Design*", IFAI Publishers, 1984, 325 p.

Giroud, J.P., "Review of Geotextile Filter Criteria", *Proceedings of the First Indian Geotextiles Conference*, Bombay, Dec 1988, pp. 1-6.

Table 1. *Giroud's Retention Criterion for Geotextile Filters.* [Giroud, 1982]

Density index of the soil (Relative density)		Linear coefficient of uniformity of the soil	
		$1 < C_u' < 3$	$C_u' > 3$
loose soil	$I_D < 35\%$	$O_{95} < C_u' \, d_{50}$	$O_{95} < (9/C_u') \, d_{50}$
medium dense soil	$35\% < I_D < 65\%$	$O_{95} < 1.5 \, C_u' \, d_{50}$	$O_{95} < (13.5/C_u') \, d_{50}$
dense soil	$I_D > 65\%$	$O_{95} < 2 \, C_u' \, d_{50}$	$O_{95} < (18/C_u') \, d_{50}$

Table 2. *FHWA Retention Criterion for Geotextile Filters.* [FHWA, 1985]

1. Less than 50% of the soil particles smaller than 75 micrometers (U.S. Sieve No. 200)

$O_{95} < B\ d_{85}$ (with B depending on C_u)

$C_u < 2$ $B = 1$

$2 < C_u < 4$ $B = 0.5\ C_u$

$4 < C_u < 8$ $B = 8/C_u$

$C_u > 8$ $B = 1$

2. More than 50% of the soil particles smaller than 75 micrometers (U.S. Sieve No. 200)

nonwovens: $O_{95} < 1.8\ d_{85}$

wovens: $O_{95} < d_{85}$

wovens and nonwovens: $O_{95} < 300$ microns (U.S. Sieve No. 50)

Table 3. *Geotextile Filter Survivability Requirements.* [FHWA, 1985]

Property	Class (A)	Class (B)	Test Method
Grab strength	800 N (180 lbs)	360 N (80 lbs)	ASTM D1682
Tear strength	220 N (50 lbs)	110 N (25 lbs)	ASTM D1117
Puncture strength	360 N (80 lbs)	110 N (25 lbs)	ASTM D3787
Burst strength	2000 kPa (290 psi)	900 kPa (130 psi)	ASTM D3786

(A) "Unprotected".

(B) "Protected", i.e., in trench, with rounded gravel; or in contact with concrete slab or geomembrane.

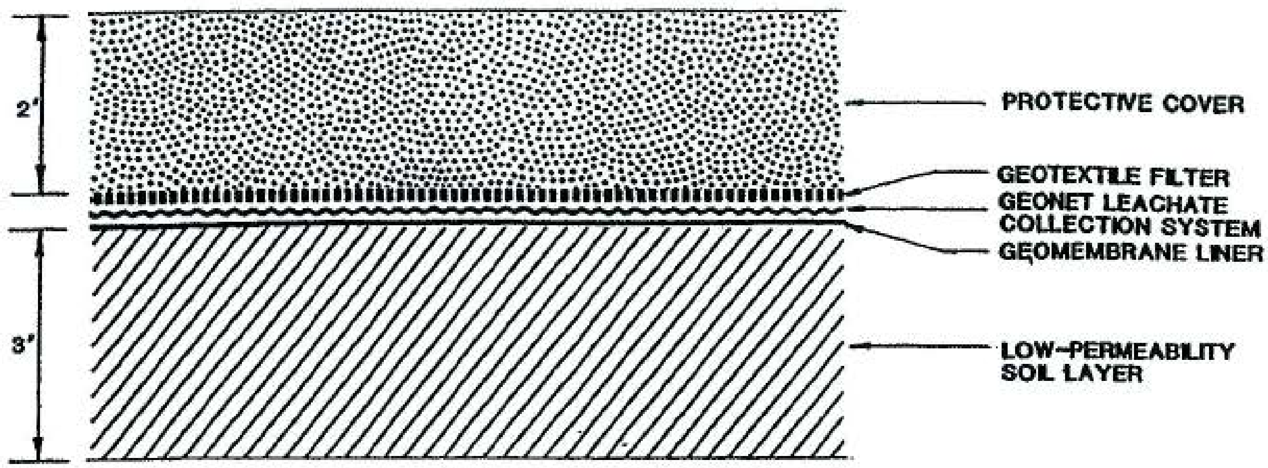

Figure 1. *Cross Section of a Landfill Lining System with a Leachate Collection* Layer.

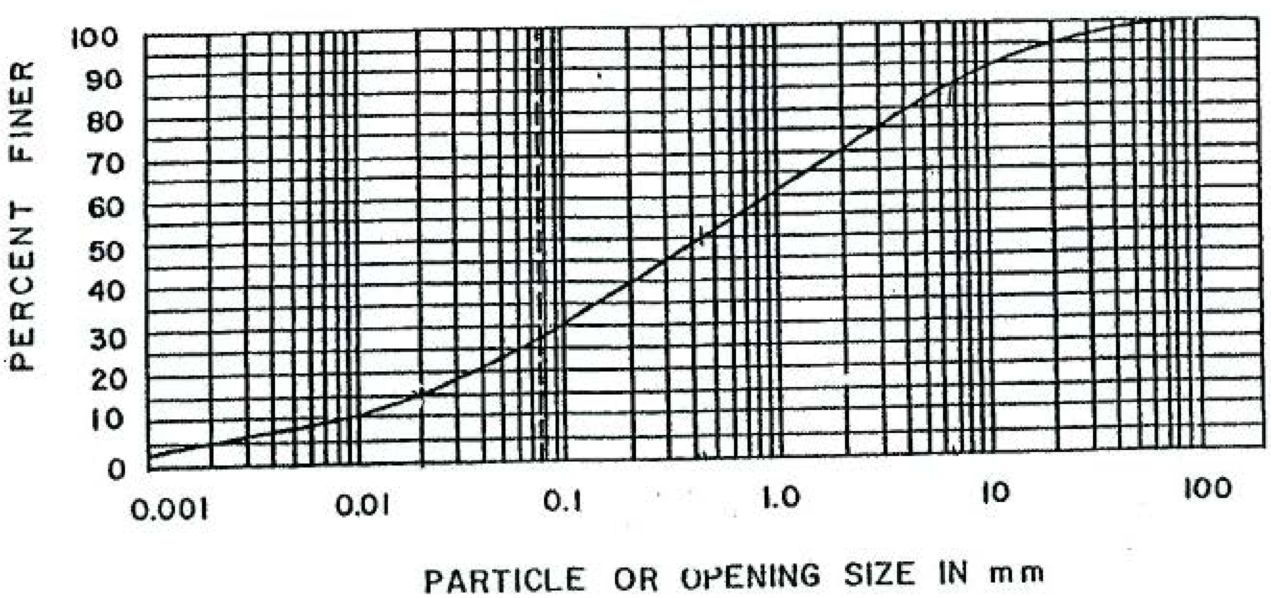

Figure 2. *Particle Size Distribution of the Protective Cover Soil.*

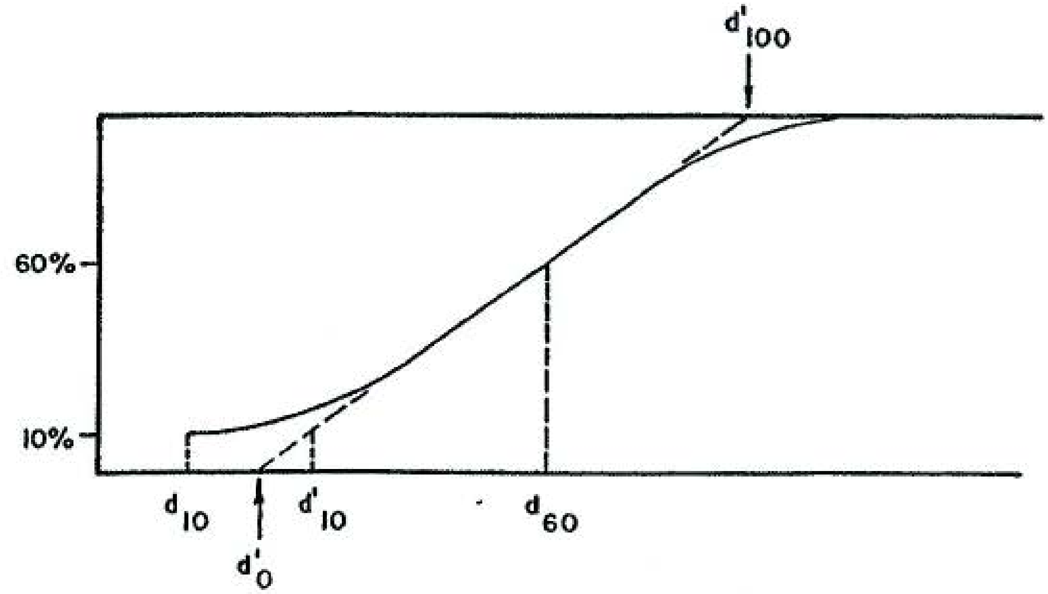

Figure 3. *Determination of the Linear Coefficient of Uniformity.*

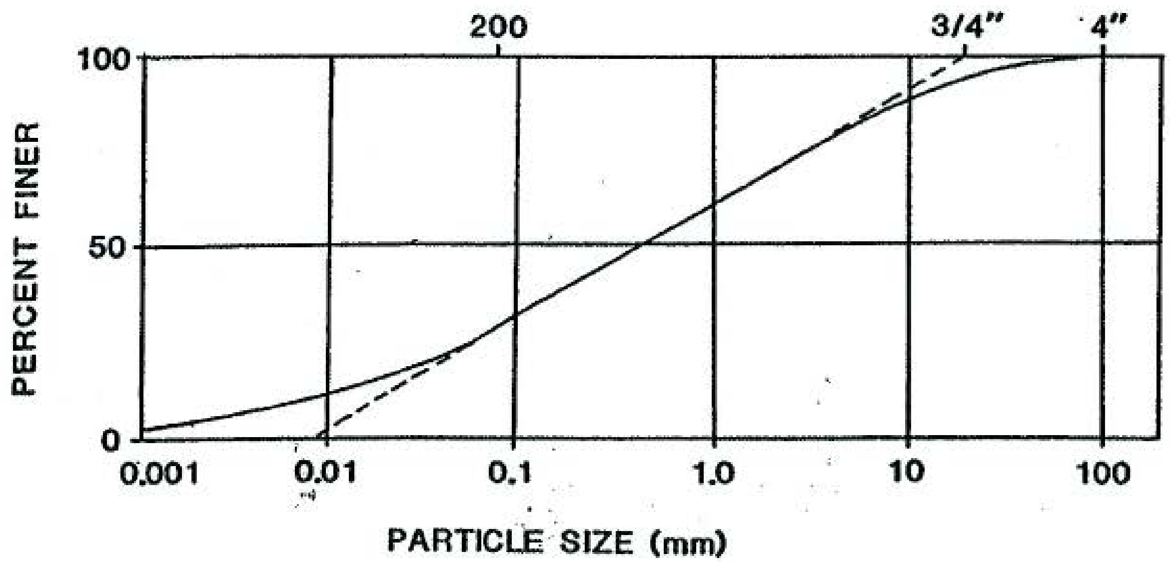

Figure 4. *Determination of the Linear Coefficient of Uniformity for the Considered Soil.*

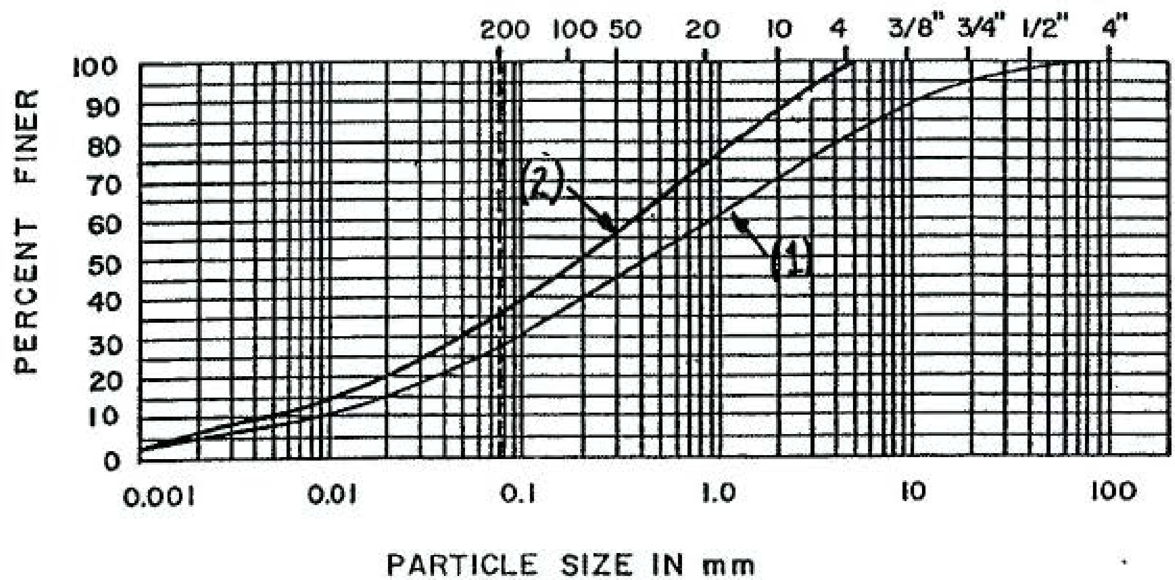

Figure 5. *Truncated Particle Size Distribution Curve.* Curve (1) is the actual curve (as shown in Figure 2) and curve (2) is the truncated curve derived from curve (1) by eliminating particles larger than 4.75 mm (U.S. Sieve No. 4).

Attachment 3

Sieve Analysis

SCS ENGINEERS

SHEET 1 OF 1

CLIENT	PROJECT	JOB NO.
Hillsborough County	Southeast County Landfill	09215600.13

SUBJECT	BY	DATE
Grain Size Distribution	FCH	10/7/2021
	CHECKED	DATE

Sieve No.	(mm)	% Passing
4	4.75	100
30	0.595	95
50	0.300	65
70	0.210	20
200	0.074	8

Refer to Division 2 Specifications Section 02220

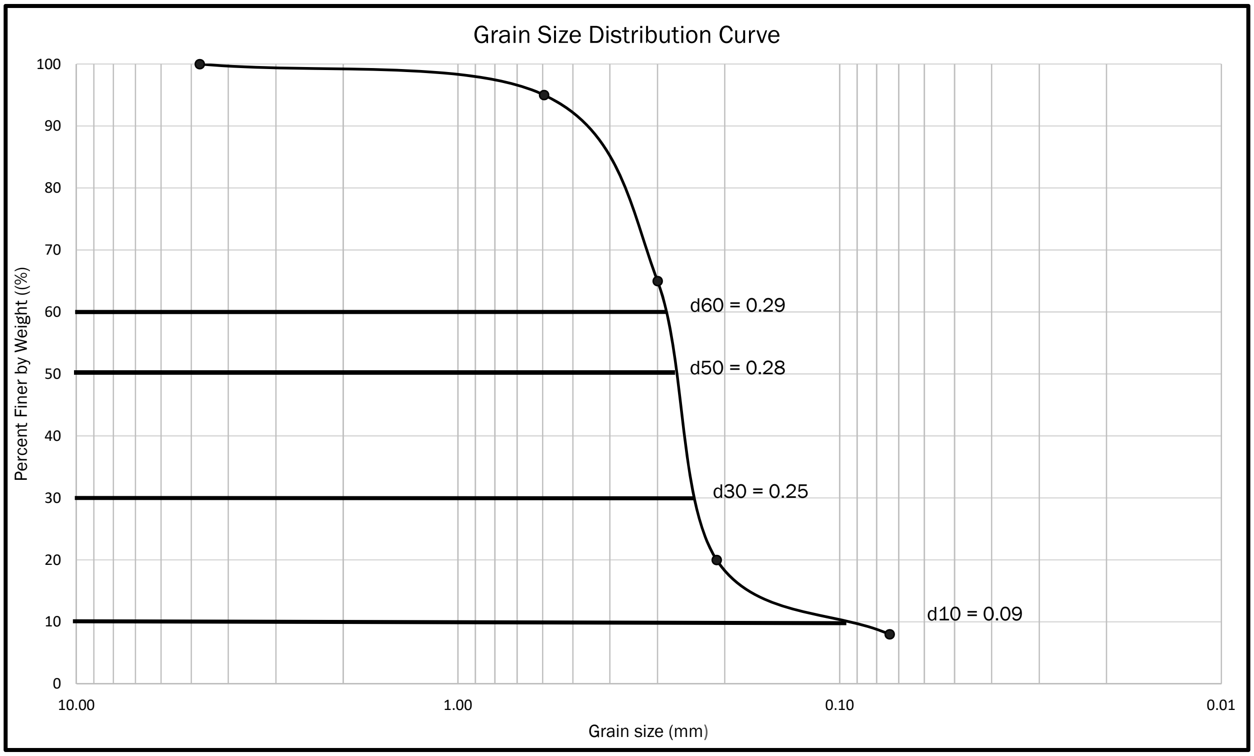

d_{10} =	0.09
d_{30} =	0.25
d_{50} =	0.28
d_{60} =	0.29

Attachment 4

Coefficient of Uniformity

631.0304 Unified Soil Classification System

The USCS provides a method of classifying and grouping unconsolidated earth materials according to their engineering properties. It is based on soil behavior, which is a reflection of the physical properties of the soil and its constituents. Refer to ASTM Standards D2487 and D2488.

The classification consists of 15 soil groups, each having distinctive engineering properties. Boundary classifications are provided for soils which have characteristics of two groups. Letter symbols have been derived from terms which are descriptive of the soil components, gradation, and liquid limit. These are combined to identify each of the 15 soil groups. Table 3–9 lists these letter symbols.

(a) Soil components

The term “soil components” applies to the solid mineral grains comprising earth materials. These components range in size from more than 12 inches to colloidal size. The particle size, gradation, shape, and mineral composition affect the behavior of the soil, as do the moisture content and the inclusion of other materials such as organic matter, gases, and coatings of cementing minerals. Table 3–10 lists various soil components with their associated grain sizes, descriptions, and some of their significant properties. Comparison of grain size boundaries of the USCS with those of other commonly used grade scales is shown in table 3–1.

A quarter-inch sieve is approximately equivalent to the No. 4 U.S. Standard Sieve. The No. 200 U.S. Standard Sieve size is about the smallest particle visible to the naked eye. The No. 40 sieve size is the limit between medium and fine sand, and Atterberg limit tests are performed on the fraction finer than the No. 40 size in the laboratory.

The Atterberg limit tests define the finer fraction plasticity. Figure 3–4, USCS plasticity chart, classifies the finer grained soil relative to liquid limit and plasticity index.

Table 3–9 USCS components and modifiers

Component		Modifier	
Symbol	**Name**	**Symbol**	**Name**
None	Boulders or cobbles	W	Well graded
G	Gravel	P	Poorly graded
S	Sand		
S	Sand	M	Silty
M	Silt	L or H	Low/high liquid limit
C	Clay	L or H	Low/high liquid limit
O	Organic	L or H	Low/high liquid limit
Pt	Peat	—	—

(b) Gradation

Coarse-grained soil gradation descriptors are shown in table 3–11. In the soil mechanics laboratory, the amounts of the various sized grains are determined by sieving and mechanical analysis and the results plotted on Form SCS–353 or equivalent. The type of gradation is readily apparent from the shape of the grain-size curve. Figure 3–5 illustrates the grain-size distribution graphs of some typical soils.

Poorly graded soils have steeply sloping curves, very flat curves, or abrupt changes in the slope of the curves, when plotted on semi-log graph paper. Well-graded soils plot as smooth curves. To qualify as well graded, the gradation must meet certain requirements in respect to coefficient of uniformity and coefficient of curvature of the plotted graph.

The coefficient of uniformity (C_u), a measure of size range of a given sample, is the ratio of that size, of which 60 percent of the sample is finer (D_{60}), to that size, of which 10 percent of the sample is finer (D_{10}). The coefficient of the curvature (C_c), which defines the shape of the grain-size curve, is the ratio of the square of that size, of which 30 percent of the sample is finer (D_{30}), to the product of the D_{60} and D_{10} sizes. These ratios can be simply written:

Table 3–10 Soil components and significant properties (Wagner 1957)

Soil component	Symbol	Grain size range and description	Significant properties
Boulder	None	Rounded to angular, bulky, hard, rock particle, average diameter greater than 12 inches	Boulders and cobbles are very stable components, used for fills, ballast, and to stabilize slopes (riprap). Because of size and weight, their occurrence in natural deposits tends to improve the stability of foundations Angularity of particles increases stability
Cobble	None	Rounded to angular, bulky, hard, rock particle, average diameter less than 12 inches and greater than 3 inches	
Gravel	G	Rounded to angular, bulky, hard, rock particle, passing 3-inch sieve (76.2 mm), retained on No. 4 sieve (4.76 mm).	Gravel and sand have essentially the same engineering properties, differing mainly in degree. The No. 4 sieve is an arbitrary division and does not correspond to a significant change in properties. They are easy to compact, are little affected by moisture, and not subject to frost action. Gravels are generally more pervious, stable, and resistant to erosion and piping than sands. Well-graded sands and gravels are generally less pervious and more stable than poorly graded sands and gravels. Irregularity of particles increases the stability slightly. Finer, uniform sand approaches the characteristics of silt; i.e., decrease in permeability and reduction in stability with increase in moisture.
Coarse		3¾ inches	
Fine		¾ inch to No. 4 sieve (4.76 mm)	
Sand	S	Rounded to angular, bulky, hard, rock particle, passing No. 4 sieve (4.76 mm), retained on No. 200 sieve (0.074 mm)	
Coarse		No. 4 to 10 sieves (4.76–2.0 mm)	
Medium		No. 10 to 40 sieves (2.0–0.42 mm)	
Fine		No. 40 to 200 sieves (0.42–0.074 mm)	
Silt	M	Particles less than No. 200 sieve (0.074 mm) identified by behavior; i.e., slightly or nonplastic regardless of moisture and exhibits little or no strength when air dried	Silt is inherently unstable, particularly when moisture is increased, with a tendency to become "quick" when saturated. It is relatively impervious, difficult to highly susceptible to frost heave, is easily erodible, and is subject to piping and boiling. Bulky grains reduce compressibility. Flaky grains, such as mica, increase compressibility and cause the silt to be "elastic."
Clay	C	Particles less than No. 200 sieve (0.074 mm) identified by behavior; i.e., it can be made to exhibit plastic properties within a certain range of moisture and exhibits considerable strength when air dried	The distinguishing characteristic of clay is cohesion or cohesive strength, which increases with decrease in moisture. The permeability of clay is low. It is difficult to compact when wet and impossible to drain by ordinary means. When compacted, clay is resistant to erosion and piping, but is subject to expansion and shrinkage with changes in moisture. The properties of clay are influenced by particle size and shape (flat, plate-like particles), and also by the types of clay minerals, which affects the base exchange capacity.
Organic matter	O	Organic matter in various sizes and stages of decomposition	Organic matter present in even moderate amounts increases the compressibility of a soil and reduces the stability of the fine-grained components. Organic matter may also decay, creating voids, or by chemical alteration change the properties of a soil. Organic soils are, therefore, not desirable for engineering uses.

Figure 3–4 Unified Soil Classification System plasticity chart

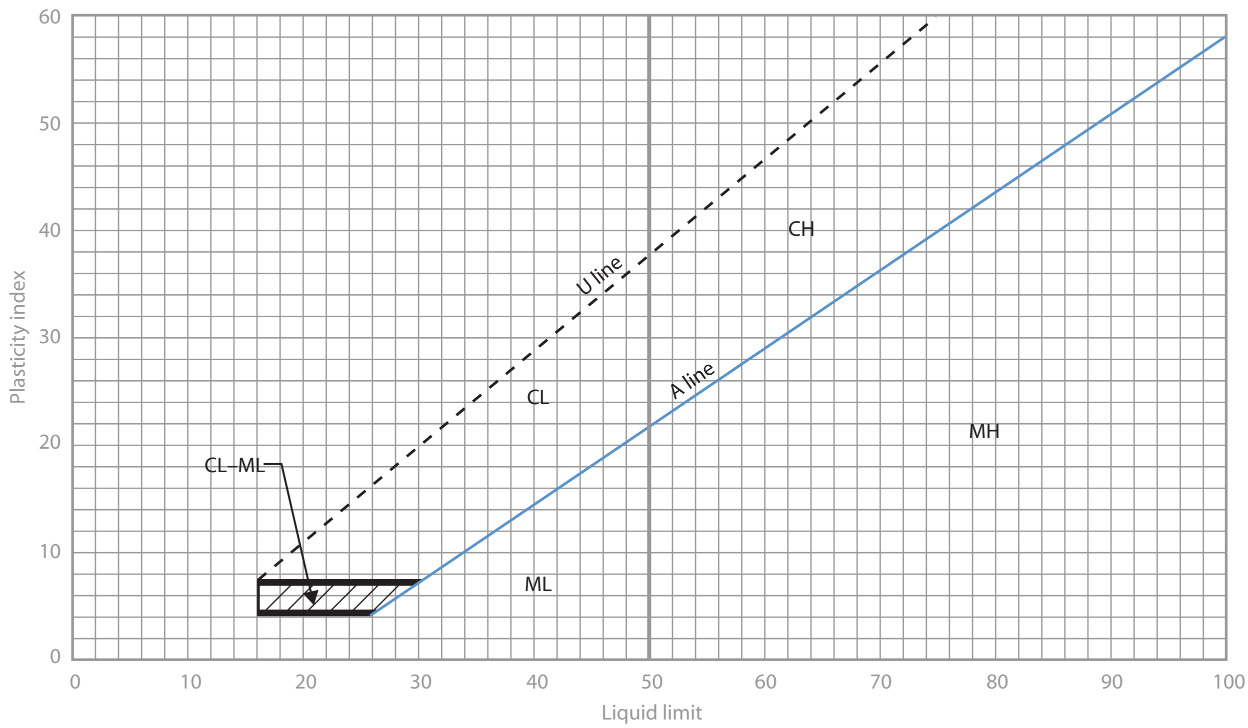

Figure 3–5 Grain size distribution graph

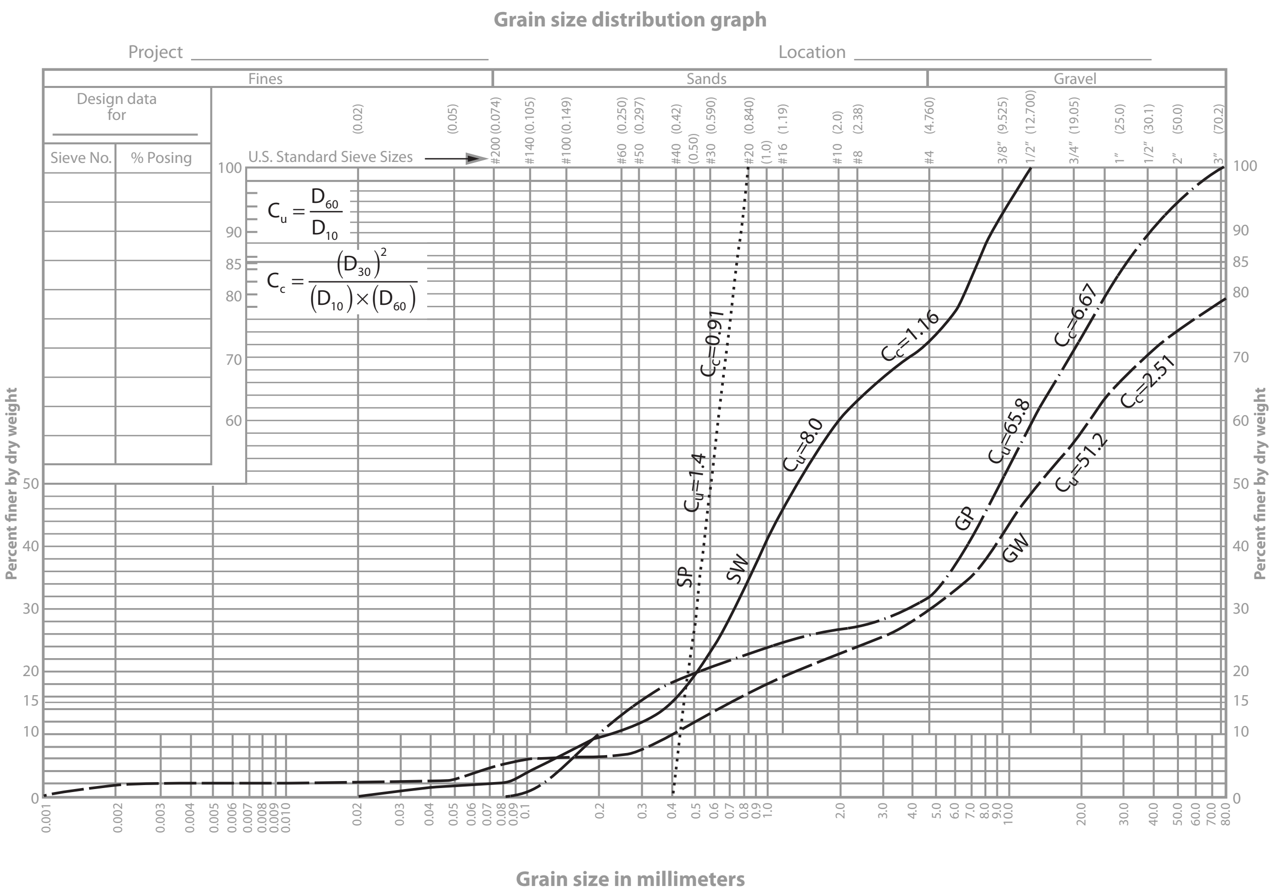

Table 3–11 Gradation descriptors for coarse-grained soils

Gradation	Description
Well graded	Soils that have a wide range of particle sizes and a good representation of all particle sizes between the largest and the smallest are said to be well graded. C_u>4 and 1<C_c<3, where $C_u = D_{60}/D_{10}$ and $C_c=(D_{30})^2/D_{60}D_{10}$
Poorly graded	Soils in which most particles are about the same size or have a range of sizes with intermediate sizes missing (skip grades) are said to be poorly graded. The gradation or grain-size distribution of soils consisting mainly of coarse grains is diagnostic of the physical properties of the soil. However, gradation is much less significant for predominantly fine-grained soils. C_u<4 and/or 1>C_c>3

Coefficient of Uniformity $C_u = \frac{D_{60}}{D_{10}}$

Coefficient of Curvature $C_c = \frac{(D_{30})^2}{D_{60} \times D_{10}}$

See figure 3–6 for an explanation of the use of these coefficients and other criteria (Atterburg limits) for laboratory identification procedures.

(c) Consistency

The most conspicuous physical property of fine-grained soils is their consistency, which is a function of their degree of plasticity. The various stages of consistency were described under mass characteristics. Atterberg limit tests are used to determine the liquid and plastic limits of soils in the laboratory. Field tests for dilatancy (reaction to shaking), dry strength (crushing characteristics), and toughness (consistency near the plastic limit) have been devised for field determinations. Figures 3–7 and 3–8 contain the procedures for making these field determinations and the methods of field classifications. The manual field tests are illustrated in figure 3–9.

(d) Field classification procedures

Complete field descriptions of soil materials encountered during a geologic investigation are needed. The following characteristics should be identified, field tested, and documented in logs of test holes, trenches, or pits:

- appoximate percentage of coarse-grain fraction, including sizes, maximum size, shape, and hardness
- mode of origin
- type of deposit
- structure
- cementation
- dispersion
- moisture and drainage conditions
- organic content
- color
- plasticity
- degree of compaction
- USCS classification (typical name and group symbol)
- local or geologic names where known or applicable

Figure 3–8, Field identification criteria, lists the classification characteristics of the soil groups. Only the primary constituents of unconsolidated material can be classified in the field in the USCS. More exact mechanical analyses must be made in the laboratory. Comparison of laboratory analyses with the original field classifications serves as an important learning and feedback loop to enable geologists to classify soils in a particular area with greater accuracy.

A representative sample is required for classification. The average size of the largest particle is estimated, boulders and cobbles are removed, and their percentage by weight removed from the total sample recorded. The amount of oversized material may be of importance in the selection of sources for embankment material. The distribution of boulders and cobbles and an estimate of their percentage in foundation materials should be noted so that their effect on physical properties of the materials and possible construction problems can be evaluated.

Step-by-step procedures for classifying soils in the field are shown in table 3–12.

Figures 3–10, 3–11, and 3–12, Engineering Properties of Unified Soil Classes, present a general evaluation of the engineering properties of the various classes. They provide guidance in determining the suitability of a soil for engineering purposes.

Figure 3–6 The Unified Soil Classification, laboratory criteria

Coarse-grained soils	**Grains** < 50% of the coarse fraction passes the No. 4 sieve size	**Clean gravels** < 5% passing the No. 200 sieve size	Borderline cases require the use of dual symbols	**Well graded** Meets gradation requirements	Gradation requirements are: $C_u = \frac{D_{60}}{D_{10}} > 4$ and $C_c = \frac{(D_{30})^2}{D_{10} \times D_{60}} > 1 < 3$	**GW**
				Poorly graded Does not meet gradation requirements		**GP**
		Gravels with fines < 12% passing the No. 200 sieve size		Plasticity limits of material passing No. 40 sieve size plots below “A” line and P.I. < 4	Plasticity limits above “A” line with P.I. > 4 < 7 are boundary cases and require use of dual symbols	**GM**
				Plasticity limits of material passing No. 40 sieve size plots below “A” line or P.I. > 7		**GC**
	Sands ≥ 50% of the coarse fraction passes the No. 4 sieve size	**Clean sands** < 5% passing the No. 200 sieve size	Borderline cases require the use of dual symbols	**Well graded** Meets gradation requirements	Gradation requirements are: $C_u = \frac{D_{60}}{D_{10}} > 6$ and $C_c = \frac{(D_{30})^2}{D_{10} \times D_{60}} > 1 < 3$	**SW**
				Poorly graded Does not meet gradation requirements		**SP**
		Sands with fines 12% passing the No. 200 sieve size		Plasticity limits of material passing No. 40 sieve size plots below “A” line and P.I. < 4	Plasticity limits above “A” line with P.I. > 4 < 7 are boundary cases and require use of dual symbols	**SM**
				Plasticity limits of material passing No. 40 sieve size plots below “A” line or P.I. > 7		**SC**
Fine-grained soils	**Silts and clays** Liquid limit < 50	Below “A” line and P.I. < 4		Above “A” line and P.I., > 4 < 7 are borderline cases requiring use of dual symbols		**ML**
		Above “A” line and P.I. > 7				**CL**
		Below “A” line and P.I. < 4 and $\frac{\text{L.L. (oven dry soil)}}{\text{L.L. (air dry soil)}} < 0.7$		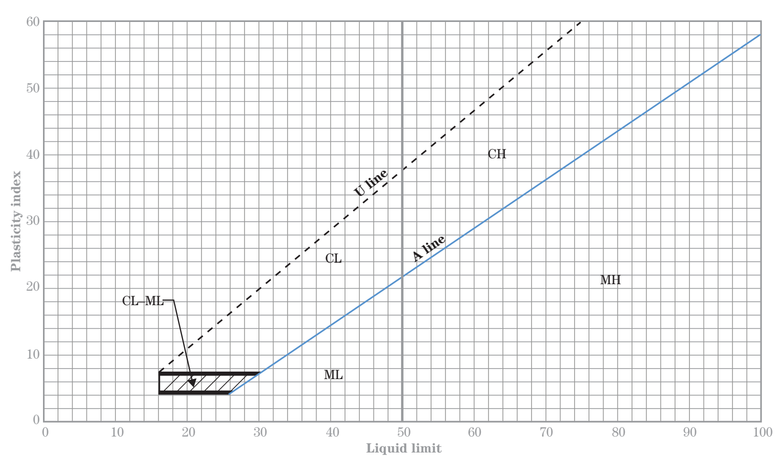		**OL**
	Silts and clays Liquid limit < 50	Below “A” line				**MH**
		Above “A” line				**CH**
		Below “A” line and P.I. < 4 and $\frac{\text{L.L. (oven dry soil)}}{\text{L.L. (air dry soil)}} < 0.7$				**OH**
Highly organic soils				$\frac{\text{L.L. (oven dry soil)}}{\text{L.L. (air dry soil)}} < 0.7$		**PT**

Figure 3–7 Unified Soil Classification, field identification criteria

Coarse-grained soils > 50% of material (by weight) is of individual grains visible to the naked eye	No. 200 sieve size is about the smallest particle visible to the naked eye	**Gravel and gravely soils** < 50% of coarse fraction passes the No. 4 sieve size	Borderline cases require the use of dual,symbols	For visual classification, the 3/4 inch size may be used as equivalent to the No. 4 sieve size	**Clean gravels** Will not leave dirt stain on a wet palm	Wide range in grain sizes and substantial amounts of all intermediate particle sizes	**GW**
						Predominately one size or a range of sizes with some intermediate sizes missing	**GP**
					Gravels with fines Will leave a dirt stain on a wet palm	Nonplastic fines or fines with low plasticity (for identification of fines, see characteristics of ML below)	**GM**
						Plastic fines (for identification of fines, see characteristics of CL below)	**GC**
		Sand and sandy soils > 50% half of the coarse fraction passes the No. 4 sieve size	Borderline cases require the use of dual symbols		**Clean sands** Will not leave a dirt stain on a wet palm	Wide range in grain sizes and substantial amounts of all intermediate particle sizes	**SW**
						Predominately one size or a range of sizes with some intermediate sizes missing	**SP**
					Sands with fines Will leave a dirt stain on a wet palm	Nonplastic fines or fines with low plasticity (for identification of fines, see characteristics of ML below)	**SM**
						Plastic fines (for identification of fines, see characteristics of CL below)	**SC**

Major division		Group		**Odor**	**Dry crushing strength**	**Dilatancy (shake) reaction**	**Toughness**	**Ribbon (near the P.L.)**	**Shine (near the P.L.)**	Symbol
Fine-grained soils > 50% of material (by weight) is of individual particle not visible to the naked eye	No. 200 sieve size is about the smallest particle visible to the naked eye	**Silts and clays** (low plastic)	See identification procedures		Slight	Rapid	Low to none	None	Dull	**ML**
					High	Medium to none	Medium	Weak	Slight to shiny	**CL**
				Pronounced	Medium	Slow to none	Low	None	Dull to slight	**OL**
		Silts and clays (highly plastic)			Medium	Very slow to none	Medium	Weak	Slight	**MH**
					Very high	None	High	Strong	Shiny	**CH**
				Pronounced	High	None	Low to medium	Weak	Dull to slight	**OH**
Highly organic soils		Readily identified by color, odor, spongy feel, and frequently by fibrous texture								**PT**

Figure 3–8 Unified Soil Classification, field identification procedures

<table>
<tr><th>Field identification procedures for fine-grained soils or fractions</th><th colspan="2">Information required during logging</th><th>GW</th></tr>
<tr><td rowspan="3">These procedures are to be performed on the minus No. 40 sieve size particles, or < 1/64 inch. For field classification purposes, screening is not intended. Simply remove the coarse particles by hand that interfere with the tests.

Dry Strength (Crushing characteristics)
After removing particles > No. 40 sieve size, mold a pat of soil to the consistency of putty, adding water if necessary. Allow the pat to dry completely by oven, sun, or air drying, and then test its strength by breaking and crumbling between the fingers. This strength is a measure of the character and quantity of the colloidal fraction contained in the soil. The dry strength increases with increasing plasticity.

High dry strength is characteristic for clays of the CH group. Inorganic silt has only very slight dry strength. Silty fine sands and silts have about the same slight dry strength, but can be distinguished by feel when powdering the dried specimen. Fine sand feels gritty, whereas silt has the smooth feel of flour.

Calcium carbonate or iron oxides may cause higher dry strength in dried material. If acid causes a fizzing reaction, calcium carbonate is present.

Dilatancy (Reaction to shaking)
After removing particles > No. 40 sieve size, prepare a pat of moist soil with a volume of about 0.5 in^3. Add enough water, if necessary, to make the soil soft but not sticky.

Place the pat in the open palm of one hand and shake horizontally, striking vigorously against the other hand several times. A positive reaction is the appearance of water on the surface of the pat, which changes to a livery consistency and becomes glossy. When the sample is squeezed between the fingers, the water and gloss disappear from the surface, the pat stiffens, and it finally cracks or crumbles. The rapidity of appearance of water during shaking and of its disappearance during squeezing assist in identifying the character of the fines in a soil.

Very fine clean sands give the quickest and most distinct reaction, whereas a plastic clay has no reaction. Inorganic silts, such as rock flour, show a moderately quick reaction.

Toughness (Consistency near plastic limit)
After removing particles > No. 40 sieve size, a specimen of soil about 0.5 in^3 in size, is molded to the consistency of putty. If too dry, water must be added and if sticky, the specimen should be spread out in a thin layer and allowed to lose some moisture by evaporation. Then the specimen is rolled out by hand on a smooth surface or between the palms into a thread about 1/8 inch in diameter. The thread is then folded and rerolled repeatedly. During this manipulation, the moisture content is gradually reduced; and the specimen stiffens, finally loses its plasticity, and crumbles when the plastic limit is reached.

After the thread crumbles, the pieces should be lumped together and a slight kneading action continued until the lump crumbles.

The tougher the thread near the plastic limit and the stiffer the lump when it finally crumbles, the greater is the colloidal clay fraction in the soil. Weakness of the thread at the plastic limit and quick loss of coherence of the lump below the plastic limit indicate either inorganic clay of low plasticity, or materials such as kaolin-type clays and organic clays, which occur below the A-line.

Highly organic clays have a very weak and spongy feel at the plastic limit. Nonplastic soils cannot be rolled into a thread at any moisture content. The toughness increases with the P.I.</td><td>**Coarse-grained soil**</td><td>For undisturbed soils add information on stratification, degree of compactness, cementation, moisture conditions, and drainage characteristics.

Give typical name: indicate approximate percentages of sand and gravel, maximum size; angularity, surface condition, and hardness of the coarse grains; local or geologic name and other pertinent descriptive information; and symbol in parentheses.

Example:
Silty sand, gravelly; about 20% hard, angular gravel particles 1/2-inch maximum size; rounded and subangular sand grains coarse to fine; about 15% nonplastic fines with low dry strength; well compacted and moist in place; alluvial sand, (SM).</td><td>GP
GM
GC
SW
SP
SM
SC</td></tr>
<tr><td>**Fine-grained soils**</td><td rowspan="2">For undisturbed soils add information on stratification, degree of compactness, cementation, moisture conditions, and drainage characteristics.

Give typical name: indicate approximate percentages of sand and gravel, maximum size; angularity, surface condition, and hardness of the coarse grains; local or geologic name and other pertinent descriptive information; and symbol in parentheses.

Example:
Clayey silt, brown, slightly plastic, small percentage of fine sand, numerous vertical root holes, firm and dry in place, loess, (ML).</td><td>ML
CL
OL
MH
CH
OH</td></tr>
<tr><td>**Organic soils**</td><td>PT</td></tr>
</table>

Attachment 5

Geotextile Thickness

From: Connie Wong, <cowong@solmax.com>
Sent: Wednesday, November 20, 2019 5:44 PM
To:
Subject: RE: geotextile thickness

============== This message originated outside of SCS Engineers ==============

We don't publish or certify the thickness of the geotextile. General speaking, typical value of 6oz/sy nonwoven geotextile is around 80mil

CONNIE WONG,
Product Manager
+1 281 230 5830
+1 832 495 5005
cowong@solmax.com

SOLMAX

19103 Gundle Road, Houston, Texas, 77073, USA

SOLMAX.COM

From:
Sent: Wednesday, November 20, 2019 1:06 PM
To: Connie Wong, <cowong@solmax.com>
Subject: geotextile thickness

Connie,
Can you please send me the thickness of the attached nonwoven geotextile for the 6 oz option

Attachment 6

Liquid Collection Systems

An official journal of the
INTERNATIONAL GEOSYNTHETICS SOCIETY

Geosynthetics International

SPECIAL ISSUE ON

Liquid Collection Systems

Editor
T.S. Ingold

Co-Editor
R.J. Bathurst

Chairman
J.P. Giroud

2000, Volume 7, Nos. 4-6
ISSN 1072-6349

Technical Paper by E.M. Palmeira and M.G. Gardoni

THE INFLUENCE OF PARTIAL CLOGGING AND PRESSURE ON THE BEHAVIOUR OF GEOTEXTILES IN DRAINAGE SYSTEMS

ABSTRACT: Nonwoven geotextiles have been used for drainage and filtration in geotechnical engineering works for many years. Concerns related to drainage capacity and clogging potential still remain as factors that restrain a broader use of geotextiles for drainage systems, particularly in major engineering projects. This paper presents the test results of the hydraulic characteristics of partially clogged geotextiles under pressure. Partial clogging can occur during spreading and compaction of soil on geotextiles or throughout the service life of the drainage system. Geotextile specimens, artificially clogged in the laboratory and exhumed from actual field works, were tested to assess their normal and longitudinal permeabilities under different levels of soil impregnation and normal stresses. The results obtained showed that partial clogging significantly influenced the mechanical and hydraulic characteristics of nonwoven geotextiles and that soil impregnation was not necessarily detrimental to the geotextile longitudinal permeability under stress. Comparisons of test and predicted results, confirmed that the expression reported by Giroud in 1996 is a useful tool for the prediction of nonwoven geotextile permeabilities under virgin and soil impregnated conditions. Data on the impregnation levels of geotextile specimens exhumed from actual field works are also presented and discussed.

KEYWORDS: Geotextile, Drainage, Filtration, Clogging, Laboratory testing, Permeability.

AUTHORS: E.M. Palmeira, Associate Professor, and M.G. Gardoni, Ph.D. Student, University of Brasilia, Department of Civil and Environmental Engineering, Faculty of Technology, 70910-900 Brasilia, DF, Brazil, Telephone: 55/61-273 7313, Telefax: 55/61-273 4644, E-mail: palmeira@unb.br.

PUBLICATION: *Geosynthetics International* is published by the Industrial Fabrics Association International, 1801 County Road B West, Roseville, Minnesota 55113-4061, USA, Telephone: 1/651-222-2508, Telefax: 1/651-631-9334. *Geosynthetics International* is registered under ISSN 1072-6349.

DATES: Original manuscript received 4 April 2000, revised version received 8 July 2000, and accepted 11 July 2000. Discussion open until 1 June 2001.

REFERENCE: Palmeira, E.M. and Gardoni, M.G., 2000, "The Influence of Partial Clogging and Pressure on the Behaviour of Geotextiles in Drainage Systems", *Geosynthetics International*, Vol. 7, Nos. 4-6, Special Issue on Liquid Collection Systems, pp. 403-431.

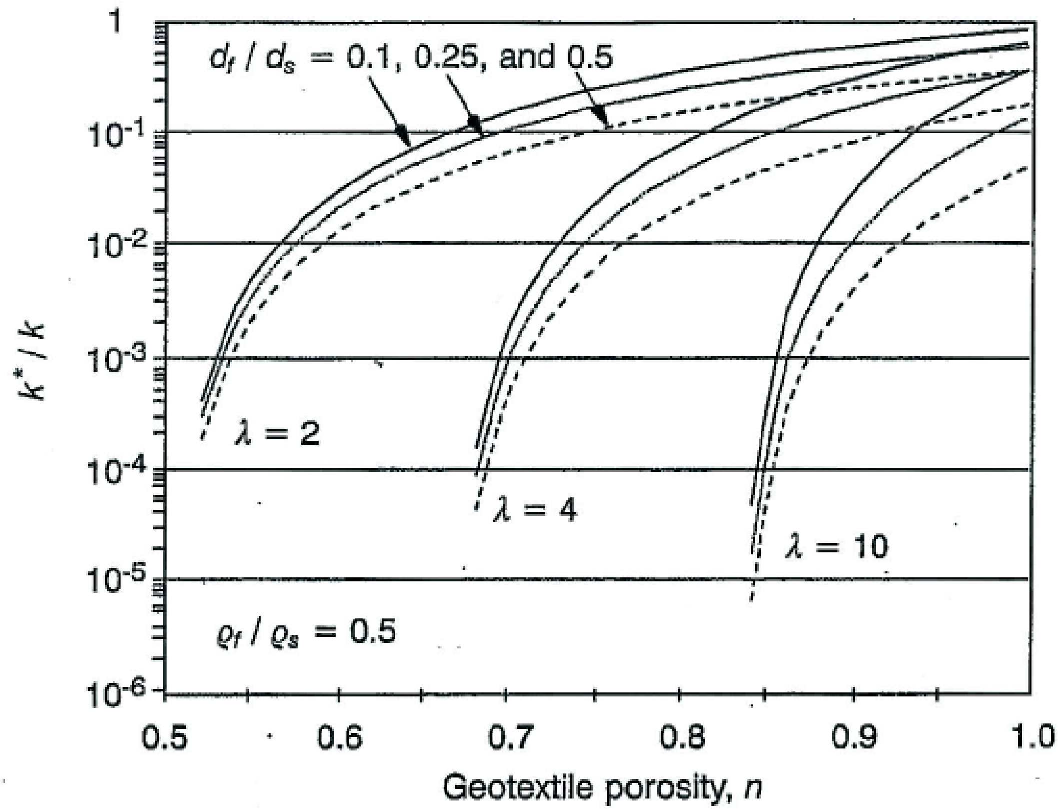

Figure 2. Variation of geotextile permeability with porosity for different λ values (Equation 9).

Note: λ = ratio of soil mass to geotextile fibre mass for partially clogged geotextiles.

3 TESTING PROGRAMME

3.1 Apparatus Used in the Testing Programme

Transmissivity and permittivity tests were performed to evaluate the behaviour of partially clogged geotextile specimens. Both transmissivity and permittivity tests were carried out with the geotextile specimen under normal stresses of up to 2,000 kPa in some cases. The behaviour of the geotextile under these high normal stresses is important in the case of drainage systems for large earth works and waste piles. In addition to the laboratory tests, the partially clogged geotextile specimens were also investigated using an image analyser and scanning microscope.

Figure 3 shows the transmissivity apparatus used in this research programme. The apparatus is similar to that proposed in the standard test method ASTM D 4716. Geosynthetic specimens, 100 mm × 100 mm in size, can be accommodated in the testing cell. The normal stress is applied by a rigid metal plate covering the entire plan area of the specimen. A hydraulic system provides the necessary vertical load, which is measured by a load cell. Rubber seals at the edges of the rigid plate, covering its entire thickness, prevent preferential flow and leakage through gaps or grooves. Distilled water reservoirs at the specimen ends allows the water to flow under a constant hydraulic gradient that can be varied between 0.2 and 3. The variation of the geotextile specimen

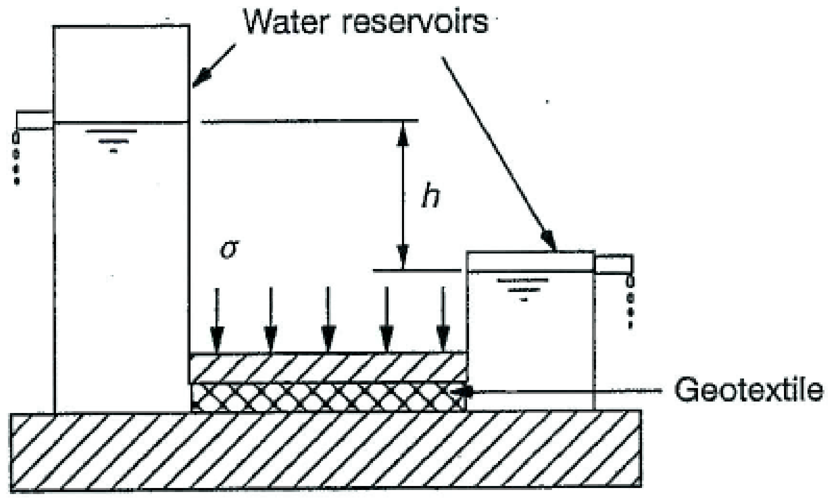

Figure 3. Apparatus for geotextile specimen transmissivity tests.

thickness during the test can also be assessed from the rigid plate vertical displacements measured by displacement transducers. Only tests with a hydraulic gradient equal to 1 are reported in the present paper. Four equally spaced (20 mm) piezometers that measure the water head variations along the geosynthetic length are connected to the base of the specimen. The piezometer measurements were useful in detecting variations of hydraulic properties along the geotextile length (Gardoni and Palmeira 1999).

The permittivity tests were carried out using two different apparatuses. The first (Figure 4a) was used at École Polytechnique, Montréal, Quebec, Canada and was designed according to ASTM D 5493. It comprises a permeameter cell, a de-aired water supply, and a hydraulic system that applies normal stresses on the specimen in the range 20 to 1,000 kPa. The permeameter cell is made of stainless steel with a diameter of 50.8 mm and a height of 280 mm. A 52 mm-diameter geotextile specimen can be accommodated in the cell for testing. A steel piston transfers the vertical load from a hydraulic loading system to the geotextile specimen, which is located between two sets of steel screen meshes for a uniform normal stress distribution. The openings of the screen meshes vary from 1 to 5 mm. Vertical displacements of the upper specimen surface can be measured using a linear variable displacement transducer (LVDT) fixed to the loading piston. Two ports located above and below the geotextile specimen measure the water head loss in the geotextile.

The second permeameter used for the permittivity tests is shown in Figure 4b. A detailed description of this permeameter is reported by Fannin et al. (1996) and Palmeira et al. (1996). In this case, the apparatus comprises a rigid metal cell capable of accommodating soil or geotextile specimens. The specimens consist of geotextile "packs" comprising several individual layers of geotextile. The body of the permeameter is made of anodised aluminium and can accommodate 102 mm-diameter geotextile specimens with heights of up to 125 mm. A pneumatic Bellofram piston transfers vertical load to the specimen. A load cell and a LVDT fixed to the loading piston measure vertical load and compression of the specimen, respectively. Water head losses measured above and below the specimen and flow rate measurements enabled the calculation of

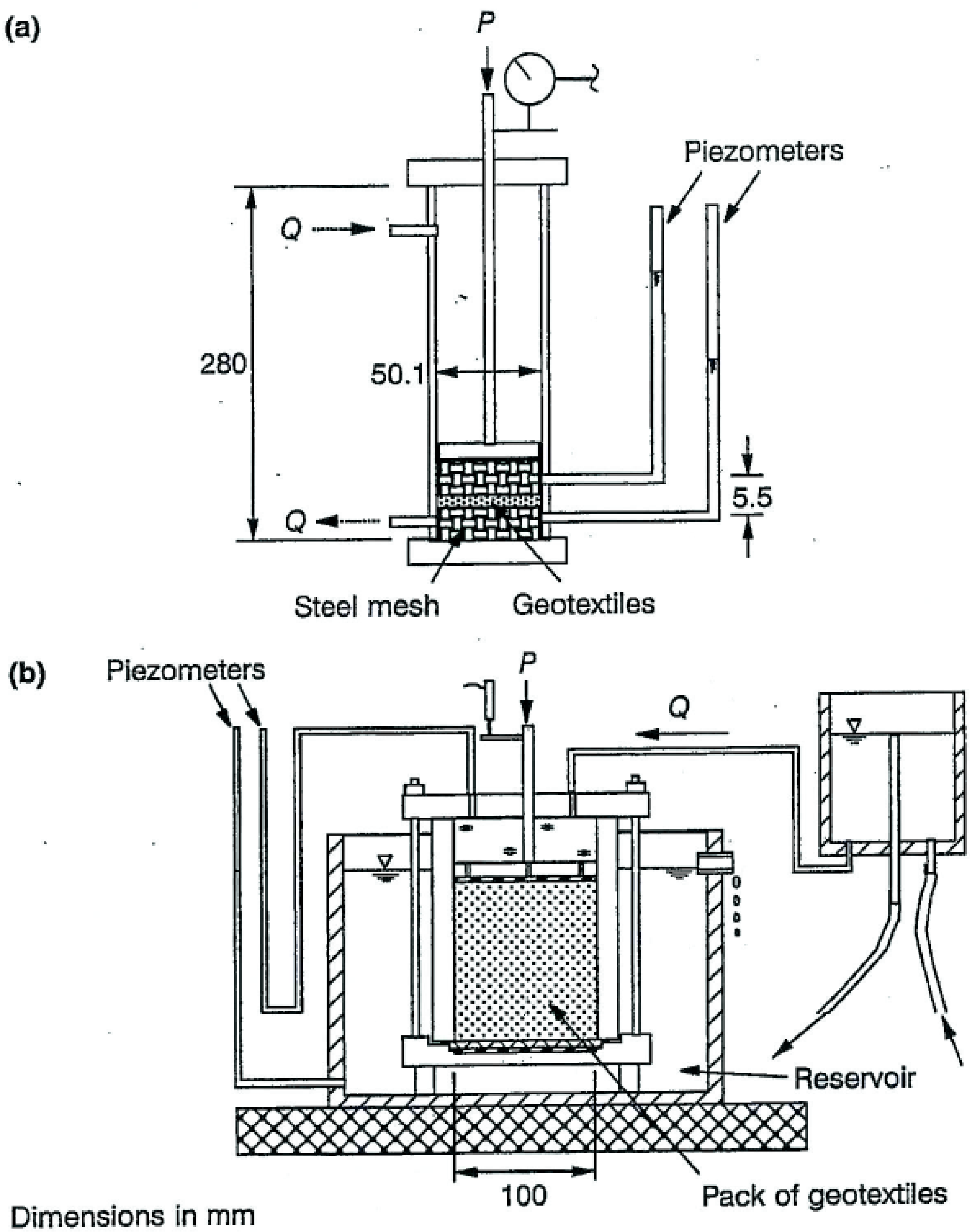

Figure 4. Apparatuses used for geotextile specimen permittivity tests: (a) apparatus for testing individual layers of geotextiles; (b) apparatus for testing packs of geotextile layers.

the average geotextile normal permeability. De-aired water was used in all of the tests performed in the present study.

To assess the dimensions of the soil particles entrapped inside the geotextile layers, investigations were carried out using a Clemex Impak Automatic Image Analizer available at the Clemex Technology Incorporation (Longueil, Quebec, Canada). The apparatus consists of a Nikon microscope with a Sony RGB photographic camera and a computer for data acquisition. Additional information on this apparatus and the measuring technique can be found in publications by Clemex (1999), Forget and Goldman (1998), and Gardoni (2000).

3.2 Materials and Methodology Employed

Eight types of needle-punched nonwoven geotextiles used worldwide were employed in the test series and will be referred to hereafter as Geotextiles GA to GH (Table 1). Geotextiles GA to GE are made of continuous polyester monofilaments (Manufacturer 1). Geotextile GF (Manufacturer 2) is also a nonwoven geotextile made of polyester. Geotextiles GG and GH are made of polypropylene (Manufacturers 3 and 4). Table 1 summarizes the main characteristics of the geotextiles. The mass per unit area of the specimens varies between 130 and 600 g/m^2 and their filtration opening sizes between 60 and 500 μm. The diameter of the geotextile fibres was measured by microscopy.

Geotextile specimens for each product were randomly chosen by mapping a layer of the product and choosing the specimens using a table of random numbers. A statistical technique associating the number of specimens tested to an allowable measuring error was employed to establish the minimum number of specimens to be tested (Gardoni 2000). For each normal stress, seven specimens of each geotextile were tested.

Table 1. Characteristics of the geotextiles tested.

Geotextile	Manufacturer	Polymer	ϱ_f (kg/m^3) (1)	M_A (g/m^2) (2)	t_{GT} (mm) (3)	n (4)	k_n (cm/s) (5)	ψ (s^{-1}) (6)	O_s (μm) (7)	d_f (μm) (8)
GA	1	Polyester	1,380	140	2.2	0.94	0.40	2.1	140	27
GB	1	Polyester	1,380	200	2.3	0.93	0.40	1.9	130	27
GC	1	Polyester	1,380	300	3.4	0.93	0.40	1.5	110	27
GD	1	Polyester	1,380	400	3.7	0.92	0.40	1.1	90	27
GE	1	Polyester	1,380	600	4.6	0.90	0.40	0.9	60	27
GF	2	Polyester	1,380	222	2.3	0.92	—	—	60	26
GG	3	Polypropylene	910	300	2.8	0.88	—	1.5	150	28
GH	4	Polypropylene	910	130	1.4	0.90	0.40	2.9	200–500	37

Notes: (1) ϱ_f = density of the fibres. (2) M_A = mass per unit area (ASTM D 3776), nominal values from manufacturers' catalogues. (3) t_{GT} = geotextile thickness under 1 kPa normal stress. (4) n = geotextile porosity under 1 kPa normal stress, calculated as $n = 1 - M_A / (\varrho_f \, t_{GT})$. (5) k_n = geotextile permeability normal to its plane (AFNOR NF G 38016 standards for Geotextiles GA to GE and ASTM D 4491 for Geotextiles GF to GH). (6) ψ = geotextile permittivity (AFNOR NF G 38016 for Geotextiles GA to GE and ASTM D 4491 for Geotextiles GF to GH) (CFG 1986). (7) O_s = opening size equal to filtration opening size (AFNOR NF G 38017) for Geotextiles GA to GE and equal to apparent opening size (ASTM D 4751) for Geotextiles GF to GH (CFG 1986). (8) d_f = diameter of the geotextile fibres obtained from microscopic measurements.

Table 2. Characteristics of the soils used.

Soil	Soil type (1)	D_{10} (mm)	D_{50} (mm)	D_{85} (mm)	C_U (2)	w_L (%)	w_P (%)	w_{opt} (%)	G	γ_{dmax} (kN/m^3)
SA	RSQ	0.016	0.11	0.2	9.4	—	—	—	2.73	20.3
SB	Sand	0.053	0.42	0.61	11.5	—	—	—	2.80	—
SC	CS	0.010	0.026	0.20	5.9	48	35	27.2	2.54	14.7
SD	GB1	0.062	0.22	0.36	3.7	—	—	—	2.38	—
SE	GB2	0.055	0.17	0.46	4.6	—	—	—	2.43	—
SF	GB3	0.089	0.11	0.18	1.4	—	—	—	2.43	—
SG	GB4	0.054	0.12	0.14	2.2	—	—	—	2.48	—

Notes: (1) RSQ = residual soil from quartzite collected from the BR-020 Highway geotextile drainage system; Sand = sand collected from the backfill of the Mucambo geotextile-reinforced wall; CS = clayey soil; GB1 = Glass beads 1; GB2 = Glass beads 2; GB3 = Glass beads 3; GB4 = Glass beads 4. (2) C_U = coefficient of uniformity (= D_{60} / D_{10}). D_{85}, D_{50}, and D_{10} = diameter of the soil particle corresponding to 85, 50, and 10% in weight passing, respectively. w_L = liquid limit, w_P = plastic limit, w_{opt} = optimum moisture content (normal Proctor energy), G = specific gravity, γ_{dmax} = maximum dry unit weight (normal Proctor energy).

The geotextile specimens were previously saturated with de-aired water and were then exposed to a vacuum for at least two hours. Installation of the geotextile specimen in the permeameter was performed under total submersion in de-aired water to maintain specimen saturation. The steel screens used in the permittivity tests (Section 3.1) were submitted to the same saturation process by vacuum.

Impregnation of the geotextile specimens with soil particles for the permittivity and transmissivity tests was made under laboratory and field conditions with the use of seven granular materials. The main physical characteristics of the granular materials are summarised in Table 2. Figures 5a and 5b show the particle size distributions of these granular materials; in Figures 5a and 5b, a wide range of particle sizes can be noted. One residual quartzite soil (Soil SA in Table 2), one sand (Soil SB), one clayey soil (Soil SC), and four types of glass beads were used to partially clog the geotextile specimens. The residual quartzite soil is common in Brasilia, Brazil, and is known for having caused severe clogging of granular highway drainage systems in Brasilia (Gardoni and Palmeira 1998). Appropriate quantities of this soil were collected at the contact with a 400 m-long nonwoven geotextile filter in the BR-020 Highway, near the city of Brasilia. Soil SB (sand) was collected from the Mucambo geotextile-reinforced retaining wall structure, built along the Linha Verde Highway, in the state of Bahia, Brazil (Palmeira and Fahel 2000). The clayey soil (Soil SC) comes from a porous clay deposit that covers most of the city of Brasilia. Glass beads SD to SG are industrial-grade glass spheres with particle sizes varying from 0.04 to 1 mm. The spherical form of the glass beads makes it convenient for assessing the accuracy of theoretical expressions developed under the assumption of spherical entrapped soil particles.

It should be noted that, for the finer materials (Soils SA and SC), there are two different particle size distribution curves (Figure 5a), depending on whether or not a deflocculant was used in the sedimentation tests. For these soils, clusters of soil particles, rather than individual particles, were retained in the geotextile filter (Gardoni and Palmeira 1998). The flocculation mechanism, aside from complicating filter design, poses the

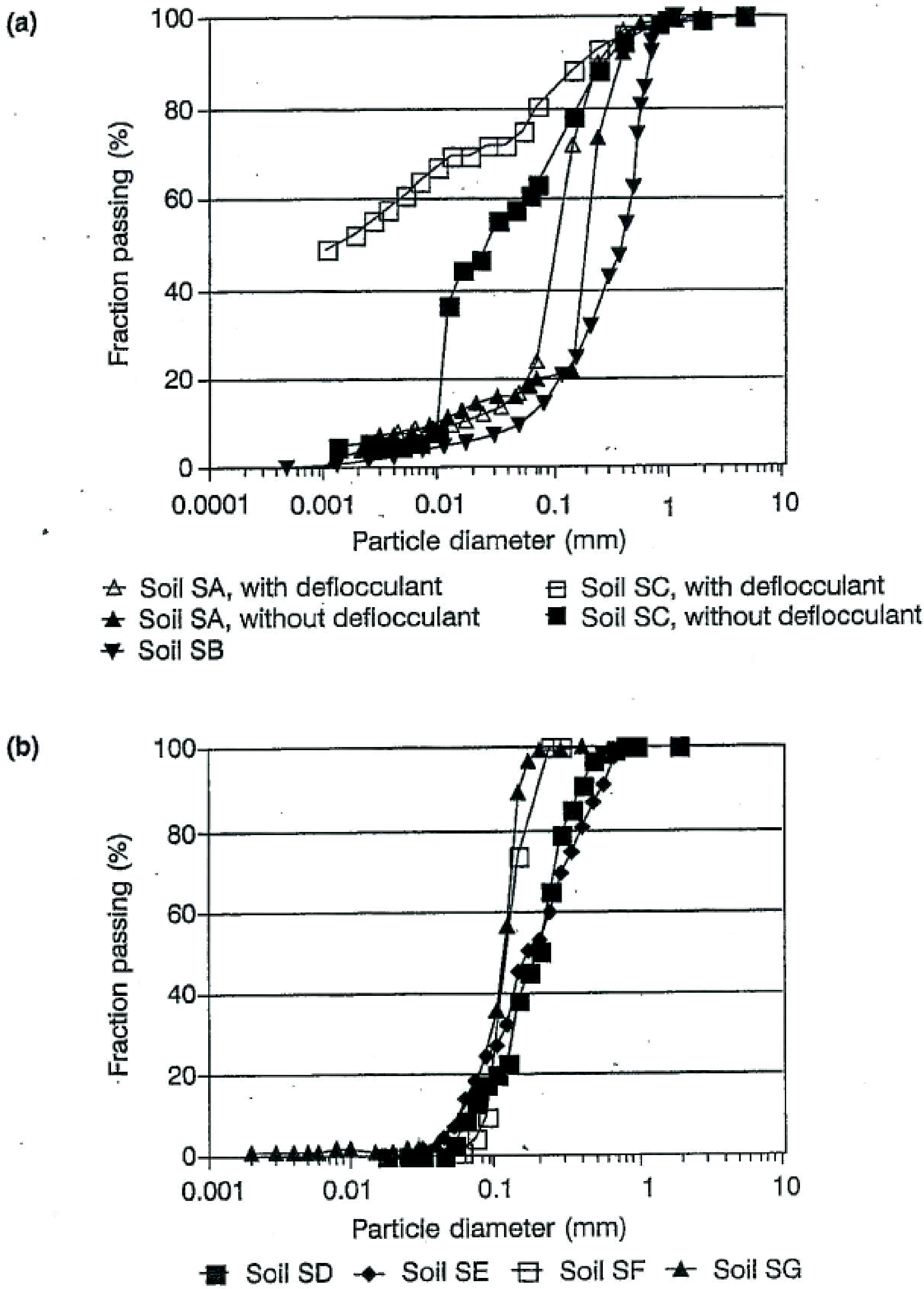

Figure 5. Particle size curves for the soils used in the test programme: (a) Soils SA, SB, and SC; (b) Soils SD, SE, SF, and SG (glass beads).

following question: can these particles be separated from one another by continuous water flow during the lifetime of the filter and then be retained inside the geotextile layer?

In the laboratory, the impregnation of the geotextile specimens with glass beads (Soils SD, SE, and SF in Table 2) was achieved by vibrating a sieve, which contained a geotextile specimen with soil on top of it. The system was vibrated for varying time periods, depending on the level of soil impregnation desired. In the case of the sandy soil, Soil SB, the geotextile specimen used in the test (transmissivity only) was exhumed from the Mucambo reinforced soil structure and tested under the conditions found after exhumation. In addition, two geotextile specimens exhumed from the BR-020 Highway drain were also tested after exhumation.

The geotextile impregnation with the clayey soil (Soil SC) was accomplished using two different procedures. For the first procedure, soil on the geotextile, which was placed at the base of a steel compaction mould used for standard compaction tests, was compacted. The compaction energy used in this case was the Proctor's normal energy and the soil optimum water content was used for compaction. The second procedure simulated geotextile impregnation with Soil SC using field test sections. In each test section, a layer of the geotextile (2 m × 1m) was laid on the ground and the fill material was spread and then compacted over it using a sheep's foot roller. The fill material was compacted under optimum moisture content conditions, using the same compaction energy that was used in the laboratory. After compaction, the geotextile specimens were carefully exhumed from the test sections for laboratory testing.

4 TEST RESULTS

4.1 Permittivity Tests

4.1.1 *Tests with Virgin Specimens*

Figures 6 and 7 show the variation of geotextile thickness, t_{GT}, normal permeability, k_n, and permittivity, ψ, versus normal stress, σ, for some of the geotextiles tested. A marked dependency of t_{GT}, k_n, and ψ on the normal stress can be observed, particularly for values of σ below 50 kPa. Figure 6a shows that the normal stress affects the geotextile thickness for values of up to 800 kPa. For the same normal stress, lighter geotextiles (i.e. low mass per unit area values) have a higher normal permeability value (Figure 6b), and, for products of the same manufacturer, the k_n value drops with increased mass per unit area values. It is also important to note that a significant difference in permeability can be observed for products with the same mass per unit area, but from different manufacturers (e.g. Geotextiles GC and GG in Figure 6b), emphasising the importance of geotextile microstructure.

The comparison of predicted and measured geotextile permeability values is shown in Figure 8. The following relevant values for the fluid (water) were used in the calculations: $\beta = 0.11$, $g = 9.81$ m/s^2, $\varrho_w = 1000$ kg/m^3, and $\eta_w = 0.001$ kg/(ms). Test results obtained by Gourc et al. (1982) for other geotextiles are also presented for comparison. Hydraulic conductivity values, predicted using Equations 2, 4, and 5, are also presented in Figure 8; it can be observed that Equation 2 (Giroud 1996) provided the best fit with the test results.

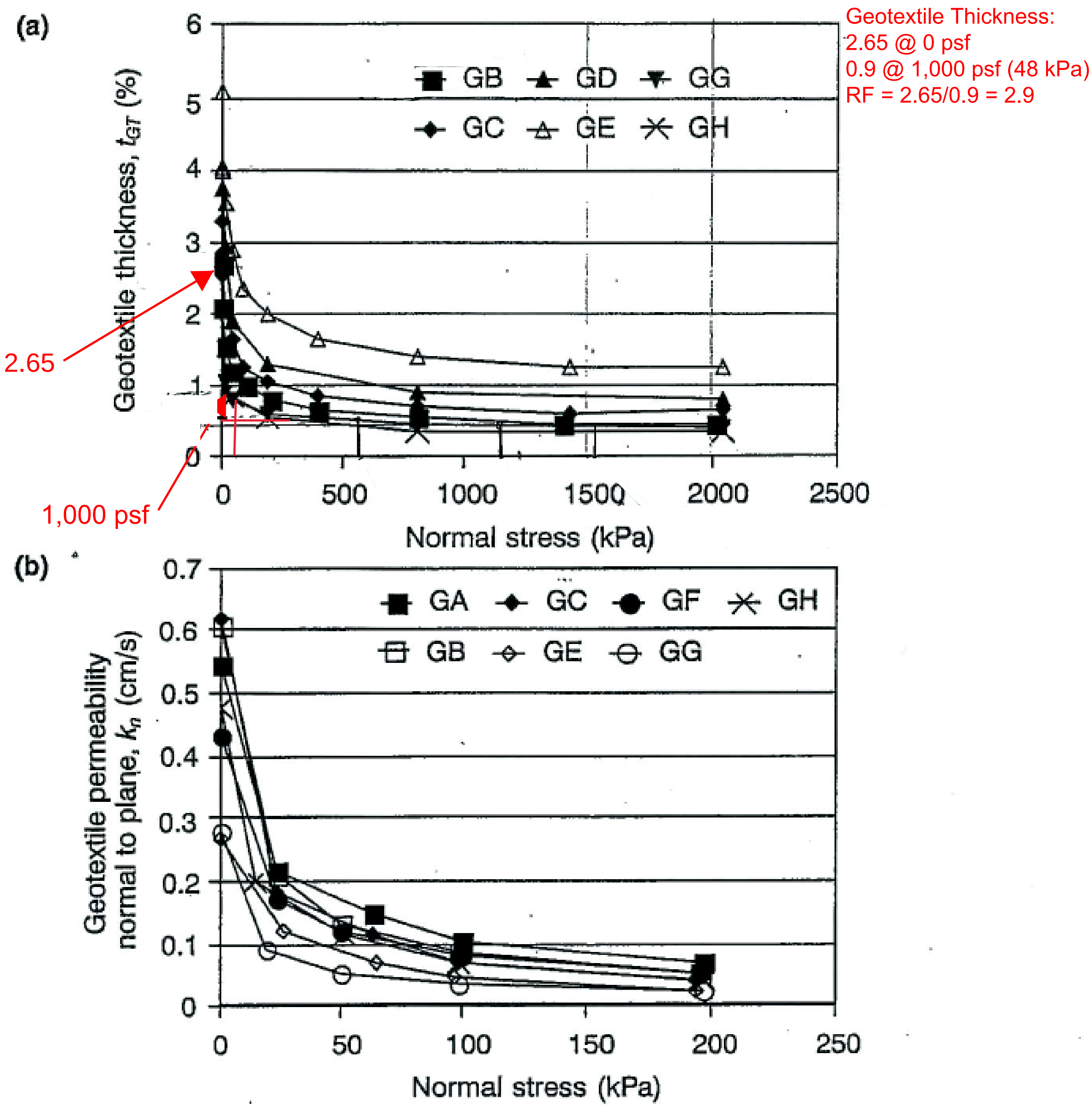

Figure 6. Variation of geotextile normal permeability with normal stress for virgin geotextile specimens: (a) average geotextile thickness versus normal stress; (b) normal permeability versus normal stress.

Figure 9 shows comparisons of test results and values predicted using Equation 2 alone in a nondimensional form. A good agreement between predicted and measured values is confirmed, particularly for geotextile porosities above 0.8 and geotextile mass per unit area values greater than 300 g/m^2.

The variation of the geotextile filtration opening size should be known to assess the accuracy of Equation 3. Figures 10a to 10c show the comparisons of predicted and mea-

Attachment 7

Darcy's Law

to obtain the closest U.S. sieve size and its number defines the AOS (or EOS) value. Thus AOS, EOS, and 0_{95} all refer to the same specific pore size, the difference being that AOS and EOS are sieve numbers, while 0_{95} is the corresponding sieve-opening size in millimeters. It should also be noted in the conversion on Table 2.6 that as the AOS sieve number increases, the 0_{95} particle size value decreases; that is, the numbers are inversely related to one another. In this book we will generally use the 0_{95} value since it is the target value for design purposes.

The AOS test is a poor test, having many problems, but the simplicity of the test and inertia seem to sustain its use in the United States. Some of the problems associated with the test are as follows:

- The glass beads can easily get trapped in the geotextile (particularly for thick nonwovens) and not pass through at all.
- Yarns in some geotextiles easily move with respect to one another (as they do in woven slit-film geotextiles), thereby allowing the beads to pass through an enlarged void not representative of the total geotextile test specimen.
- Reproducibility of the test is not good, with temperature, humidity, bead-size variation, and test duration all influencing the test results.
- The test is directed only at the 5% size (equivalent to the 95% passing size), which allows for determination of the 0_{95} size. The remainder of the pore-size curve is not defined.

As alternatives to the dry-sieving test just described, there are a number of wet-sieving methods. In Canada and France, a frame containing the geotextile specimen has a well-graded standard soil placed on it and the frame is repeatedly submerged in water. The soil fraction that escapes is analyzed and a d_{98}-equivalent particle size is obtained. In Germany, the setup is similar but a water spray is used. The soil fraction that escapes is analyzed and an effective opening diameter is calculated. The ISO/DIS 12956 test is also a wet-sieving test and will undoubtedly be seeing greater use than dry-sieving in the future. In general, these wet-sieving tests avoid many of the problems of dry sieving and are more representative of site conditions.

Permittivity (Cross-Plane Permeability). One of the major functions that geotextiles perform is filtration. (Note that most transportation agencies' specifications and some manufacturers' literature incorrectly call this "drainage.") In filtration, the liquid flows perpendicularly through the geotextile into crushed stone, a perforated pipe, or some other drainage system. It is important that the geotextile allow this flow to occur without being impeded. Hence the geotextile's cross-plane permeability must be quantified. As we discussed in the compressibility section, however, fabrics deform under load (recall Figure 2.6). Thus a new term, permittivity (Ψ), was previously defined in Eq. (2.8) (repeated here).

$$\Psi = \frac{k_n}{t} \tag{2.8}$$

where

Ψ = permittivity (s^{-1}),
k_n = permeability (properly called *hydraulic conductivity*) normal to the geotextile (m/s), and
t = thickness of the geotextile (m).

Eq. (2.8) is used in Darcy's formula as follows:

$$q = k_n iA = k_n \frac{\Delta h}{t} A$$

$$\frac{k_n}{t} = \Psi = \frac{q}{(\Delta h)(A)} \tag{2.16}$$

where

q = flow rate (m^3/s),
i = hydraulic gradient (dimensionless),
Δh = total head lost (m), and
A = total area of geotextile test specimen (m^2).

The formulation above is used for constant head tests in a manner identical to soil permeability testing. Typically, the flow rate q is measured at one value of Δh and then the test is repeated at different values of Δh. These different values of Δh produce correspondingly different values of q. When plotted (e.g., ΔhA versus q) the slope of the resulting straight line yields the desired value of Ψ.

The test can also be conducted using a falling (variable) head procedure as is also performed on soils. Here Darcy's formula is integrated over the head drop in an interval of time and used in the following equation:

$$\frac{k_n}{t} = \Psi = 2.3\frac{a}{A\Delta t}\log_{10}\frac{h_o}{h_f} \tag{2.17}$$

where

Ψ = permittivity (s^{-1}),
a = area of water supply standpipe (m^2),
A = total area of geotextile test specimen (m^2),
Δt = time change between h_o and h_f (s),
h_o = head at beginning of test (m), and
h_f = head at end of test (m).

In either case, the permittivity can be multiplied by the geotextile thickness to obtain the traditional permeability value, if so desired.

Attachment 8

Transmissivity Calculations

SCS ENGINEERS

CLIENT	PROJECT	JOB NO.
Hillsborough County	Southeast County Landfill	09215600.13

SUBJECT	BY	DATE
Geocomposite Transmissivity/Hydraulic Conductivity Calculations	FCH	11/1/2021
Phase I - VI Closure	CHECKED	DATE
	KLS	11/16/2021

OBJECTIVE: To calculate the design hydraulic conductivity, design thickness, and porosity of the geocomposite selected for use in the final cover stormwater collection system at various loads using manufacturer's testing data. The calculations for the long-term transmissivity values of the geocomposite are based on 100-hour transmissivity values.

REFERENCES:

1. Attachment 1 - GRI Standard - GC8 Technical Release, April 17, 2001, Revised January 9, 2013
2. Attachment 2 - Test results for 100 hour transmissivity values.
3. Attachment 3 - Soil properties
4. Attachment 4 - Factor of Safety

PROCEDURE:

1. The design geocomposite hydraulic conductivities are calculated by adjusting manufacturer’s transmissivity and thickness.
2. The geocomposite properties are adjusted based on the manufacturer’s recommendations and GRI Standard - GC8 to determine geocomposite properties at various specific loads of interest.
3. Calculate 100-hour transmissivity, q_{100}, at the loads of interest using manufacturer’s data.
4. Calculate geocomposite thickness at the loads of interest using manufacturer’s data.
5. Calculate the geocomposite transmissivity after applying reduction factors.
6. Calculate the design transmissivity.
7. Calculate the design hydraulic conductivity from the design transmissivity and design thickness.

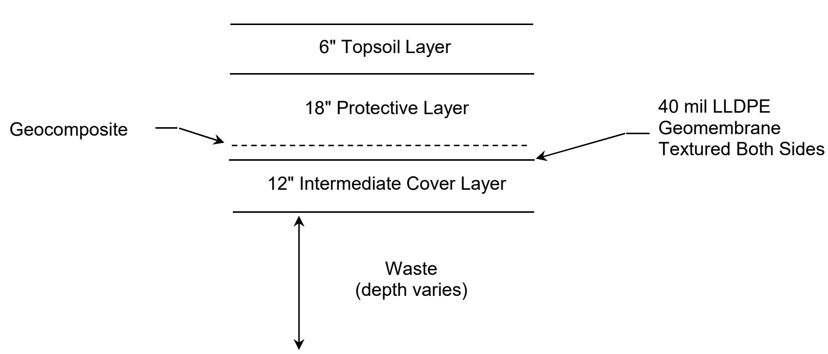

CLIENT	PROJECT	JOB NO.
Hillsborough County	Southeast County Landfill	09215600.13

SUBJECT	BY	DATE
Geocomposite Transmissivity/Hydraulic Conductivity Calculations	FCH	11/1/2021
Phase I - VI Closure	CHECKED	DATE
	KLS	11/16/2021

EQUATIONS:

Developed from Equations (1) and (2) pg GC8-3 - Refer to Attachment 1.

$$\theta_{allow} = (\theta_{ultimate})/RF_{IN} * RF_{CC} * RF_{BC} * RF_{CR} * FS)$$

Where:

θ_{allow} = Allowable transmissivity

$\theta_{ultimate}$ = Ultimate transmissivity (manufacturer's) under simulated conditions for 100 hours

RF_{IN} = Reduction Factor for elastic deformation, or intrusion of the adjacent geotextiles into the drainage channel. Since there is no long-term thickness data for material, use manufacturer provided Creep Reduction Factor at 100-hous for the design, as provided in Attachment 2

RF_{CC} = Reduction Factor for Chemical Clogging and/or precipitation of chemicals in the drainage core space

RF_{BC} = Reduction Factor for Biological Clogging in the drainage core space

RF_{CR} = Reduction Factor for Creep deformation of the drainage core and/or adjacent geotextile into the drainage channel

FS = Factor of Safety

$$RF_{CR} = \left[\frac{(t'/t) - (1 - n_{original})}{(t_{CR}/t) - (1 - n_{original})}\right]^3$$

Equation (6) pg GC8-7 - Attachment 1.

Where:

t' = Thickness at 100 hours

t = Virgin thickness

t_{CR} = Thickness at >>100 hours

$n_{original}$ = Original porosity

$= 1 - (\mu/\rho t)$ Equation (7) pg GC8-7 - Attachment 1.

μ = mass per unit area

ρ = density of formation

$$k = \frac{\theta_{allow}}{t'}$$

Developed from Equations (3) and (4) pg GC8-5 - Attachment 1.

Where:

k = Hydraulic conductivity, cm/sec

t' = Thickness at 100 hours

NOTES: RF_{IN} accounts for the geotextile encroaching on the geonet under a constant loading. A 100-hour transmissivity test accounts for intrusion. After the 100-hour seat time, the geotextile has already begun to intrude into the geonet, therefore, the transmissivity value reflects the intrusion. The transmissivity values for these calculations are all based on the 100-hour test, therefore, RF_{IN} = 1.0.

SCS ENGINEERS

SHEET 3 OF 5

CLIENT	PROJECT	JOB NO.
Hillsborough County	Southeast County Landfill	09215600.13

SUBJECT	BY	DATE
Geocomposite Transmissivity/Hydraulic Conductivity Calculations	FCH	11/1/2021
Phase I - VI Closure	CHECKED	DATE
	KLS	11/16/2021

OBJECTIVE: To determine the load on the final cover liner geocomposite under closed conditions.

KNOWN: Landfill closure cross-section.

Topsoil =	138.0	pcf	Refer to Attachment 2
Protective Cover =	138.0	pcf	Refer to Attachment 2

FINAL CLOSURE CONDITION - 54-INCH MAXIMUM DEPTH FINAL COVER:

Material	Material Density (pcf)	Depth of Material (ft)	Load (psf)		
Topsoil	138.0	0.5	69.0		
Protective Cover	138.0	5.0	690.0		
Total		5.5	759.0	<=	1,000

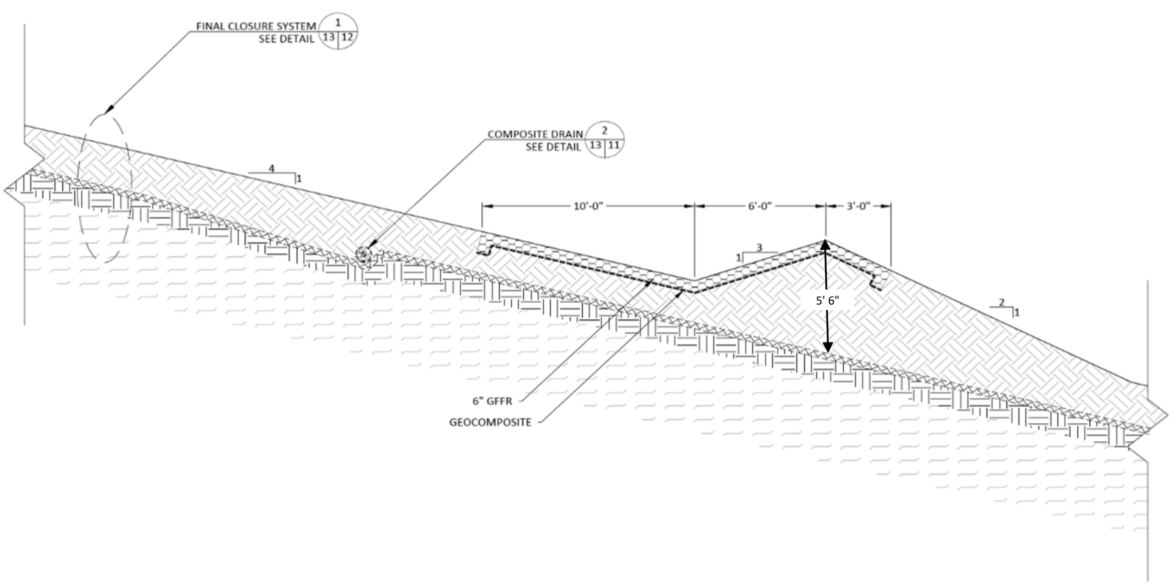

NOTES: Depth of material accounts for the thickness of soil along the side slope of the landfill.
The greater the depth of the soil, the larger the amount of loading the geocomposite could experience.
The depth of soil (5' 6") located at the berm is used to calculate the greatest load the geocomposite will experience.

CLIENT	PROJECT	JOB NO.
Hillsborough County	Southeast County Landfill	09215600.13

SUBJECT	BY	DATE
Geocomposite Transmissivity/Hydraulic Conductivity Calculations	FCH	11/1/2021
Phase I - VI Closure	CHECKED	DATE
	KLS	11/16/2021

PURPOSE: Calculate the design transmissivity, k, of a geocomposite under site specific boundary conditions for final closure loading conditions.

REFERENCES: From the AGRU technical department, the following Transmissivity (θ) and Creep values are known:

Plate/Sand/GC/Plate Manufacturer's 100 hour q_{100} Data Transmissivity	
@ 25% Gradient*	
Load (psf)	$q_{ultimate}$ (m^2/sec)
1,000	1.72E-03

* Value for 33% gradient was used for calculations.
No data available for 1,000 psf at 25% gradient.

Refer to Attachment 3

Sand/GC/GM Creep	
@ 25% Gradient	
Load (psf)	RF_{CR}
1,000	1.01

Refer to Attachment 3

Plate/Sand/GC/Plate Manufacturer's 100 hour q_{100} Data Transmissivity	
@ 5% Gradient	
Load (psf)	$q_{ultimate}$ (m^2/sec)
1,000	3.30E-03

Refer to Technical Specifications which specify a minimum transmissivity and minimum thickness for top-of-crown geocomposite

Sand/GC/GM Creep at 100-hours	
@ 5% Gradient	
Load (psf)	RF_{CR}
1,000	1.01

Refer to Attachment 3

REDUCTION FACTORS:

RF - Intrusion, RF_{IN}
RF - Chemical Clogging, RF_{CC}
RF - Biological Clogging, RF_{BC}
RF - Creep, RF_{CR}
FS - Factor of Safety

Chemical Clogging RF_{CC} =	1.0	to	1.2	Refer to Attachment 1 pg GC8-9
Biological Clogging RF_{BC} =	1.2	to	3.5	Refer to Attachment 1 pg GC8-9

EQUATIONS:

$$\theta_{allow} = (\theta_{ultimate})/RF_{IN}*RF_{CC}*RF_{BC}*RF_{CR}*FS)$$

$$t' = (t)/(RF_{CR})$$

$$k = (\theta_{allow})/(t')$$

CLIENT	PROJECT	JOB NO.
Hillsborough County	Southeast County Landfill	09215600.13

SUBJECT	BY	DATE
Geocomposite Transmissivity/Hydraulic Conductivity Calculations	FCH	11/1/2021
Phase I - VI Closure	CHECKED	DATE
	KLS	11/16/2021

FINAL CLOSURE CONDITION - 54-INCH MAXIMUM DEPTH FINAL COVER:

REDUCTION FACTORS:

RF_{IN} =	1.00	Refer to Calculation Page 2 Note	thickness, t =	300	mil
RF_{CC} =	1.00	Refer to Attachment 1 pg GC8-9		0.3	inches
RF_{BC} =	1.35	Refer to Attachment 1 pg GC8-9		0.762	cm
RF_{CR} =	1.01	Refer to Attachment 2			
FS =	2.00	Refer to Attachment 4			

@ 25% Gradient (Sideslopes)					
Load (psf)	$\theta_{Ultimate}$ (m^2/sec)	θ_{allow} (m^2/sec)	θ_{allow} (cm^2/sec)	*t' (cm)	k (cm/sec)
1,000	1.72E-03	6.31E-04	6.31	0.75446	8.36

Thickness at 100 hrs. **t' = 0.297 inches**

REDUCTION FACTORS:

RF_{IN} =	1.00	Refer to Calculation Page 2 Note	thickness, t =	330	mil
RF_{CC} =	1.00	Refer to Attachment 1 pg GC8-9		0.33	inches
RF_{BC} =	1.35	Refer to Attachment 1 pg GC8-9		0.8382	cm
RF_{CR} =	1.01	Refer to Attachment 2			
FS =	2.00	Refer to Attachment 4			

@ 5% Gradient (Top-of-crown)					
Load (psf)	$\theta_{Ultimate}$ (m^2/sec)	θ_{allow} (m^2/sec)	θ_{allow} (cm^2/sec)	*t' (cm)	k (cm/sec)
1,000	3.30E-03	1.21E-03	12.10	0.8299	14.58

Thickness at 100 hrs. **t' = 0.327 inches**

25% GRADIENT FOR VENEER STABILITY CALCULATIONS:

REDUCTION FACTORS:

FS[1] = 1.50

@ 25% Gradient for Veneer Stability					
Load (psf)	$\theta_{Ultimate}$ (m^2/sec) [2]	θ_{allow} (m^2/sec)	θ_{allow} (cm^2/sec)	*t' (cm)	k (cm/sec)
Load (psf)	1.72E-03	8.41E-04	8.41	0.75446	11.15

Thickness at 100 hrs. **t' = 0.297 inches**

"For θ_{allow} @ 25% gradient for Veneer Stability Calculation"

Notes for Veneer Stability Calculations:

1. Factor of safety adjusted from 2 to 1.5 as an additional factor of safety is applied in the veneer stability calculations.
2. A more conservative (33% gradient) θultimate value was used for 25% gradient.

Attachment 9

Aggregates

DIVISION III MATERIALS

AGGREGATES

SECTION 901
COARSE AGGREGATE

901-1 General.

901-1.1 Composition: Coarse aggregate shall consist of naturally occurring materials such as gravel, or resulting from the crushing of parent rock, to include natural rock, slags, expanded clays and shales (lightweight aggregates) and other approved inert materials with similar characteristics, having hard, strong, durable particles, conforming to the specific requirements of this Section.

Coarse aggregate for use in pipe backfill under wet conditions, underdrain aggregate, or concrete meeting the requirements of Section 347 may consist of reclaimed portland cement concrete meeting the requirements of 901-5. Coarse aggregate for use in bituminous mixtures may consist of reclaimed portland cement concrete meeting the requirements of 901-5, except that the reclaimed concrete shall be from a concrete mix which was produced and placed in accordance with applicable Department Specifications.

Materials substantially retained on the No. 4 sieve, shall be classified as coarse aggregate.

Approval of mineral aggregate sources shall be in accordance with 6-2.3.

901-1.2 Deleterious Substances: All coarse aggregates shall be reasonably free of clay lumps, soft and friable particles, salt, alkali, organic matter, adherent coatings, and other substances not defined which may possess undesirable characteristics. The weight of deleterious substances shall not exceed the following percentages:

Coal and lignite (AASHTO T 113)................................1.00
Soft and friable particles (AASHTO T 112)*................2.00
Clay lumps (AASHTO T 112)*.....................................2.00
Plant root matter (visual inspection in
AASHTO T 27)****...0.005
Wood and wood matter (visual inspection in
AASHTO T 27)****...0.005
Cinders and clinkers..0.50
Free shell**...1.00
Total Material passing the No. 200 sieve (FM 1-T 011)
At Source with Los Angeles Abrasion less than or equal
to 30 ....2.50
At Source with Los Angeles Abrasion greater than
30...1.75
At Point of Use..3.75
Fine-Grained Organic Matter (AASHTO 194)...............0.03
Chert (less than 2.40 specific gravity SSD)
(AASHTO T-113)***...3.00

* The maximum percent by weight of soft and friable particles and clay lumps together shall not exceed 3.00.

** Aggregates to be used in asphalt concrete may contain up to 5% free shell. Free shell is defined as that portion of the coarse aggregate retained on the No. 4 sieve consisting of loose, whole, or broken shell, or the external skeletal remains of other marine life, having a ratio of the maximum length of the particle to the shell wall thickness exceeding five to one. Coral, molds, or casts of other shells, and crushed clam and oyster shell indigenous to the formation will not be considered as free shell.

*** This limitation applies only to coarse aggregates in which chert appears as an impurity. It is not applicable to aggregates which are predominantly chert.

**** Plant root matter, and wood and wood matter shall be considered deleterious when any piece exceeds two inches in length or 1/2 inch in width.

The weights of deleterious substances for reclaimed Portland cement concrete aggregate shall not exceed the following percentages:

Bituminous Concrete 1.00
Bricks 1.00
Wood and other organic substances (by weight)***** 0.1
Reinforcing Steel and Welded Wire Fabric......................0.1
Plaster and gypsum board 0.1
Joint Fillers 0.1
***** Supersedes requirement for other coarse aggregate

901-1.3 Physical Properties: Coarse aggregates shall meet the following physical property requirements, except as noted herein:

Los Angeles Abrasion (FM 1-T 096) ....maximum loss 45%
Soundness (Sodium Sulfate) AASHTO T104 ....
....maximum loss 12%*
Flat or elongated pieces** .... maximum 10%

* For source approval - aggregates exceeding soundness loss limitations will be rejected unless performance history shows that the material will not be detrimental for portland cement concrete or other intended usages.

** A flat or elongated particle is defined as one having a ratio between the maximum and the minimum dimensions of a circumscribing prism exceeding five to one.

901-1.4 Gradation: Coarse aggregates shall conform to the gradation requirements of Table 1, when the stone size is specified. However, Table 1 is waived for those aggregates intended for usage in bituminous mixtures, provided the material is graded on sieves specified in production requirements contained in 6-2.3, and meets uniformity and bituminous design requirements.

TABLE 1
Standard Sizes of Coarse Aggregate

Amounts Finer than Each Laboratory Sieve (Square Openings), weight percent								
Size No.	Nominal Size Square Openings	4 inches	3 1/2 inches	3 inches	2 1/2 inches	2 inches	1 1/2 inches	1 inch

TABLE 1 Standard Sizes of Coarse Aggregate								
Amounts Finer than Each Laboratory Sieve (Square Openings), weight percent								
Size No.	Nominal Size Square Openings	4 inches	3 1/2 inches	3 inches	2 1/2 inches	2 inches	1 1/2 inches	1 inch
1	3 1/2 to 1 1/2 inches	100	90 to 100	-	25 to 60	-	0 to 15	-
2	2 1/2 inches to 1 1/2 inches	-	-	100	90 to 100	35 to 70	0 to 15	-
24	2 1/2 inches to 3/4 inch	-	-	100	90 to 100	-	25 to 60	-
3	2 inches to 1 inch	-	-	-	100	90 to 100	35 to 70	0 to 15
357	2 inches to No. 4	-	-	-	100	95 to 100	-	35 to 70
4	1 1/2 inches to 3/4 inch	-	-	-	-	100	90 to 100	20 to 55
467	1 1/2 inches to No. 4	-	-	-	-	100	95 to 100	-
5	1 inch to 1/2 inch	-	-	-	-	-	100	90 to 100
56	1 inch to 3/8 inch	-	-	-	-	-	100	90 to 100
57	1 inch to No. 4	-	-	-	-	-	100	95 to 100
6	3/4 inch to 3/8 inch	-	-	-	-	-	-	100
67	3/4 inch to No. 4	-	-	-	-	-	-	100
68	3/4 inch to No. 8	-	-	-	-	-	-	-
7	1/2 inch to No. 4	-	-	-	-	-	-	-
78	1/2 inch to No. 8	-	-	-	-	-	-	-
8	3/8 inch to No. 8	-	-	-	-	-	-	-
89	3/8 inch to No. 16	-	-	-	-	-	-	-
9	No. 4 to No. 16	-	-	-	-	-	-	-
10	No. 4 to 0	-	-	-	-	-	-	-

TABLE 1 (Continued) Standard Sizes of Coarse Aggregate								
Amounts Finer than Each Laboratory Sieve (Square Openings), weight percent								
Size No.	Nominal Size Square Openings	3/4 inch	1/2 inch	3/8 inch	No. 4	No. 8	No. 16	No. 50
1	3 1/2 inches to 1 1/2 inches	0 to 5						
2	2 1/2 inches to 1 1/2 inches	0 to 5						

TABLE 1 (Continued) Standard Sizes of Coarse Aggregate								
Amounts Finer than Each Laboratory Sieve (Square Openings), weight percent								
Size No.	Nominal Size Square Openings	3/4 inch	1/2 inch	3/8 inch	No. 4	No. 8	No. 16	No. 50
24	2 1/2 inches to 3/4 inch	0 to 10	0 to 5					
3	2 inches to 1 inch	-	0 to 5					
357	2 inches to No. 4	-	10 to 30	-	0 to 5			
4	1 1/2 inches to 3/4 inch	0 to 15	-	0 to 5				
467	1 1/2 inches to No. 4	35 to 70	-	10 to 30	0 to 5			
5	1 inch to 1/2 inch	20 to 55	0 to 10	0 to 5				
56	1 inch to 3/8 inch	40 to 85	10 to 40	0 to 15	0 to 5			
57	1 inch to No. 4	-	25 to 60	-	0 to 10	0 to 5		
6	3/4 inch to 3/8 inch	90 to 100	20 to 55	0 to 15	0 to 5			
67	3/4 inch to No. 4	90 to 100	-	20 to 55	0 to 10	0 to 5		
68	3/4 inch to No. 8	90 to 100	-	30 to 65	5 to 25	0 to 10	0 to 5	
7	1/2 inch to No. 4	100	90 to 100	40 to 70	0 to 15	0 to 5		
78	1/2 inch to No. 8	100	90 to 100	40 to 75	5 to 25	0 to 10	0 to 5	
8	3/8 inch to No. 8	-	100	85 to 100	10 to 30	0 to 10	0 to 5	
89	3/8 inch to No. 16	-	100	90 to 100	20 to 55	0 to 30	0 to 10	0 to 5
9	No. 4 to No. 16	-	-	100	85 to 100	10 to 40	0 to 10	0 to 5
10	No. 4 to 0	-	-	100	85 to 100	-	-	-

The gradations in Table 1 represent the extreme limits for the various sizes indicated which will be used in determining the suitability for use of coarse aggregate from all sources of supply. For any grade from any one source, the gradation shall be held reasonably uniform and not subject to the extreme percentages of gradation specified above.

901-2 Natural Stones.

Course aggregate may be processed from gravels, granites, limestones, dolomite, sandstones, or other naturally occurring hard, sound, durable materials meeting the requirements of this Section.

901-2.1 Gravels: Gravel shall be composed of naturally occurring quartz, free from deleterious coatings of any kind. The minimum dry-rodded weight AASHTO T19 shall be 95 lb/ft^3.

Crushed gravel shall consist of a minimum of 85%, by weight, of the material retained on the No. 4 sieve, having at least three fractured faces.

901-2.2 Granites: Coarse aggregate produced from the crushing of granites shall be sound and durable. For granites to be used in bituminous mixtures and surface treatments, the Los Angeles Abrasion requirement of 901-1.3 is modified to permit a maximum loss up to 50 (FM 1-T 096). Maximum amount of mica schist permitted is 5% (FM 5-584).

901-2.3 Limestones, Dolomite and Sandstone: Coarse aggregates may be produced from limestone, dolomite, sandstones, and other naturally occurring hard, durable materials meeting the requirements of this Section.

Pre-Cenozoic limestones and dolomite shall not be used as crushed stone aggregates either coarse or fine for Asphalt Concrete Friction Courses, or any other asphalt concrete mixture or surface treatment serving as the final wearing course. This specifically includes materials from the Ketone Dolomite (Cambrian) Newala Limestone (Mississippian), and Northern Alabama and Georgia.

As an exception to the above up to 20% fine aggregate from these materials may be used in asphalt concrete mixtures other than Friction Courses which serve as the final wearing course.

901-2.4 Cemented Coquina Rock: For Cemented Coquina Rock to be used in bituminous mixtures, the Los Angeles Abrasion requirement of 901-1.3 is modified to permit a maximum loss up to 50 (FM 1-T 096) provided that the amount of material finer than No. 200 generated during the Los Angeles Abrasion test is less than 18%.

901-3 Manufactured Stones.

901-3.1 Slags: Coarse aggregate may be produced from molten nonmetallic by-products consisting essentially of silicates and aluminosilicates of calcium and other bases, such as air-cooled blast-furnace slag or phosphate slag, provided it is reasonably uniform in density and quality, and reasonably free from deleterious substances as specified in 901-1.2. In addition, it must meet the following specific requirements:

Sulphur content .... not more than 1.5%
Dry rodded weight AASHTO T 19..................... minimum 70 lb/ft^3
Glassy Particles .... not more than 10%

Slag shall not be used as an aggregate for Portland cement concrete.

For Air-Cooled Blast Furnace Slag, the Los Angeles Abrasion requirement of 901-1.3 is modified to permit a maximum loss up to 50 (FM 1-T 096) provided that the amount of material finer than No. 200 sieve generated during the Los Angeles Abrasion test is less than 18%.

901-4 Lightweight Aggregates.

901-4.1 Lightweight Coarse Aggregate for Bituminous Construction: Lightweight coarse aggregate may be produced from naturally occurring materials such as pumice, scoria and tuff or from expanded clay, shale or slate fired in a rotary kiln. It shall be reasonably uniform in quality and density, and free of deleterious substances as specified in 901-1.2, except that the term cinders and clinkers shall apply to those particles clearly foreign to the extended aggregate in question.

In addition, it must meet the following specific requirements:

Material passing the No. 200 Sieve ....maximum 3.00%, (FM 1-T 011)
Dry loose weight (AASHTO T 19)*....... 33-55 lb/ft^3
Los Angeles Abrasion (FM 1-T 096) maximum 35%
Ferric Oxide (ASTM C 641)......... maximum 1.5 mg

* Source shall maintain dry-loose unit weight within plus or minus 6% of Quality Control average. Point of use dry-loose unit weight shall be within plus or minus 10% of Source Quality Control average.

901-4.2 Lightweight Coarse Aggregate for Structural Concrete: The requirements of 901-4.1 are modified as follows:

Aggregates shall not be produced from pumice and scoria.

Los Angeles Abrasion (FM 1-T 096, Section 12) shall be 45%, maximum.

Gradation shall meet the requirements of AASHTO M195 for 3/4 inch, 1/2 inch and 3/8 inch.

901-5 Reclaimed Portland Cement Concrete.

The reclaimed portland cement concrete shall be crushed and processed to provide a clean, hard, durable aggregate having a uniform gradation free from adherent coatings.

The Contractor's (Producer's) crushing operation shall produce an aggregate meeting the applicable gradation requirements. The physical property requirements of 901-1.3 for soundness shall not apply and the maximum loss as determined by the Los Angeles Abrasion (FM 1-T 096) is changed to 50.

The sources of reclaimed portland cement concrete will be treated as a mine and subject to the requirements of Section 6 and Section 105. These sources shall qualify as facilities generating clean debris, defined in Rule 62-701.200(15), Florida Administrative Code (FAC), as uncontaminated concrete exempt from solid waste regulation in accordance with Rule 62-701.220(2)(f), FAC.

If the Department determines that the concrete has been contaminated with petroleum products or lead-based paint, the concrete shall not be considered clean debris and the source shall be required to be permitted and to perform testing in accordance with Rule 62-701, FAC, subject to any ensuing enforcement action by the Florida Department of Environmental Protection.

Concrete shall be asbestos free.

Operators of demolition recycling facilities shall demonstrate that they are in compliance with 40 Code of Federal Regulations (CFR) 61.141 and 61.145. Notification requirements from each owner or operator of a demolition or renovation activity supplying reclaimed concrete shall be available at the recycling facility.

901-6 Exceptions, Additions and Restrictions.

Pertinent specification modifications, based on material usage, will be found in other Sections of the specifications.

Attachment 10

CAT Tire Pressure

2016 Cat® Tire Maintenance Guide

Tire and Service Literature Information

Safety Recommendations

Safety Instructions

Any tire, no matter how well constructed, may fail as a result of punctures, impact damage, improper inflation, or other conditions resulting from use or misuse. Tire failure may create a risk of property damage, personal injury, or death. To reduce the risk of tire failure, read and follow all safety information contained in this manual and in industry publications.

The safety related information provided in this manual is designed to assist supervisory and service technicians in servicing rim wheel assemblies. Responsibility for implementing these safety guidelines rests with supervisors and service technicians doing the actual service work. Read and fully understand all procedures before attempting to service a rim wheel assembly.

These instructions are not designed to apply to any specific tire, rim, or rim wheel assembly. Therefore, contact the tire, rim, or rim wheel assembly manufacturer for correct servicing procedures. Always follow instructions from the manufacturers of the tires, rim, and vehicle for deflating, demounting, and inflating . Always follow applicable industry guidelines when servicing rim wheel assemblies. Also, follow all State and Federal health and safety laws and/or local regulations.

Never perform inspection, service, or inflation operations while in the rim wheel assembly trajectory path.

Misapplication, improper inflation, overloading, and exceeding maximum speed may cause tire failure, possibly resulting in injury or death. Proper care is your responsibility. If you have any doubt about the correct, safe method of performing any step in the demounting, mounting, adding or removing fill, or inflating process – STOP! Seek out expert assistance from a qualified person.

Inspection Checklist

Many tire failures are preceded by vibration, bumps, bulges, or irregular wear. Have vehicle operators report any unusual vibrations and perform regularly scheduled inspections on all tires.

– Inspect tires for excessive wear, damage, or imperfections that may affect the wear life and capacity of tires. Replace any tires that appear to show signs of excessive wear, are damaged, or defective in any way

– Inspect tires for cuts, cracks, splits, or bruises in the tread and sidewall area. Bumps or bulges may indicate tire separation within the tire body.

– Inspect tires for a safe tread depth. Any tire worn to the built-in wear indicators (where available) or less tread groove depth or with a tire cord or fabric exposed must be replaced immediately.

– Inspect tired for uneven wear. Wear on one side of the tread or flat spots in the tread may indicate a problem with the tire or the vehicle.

– Remove water and foreign material from the tire. Tires and tubes with excessive or uneven wear, cracks, tears, punctures, blisters
and /or other damage may explode during inflation of service. If potential failure of a tire or tube is suspected, destroy the tire or tube
and replace it with a serviceable tire or tube of the correct size, type, and manufacture for the assembly, machine, and application.

– When conducting routine tire inspections, also make a visual inspection of tire and rim parts. Always replace any parts found
to have damage or non-conformities. Parts that are cracked, worn, pitted with corrosion, or damaged must be destroyed and
replaced with serviceable parts.

– Always inspect both sides of the tire to assure a proper bead seat. When conducting routine tire inspections also make a visual inspection of wheel and rim components. Always correct any damage found.

Safety Checklist

Rims

– Always use approved tire and rim combinations for sizes and contours.
– Always verify that part umbers and size designations of rims match machine specs.
– DO NOT use a steel hammer on any part of the rim, because this can damage the rim. If you must reposition tire or rim parts, use a rubber, plastic, or brass-faced hammer.
–Never try to repair a rim assembly
– Rims that are cracked, worn, pitted with corrosion, or otherwise damaged must be destroyed and replaced with serviceable parts.
– Destroy old rims. Using damaged rims can result in serious injury or death.

Tires

– Always replace damaged or badly worn tires. When replacing tires, always use the recommended replacement.
– Destroy old tires. Using badly worn or damaged tires can result in serious injury or death.
– Never put flammable substances in a rim wheel assembly, such as starting fluid, ether, gasoline, or any other flammable material to lubricate, seal, or seal the bead of tire. Never attempt to seal tire beads by igniting flammable substances on the rim wheel assembly. These actions can cause an explosion resulting in serious injury or death.

– Never reinflate a tire that has lost air pressure without determining and correcting the problem.

Inflation

– Always exhaust all air from the tire prior to demounting
– Always use restraining devices (safety cages) when inflating tires. Not using a restraining device or safety cage can result in serious injury or death.
– Always use a clip-on air chuck and a hose that is long enough to allow you to stand outside the tire trajectory. The air line must be equipped with an in-line valve with a pressure gauge or a regulator that can be preset.
– Never inflate a tire beyond 2.41 bar (35 psi) to seat a tire bead. Always inspect both sides of the tire to assure a proper bead seat. If the tire bead is not fully seated at 2.41 bar (35 psi): STOP! Deflate the tire and correct the problem.
– Never exceed manufacturer's recommended tire inflation pressure. Misapplication, improper inflation, and overloading a vehicle may cause tire failure resulting in serious injury or death.

Wheel Assembly

– Servicing tires and rims can be extremely dangerous and should be performed by trained personnel only, using the correct tools, and following the procedures presented in this manual, in OEM manufacturers' manuals, or in other industry and
government instructions.
– Never leave a rim wheel assembly unsecured in a vertical position.
– Always be careful when moving tires and rims to prevent endangering bystanders.
– Always use proper lifting techniques or mechanized lifting aids to move heavy objects, assemblies, components, and parts. DO NOT attempt to lift objects that are too heavy.

Safety Recommendations

Safety Checklist (Cont'd.)

– Failure to chock the tires and crib the vehicle can result in serious injury or death. DO NOT work under an unblocked load.
– Several types of tire changing equipment are available. Installers should be fully trained in correct operating procedures and safety instructions for the specific equipment being used. Always read and understand any manufacturer's warning contained in the product literature or attached to the equipment.
– Never hammer, strike, or pry an inflated or partly inflated rim wheel assembly. If any rim part does not seat correctly, deflate the tire and inspect the rim wheel assembly. If any rim part does not seat correctly, deflate the tire and inspect for warped or incorrectly seated parts, such as lock rings.
– If the rim wheel assembly does not slide on the vehicle: DO NOT force the rim wheel assembly by hammering it. Deflate the tire and inspect the rim wheel assembly.
– NEVER weld on an inflated or partially inflated rim wheel assembly, because it may cause an explosion, resulting in serious injury or death.

General Technician Warnings

Training

Servicing tires and rims should only be performed by trained personnel using proper tools and following specific procedures. Servicing tires and rims can be extremely dangerous and failure to follow these warnings could lead to serious injury or death.

Any person assigned to service rim wheel assemblies must be able to demonstrate and maintain the ability to service rim wheel assemblies safely, including (but not limited to):

- handling rim wheel assemblies,
- demounting tires (including deflation),
- installing and removing rim wheel assemblies,
- inspecting and identifying rim parts,
- mounting tires (including tire inflation with the required safeguards),
- inflating a tire on a rim assembly while it is mounted on the vehicle,
- using a restraining device or barrier,
- standing outside the trajectory path during inflation of the tire, and
- inspecting the rim wheel assembly following inflation of the tire.

Slips or Falls

Personal injury can result from slips or falls. DO NOT leave tools or parts laying around the work area and clean up all spilled fluids immediately

General Technician Warnings (Cont'd.)

Pinch Points

Keep loose clothing and fingers away from pinch areas to prevent pinching and crushing. It is recommended to remove finger rings.

Eye Protection

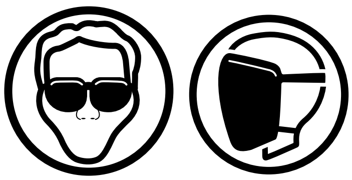

To avoid eye injury, always wear protective glasses or face shield when using any equipment, a hammer, or similar tool. Chips and debris can fly off objects when struck. Make sure no one can be injured by flying debris before striking any object.

Proper Techniques

To prevent personal injury, always use proper lifting techniques or mechanized lifting aids to move heavy objects, assemblies, and parts. DO NOT attempt to lift objects that are too heavy.

Hoist Awareness

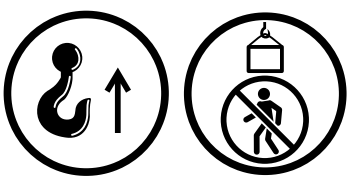

When a hoist is used to lift any part or assembly, stand clear of the area under the part being raised. Make sure the lifting cables and other lifting devices are strong enough to support the part.

Eye Protection

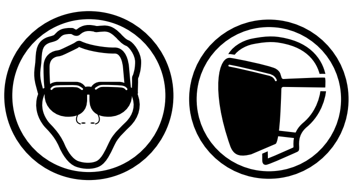

To avoid eye injury, always wear protective glasses or face shield. Make sure no one can be injured by flying objects or debris when using tools or working on the equipment or the vehicle.

Air Protection

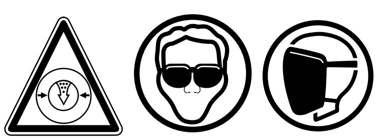

Personal injuries can occur as a result of using pressurized air. Maximum air pressure at the nozzle must be below 205 kPa (30 psi) for cleaning purposes. Wear protective clothing, protective glasses, and a protective face shield when using pressure air or when releasing pressure air from a tire.

Protective Gear

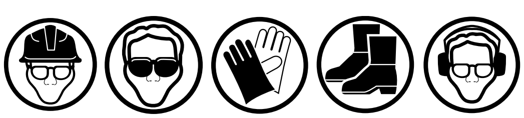

To avoid serious personal injury, always wear proper protective gear, such as hard hats, safety glasses, gloves, steel toe shoes, and hearing protection when servicing tires and rims.

General Technician Warnings (Cont'd.)

Matching Tires, Rims, and Rim Parts
Always use approved tire and rim combinations, sizes, contours, and tapers. Most tires will fit on more than one rim width. Always use the correct tire for the rim.

There is a danger of serious injury or death if a tire of one bead diameter is installed on a rim with a different diameter. Always replace a tire with another tire of exactly the same bead diameter designation and suffix letters.

Example

- Mount a 16 inch tire on a 16 inch rim.
- Never mount a 16 inch tire on a 16.1 inch or 16.5 inch rim.
- Mount a 16.5 inch tire on a 16.5 inch rim.
- Never mount a 16.5 inch tire on a 16 inch or 16.1 inch rim.

Repairing Tires and Rims

DO NOT make any repairs to a tire unless the repairs are authorized and recommended by the tire industry and/or tire manufacturer.

Never drive on an improperly repaired tire, which may cause further damage and eventual tire failure resulting in personal injury or death.

Never repair a tire without removing the tire from the rim assembly and never use a tube as a substitute for a tire repair or replacement. Always use an inside patch and a plug to repair a tire unless the hole is too small to insert a plug. DO NOT use a plug without an inside patch to repair a tire.

Never repair a tire with less tread than the tread wear indicators (where available), with a puncture larger than 6.4 mm (.25 in)diameter, and/or damage outside the tread or sidewall area. These tires must be replaced because they cannot be safely repaired.

DO NOT attempt to repair a tire using an aerosol fixer to inflate and seal the tire. An aerosol fixer may contain highly volatile gas that can be ignited by an excessive heat source, flame, or sparks, Any tire with an aerosol fixer must be removed from all heat sources and be completely deflated before removing the tire from the rim.

Tire Changing Equipment / Tools

Several types of tire changing equipment are available and service technicians must be fully trained in the correct safety procedures and instructions for any specific tire changing machine. Always read and understand any warnings contained in the manufacturer's manuals or attached to the equipment.

If used, keep a firm grip on tire irons. They may spring back, resulting in personal injury.

When using a bead breaker, always stand to one side of the rim to maintain control of the bead breaker and DO NOT hold the bead breaker when breaking the tire bead. If the bead breaker is not seated properly and flies off the rim, it could cause serious injury or death.

Pressure

Warning

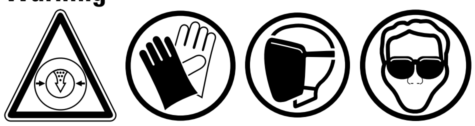

Personal injury can result from pressurized air. When releasing pressure air from the tire, wear a protective face shield or protective glasses.

Pressure

Always purge all air from the tire prior to demounting. Never reinflate a tire that has lost air pressure without determining and correcting the problem. Never exceed 241 kPa (35 psi) or the maximum tire inflation pressure when seating beads. Never exceed the manufacturer's recommended tire inflation pressure. Always use restraining devices (safety cages) when inflating tires.

Misapplication, improper inflation, overloading the vehicle, or exceeding maximum speed may cause tire failure resulting in injury or death.

Never inflate a tire unless it is secured to the vehicle or enclosed in a restraining device. Never reinflate a tire that has lost air pressure or operate a vehicle with a tire that has been reinflated without determining and correcting the problem.

Driving on damaged or underinflated tires is dangerous. Underinflated tires may:
- reduce the wear life of the tire,
- adversely affect vehicle handling,
- increase fuel consumption,
- become overheated, and damage the tire resulting in tire failure.

Check air pressure at least once a week and make sure the air pressure gauge is accurate. If tires lose more than 14 kPa (2 psi) per month, the tire, the valve, or rim assembly may become damaged, creating a dangerous situation, and possibly resulting in serious injury or death.

Check the air pressure when tires are "cold". Tires are "cold" when the vehicle has been driven less than a mile at moderate speed or after being stopped for three or more hours.

Never exceed a manufacturer's recommended tire inflation pressure. If air pressure must be added when a tire is hot, add 28 kPa (4 psi) above the recommended "cold" air pressure and recheck the inflation pressure when the tire is "cold".

Driving on tires with too much air pressure can be dangerous. Tires with too much air pressure are more likely to be cut, punctured, or broken by sudden impact.

Never release air from a "hot" tire to reach the recommended "cold" tire air pressure. Normal driving causes tires to run hotter and air pressure to increase. If air is released from a "hot" tire it may cause the tire to be dangerously underinflated.

Tire Maintenance

Deflating Tires

⚠ Deflating Tires

To prevent personal injury or death, DO NOT attempt to repair a rim wheel assembly until you are certain the tire has been deflated appropriately. Always remove the valve core and exhaust all possible air from the tire prior to demounting. Always deflate tires before removing the rim or a rim part, such as a rim clamp or nut.

NOTE:

The configuration of the valve stem will not be the same for every tire.

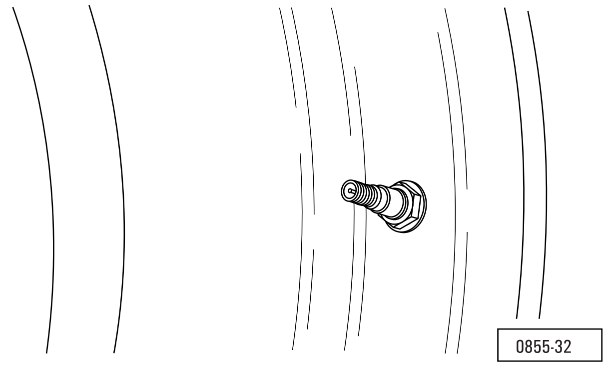

Step 1

Use a valve core removal tool to remove the valve core.

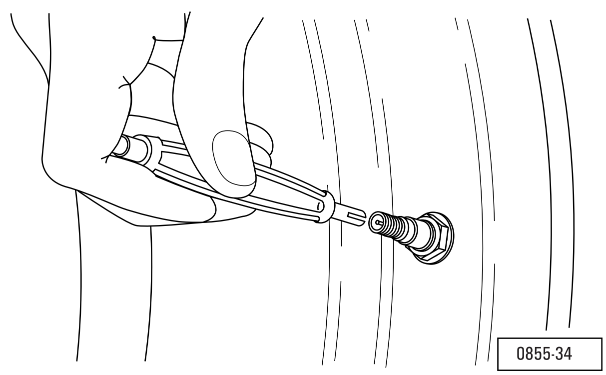

⚠ WARNING

Use extreme caution when removing the valve core from a tire with liquid filler. Pressure on the valve core could cause the valve core to be violently propelled, resulting in severe injury. Avoid standing in the trajectory path of the valve stem when removing the valve core.

Step 2

Turn the valve core counterclockwise for removal and clockwise for installation.

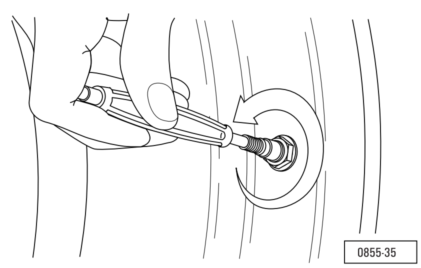

Deflating Tires (Cont'd.)

Step 3

With the valve core removed, run a wire inside the valve stem to make sure the valve stem is not plugged and all possible air is released. If the tire is part of a dual tire assembly, make sure the air is removed from both tires.

NOTICE: DO NOT puncture, rupture, bend, or twist the valve stem while releasing air from the tire.

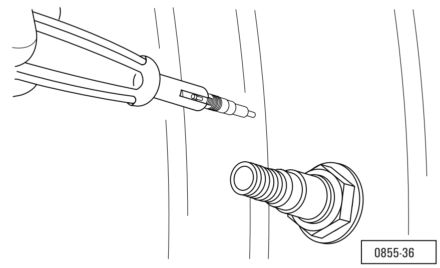

Trajectory Path

WARNING

Basic Inspection and Service Principles

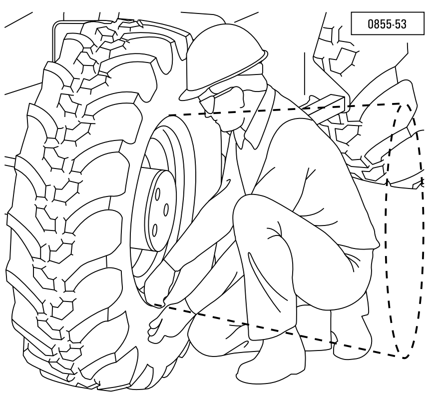

Stay completely out of the trajectory path indicated by the marked areas in the following illustrations. NEVER stand, lean, or reach across the rim wheel assembly trajectory path during inspection, service, or inflation operations.

Trajectory Path

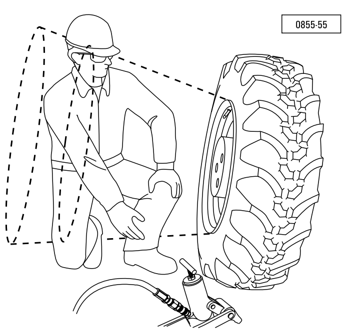

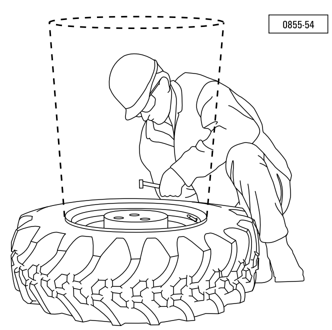

The trajectory path may be the gravest area of danger if a tire bead ruptures and/or a tire violently explodes due to misapplication, improper inflation, overloading, or for any other possible reason.

The trajectory path is any potential path or route that pieces of the rim wheel assembly may travel due to an explosive separation or sudden release of pressurized air, or an area at which an air blast from a single-piece rim wheel may be released. Be aware that under some circumstances, the trajectory path may deviate from the expected trajectory paths, which are perpendicular to the assembled position of the rim wheel at the time of separation or explosion

Tire Maintenance

Trajectory Path (Cont'd.)

Bystander Awareness

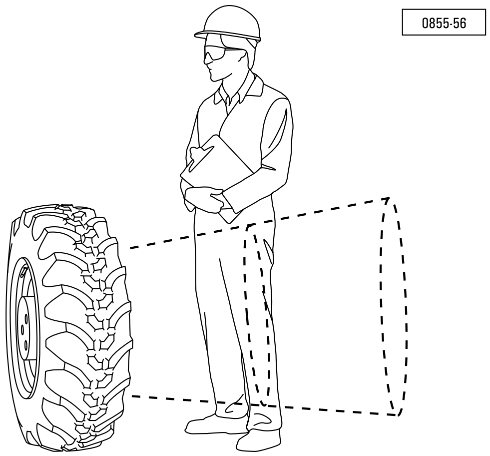

NEVER allow a bystander to stand, lean, or reach across the rim wheel assembly trajectory path while inspecting, servicing, or inflating a tire.

Restraining Devices

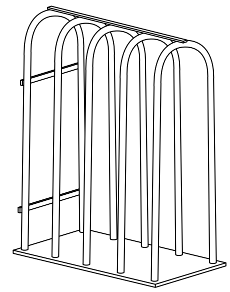

The task of servicing tires and rims can be extremely dangerous and should be performed by trained personnel only, using the correct tools, and following the procedures presented in this manual, OEM manufacturers' instruction manuals, or other industry and government instructions.

Always use restraining devices (safety cages) when inflating tires removed from a vehicle. Not using a restraining device can result in serious injury or death.

Restraining devices are safety cages that are manufactured in a variety of styles and shapes. Restraining devices are designed to reduce the possibility of injury or death from explosive projection from rim wheel assemblies, but should never be relied upon for total protection. Allow as much distance as possible and remain out of the trajectory path while servicing or inflating tires. Not using a restraining device can result in serious injury or death.

Each restraining device or barrier must:
- have the capacity to withstand the maximum force that would be transferred to it during a rim wheel separation occurring at 150 percent of the maximum tire specification pressure for the type of tire being serviced.
- be capable of preventing rim wheel parts from being thrown outside or beyond the restraining device or barrier from any rim wheel within or behind the restraining device.
- be visually inspected prior to each day's use, after any separation of rim wheel parts, or the sudden release of contained air.

Any restraining device or barrier must be removed from service if there is any sign of damage caused by mishandling, abuse, tire explosion, rim wheel separation, or corrosion, such as:
- cracks at welds
- cracked or broken framing
- bent or sprung framing
- corroded framing or parts,
- or any other structural damage which would decrease the effectiveness of the restraining device.

Restraining devices or barriers removed from service must not be returned to service until they are repaired and reinspected. Devices requiring structural repair, such as framing replacement or rewelding, must not be returned to service until they are certified by either the manufacturer or a Registered Professional Engineer as meeting the original strength requirements.

Tire Maintenance

Inspection

Step 1

Inspect the rim for damage or irregular wear.

Step 2

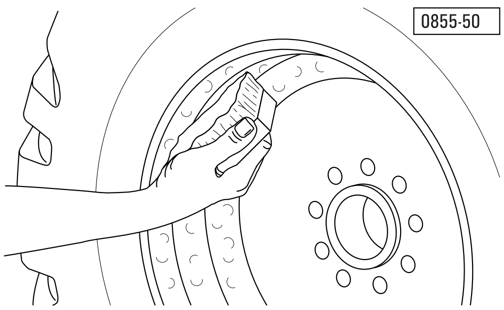

Clean the rim by removing all rust, dirt, and foreign material.

Warning

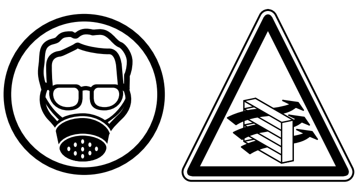

To prevent personal injury or death, always follow all of the procedures and safety precautions prescribed by the paint manufacturer. Paint may contain products of combustion which are harmful to your health. Only use paint in a well-ventilated area or if in an enclosed area, vent the paint fumes to the outside.

Step 3

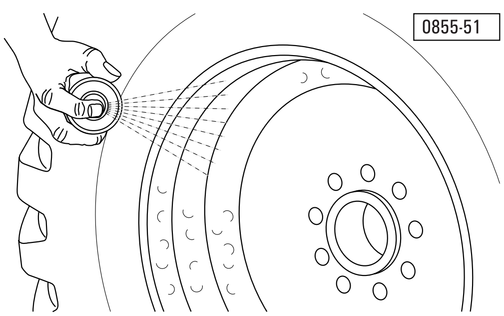

Paint bare metal areas on rim parts.

Step 4

Visually inspect the tire and rim to make sure they are seated properly.

Inflating the Tire

Warnings

A service technician should NEVER inflate a tire while remaining in or with bystanders in the rim wheel assembly trajectory path.

To prevent personal injury or death, NEVER inflate a tire beyond 241 kPa (35 psi) or the maximum tire inflation pressure to seat a tire bead. If the tire bead is not fully seated at 241 kPa (35 psi): STOP! Deflate the tire and correct the problem.
To prevent personal injury or death, only inflate and load tires to the manufacturer's specifications. DO NOT over-inflate or overload a tire, which can cause the tire to explode.

Never inflate a tire unless it is secured to the vehicle or enclosed in a restraining device (safety cage).

Never exceed 241 kPa (35 psi) or the maximum tire inflation pressure when seating beads.

Always inspect both sides of the tire to assure a proper bead seat.

In addition to having the tire in a restraining device, the service technician must use an air line assembly for inflating tires. It should have:

- a clip-on chuck and
- an in-line valve with a pressure gauge or a presettable regulator.
- A sufficient length of air line should be used to allow the service technician to stand outside the trajectory path.

Step 1
Place the tire in a safety cage or other restraining device before inflating the tire, in compliance with OSHA Regulation 29CFR 1910.177.

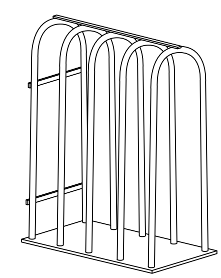

0855-24B

Note

Use a clip-on air chuck, an in-line valve with pressure gauge or regulator that can be preset, and hose that is long enough to allow you to stand outside the rim wheel trajectory.

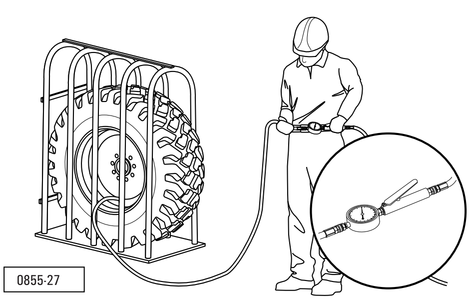

0855-27

Inflating the Tire (Cont'd.)

Step 2
Inflate the tire to 0.345 bar (5 psi)
a. Check all tire and rim parts again for proper positioning.
b. If tire/rim parts are not seated properly, deflate the tire and correct the problem before proceeding.
c. If tire and rim parts are seated properly, continue to inflate the tire.

Step 3

Inflate the tire to 1.38 bar (20 psi)
a. Check the tire bead for proper seating.
b. If tire and rim parts are not seated properly, deflate the tire and correct the problem before proceeding.
c. If tire and rim parts are seated properly, continue to inflate the tire.

⚠ WARNING

To prevent personal injury or death, NEVER inflate a tire beyond 241 kPa (35 psi) or the maximum tire inflation pressure to seat a tire bead. If the tire bead is not fully seated at 241 kPa (35 psi): STOP! Deflate the tire and correct the problem.

Step 4
Inflate the tire to 241 kPa (35 psi) or the maximum tire inflation pressure.
a. Check the tire bead for proper seating.
b. If tire/rim parts are not seated properly, deflate the tire and correct the problem before proceeding.
c. Once the tire bead is fully seated at 241 kPa (35 psi) or the maximum tire inflation pressure, deflate the tire completely.

⚠ WARNING

To prevent personal injury or death, only inflate and load tires to the manufacturer's specifications. DO NOT overinflate or overload a tire, which can cause the tire to explode.

Step 5
Reinflate the tire slowly to a pressure within the manufacturer's specifications. Tire pressures for Cat equipment can be found in the Tire section of the Caterpillar Performance Handbook.

Rotational Direction

Cat pneumatic skid steer and Flexport Construction tread tires are directional tires. The lug or "tread" pattern is designed to enhance traction. By specifying the rotational direction of a tire, cross ribs and grooves are laid out so that traction improves in slippery applications. When ordering a tire and wheel assembly, it is critical to know on which side the tire will be mounted. If an incorrect tire is specified, it will need to be remounted in the correct direction of rotation.

Skid Steer Loader - Determining Inset / Outset

Skid Steer Loaders

Standard Wheel — Definitions

The terms inset and outset are used to describe how much a wheel mounting surface differs from the centerline of the wheel.

When the wheel mounting surface is positioned off of the centerline and toward the machine (pictured), the wheel is outset. This causes the tire to move away from (out from) the side of the machine.

When the wheel mounting surface is positioned off of the centerline and away from the machine, the wheel is inset. This causes the tire to move toward (in toward) the side of the machine.

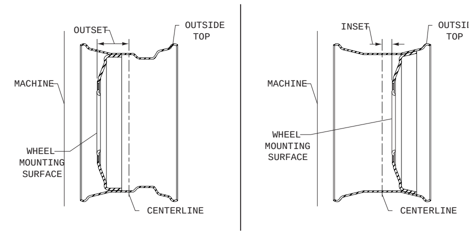

Standard Wheel — Steps to Determine Inset or Outset

1. Determine the centerline of the wheel. Measure the width of the wheel and divide it by two.

2. Measure the distance from the outside, top (stem side) of the wheel to the face of the wheel mounting surface. Place a flat bar across the wheel and drop the ruler down into the wheel until it hits the face near the bolt holes.

3. Subtract the centerline measurement in Step 1 from the measured distance in Step 2. A positive value is an outset. A negative value is an inset.

Solid Wheels

The Cat extreme duty solid tire and wheel assembly has an offset of two inches. The position in which the wheel assembly is installed on a machine depends on the machine's make and model.
The same solid wheel assembly is used with all makes and models that have identical bolt hole patterns and pilot holes. Machines with a pneumatic wheel "inset" will turn the solid wheel assembly position so that the two inch offset is an "inset". Machines with a pneumatic wheel "outset" will turn the solid wheel so that the two inch offset is an "outset".

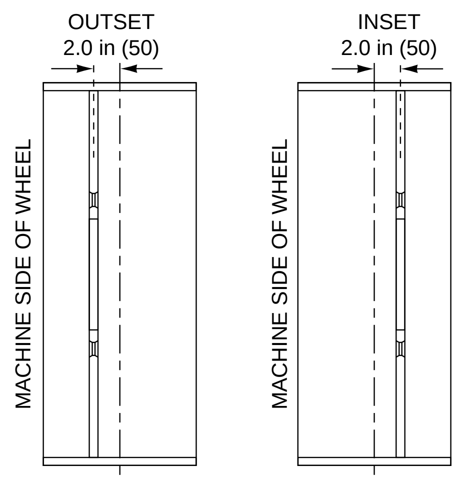

Skid Steer Loaders (Cont'd.)

Width Over Tire

Cat skid steer loaders can be ordered with varying "widths-over-tire." The width-over-tire measurement "X" can be changed by ordering a different wheel offset.

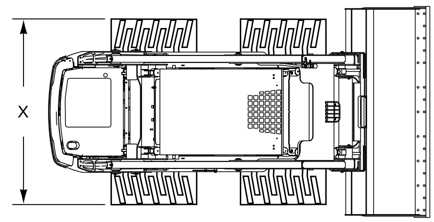

Various wheel offsets are available for Cat and competitive skid steer models.

Various wheel offset options are available in order to better accommodate varying bucket widths. A skid steer with a larger bucket on the front can perform better with the wider width-over-tire option. Tire clearance, when utilizing the wider width-over-tire option, may be a problem if the outside edge of the tires extend beyond the width of a smaller bucket.

For Cat skid steers it is important to not only know the model, but the width-over-tire dimension "X" when ordering replacement wheel assemblies.

Flexport Two-Piece Assembly for Wheel Loaders and Integrated Toolcarriers

Wheel Loaders and Integrated Toolcarriers

Flexport Tires are available for small and medium wheel loaders and integrated toolcarriers. A mounting disc which attaches to the wheel is required. The tire/wheel assembly is then attached to the machine using Cat mounting hardware.
All mounting discs attach to the tire with 900 ± 100 N·m (664 ± 74 ft. lbs.) of torque. The tire/wheel assembly then attaches to the machine using the specified bolt torque for that particular machine.

20.5X25 Flexport
926M, 930M, 938M
Bolt Torque: 900+/- 100 Nm
Apply Threadlocker to threads

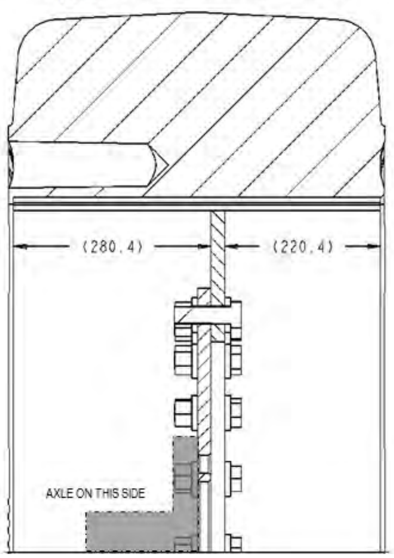

23.5X25 Flexport
950M, 962M
Bolt Torque: 900+/- 100 Nm

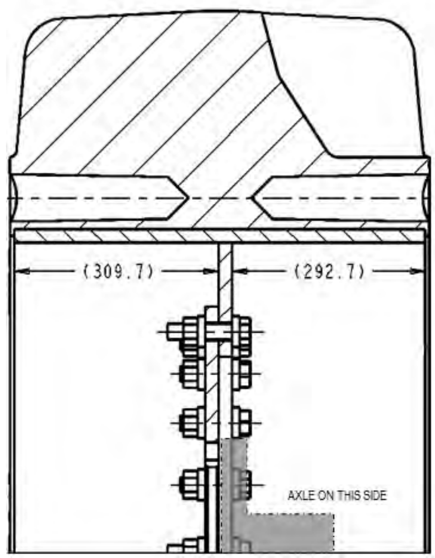

26.5X25 Flexport
966M, 972M
Bolt Torque: 900+/- 100 Nm

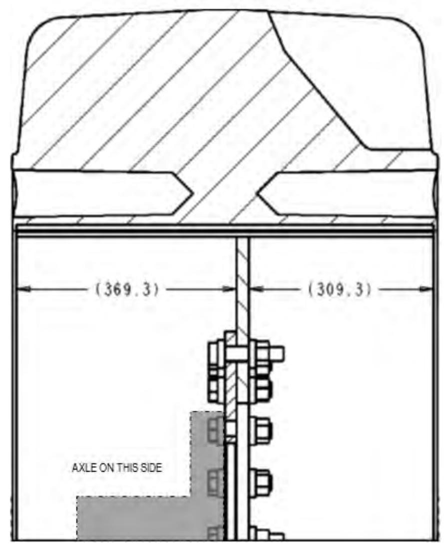

Data Codes

How to Find and Read Date Codes

When checking for the date code on pneumatic tires, one side of the tire will have a date code that starts with the letters CF, followed by four numbers. The first two numbers are the week of the year, and the last two numbers are the year of manufacture. These date codes are used in case of a warranty situation.

How to Find and Read Serial Numbers on Cat Flexport Tires

The serial number on a Cat Flexport Tire will be found underneath the Cat part number, just below the elliptical ports. Serial numbers are used in case of warranty situations.

Evaluating Conditions of Cat Tires for Warranty Replacement

Skid Steer Loaders

Reference: Warranty Statement, SELF5330, "Caterpillar Tire Warranty"

Reference: Warranty Bulletin, SELD0869, "Caterpillar Tire Warranty"

This section addresses the conditions of Cat tires as the conditions relate to warranty replacement. Under the subjects of the warranty, tire failures are attributed to one of the following causes:

- Defects in material or in workmanship
- Application

Tire failures that are attributed to defects in material or in workmanship are covered by the warranty. Tire failures that are related to the application are not covered by the warranty. See "Warranty Replacement Guidelines" in the Warranty Bulletin for additional information on the causes of failures.

BUILT FOR IT.™

PECP9064-10
www.cat.com

Attachment 11

Designing with Geosythetics

Fourth Edition

Designing with Geosynthetics

Robert M. Koerner, Ph.D., P.E.

H. L. Bowman Professor of Civil Engineering,
Drexel University and Director, Geosynthetic
Research Institute

PRENTICE HALL
Upper Saddle River, New Jersey 07458

TABLE 2.12 RECOMMENDED REDUCTION FACTOR VALUES FOR USE IN EQ. (2.25a)

	Range of Reduction Factors				
Application	Soil Clogging and Blinding*	Creep Reduction of Voids	Intrusion into Voids	Chemical Clogging†	Biological Clogging
Retaining wall filters	2.0 to 4.0	1.5 to 2.0	1.0 to 1.2	1.0 to 1.2	1.0 to 1.3
Underdrain filters	5.0 to 10	1.0 to 1.5	1.0 to 1.2	1.2 to 1.5	2.0 to 4.0
Erosion-control filters	2.0 to 10	1.0 to 1.5	1.0 to 1.2	1.0 to 1.2	2.0 to 4.0
Landfill filters	5.0 to 10	1.5 to 2.0	1.0 to 1.2	1.2 to 1.5	5 to 10‡
Gravity drainage	2.0 to 4.0	2.0 to 3.0	1.0 to 1.2	1.2 to 1.5	1.2 to 1.5
Pressure drainage	2.0 to 3.0	2.0 to 3.0	1.0 to 1.2	1.1 to 1.3	1.1 to 1.3

*If stone riprap or concrete blocks cover the surface of the geotextile, use either the upper values or include an additional reduction factor.

†Values can be higher particularly for high alkalinity groundwater.

‡Values can be higher for turbidity and/or for microorganism contents greater than 5000 mg/l.

$$\boxed{q_{\text{allow}} = q_{\text{ult}}\left(\frac{1}{\Pi \text{RF}}\right)} \tag{2.25b}$$

where

q_{allow} = allowable flow rate,
q_{ult} = ultimate flow rate,
RF_{SCB} = reduction factor for soil clogging and blinding,
RF_{CR} = reduction factor for creep reduction of void space,
RF_{IN} = reduction factor for adjacent materials intruding into geotextile's void space,
RF_{CC} = reduction factor for chemical clogging,
RF_{BC} = reduction factor for biological clogging, and
ΠRF = value of cumulative reduction factors.

As with Eqs. (2.24) for strength reduction, this flow-reduction equation could also have included additional site-specific terms, such as blocking of a portion of the geotextile's surface by riprap or concrete blocks.

2.5 DESIGNING FOR SEPARATION

Application areas for geotextiles used for the separation function were given in Section 1.3.3. There are many specific applications, and it could be said, in a general sense, that geotextiles always serve a separation function. If they do not also serve this function, any other function, including the primary one, will not be served properly. This should not give the impression that the geotextile function of separation always plays a secondary role. Many situations call for separation only, and in such cases the geotextiles serve a significant and worthwhile function.

2.5.1 Overview of Applications

Perhaps the target application that best illustrates the use of geotextiles as separators is their placement between a reasonably firm soil subgrade (beneath) and a stone base course, aggregate, or ballast (above). We say "reasonably firm" because it is assumed that the subgrade deformation is not sufficiently large to mobilize uniformly high tensile stress in the geotextile. (The application of geotextiles in unpaved roads on soft soils with membrane-type reinforcement is treated later in Section 2.6.1.) Thus for a separation function to occur the geotextile has only to be placed on the soil subgrade and then have stone placed, spread, and compacted on top of it. The subsequent deformations are very localized and occur around each individual stone particle. A number of scenarios can be developed showing which geotextile properties are required for a given situation.

2.5.2 Burst Resistance

Consider a geotextile on a soil subgrade with stone of average particle diameter (d_a) placed above it. If the stone is uniformly sized, there will be voids within it that will be available for the geotextile to enter. This entry is caused by the simultaneous action of the traffic loads being transmitted to the stone, through the geotextile, and into the underlying soil. The stressed soil then tries to push the geotextile up into the voids within the stone. The situation is shown schematically in Figure 2.28. Giroud [64] provides a formulation for the required geotextile strength that can be adopted for this application.

$$\boxed{T_{\text{reqd}} = \frac{1}{2} p' d_v [f(\varepsilon)]} \tag{2.26}$$

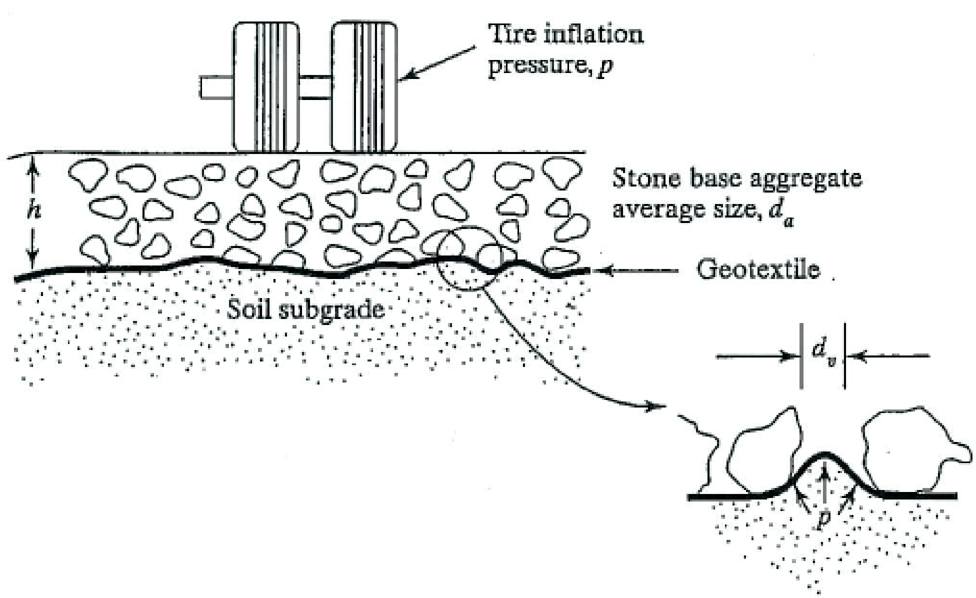

Figure 2.28 Geotextile being forced up into voids of stone base by traffic tire loads.

where

T_{reqd} = required geotextile burst strength;
p' = stress at the geotextile's surface, which is less than or equal to p, the ti inflation pressure at the ground surface;
d_v = maximum void diameter of the stone $\cong 0.33d_a$;
d_a = the average stone diameter,
$f(\varepsilon)$ = strain function of the deformed geotextile
$= \frac{1}{4}\left(\frac{2y}{b} + \frac{b}{2y}\right)$, in which
b = width of opening (or void), and
y = deformation into the opening (or void).

The field situation is analogous to the ASTM D3786 (Mullen) burst test, which has t geotextile being stressed into a gradually increasing hemispherical shape until it fails radial tension (recall Section 2.3.3). Thus, the adapted form of Eq. (2.26) is:

$$T_{ult} = \frac{1}{2} p_{test} d_{test} [f(\varepsilon)] \tag{2.2}$$

where

T_{ult} = ultimate geotextile strength,
p_{test} = burst test pressure, and
d_{test} = diameter of the burst test device (= 30 mm).

Knowing that $T_{allow} = T_{ult}/(\Pi RF)$, where ΠRF = cumulative reduction factors, we ca formulate an expression for the FS as follows:

$$FS = \frac{T_{allow}}{T_{reqd}} = \frac{(p_{test} d_{test})}{(\Pi RF) p' d_v}$$

For example, if $d_{test} = 30$ mm, $d_v = 0.33\, d_a$, and $\Pi FS = 1.5$ (which is not particularly low since creep is not an issue with this application), then the FS is the following, with d_a in mm.

$$FS = \frac{p_{test}(30)}{(1.5)p'(0.33d_a)}$$

$$FS = \frac{60.6 p_{test}}{p' d_a} \tag{2.28}$$

Example 2.7

Given a 700 kPa truck tire inflation pressure on a poorly graded stone-base course consisting of 50 mm maximum-size stone, what is the factor of safety using a geotextile with an ultimate burst strength of 2000 kPa and cumulative reduction factors of 1.5?

Solution: Assuming that the tire inflation pressure is not significantly reduced through the thickness of the stone base, we can solve Eq. (2.28) as follows.

$$\begin{aligned} FS &= \frac{60.6(2000)}{700(50)} \\ &= 3.5 \end{aligned}$$

Note that with the cumulative reduction factors of 1.5 already included, the resulting factor of safety value is acceptable.

For a range of stone-base particle diameters (d_a), values of tire inflation pressure (p'), and cumulative reduction factors of 1.5, along with a factor of safety of 2.0, we get the design guide in Figure 2.29. Here it can be seen that stone size is quite significant insofar as the required burst-pressure values are concerned. Note also that these are poorly graded aggregates and that the presence of fines will lessen the severity of the design; hence this approach should be considered to be a worst-case design.

REQUIRED BURST RESISTANCE FOR 1½" STONE AT ~~32,000~~ ~~24,000~~ 12,000 PSF EQUALS: ~~1150.2 kPa~~ 574 kPa
~~1875 kPa =~~
~~272 psi~~
= [illegible]

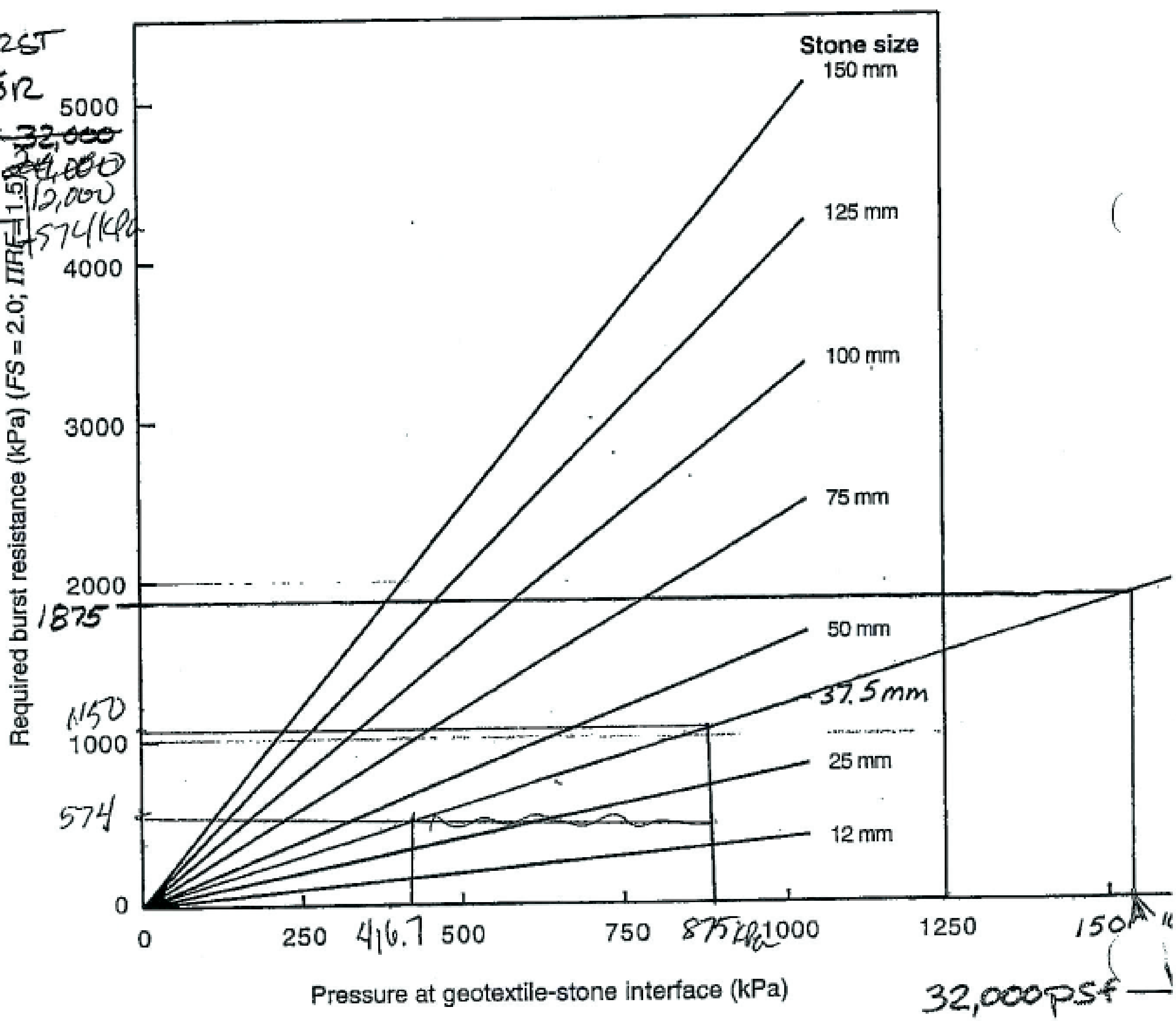

Figure 2.29 Design guide for burst analysis of geotextile used in a separation function based on cumulative reduction factors of 1.5 and a factor of safety of 2.0.

2.5.3 Tensile Strength Requirement

Continuing the discussion of the general problem, there is a process acting on the ge textile simultaneously as its tendency to burst in an out-of-plane mode: tensile stre mobilized by in-plane deformation. This occurs as the geotextile is locked into positic by the stone-base aggregate above it and soil subgrade below it. A lateral or in-plar tensile stress in the geotextile is mobilized when an upper piece of aggregate is force between two lower pieces that lie against the geotextile. The analogy to the grab tensil test can be readily visualized, as illustrated in Figure 2.30. Here we can estimate th maximum strain that the geotextile will undergo as the upper stone wedges itself dow to the level of the geotextile. Using the dimensions shown (where $S \sim d/2$ and l_f = de formed geotextile length), the maximum strain with no slippage or stone breakage ca be calculated.

$$\begin{aligned}
\varepsilon &= \frac{l_f - l_o}{l_o}(100) \\
&= \frac{[d + 2(d/2)] - 3(d/2)}{3(d/2)}(100) \\
&= \frac{4(d/2) - 3(d/2)}{3(d/2)}(100) \\
&= 33\%
\end{aligned}$$

Note that the preceding assumptions result in a strain that is independent of particle size. Thus the strain in the geotextile could be as high as 33% given the idealized

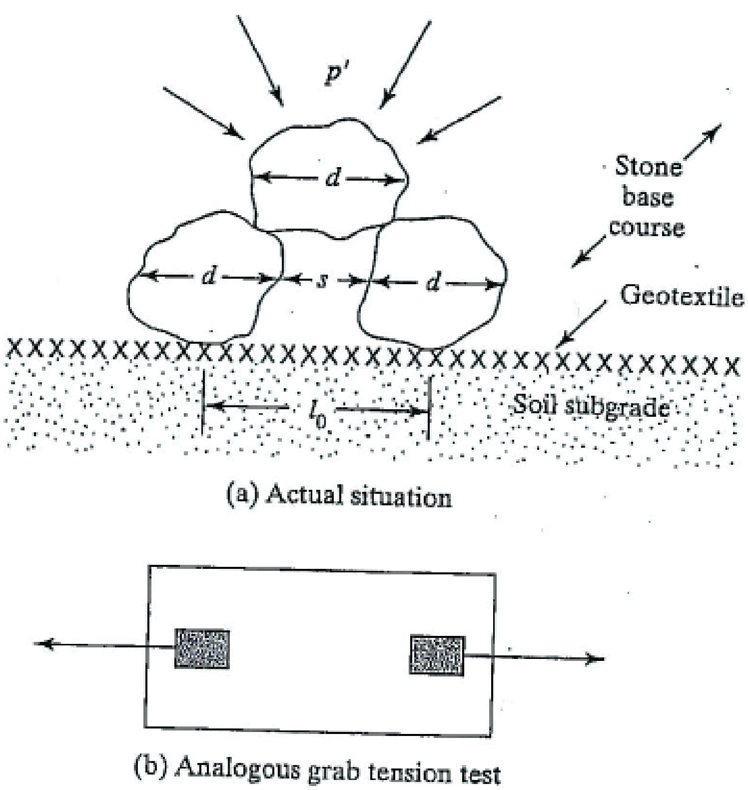

(a) Actual situation

(b) Analogous grab tension test

Figure 2.30 Geotextile being subjected to tensile stress as surface pressure is applied and stone base attempts to spread laterally.

(upper-bound) assumptions stated above. The tensile force being mobilized is related to the pressure exerted on the stone as follows [64].

$$\boxed{T_{\text{reqd}} = p'(d_v)^2[f(\varepsilon)]} \tag{2.29}$$

where

T_{reqd} = required grab tensile force;
p' = applied pressure;
d_v = maximum void diameter $\simeq 0.33\, d_a$, where
d_a = average stone diameter; and
$f(\varepsilon)$ = strain function of the deformed geotextile;
$= \frac{1}{4}\left(\frac{2y}{b} + \frac{b}{2y}\right)$, where
b = width of stone void, and
y = deformation into stone void.

Example 2.8 illustrates the design procedure above.

Example 2.8

Given a 700 kPa truck-tire inflation pressure on a stone-base course consisting of 50 mm maximum-size stone with a geotextile beneath it, calculate **(a)** the required grab tensile stress on the geotextile, and **(b)** the factor of safety for a geotextile whose grab strength at 33% is 500 N with cumulative reduction factors of 2.5 and $f(\varepsilon) = 0.52$.

Solution: **(a)** Using an empirical relationship that $d_v = 0.33\, d_a$ and $f(\varepsilon) = 0.52$, the required grab tensile strength from Eq. (2.29) is as follows.

$$\begin{aligned} T_{\text{reqd}} &= p'(d_v)^2(0.52) \\ &= p'(0.33d_a)^2(0.52) \\ &= 0.057\, p'd_a^2 \\ &= 0.057(700)(1000)(0.0 \\ &= 100 \text{ N} \end{aligned}$$

$f(\varepsilon) = \frac{1}{4}\left(\frac{2y}{b} + \frac{b}{2y}\right)$? y & b

$= \frac{1}{4}(2$

(b) The factor of safety for a 500 N grab tensile geotexti reduction factors of 2.5 is as follows.

$$\begin{aligned} \text{FS} &= \frac{T_{\text{allow}}}{T_{\text{reqd}}} \\ &= \frac{500/2.5}{100} \\ &= 2.0 \quad \text{which is acceptabl.} \end{aligned}$$

2.5.4 Puncture Resistance

The geotextile must survive the installation process. This is not just related to the function of separation; indeed, fabric survivability is critical in all types of applications—without it the best of designs are futile (recall Figure 2.19). In this regard, sharp stones,

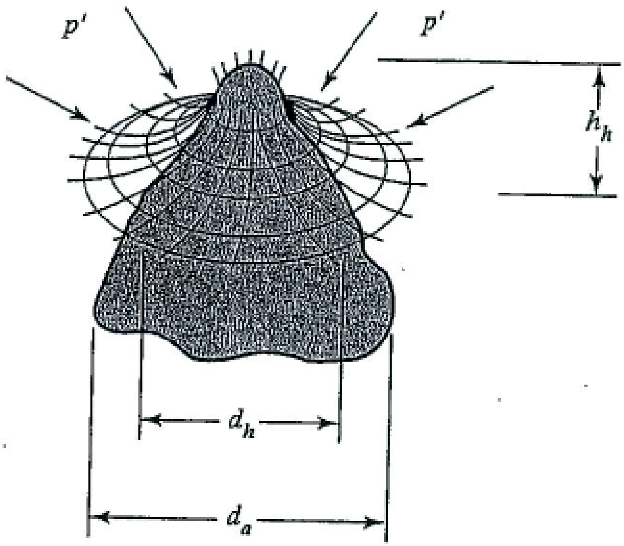

Figure 2.31 Visualization of a stone puncturing a geotextile as pressure is applied from above.

tree stumps, roots, miscellaneous debris, and other items, either on the ground surface beneath the geotextile or placed above it, could puncture through the geotextile after backfilling and traffic loads are imposed. The design method suggested for this situation is shown schematically in Figure 2.31. For these conditions, the vertical force exerted on the geotextile (which is gradually tightening around the protruding object) is as follows:

$$F_{\text{reqd}} = p' d_a^2 S_1 S_2 S_3 \tag{2.30}$$

where

F_{reqd} = required vertical force to be resisted;
d_a = average diameter of the puncturing aggregate or sharp object;
p' = pressure exerted on the geotextile (approximately 100% of tire inflation pressure at the ground surface for thin covering thicknesses);
S_1 = protrusion factor = h_h/d_a;
h_h = protrusion height $\leq d_a$;
S_2 = scale factor to adjust the ASTM D4833 puncture test value (which uses an 8.0 mm diameter puncture probe) to the diameter of the actual puncturing object = d_{probe}/d_a;
S_3 = shape factor to adjust the ASTM D4833 flat puncture probe to the actual shape of puncturing object = $1 - A_p/A_c$, (values for A_p/A_c range from 0.8 for rounded sand, to 0.7 for run-of-bank gravel, to 0.4 for crushed rock, to 0.3 for shot rock);
A_p = projected area of puncturing particle;
A_c = area of smallest circumscribed circle around puncturing particle.

Example 2.9

What is the factor of safety against puncture of a geotextile from a 50 mm stone on the ground surface mobilized by a loaded truck with a tire inflation pressure of 550 kPa traveling on the surface of the base course? The geotextile has an ultimate puncture strength of 200 N, according to ASTM D4833.

Solution: Using the full stress on the geotextile of 550 kPa and the values 0.33, 0.15, and 0.6 for the factors S_1, S_2, and S_3, respectively,

$$F_{reqd} = p' d_a^2 S_1 S_2 S_3$$
$$= (550)(1000)(50 \times 0.001)^2(0.33)(0.15)(0.6)$$
$$= 40.8 \text{ N}$$

Assuming that the cumulative reduction factors are 2.0, the factor of safety is as follows:

$$FS = \frac{F_{allow}}{F_{reqd}}$$
$$= \frac{200/2.0}{40.8}$$
$$= 2.4 \quad \text{which is acceptable}$$

Using the following assumptions (which can be modified as desired), a design guide can be developed as shown in Figure 2.32: the geotextile has an angular subgrade

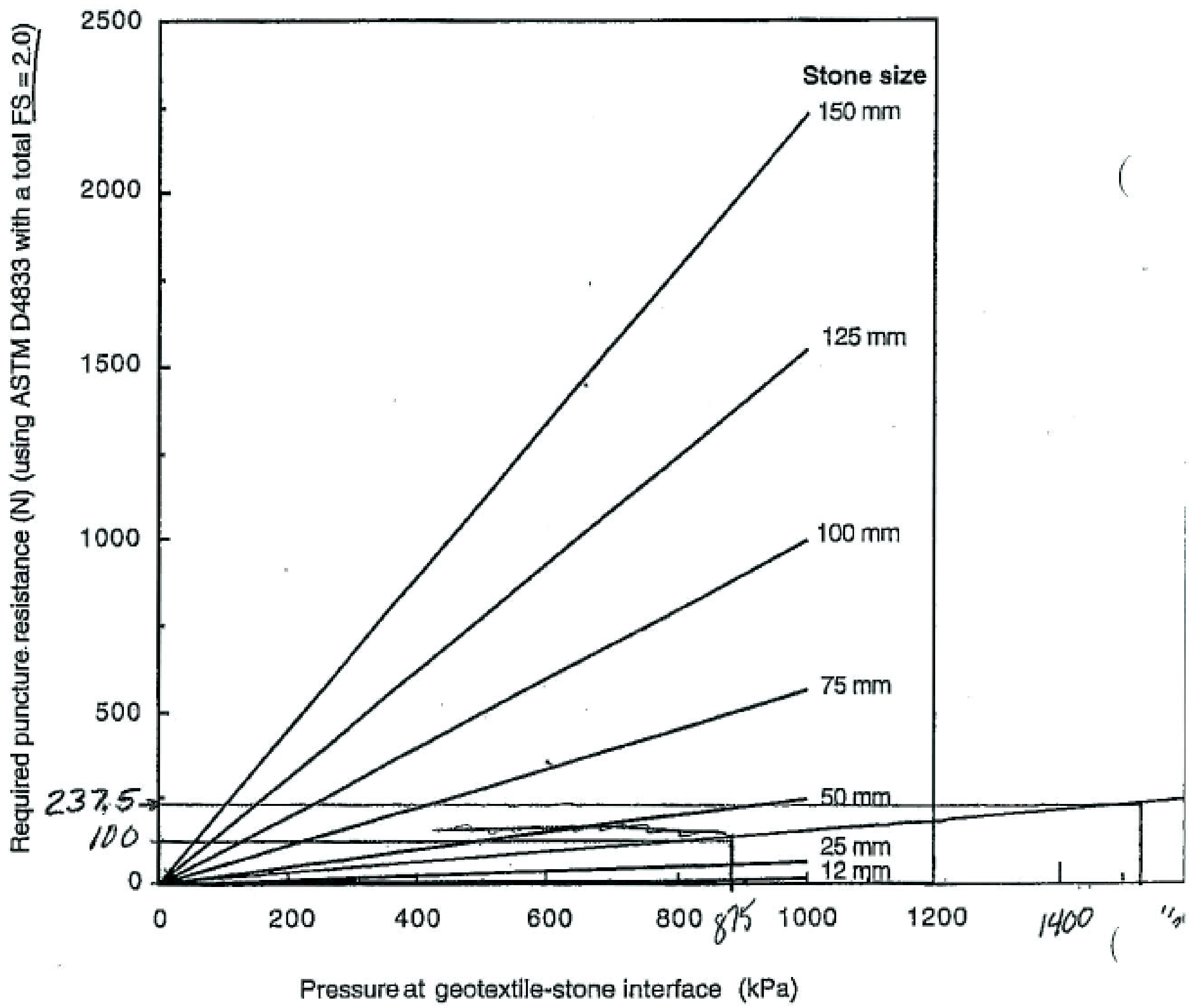

Figure 2.32 Puncture resistance design guide based on cumulative reduction factors of 2.0, a factor of safety of 2.0, and conditions stated in text.

above it such that $S_1 = 0.33$, $S_2 = 0.15$, and $S_3 = 0.5$; the cumulative reduction factors are 2.0; and the factor of safety is also 2.0.

$$F_{\text{reqd}} = p'd_a^2(0.33)(0.15)(0.5)$$

$$= 0.0248p'd_a^2$$

$$\text{FS} = \frac{F_{\text{ult}}/\Pi\text{RF}}{F_{\text{reqd}}}$$

$$2.0 = \frac{F_{\text{ult}}/2.0}{0.0248p'd_a^2}$$

$$F_{\text{ult}} = 0.099p'd_a^2$$ which is graphed accordingly.

2.5.5 Impact (Tear) Resistance

As with the puncture requirement just described, the resistance of a geotextile to impact is as much a survivability criterion as it is a separation function. Yet in many applications of separation, the geotextile must resist the impact of various objects. The most obvious one is a rock falling on it, but there are also situations in which construction equipment and materials can cause or contribute to impact damage on geotextiles.

The problem concerns the energy mobilized by a free-falling object of known weight and the height of the drop. Rarely will an object be intentionally impelled onto an exposed geotextile with additional force, so only gravitational energy will be assumed.

To develop a design guide, we assume free-falling stones of specific gravity of 2.60, varying in diameter from 25 to 600 mm and falling from heights of 0.5 to 5 m. Using this data the design curves of Figure 2.33 are developed. The relationship is as follows.

$$E = mgh$$

$$= (V \times \rho)gh$$

$$= [V \times (\rho_w G_s)]gh$$

$$= \left(\frac{\pi(d_a/1000)^3}{6}\right)\left(\frac{1000 kg}{m^3}\right)(2.6)(9.81)h$$

$$E = 13.35 \times 10^{-6} d_a^3 h \tag{2.31}$$

where

E = energy developed (joules),
m = mass of the object (kg),
g = acceleration due to gravity (m/s²),
h = height of fall (m),

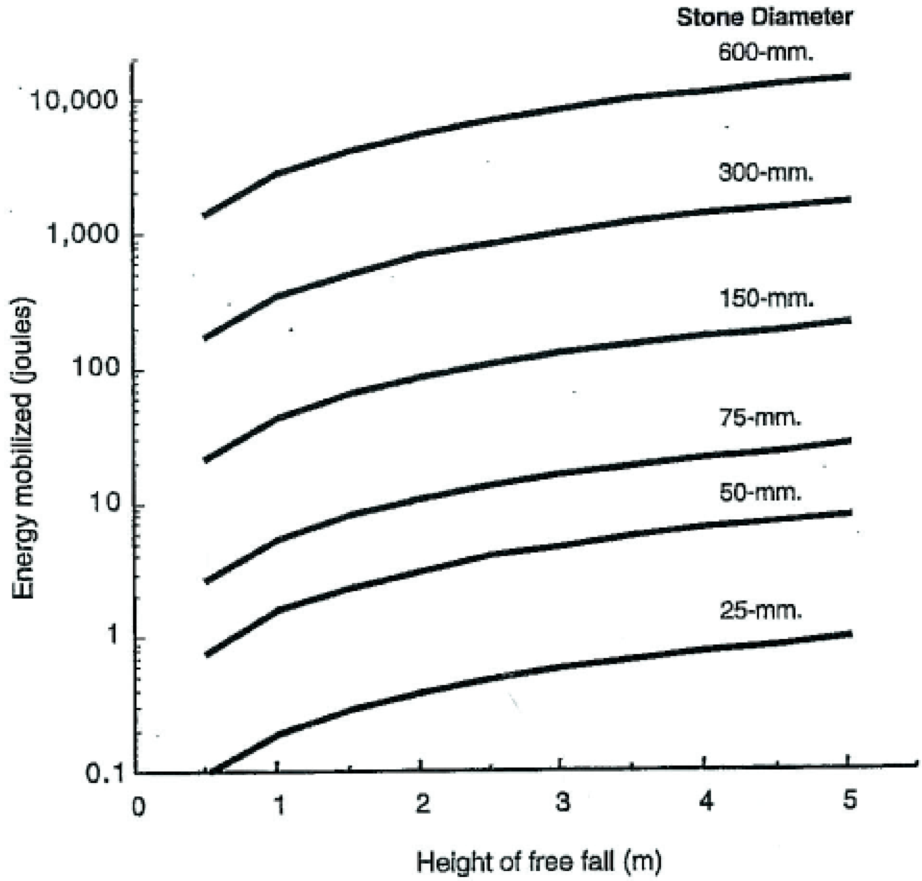

Figure 2.33 Energy mobilization by a free-falling rock on a geotextile with an unyielding support.

V = volume of the object (m^3),
ρ = density of the object (kg/m^3),
ρ_w = density of water (kg/m^3),
G_s = specific gravity of the object (dimensionless), and
d_a = diameter of the object (mm).

Note that these calculated energies are based on the geotextile resting on an unyielding surface, that is, the worst possible condition. As the soil beneath the geotextile deforms, the geotextile can absorb greater amounts of impacting energy. Since this is always the case, the reduction factors of Figure 2.34 are to be used in conjunction with the curves of Figure 2.33. Once the required energy is calculated, it should be compared to the allowable impact strength of the geotextile (e.g., the Elmerdorf tear or other impact test as discussed in Section 2.3.3). Example 2.10 illustrates the procedure.

Example 2.10

What energy is mobilized by a free-falling stone of 300 mm size falling 1.5 m onto a geotextile? The geotextile is supported by a poor subsoil having an unsoaked CBR strength of 4. If the geotextile has an allowable impact strength of 36 J, what is the factor of safety?

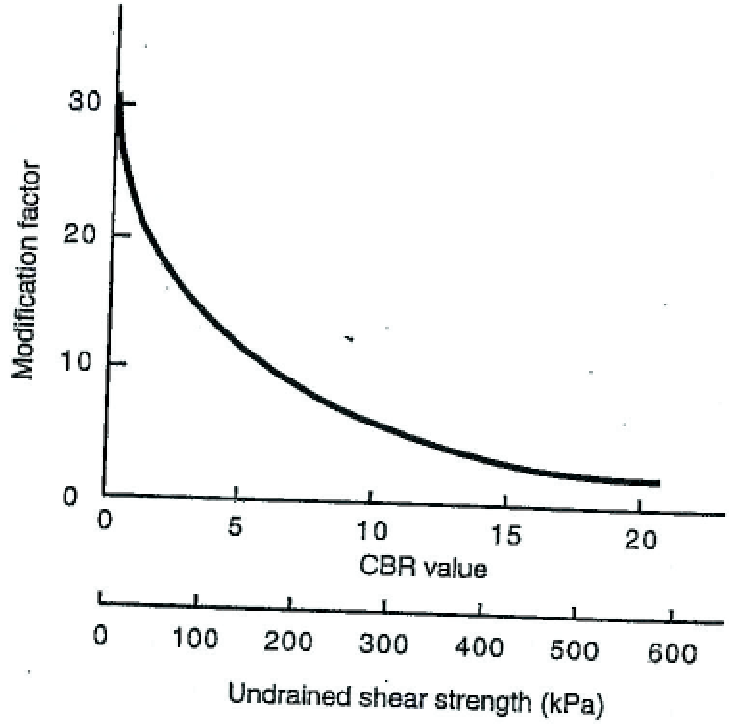

Figure 2.34 Modification factors to be used with energy mobilized by objects falling on geotextiles of varying suppor resistances characterized by their unsoaked CBR values or undrained shear strength.

Solution: Using Eq. (2.31) one calculates the required impact energy

$$E_{\max} = 13.35 \times 10^{-6}(d_a^3)(\mathrm{h})$$
$$= 13.35 \times 10^{-6}(300)^3(1.5)$$
$$E_{\max} = 540 \text{ J}$$

Note that this value is substantiated by the design chart in Figure 2.33. Of course, other d sign charts can be made for different assumptions.

This value is reduced according to the subgrade conditions of Figure 2.34.

$$E_{\text{reqd}} = 540/13$$
$$= 41.5 \text{ J}$$

This results in a global factor of safety calculation as follows.

$$\text{FS} = \frac{E_{\text{allow}}}{E_{\text{reqd}}}$$
$$= \frac{36}{41.5}$$
$$\text{FS} = 0.87 \qquad \text{which is not acceptable.}$$

Thus holes are likely to be formed when free-falling rocks of this size fall directly on th exposed geotextile. Not included in this analysis is the effect of the contact area of th falling object on the geotextile; for a very rounded rock, the effect is much less severe tha for a sharp, angular one, which could easily cut through the fabric. A more sophisticate design of this nature for puncture of geomembranes, along with geotextile protection, wi be developed in Section 5.6.7.

It should be emphasized that the last two methods of puncture and impact desig refer not only to separation per se, but to the construction survivability of geotextiles i general (recall Table 2.2a). In all cases these considerations should be examined, for they are critical in many situations.

2.5.6 Summary

Separation, the *most underrated of all geotextile functions,* was addressed in this section. I say underrated because every use of geotextiles carries with it the separation function, yet rarely is separation designed on its own merit. Hopefully, the designs in this section will allow the engineer to determine quantitatively which geotextile is suitable for a specific situation.

Last, and in a sense most important, is the economic justification for the use of geotextiles in the separation function. It lies in the greater use and service lifetime of the system with geotextiles than without. When a geotextile separator is used in roadway cross sections, geotextiles could well double or triple the lifetime; however, field data for such quantification is sparse and greater efforts should be taken to provide test sites for this. Figure 2.35 is the photograph of a 40 m long driveway test plot, which was subdivided into four elongated quadrants, two with geotextiles and two without. Further, the two geotextiles were different and placed diagonally across from one another. After nine years of service, no cracks have surfaced on the paving and the test is continuing with the objective of providing lifetime data with and without geotextiles, and on which is the preferred type of geotextile. A database of like projects is being developed; see [65].

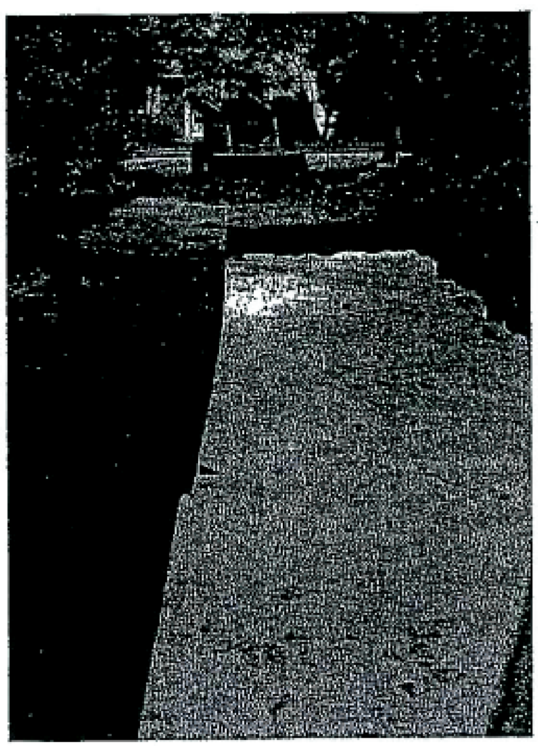

Figure 2.35 Different separation geotextiles being used to determine pavement (driveway) lifetime contrasted to sections with no geotextile.

SCS ENGINEERS

SHEET 1 OF 5

CLIENT Hillsborough County	PROJECT Southeast County Landfill	JOB NO. 09215600.13

SUBJECT Southeast County Landfill Phase II-III Closure Veneer Stability Calculations	BY TMA	DATE 11/16/2021
	CHECKED KLS	DATE 12/17/2021

OBJECTIVE: To evaluate the stability of the protective cover soil with seepage forces applied using the method described by Koerner and Soong (1998) referenced below.

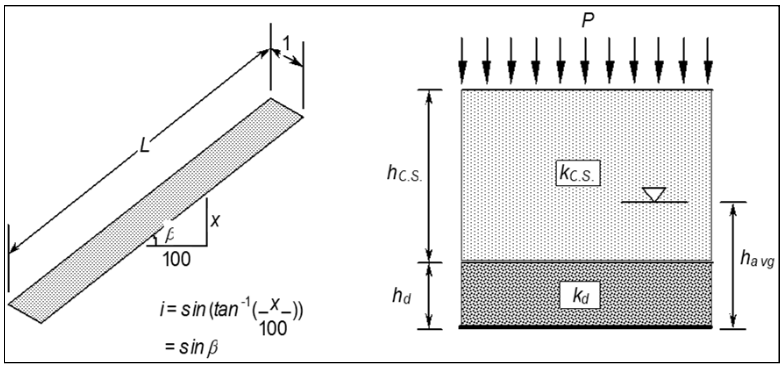

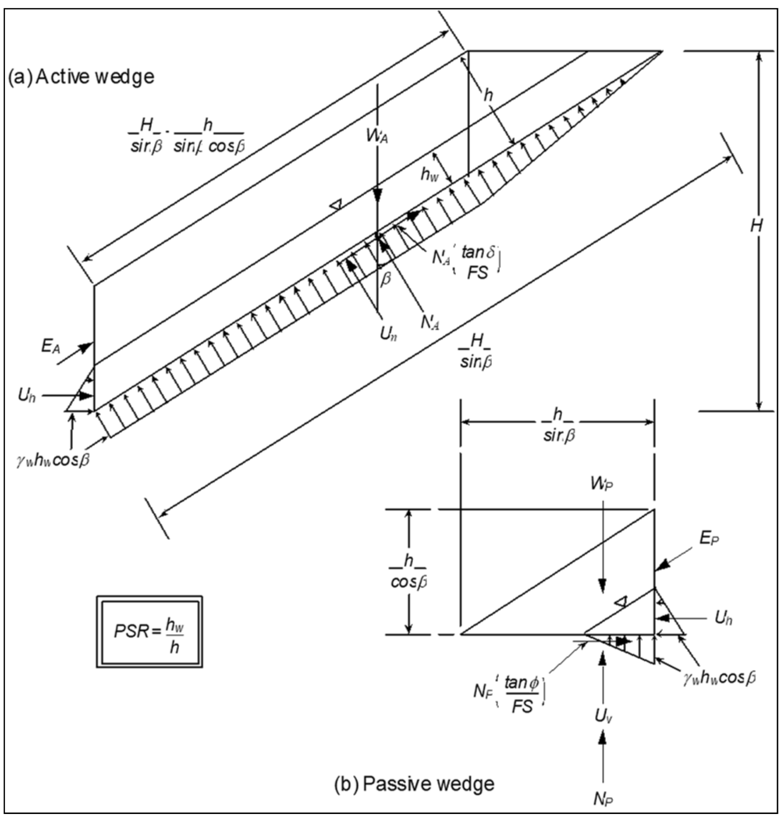

R.M. Koerner, and T-Y.Soong, 1998. "Analysis and Design of Veneer Cover Soils". Proceeding of 6th International Conference on Geosynthetics, Vol. 1, pp. 1-23, Atlanta, Georgia, USA. Refer to Attachment 1.

CLIENT	PROJECT	JOB NO.
Hillsborough County	Southeast County Landfill	09215600.13

SUBJECT	BY	DATE
Southeast County Landfill Phase II-III Closure	TMA	11/16/2021
Veneer Stability Calculations	CHECKED	DATE
	KLS	12/17/2021

PARAMETERS:

DLC	=	drainage layer capacity
$FLUX_{allow}$	=	allowable flow rate of the drainage layer per unit width of slope
k_d	=	permeability of drainage soil or geocomposite
h_d	=	thickness of the drainage soil or geocomposite
i	=	sin β = slope gradient
$FLUX_{req'd}$	=	actual flow rate per unit width of slope
PERC	=	the rate of percolation
P	=	probable maximum (hourly) precipitation (25-year storm event)
RC	=	runoff coefficient
L	=	length of drainage slope
k_{cs}	=	permeability of cover soil
β	=	slope angle
w	=	1.0 m = unit width of drainage slope
PSR	=	parallel submergence ratio
h_{avg}	=	average head buildup above the geomembrane
h_{cs}	=	thickness of cover soil
FS	=	factor of safety against instability
W_A	=	total weight of the active wedge
W_P	=	total weight of the passive wedge
U_h	=	resultant of the pore pressures acting on the interwedge surfaces
U_n	=	resultant of the pore pressures acting perpendicular to the slope
U_v	=	resultant of the vertical pore pressures acting on the passive wedge
N_A	=	effective force normal to the failure plane of the active wedge
h	=	thickness of the cover soil
H	=	vertical height of the slope measured from the toe
h_w	=	(PSR)(h) = height of the free water surface measured from the geomembrane
γ_{dry}	=	dry unit weight of the cover soil
$\gamma_{sat'd}$	=	saturated unit weight of the cover soil
γ_w	=	unit weight of water
ϕ	=	cover soil friction angle
δ	=	interface friction angle between weakest interface of the final cover system

REFERENCES:

1. Attachment 1 - R.M. Koerner, "Analysis and Design of Veneer Cover Soils"
2. Attachment 2 - Te-Yand Soong and R.M. Koerner, "The Design of Drainage Systems Over Geosynthetically Lined Slopes"
3. Attachment 3 - NOAA 25-Year 24-Hour Storm Event
4. Attachment 4 - Soil properties
5. Attachment 5 - Soil Friction Angle
6. Attachment 6 - GRI Report #30, June 14, 2005

CLIENT	PROJECT	JOB NO.
Hillsborough County	Southeast County Landfill	09215600.13

SUBJECT	BY	DATE
Southeast County Landfill Phase II-III Closure	TMA	11/16/2021
Veneer Stability Calculations	CHECKED	DATE
	KLS	12/17/2021

CALCULATE DRAINAGE LAYER CAPACITY (DLC):

$PERC = P(1\text{-}RC)$, for $P(1\text{-}RC) \leq k_{cs}$
$PERC = k_{cs}$, for $P(1\text{-}RC) > k_{cs}$

See Equations 21a, 21b on p. 34 in Attachment 2

k_{CS} =	5.00E-04	cm/s	=	18.00	mm/hr	Value included in the technical specifications.
P =	3.34	in/hr	=	84.84	mm/hr	Refer to Attachment 3 for Rainfall Data.
RC =	0.40					Refer to page 26 of Attachment 2 for RC values, this was taken as the default value for this design.
P(1-RC) =	50.90	mm/hr				
PERC =	18.00	mm/hr				

$$FLUX_{req'd} = \frac{PERC}{1000} \times L(\cos\beta) \times w$$

See Equation 22 on p. 40 in Attachment 2

L =	150	feet	=	45.72	m	"L" represents the slope length between sideslope composite drains
β =	14.4	°	=	0.25	rad	w = 1.0 = unit width (constant) of drainage slope
$L(\cos\beta)$ =	44.28	m				
$FLUX_{req'd}$ =	0.80	m^3/hr				

$$FLUX_{allow} = k_d \times i \times h_d$$

k_d =	11.15	cm/s	=	0.11	m/s	Refer to Geocomposite Transmissivity for calculations and resulting h_d
h_d =	297	mil				
h_d =	10.06	mm	=	0.01	m	
i =	0.25					
$FLUX_{allow}$ =	1.00	m^2/hr				

$$DLC = \frac{FLUX_{allow}}{FLUX_{req'd}}$$

See Equation 23 on p. 40 in Attachment 2

DLC = 1.26

NOTES: If only one soil layer above geomembrane, treat it as a drainage layer.
DLC needs to be greater than one to avoid saturation of the drainage layer.
Therefore, the proposed geocomposite meets drainage capacity requirements.

CLIENT	PROJECT	JOB NO.
Hillsborough County	Southeast County Landfill	09215600.13

SUBJECT	BY	DATE
Southeast County Landfill Phase II-III Closure	TMA	11/16/2021
Veneer Stability Calculations	CHECKED	DATE
	KLS	12/17/2021

CALCULATE PARALLEL SUBMERGENCE RATIO (PSR):

$h_{avg} = \frac{FLUX_{req'd}/3600}{k_d \times i}$, for DLC $\geq$ 1.0 — See Equation 24 on p. 42 in Attachment 2

$h_{avg} = \frac{[FLUX_{req'd}/(3600 \times i)] - [h_d \times (k_d - k_{cs})]}{k_{cs}}$, for DLC < 1.0 — See Equation 26 on p. 42 in Attachment 2

h_{avg} for DLC $\geq$ 1.0 = 0.008 m

h_{avg} for DLC < 1.0 = -46.22 m

h_{avg} = 0.008 m

$PSR = \frac{h_{avg}}{h_{cs} + h_d}$ — See Equation 27 on p. 42 in Attachment 2

if PSR $\geq$ 1, set PSR = 1

h_{CS} = 609.6 mm = 0.61 m — Thickness of cover soil (2 ft)

PSR = 0.013

PSR = 0.013

CALCULATE FACTOR OF SAFETY (FS):

$W_A = \frac{\gamma_{dry}(h - h_w)[2H\cos\beta - (h + h_w)] + \gamma_{sat'd}(h_w)(2H\cos\beta - h_w)}{\sin 2\beta}$ — See Equation 32 on p. 12 in Attachment 1

γ_{dry} = 138 lb/ft^3 = 21.68 kN/m^3 — Refer to Attachment 4

$\gamma_{sat'd}$ = 138 lb/ft^3 = 21.68 kN/m^3

$h = h_d + h_{cs}$ = 619.66 mm = 0.62 m

h_w = 7.99 mm = 0.01 m

$H = L \times \sin\beta$ = 11.37 m

W_A = 596.88 kN

$U_h = \frac{\gamma_w (h_w)^2}{2}$ — See Equation 34 on p. 12 in Attachment 1

γ_w = 9.81 kN/m^3

U_h = 0.0003 kN

$U_n = \frac{\gamma_w(h_w)(\cos\beta)(2H\cos\beta - h_w)}{\sin 2\beta}$ — See Equation 33 on p. 12 in Attachment 1

U_n = 3.47 kN

CLIENT	PROJECT	JOB NO.
Hillsborough County	Southeast County Landfill	09215600.13

SUBJECT	BY	DATE
Southeast County Landfill Phase II-III Closure	TMA	11/16/2021
Veneer Stability Calculations	CHECKED	DATE
	KLS	12/17/2021

$N_A = W_A(\cos\beta) + U_h(\sin\beta) - U_n$ — See Equation 26 on p. 10 in Attachment 1

$N_A =$ 574.66 kN

$$W_P = \frac{\gamma_{dry}(h^2 - h_w^2) + \gamma_{sat'd}(h_w)^2}{\sin 2\beta}$$

See Equation 35 on p. 12 in Attachment 1

$W_P =$ 17.28 kN

$U_V = U_h(\cot\beta)$ — See Equation 29 on p. 11 in Attachment 1

$U_V =$ 0.001218 kN

$$FS = \frac{-b + (b^2 - 4ac)^{1/2}}{2a}$$

See Equation 15 on p. 5 in Attachment 1

$a = W_A(\sin\beta)(\cos\beta) - U_h(\cos^2\beta) + U_h$

See Equation 31 on p. 11 in Attachment 1
for quadratic equation variables "a", "b", and "c"

a = 143.77

$b = -W_A(\sin^2\beta)(\tan\phi) + U_h(\sin\beta)(\cos\beta)(\tan\phi) - N_A(\cos\beta)(\tan\delta) - (W_P - U_V)(\tan\phi)$

Friction angle ϕ =	33.0 °	=	0.58	rad	Refer to Attachment 5
Shear resistance δ =	26.0 °	=	0.45	rad	Refer to Attachment 6

b = -306.67

$c = N_A(\sin\beta)(\tan\delta)(\tan\phi)$

c = 45.27

FS = 1.97

SUMMARY:

DLC	1.3
PSR	0.01
δ =	26.0
FS	1.97

At the minimum interface friction angle indicated in the summary table for all soil-geosynthetic and geosynthetic-geosynthetic interfaces, the calculated factor of safety is (static), indicating that there is adequate shear strength available to prevent the cover soil from sliding. Therefore, the cover soil will be stable under the slope conditions analyzed. The resulting DLC of greater than 1.0, indicating the saturation of the cover soil above the liner would not occur. Therefore the anticipated flow capacity within the drainage layer is sufficient to handle a 25-year 24-hour storm event.

Attachment 1

Analysis of Veneer Cover Soil Koerner and Soong 1998

Analysis and Design of Veneer Cover Soils

Robert M. Koerner
Professor and Director, Geosynthetic Research Institute, Drexel University, Philadelphia, Pennsylvania, USA

Te-Yang Soong
Research Engineer, Geosynthetic Research Institute, Drexel University, Philadelphia, Pennsylvania, USA

ABSTRACT: The sliding of cover soils on slopes underlain by geosynthetics is obviously an unacceptable situation and, if the number of occurrences becomes excessive, will eventually reflect poorly on the entire technology. Steeply sloped leachate collection layers and final covers of landfills are situations where incidents of such sliding have occurred. Paradoxically, the analytic formulation of the situation is quite straightforward. This paper presents an analysis of the common problem of a veneer of cover soil (0.3 to 1.0 m thick) on a geosynthetic material at a given slope angle and length so as to arrive at a FS-value. The paper then presents different scenarios that create lower FS-values than the gravitational stresses of the above situation, e.g., equipment loads, seepage forces and seismic loads. As a counterpoint, different scenarios that create higher FS-values also are presented, e.g., toe berms, tapered thickness cover soils and veneer reinforcement. In this latter category, a subdivision is made between intentional reinforcement (using geogrids or high strength geotextiles) and nonintentional reinforcement (cases where geosynthetics overlay a weak interface within a multilayered slope). Hypothetical numeric examples are used in each of the above situations to illustrate the various influences on the resulting FS-value. In many cases, design curves are also generated. Suggested minimum FS-values are presented for final closures of landfills, waste piles, leach pads, etc., which are the situations where veneer slides of this type are the most troublesome. Hopefully, the paper will serve as a vehicle to bring a greater awareness to such situations so as to avert slides from occurring in the future.

KEYWORDS: Analysis, Design, Limit Equilibrium Methods, Steep Slopes, Veneer Stability.

1 INTRODUCTION

There have been numerous cover soil stability problems in the past resulting in slides that range from being relatively small (which can be easily repaired), to very large (involving litigation and financial judgments against the parties involved). Furthermore, the number of occurrences appears to have increased over the past few years. Soong and Koerner (1996) report on eight cover soil failures resulting from seepage induced stresses alone. While such slides can occur in transportation and geotechnical applications, it is in the environmental applications area where they are most frequent. Specifically, the sliding of relatively thin cover soil layers (called "veneer") above both geosynthetic and natural soil liners, i.e., geomembranes (GM), geosynthetic clay liners (GCL) and compacted clay liners (CCL) are the particular materials of concern. These situations represent a major challenge due (in part) to the following reasons:

(a) The underlying barrier materials generally represent a low interface shear strength boundary with respect to the soil placed above them.
(b) The liner system is oriented precisely in the direction of potential sliding.
(c) The potential shear planes are usually linear and are essentially uninterrupted along the slope.
(d) Liquid (water or leachate) cannot continue to percolate downward through the cross section due to the presence of the barrier material.

When such slopes are relatively steep, long and uninterrupted in their length (which is the design goal for landfills, waste piles and surface impoundments so as to maximize containment space and minimize land area), the situation is exacerbated.

There are two specific applications in which cover soil stability has been difficult to achieve in light of this discussion.

- Leachate collection soil placed above a GM, GCL and/or CCL along the sides of a landfill before waste is placed and stability achieved accordingly.
- Final cover soil placed above a GM, GCL and/or CCL in the cap or closure of a landfill or waste pile after the waste has been placed to its permitted height.

For the leachate collection soil situation, the time frame is generally short (from months to a few years) and the implications of a slide may be minor in that repairs can oftentimes be done by on-site personnel. For the final cover soil situation, the time frame is invariably long (from decades to centuries) and the implications of a slide can be serious in that repairs often call for a forensic analysis, engineering redesign, separately engaged contractors and quite high remediation costs. These latter cases sometime involve litigation, insurance carriers, and invariably technical experts, thus becoming quite contentious.

Since both situations (leachate collection and final covers) present the same technical issues, the paper will address them simultaneously. It should be realized, however, that the final cover situation is of significantly greater concern.

In the sections to follow, geotechnical engineering considerations will be presented leading to the goal of establishing a suitable factor of safety (FS) against slope instability. A number of common situations will then be analyzed, all of which have the tendency to decrease stability. As a counterpoint, a number of design options will follow, all of which have the objective of increasing stability. A summary and conclusions section will compare the various situations which tend to either create slope instability or aid in slope stability. It is hoped that an increased awareness in the analysis and design details offered herein, and elsewhere in the published literature which is referenced herein, leads to a significant decrease in the number of veneer cover soil slides that have occurred.

2 GEOTECHNICAL ENGINEERING CONSIDERATIONS

As just mentioned, the potential failure surface for veneer cover soils is usually linear with the cover soil sliding with respect to the lowest interface friction layer in the underlying cross section. The potential failure plane being linear allows for a straightforward stability calculation without the need for trial center locations and different radii as with soil stability problems analyzed by rotational failure surfaces. Furthermore, full static equilibrium can be achieved without solving simultaneous equations or making simplified design assumptions.

2.1 Limit Equilibrium Concepts

The free body diagram of an *infinitely* long slope with uniformly thick cohesionless cover soil on an incipient planar shear surface, like the upper surface of a geomembrane, is shown in Figure 1. The situation can be treated quite simply.

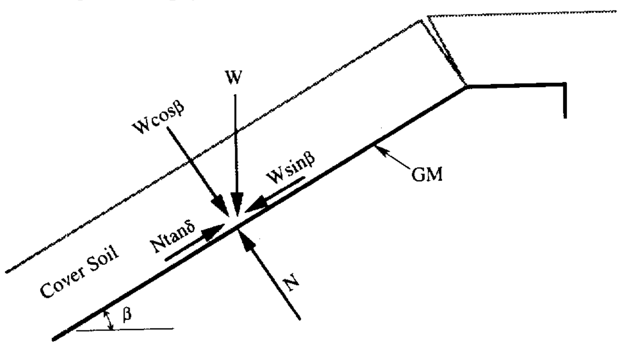

Figure 1. Limit equilibrium forces involved in an infinite slope analysis for a uniformly thick cohesionless cover soil.

By taking force summation parallel to the slope and comparing the resisting force to the driving or mobilizing force, a global factor of safety (FS) results;

$$FS = \frac{\sum \text{Resisting Forces}}{\sum \text{Driving Forces}}$$

$$= \frac{N \tan\delta}{W \sin\beta} = \frac{W \cos\beta \tan\delta}{W \sin\beta}$$

hence:

$$FS = \frac{\tan\delta}{\tan\beta} \qquad (1)$$

Here it is seen that the FS-value is the ratio of tangents of the interface friction angle of the cover soil against the upper surface of the geomembrane (δ), and the slope angle of the soil beneath the geomembrane (β). As simple as this analysis is, its teachings are very significant, for example:

- To obtain an accurate FS-value, an accurately determined laboratory δ-value is absolutely critical. The accuracy of the final analysis is only as good as the accuracy of the laboratory obtained δ-value.
- For low δ-values, the resulting soil slope angle will be proportionately low. For example, for a δ-value of 20 deg., and a required FS-value of 1.5, the maximum slope angle is 14 deg. This is equivalent to a 4(H) on 1(V) slope which is relatively low. Furthermore, many geosynthetics have even lower δ-values than 20 deg.
- This simple formula has driven geosynthetic manufacturers to develop products with high δ-values, e.g., textured geomembranes, thermally bonded drainage geocomposites, internally reinforced GCLs, etc.

Unfortunately, the above analysis is too simplistic to use in most realistic situations. For example, the following situations cannot be accommodated:

- A finite length slope with the incorporation of a passive soil wedge at the toe of the slope
- The consideration of equipment loads on the slope
- Consideration of seepage forces within the cover soil
- Consideration of seismic forces acting on the cover soil
- The use of soil masses acting as toe berms
- The use of tapered covered soil thicknesses
- Reinforcement of the cover soil using geogrids or high strength geotextiles

These specific situations will be treated in subsequent sections. For each situation, the essence of the theory will be presented, followed by the necessary design equations. This will be followed, in each case, with a design graph and a numeric example. First, however, the important issue of interface shear testing will be discussed.

2.2 Interface Shear Testing

The interface shear strength of a cover soil with respect to the underlying material (often a geomembrane) is critical so as to properly analyze the stability of the cover soil. This value of interface shear strength is obtained by laboratory testing of the project specific materials at the site specific conditions. By project specific materials, we mean sampling of the candidate geosynthetics to be used at the site, as well as the cover soil at its targeted density and moisture conditions. By site specific conditions we mean normal stresses, strain rates, peak or residual shear strengths and temperature extremes (high and/or low). Note that it is completely inappropriate to use values of interface shear strengths from the literature for final design.

While the above list of items is formidable, at least the type of test is established. It is the direct shear test which has been utilized in geotechnical engineering testing for many years. The test has been adapted to evaluate geosynthetics in the USA as ASTM D5321 and in Germany as DIN 60500.

In conducting a direct shear test on a specific interface, one typically performs three replicate tests with the only variable being different values of normal stress. The middle value is usually targeted to the site specific condition, with a lower and higher value of normal stress covering the range of possible values. These three tests result in a set of shear displacement versus shear stress curves, see Figure 2a. From each curve, a peak shear strength (τ_p) and a residual shear strength (τ_r) are obtained. As a next step, these shear strength values, together with their respective normal stress values, are plotted on Mohr-Coulomb stress space to obtain the shear strength parameters of friction and adhesion, see Figure 2b.

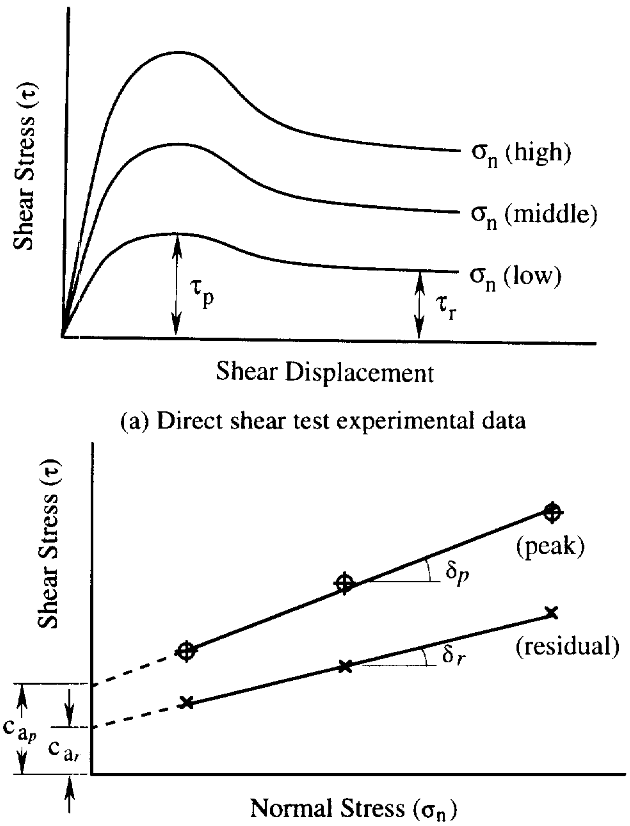

(a) Direct shear test experimental data

(b) Resulting behavior on Mohr - Coulomb stress space

Figure 2. Direct shear test results and analysis procedure to obtain shear strength parameters.

The points are then connected (usually with a straight line), and the two fundamental shear strength parameters are obtained. These shear strength parameters are:

δ = the angle of shearing resistance, peak and/or residual, of the two opposing surfaces (often called the interface friction angle)

c_a = the adhesion of the two opposing surfaces, peak and/or residual (synonymous with cohesion when testing fine grained soils against one another)

Each set of parameters constitute the equation of a straight line which is the Mohr-Coulomb failure criterion common to geotechnical engineering. The concept is readily adaptable to geosynthetic materials in the following form:

$$\tau_p = c_{ap} + \sigma_n \tan \delta_p \quad (2a)$$

$$\tau_r = c_{ar} + \sigma_n \tan \delta_r \quad (2b)$$

The upper limit of "δ" when soil is involved as one of the interfaces is "ϕ", the angle of shearing resistance of the soil component. The upper limit of the "c_a" value is "c", the cohesion of the soil component. In the slope stability analyses to follow, the "c_a" term will be included for the sake of completeness, but then it will be neglected (as being a conservative assumption) in the design graphs and numeric examples. To utilize an adhesion value, there must be a clear physical justification for use of such values when geosynthetics are involved. Some unique situations such as textured geomembranes with physical interlocking of soils having cohesion, or the bentonite component of a GCL are valid reasons for including such a term.

Note that residual strengths are equal, or lower, than peak strengths. The amount of difference is very dependent on the material and no general guidelines can be given. Clearly, material specific and site specific direct shear tests must be performed to determine the appropriate values. Further, each direct shear test must be conducted to a relatively large displacement to determine the residual behavior, see Stark and Poeppel (1994). The decision as to the use of peak or residual strengths in the subsequent analysis is a very subjective one. It is both a materials specific and site specific issue which is left up to the designer and/or regulator. Even further, the use of peak values at the crest of a slope and residual values at the toe may be justified. As such, the analyses to follow will use an interface δ-value with no subscript thereby concentrating on the computational procedures rather than this particular detail. However, the importance of an appropriate and accurate δ-value should not be minimized.

Due to the physical structure of many geosynthetics, the size of the recommended shear box is quite large. It must be at least 300 mm by 300 mm unless it can be shown that data generated by a smaller device contains no scale or edge effects, i.e., that no bias exists with a smaller shear box. The implications of such a large shear box should not be taken lightly. Some issues which should receive particular attention are the following:

- Unless it can be justified otherwise, the interface will usually be tested in a saturated state. Thus complete and uniform saturation over the entire specimen area must be achieved. This is particularly necessary for CCLs and GCLs, Daniel, et al. (1993). Hydration takes relatively long in comparison to soils in conventional (smaller) testing shear boxes.
- Consolidation of soils (including CCLs and GCLs) in larger shear boxes is similarly affected.
- Uniformity of normal stress over the entire area must be maintained during consolidation and shearing so as to avoid stress concentrations from occurring.
- The application of relatively low normal stresses, e.g., 10, to 30 kPa simulating typical cover soil thicknesses, challenges the accuracy of some commercially available shear box setups and monitoring systems, particularly the accuracy of pressure gages.

- The issue of appropriate normal stress is greatly complicated if gas pressures are generated in the underlying waste. These gas pressures will counteract some (or all) of the gravitational stress of the cover soil. The resulting shear strength, and subsequent stability, can be significantly decreased. See Liu et al (1997) for insight into this possibility.
- Shear rates necessary to attain drained conditions (if this is the desired situation) are extremely slow, requiring long testing times.
- Deformations necessary to attain residual strengths require large relative movement of the two respective halves of the shear box. So as not to travel over the edges of the opposing shear box sections, devices should have the lower shear box significantly longer than 300 mm. However, with a lower shear box longer than the upper traveling section, new surface is constantly being added to the shearing plane. This influence is not clear in the material's response or in the subsequent behavior.
- The attainment of a true residual strength is difficult to achieve. ASTM D5321 states that one should "run the test until the applied shear force remains constant with increasing displacement". Many commercially available shear boxes have insufficient travel to reach this condition.
- The ring torsion shearing apparatus is an alternative device to determine true residual strength values, but is not without its own problems. Some outstanding issues are the small specimen size, nonuniform shear rates along the width of the specimen, anisotropic shearing with some geosynthetics and no standardized testing protocol. See Stark and Poeppel (1994) for information and data using this alternative test method.

2.3 Various Types of Loadings

There are a large variety of slope stability problems that may be encountered in analyzing and/or designing final covers of engineered landfills, abandoned dumps and remediation sites as well as leachate collection soils covering geomembranes beneath the waste. Perhaps the most common situation is a uniformly thick cover soil on a geomembrane placed over the soil subgrade at a given and constant slope angle. This "standard" problem will be analyzed in the next section. A variation of this problem will include equipment loads used during placement of cover soil on the geomembrane. This problem will be solved with equipment moving up the slope and then moving down the slope.

Unfortunately, cover soil slides have occurred and it is felt that the majority of the slides have been associated with seepage forces. Indeed, drainage above a geomembrane (or other barrier material) in the cover soil cross section must be accommodated to avoid the possibility of seepage forces. A section will be devoted to this class of slope stability problems.

Lastly, the possibility of seismic forces exists in earthquake prone locations. If an earthquake occurs in the vicinity of an engineered landfill, abandoned dump or remediation site, the seismic wave travels through the solid waste mass reaching the upper surface of the cover. It then decouples from the cover soil materials, producing a horizontal force which must be appropriately analyzed. A section will be devoted to the seismic aspects of cover soil slope analysis as well.

All of the above actions are destabilizing forces tending to cause slope instability. Fortunately, there are a number of actions that can be taken to increase the stability of slopes.

Other than geometrically redesigning the slope with a flatter slope angle or shorter slope length, a designer can add soil mass at the toe of the slope thereby enhancing stability. Both toe berms and tapered soil covers are available options and will be analyzed accordingly. Alternatively, the designer can always use geogrids or high strength geotextiles within the cover soil acting as reinforcement materials. This technique is usually referred to as veneer reinforcement. Cases of both intentional and nonintentional veneer reinforcement will be presented.

Thus it is seen that a number of strategies influence slope stability. Each will be described in the sections to follow. First, the basic gravitational problem will be presented followed by those additional loading situations which tend to decrease slope stability. Second, various actions that can be taken by the designer to increase slope stability will be presented. The summary will contrast the FS-values obtained in the similarly crafted numeric examples.

3 SITUATIONS CAUSING DESTABILIZATION OF SLOPES

This section treats the standard veneer slope stability problem and then superimposes upon it a number of situations, all of which tend to destabilize slopes. Included are gravitational, construction equipment, seepage and seismic forces. Each will be illustrated by a design graph and a numeric example.

3.1 Cover Soil (Gravitational) Forces

Figure 3 illustrates the common situation of a *finite* length, uniformly thick cover soil placed over a liner material at a slope angle "β". It includes a passive wedge at the toe and has a tension crack of the crest. The analysis that follows is after Koerner and Hwu (1991), but comparable analyses are available from Giroud and Beech (1989), McKelvey and Deutsch (1991), Ling and Leshchinsky (1997) and others.

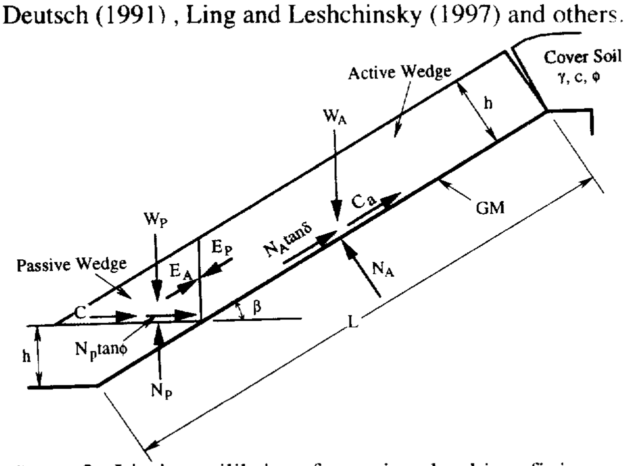

Figure 3. Limit equilibrium forces involved in a finite length slope analysis for a uniformly thick cover soil.

The symbols used in Figure 3 are defined below.

W_A = total weight of the active wedge
W_P = total weight of the passive wedge
N_A = effective force normal to the failure plane of the active wedge
N_P = effective force normal to the failure plane of the passive wedge
γ = unit weight of the cover soil
h = thickness of the cover soil
L = length of slope measured along the geomembrane
β = soil slope angle beneath the geomembrane
ϕ = friction angle of the cover soil
δ = interface friction angle between cover soil and geomembrane
C_a = adhesive force between cover soil of the active wedge and the geomembrane
c_a = adhesion between cover soil of the active wedge and the geomembrane
C = cohesive force along the failure plane of the passive wedge
c = cohesion of the cover soil
E_A = interwedge force acting on the active wedge from the passive wedge
E_P = interwedge force acting on the passive wedge from the active wedge
FS = factor of safety against cover soil sliding on the geomembrane

The expression for determining the factor of safety can be derived as follows:

Considering the active wedge,

$$W_A = \gamma h^2\left(\frac{L}{h} - \frac{1}{\sin\beta} - \frac{\tan\beta}{2}\right) \qquad (3)$$

$$N_A = W_A \cos\beta \qquad (4)$$

$$C_a = c_a\left(L - \frac{h}{\sin\beta}\right) \qquad (5)$$

By balancing the forces in the vertical direction, the following formulation results:

$$E_A \sin\beta = W_A - N_A \cos\beta - \frac{N_A \tan\delta + C_a}{FS}\sin\beta \qquad (6)$$

Hence the interwedge force acting on the active wedge is:

$$E_A = \frac{(FS)(W_A - N_A\cos\beta) - (N_A\tan\delta + C_a)\sin\beta}{\sin\beta(FS)} \qquad (7)$$

The passive wedge can be considered in a similar manner:

$$W_P = \frac{\gamma h^2}{\sin 2\beta} \qquad (8)$$

$$N_p = W_P + E_P \sin\beta \qquad (9)$$

$$C = \frac{(c)(h)}{\sin\beta} \qquad (10)$$

By balancing the forces in the horizontal direction, the following formulation results:

$$E_P \cos\beta = \frac{C + N_P \tan\phi}{FS} \qquad (11)$$

Hence the interwedge force acting on the passive wedge is:

$$E_P = \frac{C + W_P \tan\phi}{\cos\beta(FS) - \sin\beta\tan\phi} \qquad (12)$$

By setting $E_A = E_P$, the resulting equation can be arranged in the form of the quadratic equation $ax^2 + bx + c = 0$ which in our case, using FS-values, is:

$$a(FS)^2 + b(FS) + c = 0 \qquad (13)$$

where

$$a = (W_A - N_A\cos\beta)\cos\beta$$

$$b = -\left[(W_A - N_A\cos\beta)\sin\beta\tan\phi + (N_A\tan\delta + C_a)\sin\beta\cos\beta + \sin\beta(C + W_P\tan\phi)\right]$$

$$c = (N_A\tan\delta + C_a)\sin^2\beta\tan\phi \qquad (14)$$

The resulting FS-value is then obtained from the solution of the quadratic equation:

$$\boxed{FS = \frac{-b + \sqrt{b^2 - 4ac}}{2a}} \qquad (15)$$

When the calculated FS-value falls below 1.0, sliding of the cover soil on the geomembrane is to be anticipated. Thus a value of greater than 1.0 must be targeted as being the minimum factor of safety. How much greater than 1.0 the FS-value should be, is a design and/or regulatory issue. The issue of minimum allowable FS-values under different conditions will be assessed at the end of the paper. In order to better illustrate the implications of Eqs. 13, 14 and 15, typical design curves for various FS-values as a function of slope angle and interface friction angle are given in Figure 4. Note that the curves are developed specifically for the variables stated in the legend of the figure. Example 1 illustrates the use of the curves in what will be the standard example to which other examples will be compared.

Example 1:
Given a 30 m long slope with a uniformly thick 300 mm cover soil at a unit weight of 18 kN/m³. The soil has a friction angle of 30 deg. and zero cohesion, i.e., it is a sand. The cover soil is placed directly on a geomembrane as shown in Figure 3. Direct shear testing has resulted in a interface friction angle between the cover soil and geomembrane of 22 deg. with zero adhesion. What is the FS-value at a slope angle of 3(H)-to-1(V), i.e., 18.4 deg?

Solution:

Substituting Eq. 14 into Eq. 15 and solving for the FS-value results in the following which is seen to be in agreement with the curves of Figure 4.

$$\left.\begin{aligned} a &= 14.7\,\mathrm{kN/m} \\ b &= -21.3\,\mathrm{kN/m} \\ c &= 3.5\,\mathrm{kN/m} \end{aligned}\right\} \quad FS = 1.25$$

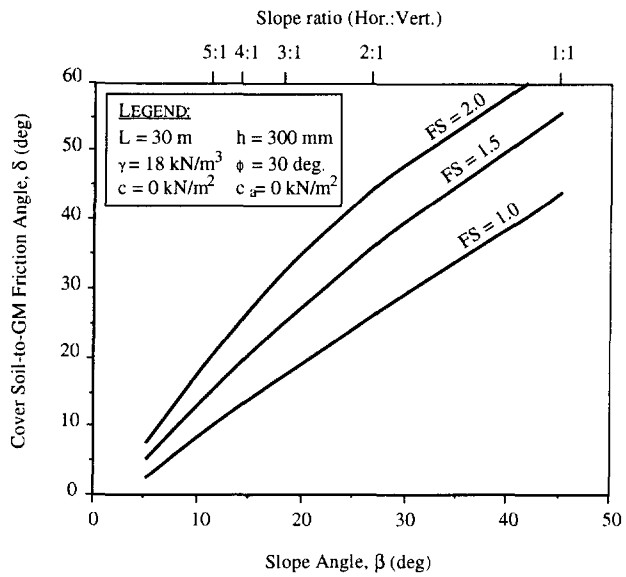

Figure 4. Design curves for stability of uniform thickness cohesionless cover soils on linear failure planes for various global factors-of-safety.

Comment:
In general, this is too low of a value for a final cover soil factor-of-safety and a redesign is necessary. While there are many possible options of changing the geometry of the situation, the example will be revisited later in this section using toe berms, tapered cover soil thickness and veneer reinforcement. Furthermore, this general problem will be used throughout the main body of this paper for comparison purposes to other cover soil slope stability situations.

3.2 Tracked Construction Equipment Forces

The placement of cover soil on a slope with a relatively low shear strength inclusion (like a geomembrane) should always be from the toe upward to the crest. Figure 5a shows the recommended method. In so doing, the gravitational forces of the cover soil and live load of the construction equipment are compacting previously placed soil and working with an ever present passive wedge and stable lower-portion beneath the active wedge. While it is necessary to specify low ground pressure equipment to place the soil, the reduction of the FS-value for this situation of equipment working up the slope will be seen to be relatively small.

For soil placement down the slope, however, a stability analysis cannot rely on toe buttressing and also a dynamic stress should be included in the calculation. These conditions decrease the FS-value and in some cases to a great extent. Figure 5b shows this procedure. Unless absolutely necessary, it is not recommended to place cover soil on a slope in this manner. If it is necessary, the design must consider the unsupported soil mass and the dynamic force of the specific type of construction equipment and its manner of operation.

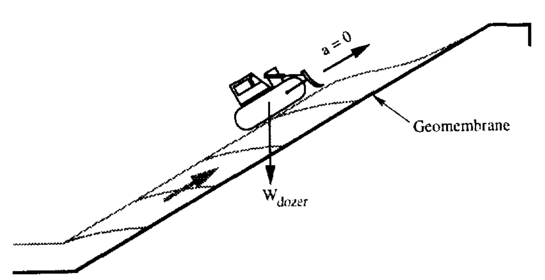

(a) Equipment backfilling up slope
(the recommended method)

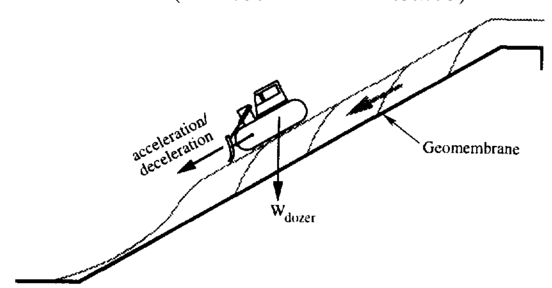

(b) Equipment backfilling down slope
(method is not recommended)

Figure 5. Construction equipment placing cover soil on slopes containing geosynthetics.

For the first case of a bulldozer pushing cover soil up from the toe of the slope to the crest, the analysis uses the free body diagram of Figure 6a. The analysis uses a specific piece of tracked construction equipment (like a bulldozer characterized by its ground contact pressure) and dissipates this force or stress through the cover soil thickness to the surface of the geomembrane. A Boussinesq analysis is used, see Poulos and Davis (1974). This results in an equipment force per unit width as follows:

$$W_e = q\,w\,I \tag{16}$$

where

W_e = equivalent equipment force per unit width at the geomembrane interface
q = $W_b / (2 \times w \times b)$

W_b = actual weight of equipment (e.g., a bulldozer)
w = length of equipment track
b = width of equipment track
I = influence factor at the geomembrane interface see Figure 7

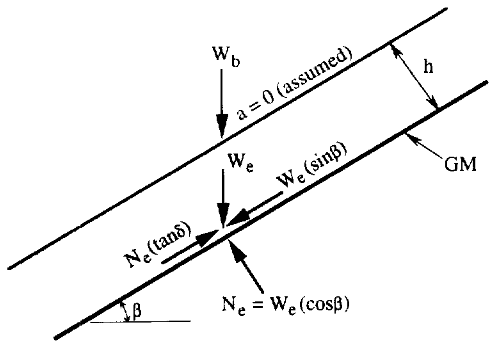

(a) Equipment moving up slope
(load with no assumed acceleration)

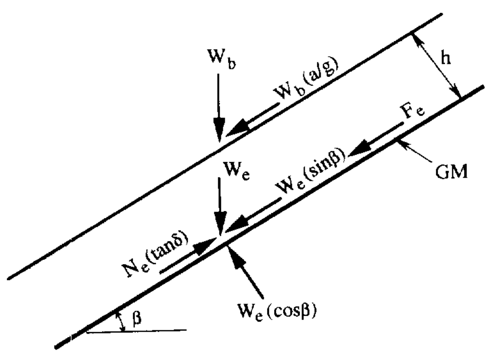

(b) Equipment moving down slope
(load plus acceleration or deceleration)

Figure 6. Additional (to gravitational forces) limit equilibrium forces due to construction equipment moving on cover soil (see Figure 3 for the gravitational soil force to which the above forces are added).

Upon determining the additional equipment force at the cover soil-to-geomembrane interface, the analysis proceeds as described in Section 3.1 for gravitational forces only. In essence, the equipment moving up the slope adds an additional term, W_e, to the W_A-force in Eq. 3. Note, however, that this involves the generation of a resisting force as well. Thus, the net effect of increasing the driving force as well as the resisting force is somewhat neutralized insofar as the resulting FS-value is concerned. It should also be noted that no acceleration/deceleration forces are included in this analysis which is somewhat optimistic. Using these concepts (the same equations used in Section 3.1 are used here), typical design curves for various FS-values as a function of equivalent ground contact equipment pressures and cover soil thicknesses are given in Figure 8. Note that the curves are developed specifically for the variables stated in the legend. Example 2a illustrates the use of the formulation.

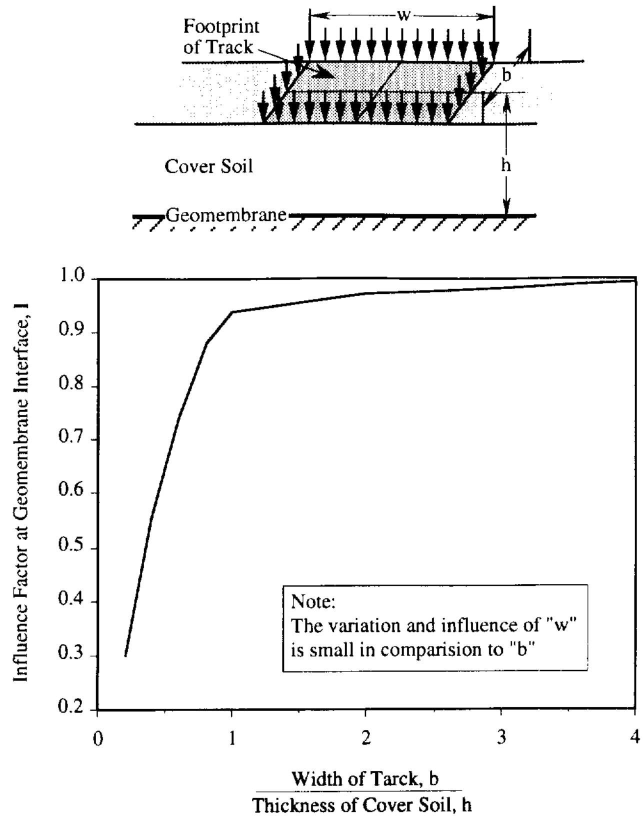

Figure 7. Values of influence factor, "I", for use in Eq. 16 to dissipate surface force of tracked equipment through the cover soil to the geomembrane interface, after Poulos and Davis (1974).

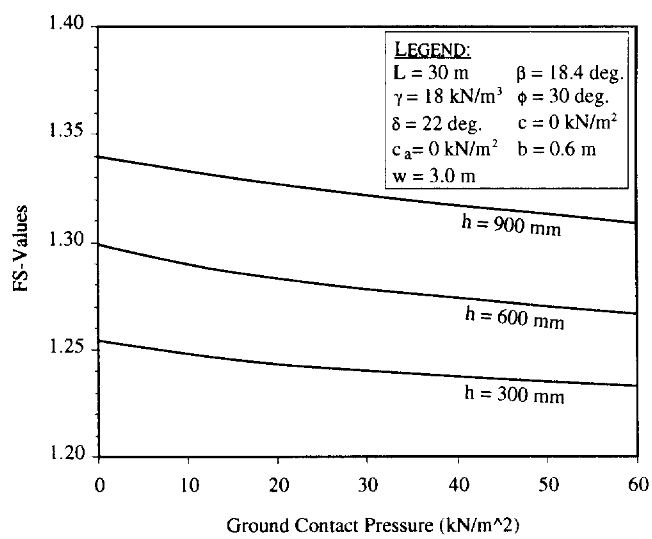

Figure 8. Design curves for stability of different thickness of cover soil for various values of tracked ground contact pressure construction equipment.

Example 2a:

Given 30 m long slope with uniform cover soil of 300 mm thickness at a unit weight of 18 kN/m^3. The soil has a friction angle of 30 deg. and zero cohesion, i.e., it is a sand. It is placed on the slope using a bulldozer moving from the toe of the slope up to the crest. The bulldozer has a ground pressure of 30 kN/m^2 and tracks that are 3.0 m long and 0.6 m wide. The cover soil to geomembrane friction angle is 22 deg. with zero adhesion. What is the FS-value at a slope angle of 3(H)-to-1(V), i.e., 18.4 deg.

Solution:
This problem follows Example 1 exactly except for the addition of the bulldozer moving up the slope. Using the additional equipment load Eq. 16, substituted into Eqs. 14 and 15 results in the following.

$$\left.\begin{array}{l} a = 73.1\,\mathrm{kN/m} \\ b = -104.3\,\mathrm{kN/m} \\ c = 17.0\,\mathrm{kN/m} \end{array}\right\} FS = 1.24$$

Comment:
While the resulting FS-value is low, the result is best assessed by comparing it to Example 1, i.e., the same problem except without the bulldozer. It is seen that the FS-value has only decreased from 1.25 to 1.24. Thus, in general, a low ground contact pressure bulldozer placing cover soil up the slope with negligible acceleration/ deceleration forces does not significantly decrease the factor-of-safety.

For the second case of a bulldozer pushing cover soil down from the crest of the slope to the toe as shown in Figure 5b, the analysis uses the force diagram of Figure 6b. While the weight of the equipment is treated as just described, the lack of a passive wedge along with an additional force due to acceleration (or deceleration) of the equipment significantly changes the resulting FS-values. This analysis again uses a specific piece of construction equipment operated in a specific manner. It produces a force parallel to the slope equivalent to W_b (a/g), where W_b = the weight of the bulldozer, a = acceleration of the bulldozer and g = acceleration due to gravity. Its magnitude is equipment operator dependent and related to both the equipment speed and time to reach such a speed, see Figure 9. A similar behavior will be seen for deceleration.

The acceleration of the bulldozer, coupled with an influence factor "I" from Figure 7, results in the dynamic force per unit width at the cover soil to geomembrane interface, "F_e". The relationship is as follows:

$$F_e = W_e\left(\frac{a}{g}\right) \tag{17}$$

where

F_e = dynamic force per unit width parallel to the slope at the geomembrane interface,

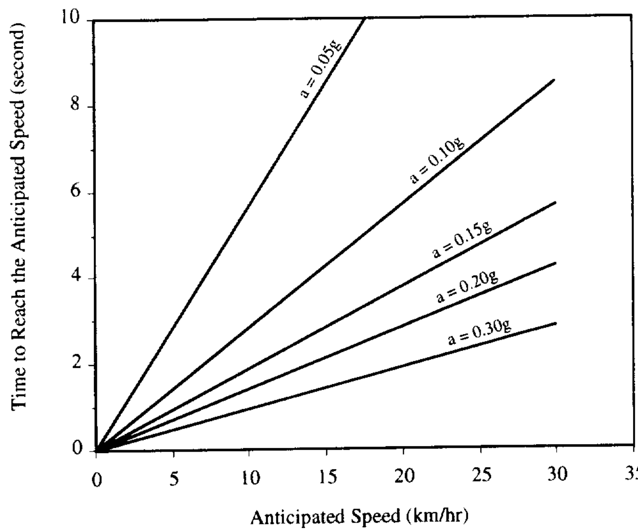

Figure 9. Graphic relationship of construction equipment speed and rise time to obtain equipment acceleration.

W_e = equivalent equipment (bulldozer) force per unit width at geomembrane interface, recall Eq. 16.
β = soil slope angle beneath geomembrane
a = acceleration of the bulldozer
g = acceleration due to gravity

Using these concepts, the new force parallel to the cover soil surface is dissipated through the thickness of the cover soil to the interface of the geomembrane. Again, a Boussinesq analysis is used, see Poulos and Davis (1974). The expression for determining the FS-value can now be derived as follows:

Considering the active wedge, and balancing the forces in the direction parallel to the slope, the following formulation results:

$$E_A + \frac{(N_e + N_A)\tan\delta + C_a}{FS} = (W_A + W_e)\sin\beta + F_e \tag{18}$$

where

N_e = effective equipment force normal to the failure plane of the active wedge
= $W_e \cos\beta$ (19)

Note that all the other symbols have been previously defined.

The interwedge force acting on the active wedge can down be expressed as:

$$E_A = \frac{(FS)\left[(W_A + W_e)\sin\beta + F_e\right]}{FS} - \frac{\left[(N_e + N_A)\tan\delta + C_a\right]}{FS} \tag{20}$$

The passive wedge can be treated in a similar manner. The following formulation of the interwedge force acting on the passive wedge results:

$$E_P = \frac{C + W_P \tan\phi}{\cos\beta(FS) - \sin\beta\tan\phi} \quad (21)$$

By setting $E_A = E_P$, the following equation can be arranged in the form of Eq. 13 in which the "a", "b" and "c" terms are as follows:

$$a = \left[\left(W_A + W_e\right)\sin\beta + F_e\right]\cos\beta$$

$$b = -\left\{\left[\left(N_e + N_A\right)\tan\delta + C_a\right]\cos\beta + \left[\left(W_A + W_e\right)\sin\beta + F_e\right]\sin\beta\tan\phi + \left(C + W_P\tan\phi\right)\right\}$$

$$c = \left[\left(N_e + N_A\right)\tan\delta + C_a\right]\sin\beta\tan\phi \quad (22)$$

Finally, the resulting FS-value can be obtained using Eq. 15. Using these concepts, typical design curves for various FS-values as a function of equipment ground contact pressure and equipment acceleration can be developed, see Figure 10. Note that the curves are developed specifically for the variables stated in the legend. Example 2b illustrates the use of the formulation.

Example 2b:

Given a 30 m long slope with uniform cover soil of 300 mm thickness at a unit weight of 18 kN/m^3. The soil has a friction angle of 30 deg. and zero cohesion, i.e., it is a sand. It is placed on the slope using a bulldozer moving from the crest of the slope down to the toe. The bulldozer has a ground contact pressure of 30 kN/m^2 and tracks that are 3.0 m long and 0.6 m wide. The estimated equipment speed is 20 km/hr and the time to reach this speed is 3.0 sec. The cover soil to geomembrane friction angle is 22 deg. with zero adhesion. What is the FS-value at a slope angle of 3(H)-to-1(V), i.e., 18.4 deg.

Solution:

Using the design curves of Figure 10 along with Eqs. 22 substituted into Eq. 15 the solution can be obtained:

- From Figure 9 at 20 km/hr and 3.0 sec. the bulldozer's acceleration is 0.19g.
- From Eq. 22 substituted into Eq. 15 we obtain

$$\left.\begin{aligned} a &= 88.8\,\text{kN/m} \\ b &= -107.3\,\text{kN/m} \\ c &= 17.0\,\text{kN/m} \end{aligned}\right\} \quad FS = 1.03$$

Comment:

This problem solution can now be compared to the previous two examples:

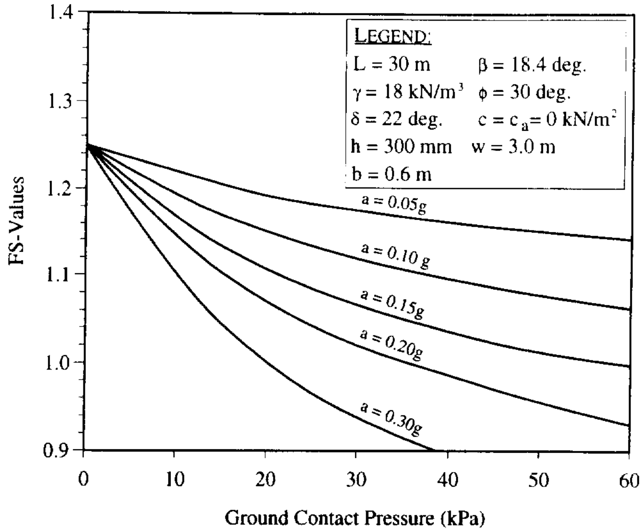

Figure 10. Design curves for stability of different construction equipment ground contact pressure for various equipment accelerations.

Ex. 1:	cover soil alone with no bulldozer loading	FS = 1.25
Ex. 2a:	cover soil plus bulldozer moving up slope	FS = 1.24
Ex. 2b:	cover soil plus bulldozer moving down slope	FS = 1.03

The inherent danger of a bulldozer moving down the slope is readily apparent. Note, that the same result comes about by the bulldozer decelerating instead of accelerating. The sharp breaking action of the bulldozer is arguable the more severe condition due to the extremely short times involved when stopping forward motion. Clearly, only in unavoidable situations should the cover soil placement equipment be allowed to work down the slope. If it is unavoidable, an analysis should be made of the specific stability situation and the construction specifications should reflect the exact conditions made in the design. The maximum allowable weight and ground contact pressure of the equipment should be stated along with suggested operator movement of the cover soil placement operations. Truck traffic on the slopes can also give as high, or even higher, stresses and should be avoided unless adequately designed. Additional detail is given in McKelvey (1994). The issue of access ramps is a unique subset of this example and one which deserves focused attention due to the high loads and decelerations that often occur.

3.3 Consideration of Seepage Forces

The previous sections presented the general problem of slope stability analysis of cover soils placed on slopes under different conditions. The tacit assumption throughout was that either permeable soil or a drainage layer was placed above the barrier layer with adequate flow capacity to efficiently remove permeating water safely way from the cross section. The amount of water to be removed is obviously a site specific situation. Note that in extremely arid areas, or with very low permeability cover soils drainage may not be required although this is generally the exception.

Unfortunately, adequate drainage of final covers has sometimes not been available and seepage induced slope stability problems have occurred. The following situations have resulted in seepage induced slides:

- Drainage soils with hydraulic conductivity (permeability) too low for site specific conditions.
- Inadequate drainage capacity at the toe of long slopes where seepage quantities accumulate and are at their maximum.
- Fines from quarried drainage stone either clogging the drainage layer or accumulating at the toe of the slope thereby decreasing the as-constructed permeability over time.
- Fine, cohesionless, cover soil particles migrating through the filter (if one is present) either clogging the drainage layer, or accumulating at the toe of the slope thereby decreasing the as-constructed outlet permeability over time.
- Freezing of the drainage layer at the toe of the slope, while the soil covered top of the slope thaws, thereby mobilizing seepage forces against the ice wedge at the toe.

If seepage forces of the types described occur, a variation in slope stability design methodology is required. Such an analysis is the focus of this subsection. Note that additional discussion is given in Cancelli and Rimoldi (1989), Thiel and Stewart (1993) and Soong and Koerner (1996).

Consider a cover soil of uniform thickness placed directly above a geomembrane at a slope angle of "β" as shown in Figure 11. Different from previous examples, however, is that within the cover soil exists a saturated soil zone for part or all of the thickness. The saturated boundary is shown as two possibly different phreatic surface orientations. This is because seepage can be built-up in the cover soil in two different ways: a horizontal buildup from the toe upward or a parallel-to-slope buildup outward. These two hypotheses are defined and quantified as a horizontal submergence ratio (HSR) and a parallel submergence ratio (PSR). The dimensional definitions of both ratios are given in Figure 11.

When analyzing the stability of slopes using the limit equilibrium method, free body diagrams of the passive and active wedges are taken with the appropriate forces (now including pore water pressures) being applied. The formulation for the resulting factor-of-safety, for horizontal seepage buildup and then for parallel-to-slope seepage buildup, follows.

<u>The Case of the Horizontal Seepage Buildup</u>. Figure 12 shows the free body diagram of both the active and passive wedge assuming horizontal seepage. Horizontal seepage buildup can occur when toe blockage occurs due to inadequate outlet capacity, contamination or physical blocking of outlets, or freezing conditions at the outlets.

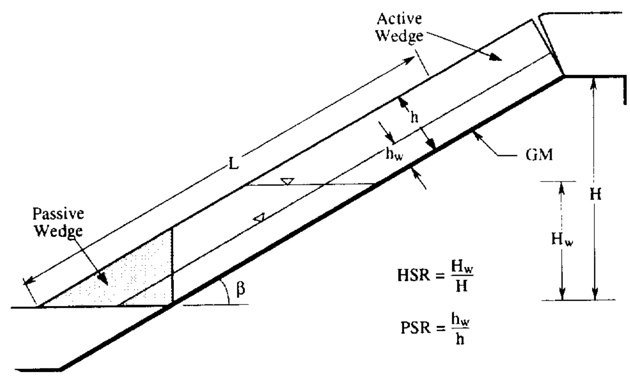

Figure 11. Cross section of a uniform thickness cover soil on a geomembrane illustrating different submergence assumptions and related definitions, Soong and Koerner (1996).

All symbols used in Figure 12 were previously defined except the following:

$\gamma_{sat'd}$ = saturated unit weight of the cover soil
γ_t = total (moist) unit weight of the cover soil
γ_w = unit weight of water
H = vertical height of the slope measured from the toe
H_w = vertical height of the free water surface measured from the toe
U_h = resultant of the pore pressures acting on the interwedge surfaces
U_n = resultant of the pore pressures acting perpendicular to the slope
U_v = resultant of the vertical pore pressures acting on the passive wedge

The expression for finding the factor-of-safety can be derived as follows:

Considering the active wedge,

$$W_A = \left(\frac{\gamma_{sat'd}(h)(2H_w\cos\beta - h)}{\sin 2\beta}\right) + \left(\frac{\gamma_t(h)(H - H_w)}{\sin\beta}\right) \tag{23}$$

$$U_n = \frac{\gamma_w(h)(\cos\beta)(2H_w\cos\beta - h)}{\sin 2\beta} \tag{24}$$

$$U_h = \frac{\gamma_w h^2}{2} \tag{25}$$

$$\boxed{N_A = W_A(\cos\beta) + U_h(\sin\beta) - U_n} \tag{26}$$

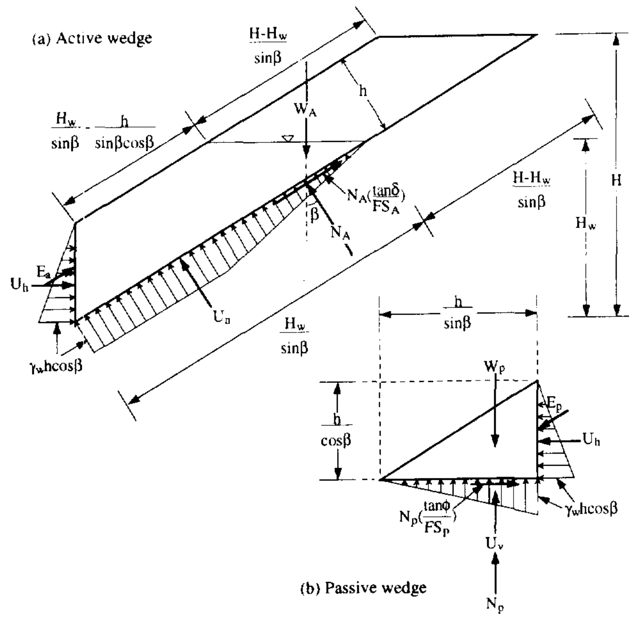

Figure 12. Limit equilibrium forces involved in a finite length slope of uniform cover soil with horizontal seepage buildup.

The interwedge force acting on the active wedge can then be expressed as:

$$E_A = W_A \sin\beta - U_h \cos\beta - \frac{N_A \tan\delta}{FS} \tag{27}$$

The passive wedge can be considered in a similar manner and the following expressions result:

$$W_P = \frac{\gamma_{sat'd} h^2}{\sin 2\beta} \tag{28}$$

$$U_V = U_h \cot\beta \tag{29}$$

The interwedge force acting on the passive wedge can then be expressed as:

$$E_P = \frac{U_h(FS) - (W_P - U_V)\tan\phi}{\sin\beta\tan\phi - \cos\beta(FS)} \tag{30}$$

By setting $E_A = E_P$, the following equation can be arranged in the form of $ax^2 + bx + c = 0$ which in this case is:

$$a(FS)^2 + b(FS) + c = 0 \tag{13}$$

where

$$\begin{aligned} a &= W_A \sin\beta\cos\beta - U_h \cos^2\beta + U_h \\ b &= -W_A \sin^2\beta\tan\phi + U_h \sin\beta\cos\beta\tan\phi \\ &\quad - N_A \cos\beta\tan\delta - (W_P - U_V)\tan\phi \\ c &= N_A \sin\beta\tan\delta\tan\phi \end{aligned} \tag{31}$$

As with previous solution, the resulting FS-value is obtained using Eq. 15.

The Case of Parallel-to-Slope Seepage Buildup. Figure 13 shows the free body diagrams of both the active and passive wedges with seepage buildup in the direction parallel to the slope. Parallel seepage buildup can occur when soils placed above a geomembrane are initially too low in their hydraulic conductivity, or become too low due to long-term clogging from overlying soils which do not have a filter. Identical symbols as defined in the previous cases are used here with an additional definition of h_w equal to the height of free water surface measured in the direction perpendicular to the slope.

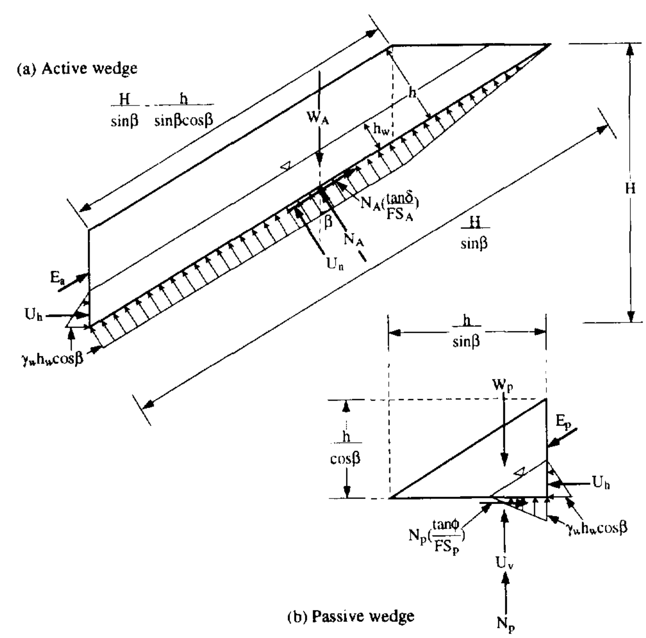

Figure 13. Limit equilibrium forces involved in a finite length slope of uniform cover soil with parallel-to-slope seepage buildup.

Note that the general expression of factor-of-safety shown in Eq. 15 is still valid. However, the a, b and c terms given in Eq. 31 have different definitions in this case owing to the new definitions of the following terms:

$$W_A = \frac{\gamma_t(h - h_w)(2H\cos\beta - (h + h_w))}{\sin 2\beta} + \frac{\gamma_{sat'd}(h_w)(2H\cos\beta - h_w)}{\sin 2\beta} \quad (32)$$

$$U_n = \frac{\gamma_w h_w \cos\beta(2H\cos\beta - h_w)}{\sin 2\beta} \quad (33)$$

$$U_h = \frac{\gamma_w (h_w)^2}{2} \quad (34)$$

$$W_P = \frac{\gamma_t(h^2 - h_w^2) + \gamma_{sat'd}(h_w^2)}{\sin 2\beta} \quad (35)$$

In order to illustrate the behavior of these equations, the design curves of Figure 14 have been developed. They show the decrease in FS-value with increasing submergence ratio for all values of interface friction. Furthermore, the differences in response curves for the parallel and horizontal submergence ratio assumptions are seen to be very small. Note that the curves are developed specifically for variables stated in the legend. Example 3 illustrates the use of the design curves.

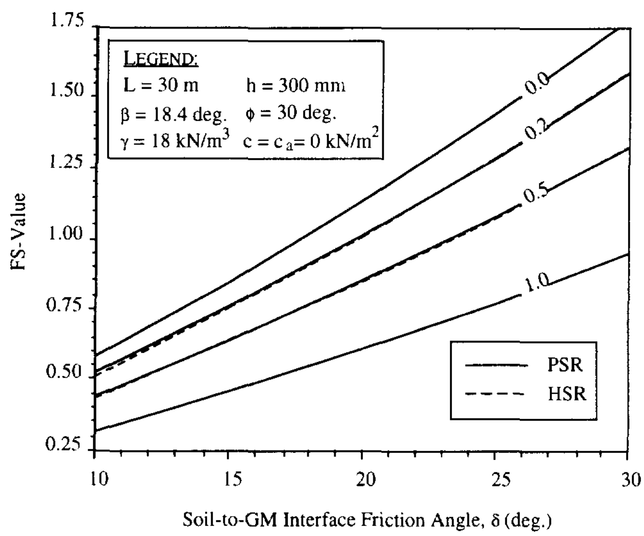

Figure 14. Design curves for stability of cohesionless, uniform thickness, cover soils for different submergence ratios.

Example 3:

Given a 30 m long slope with a uniform thickness cover soil of 300 mm at a dry unit weight of 18 kN/m^3. The soil has a friction angle of 30 deg. and zero cohesion, i.e., it is a sand. The soil becomes saturated through 50% of its thickness, i.e., it is a parallel seepage problem with PSR = 0.5, and its saturated unit weight increases to 21 kN/m^3. Direct shear testing has resulted in an interface friction angle of 22 deg. with zero adhesion. What is the factor-of-safety at a slope of 3(H)-to-1(V), i.e., 18.4 deg.

Solution:

Solving Eqs. 31 with the values of Eqs. 32 to 35 for the a, b and c terms and then substituting them into Eq. 15 results in the following.

$$\left.\begin{aligned} a &= 51.7\,\text{kN/m} \\ b &= -57.8\,\text{kN/m} \\ c &= 9.0\,\text{kN/m} \end{aligned}\right\} \quad FS = 0.93$$

Comment:

The seriousness of seepage forces in a slope of this type are immediately obvious. Had the saturation been 100% of the drainage layer thickness, the FS-value would have been even lower. Furthermore, the result using a horizontal assumption of saturated cover soil with the same saturation ratio will give identically low FS-values. Clearly, the teaching of this example problem is that adequate long-term drainage above the barrier layer in cover soil slopes must be provided to avoid seepage forces from occurring.

3.4 Consideration of Seismic Forces

In areas of anticipated earthquake activity, the slope stability analysis of a final cover soil over an engineered landfill, abandoned dump or remediated site must consider seismic forces. In the United States, the Environmental Protection Agency (EPA) regulations require such an analysis for sites that have a probability of ≥ 10% of experiencing a 0.10 g peak horizontal acceleration within the past 250 years. For the continental USA this includes not only the western states, but major sections of the midwest and northeast states, as well. If practiced worldwide, such a criterion would have huge implications.

The seismic analysis of cover soils of the type under consideration in this paper is a two-part process:

- The calculation of a FS-value using a pseudo-static analysis via the addition of a horizontal force acting at the centroid of the cover soil cross section.
- If the FS-value in the above calculation is less than 1.0, a permanent deformation analysis is required. The calculated deformation is then assessed in light of the potential damage to the cover soil section and is either accepted, or the slope requires an appropriate redesign. The redesign is then analyzed until the situation becomes acceptable.

The first part of the analysis is a pseudo-static approach which follows the previous examples except for the addition of a horizontal force at the centroid of the cover soil in proportion to the anticipated seismic activity. It is first necessary to obtain an average seismic coefficient (C_S). The bedrock acceleration can be estimated from a seismic zone map, e.g., Algermissen (1991), using the procedures embodied in Richardson, et al (1995). Such maps are available on a worldwide basis. The value of C_s is nondimensional and is a ratio of the bedrock acceleration to gravitational acceleration. This value of C_s is modified using available computer codes such as "SHAKE", see

Schnabel, et al. (1972), for propagation to the site and then to the landfill cover. The computational process within such programs is quite intricate. For detailed discussion see Seed and Idriss (1982) and Idriss (1990). The analysis is then typical to those previously presented.

Using Figure 15, the additional seismic force is seen to be $C_S W_A$ acting horizontally on the active wedge. All additional symbols used in Figure 15 have been previously defined and the expression for finding the FS-value can be derived as follows:

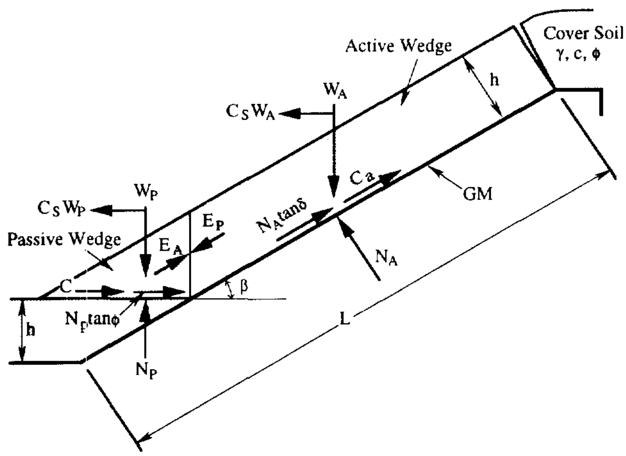

Figure 15. Limit equilibrium forces involved in pseudo-static analysis including use of an average seismic coefficient

Considering the active wedge, by balancing the forces in the horizontal direction, the following formulation results:

$$E_A \cos\beta + \frac{(N_A \tan\delta + C_a)\cos\beta}{FS} = C_S W_A + N_A \sin\beta \qquad (36)$$

Hence the interwedge force acting on the active wedge results:

$$E_A = \frac{(FS)(C_S W_A + N_A \sin\beta)}{(FS)\cos\beta} - \frac{(N_A \tan\delta + C_a)\cos\beta}{(FS)\cos\beta} \qquad (37)$$

The passive wedge can be considered in a similar manner and the following formulation results:

$$E_P \cos\beta + C_S W_P = \frac{C + N_P \tan\phi}{FS} \qquad (38)$$

Hence the interwedge force acting on the passive wedge is:

$$E_P = \frac{C + W_P \tan\phi - C_S W_P (FS)}{(FS)\cos\beta - \sin\beta \tan\phi} \qquad (39)$$

Again, by setting $E_A = E_P$, the following equation can be arranged in the form of $ax^2 + bx + c = 0$ which in this case is:

$$a(FS)^2 + b(FS) + c = 0 \qquad (13)$$

where

$$\begin{aligned} a &= (C_S W_A + N_A \sin\beta)\cos\beta + C_S W_P \cos\beta \\ b &= -[(C_S W_A + N_A \sin\beta)\sin\beta \tan\phi \\ &\quad + (N_A \tan\delta + C_a)\cos^2\beta \\ &\quad + (C + W_P \tan\phi)\cos\beta] \\ c &= (N_A \tan\delta + C_a)\cos\beta \sin\beta \tan\phi \end{aligned} \qquad (40)$$

The resulting FS-value is then obtained from the following equation:

$$FS = \frac{-b + \sqrt{b^2 - 4ac}}{2a} \qquad (15)$$

Using these concepts, a design curve for the general problem under consideration as a function of seismic coefficient can be developed, see Figure 16. Note that the curve is developed specifically for the variables stated in the legend. Example 4a illustrates the use of the curve.

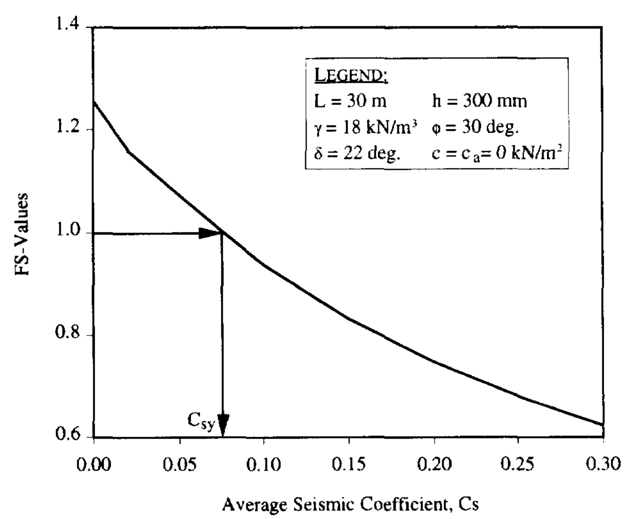

Figure 16. Design curve for a uniformly thick cover soil pseudo-static seismic analysis with varying average seismic coefficients.

Example 4a:

Given a 30 m long slope with uniform thickness cover soil of 300 mm at a unit weight of 18 kN/m^3. The soil has a friction angle of 30 deg. and zero cohesion, i.e., it is a sand. The cover soil is on a geomembrane as shown in Figure 15. Direct shear testing has resulted in an interface friction angle of 22 deg. with zero adhesion. The slope angle is 3(H)-to-1(V), i.e., 18.4 deg. A design earthquake appropriately transferred to the site's cover soil results in an average seismic coefficient of 0.10. What is the FS-value?

Solution:
Solving Eqs. 40 for the values given in the example and substituting into Eq. 15 results in the following FS-value.

$$\left.\begin{aligned} a &= 59.6\,\text{kN}/\text{m} \\ b &= -66.9\,\text{kN}/\text{m} \\ c &= 10.4\,\text{kN}/\text{m} \end{aligned}\right\} \quad FS = 0.94$$

Note that the value of FS = 0.94 agrees with the design curve of Figure 16 at a seismic coefficient of 0.10.

Comment:
Had the above FS-value been greater than 1.0, the analysis would be complete. The assumption being that cover soil stability can withstand the short-term excitation of an earthquake and still not slide. However, since the value in this example is less than 1.0, a second part of the analysis is required.

The second part of the analysis is directed toward calculating the estimated deformation of the lowest shear strength interface in the cross section under consideration. The deformation is then assessed in light of the potential damage that may be imposed on the system.

To begin the permanent deformation analysis, a yield acceleration, "C_{sy}", is obtained from a pseudo-static analysis under an assumed FS = 1.0. Figure 16 illustrates this procedure for the assumptions stated in the legend. It results in a value of C_{sy} = 0.075. Coupling this value with the time history response obtained for the actual site location and cross section, results in a comparison as shown in Figure 17a. If the earthquake time history response never exceeds the value of C_{sy}, there is no anticipated permanent deformation. However, whenever any part of the time history curve exceeds the value of C_{sy}, permanent deformation is expected. By double integration of the time history curve (which is acceleration), to velocity (Figure 17b) and then to displacement (Figure 17c), the anticipated value of deformation can be obtained. This value is considered to be permanent deformation and is then assessed based on the site-specific implications of damage to the final cover system. Empirical charts, e.g., Makdisi and Seed (1978) can also be used to estimate the permanent deformation. Example 4b continues the previous pseudo-static analysis into the deformation calculation.

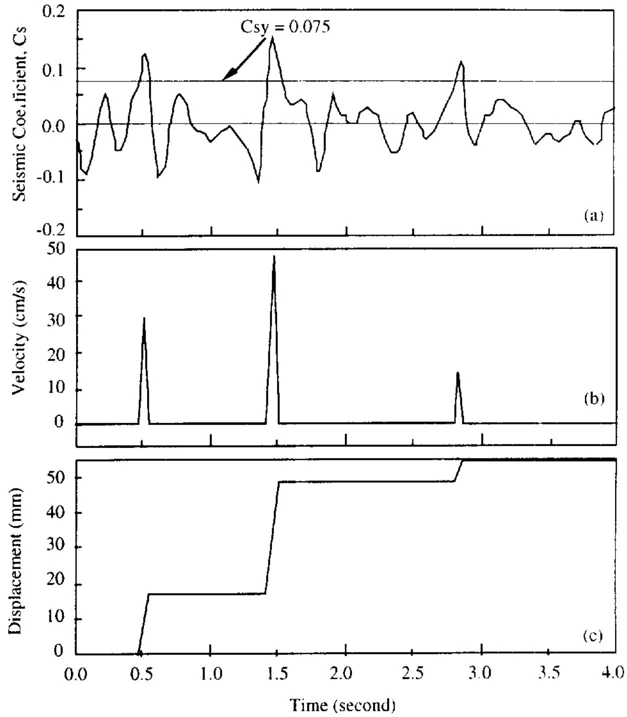

Figure 17. Hypothetical design curves to obtain permanent deformation utilizing (a) acceleration, (b) velocity and (c) displacement curves.

Example 4b:
Continue Example 4a and determine the anticipated permanent deformation of the weakest interface in the cover soil system. The site-specific seismic time-history diagram is given in Figure 17a.

Solution:
The interface of concern is the cover soil-to-geomembrane for this particular example. With a yield acceleration of 0.075 from Figure 16 and the site-specific (design) time history shown in Figures 17a, integration produces Figure 17b and then 17c. The three peaks exceeding the yield acceleration value of 0.075, produce a cumulative deformation of approximately 54 mm. This value is now viewed in light of the deformation capability of the cover soil above the particular interface used at the site. Note that current practice limits such deformation to either 100 or 300 mm depending on site-specific situations, see Richardson et al (1995).

Comments:
An assessment of the implications of deformation (in this example it is 54 mm) is very subjective. For example, this problem could easily have been framed to produce much higher permanent deformation. Such deformation can readily be envisioned in high seismic-prone areas. In addition to an assessment of cover soil stability, the concerns for appurtenances and ancillary piping must also be addressed.

4 SITUATIONS CAUSING THE ENHANCED STABILIZATION OF SLOPES

This section represents a counterpoint to the previous section on slope destabilization situations, in that all situations presented here tend to increase the stability of the slopes. Thus they represent methods to increase the cover soil FS-value. Included are toe berms, tapered cover soils and veneer reinforcement (both intentional and nonintentional). Not included, but very practical in site-specific situations, is to simply decrease the slope angle and/or decrease the slope length. These solutions, however, do not incorporate new design techniques and are therefore not illustrated. They are, however, very viable alternatives for the design engineer.

4.1 Toe (Buttress) Berm

A common method of stabilizing highway slopes and earth dams is to place a soil mass, i.e., a berm, at the toe of the slope. In so doing one provides a soil buttress, acting in a passive state thereby providing a stabilizing force. Figure 18 illustrates the two geometric cases necessary to provide the requisite equations. While the force equilibrium is performed as previously described, i.e., equilibrium along the slope with abutting interwedge forces aligned with the slope angle or horizontal, the equations are extremely long. Due to space limitations (and the resulting trends in FS-value improvement) they are not presented.

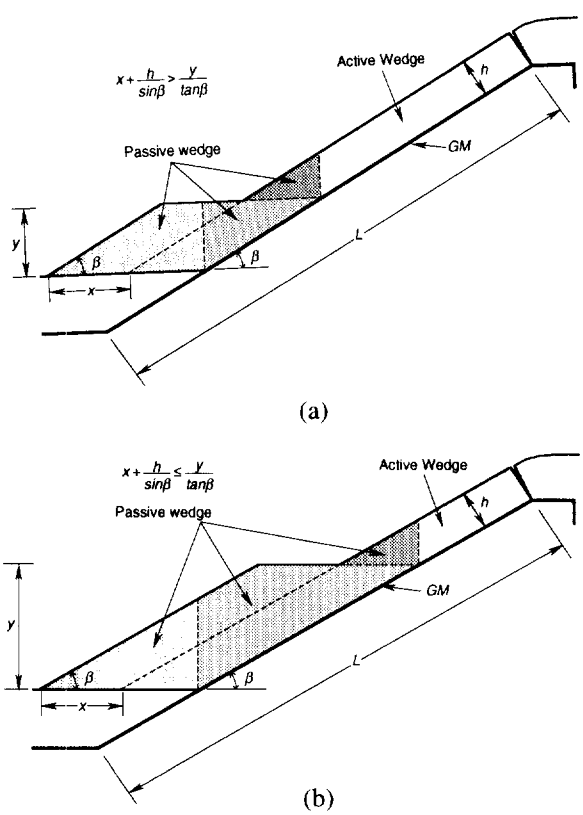

Figure 18. Dimensions of toe (buttress) berms acting as passive wedges to enhance stability.

Example 5:

Given a 30 m long slope with a uniform cover soil thickness of 300 mm and a unit weight of 18 kN/m^3. The soil has a friction angle of 30 deg. and zero cohesion, i.e., it is a sand. The cover soil is on a geomembrane as shown in Figure 18. Direct shear testing has resulted in a interface friction angle between the cover soil and geomembrane of 22 deg. and zero adhesion. The FS-value at a slope angle of 3(H)-to-1(V), i.e., 18.4 deg., was shown in Section 3.1 to be 1.25. What is the increase in FS-value using different sized toe berms with values of x = 1, 2 and 3 m, and gradually increasing y-values?

Solution:

The FS-value response to this type of toe berm stabilization is given in two parts, see Figure 19. Using thickness values of x = 1, 2 and 3 m, the lower berm section by itself is seen to have high FS-values initially, which decrease rapidly as the height of the toe berm increases. This is a predictable response for this passive wedge zone. Unfortunately, the upper layer of soil above the toe berm

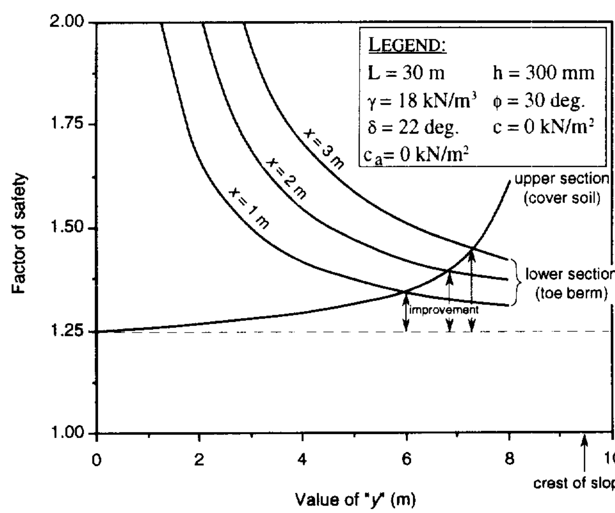

Figure 19. Design curves for FS-values using toe (buttress) berms of different dimensions.

(the active zone) is only nominally increasing in its FS-value. Note that at the crossover points of the upper and lower FS-values (which is the optimum solution for each set of conditions), the following occurs:

- For x = 1 m; y = 6.0 m (63% of the slope height) and FS = 1.35 (only an 8% improvement in stability)
- For x = 2 m; y = 6.8 m (72% of the slope height) and FS = 1.37 (only a 12% improvement in stability)
- For x = 3 m; y = 7.3 m (77% of the slope height) and FS = 1.40 (only a 16% improvement in stability)

Comment:

Readily seen is that construction of a toe berm is not a viable strategy to stabilize relatively thin layers of sloped cover soil of the type under investigation. Essentially what is happening is that the upper section of the cover soil (the active wedge) above the berm is sliding off of the top of the toe berm. While the upper slope length is becoming shorter (as evidenced by the slight improvement in FS-values), it is only doing so with the addition of a tremendous amount of soil fill. Thus this toe berm concept is a poor strategy for the stabilization of forces oriented in the slope's direction. Conversely, it is an excellent strategy for embankments and dams where the necessary resisting force for the toe berm is horizontal thereby counteracting a horizontal thrust by the potentially unstable soil and/or water mass.

4.2 Slopes with Tapered Thickness Cover Soil

An alternative method available to the designer to increase the FS-value of a given slope is to uniformly taper the cover soil thickness from thick at the toe, to thin at the crest, see Figure 20. The FS-value will increase in approximate proportion to the thickness of soil at the toe. The analysis for tapered cover soils includes the design assumptions of a tension crack at the top of the slope, the upper surface of the cover soil tapered at a constant angle "ω", and the earth

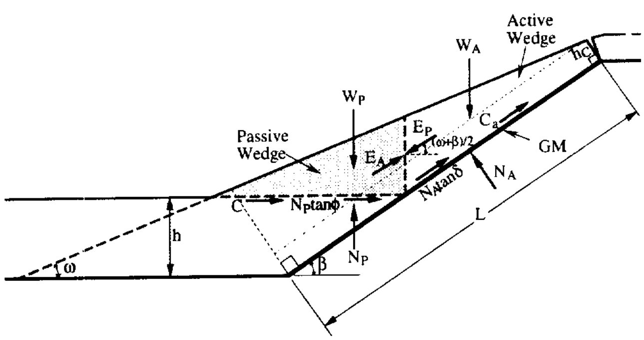

Figure 20. Limit equilibrium forces involved in a finite length slope analysis with tapered thickness cover soil from toe to crest.

pressure forces on the respective wedges oriented at the average of the surface and slope angles, i.e., the E-forces are at an angle of $(\omega + \beta)/2$. The procedure follows that of the uniform cover soil thickness analysis. Again, the resulting equation is not an explicit solution for the FS, and must be solved indirectly.

All symbols used in Figure 20 were previously defined (see Section 3.1) except the following:

h = thickness of cover soil at bottom of the landfill, measured perpendicular to the base liner

h_c = thickness of cover soil at crest of the slope, measured perpendicular to the slope

y = see Figure 20

$$= \left(L - \frac{h}{\sin\beta} - h_c \tan\beta\right)(\sin\beta - \cos\beta \tan\omega)$$

ω = finished slope angle of cover soil, note that $\omega < \beta$

The expression for determining the FS-value can be derived as follows:

Considering the active wedge,

$$W_A = \gamma\left[\left(L - \frac{h}{\sin\beta} - h_c \tan\beta\right)\left(\frac{y\cos\beta}{2} + h_c\right) + \frac{h_c^2 \tan\beta}{2}\right] \tag{41}$$

$$N_A = W_A \cos\beta \tag{42}$$

$$C_a = c_a\left(L - \frac{h}{\sin\beta}\right) \tag{43}$$

By balancing the forces in the vertical direction, the following formulations result:

$$E_A \sin\left(\frac{\omega+\beta}{2}\right) = W_A - N_A \cos\beta - \frac{N_A \tan\delta + C_a}{FS}(\sin\beta) \tag{44}$$

Hence the interwedge force acting on the active wedge is:

$$E_A = \frac{(FS)(W_A - N_A\cos\beta) - (N_A \tan\delta + C_a)\sin\beta}{\sin\left(\frac{\omega+\beta}{2}\right)(FS)} \tag{45}$$

The passive wedge can be considered in a similar manner:

$$W_P = \frac{\gamma}{2\tan\omega}\left[\left(L - \frac{h}{\sin\beta} - h_c \tan\beta\right)(\sin\beta - \cos\beta\tan\omega) + \frac{h_c}{\cos\beta}\right]^2 \tag{46}$$

$$N_p = W_P + E_P \sin\left(\frac{\omega+\beta}{2}\right) \tag{47}$$

$$C = \frac{\gamma}{\tan\omega}\left[\left(L - \frac{h}{\sin\beta} - h_c \tan\beta\right)(\sin\beta - \cos\beta\tan\omega) + \frac{h_c}{\cos\beta}\right] \tag{48}$$

By balancing the forces in the horizontal direction, the following formulation results:

$$E_P \cos\left(\frac{\omega+\beta}{2}\right) = \frac{C + N_P \tan\phi}{FS} \tag{49}$$

Hence the interwedge force acting on the passive wedge is:

$$E_P = \frac{C + W_P \tan\phi}{\cos\left(\frac{\omega+\beta}{2}\right)(FS) - \sin\left(\frac{\omega+\beta}{2}\right)\tan\phi} \tag{50}$$

By setting $E_A = E_P$, the following equation can be arranged in the form of $ax^2 + bx + c = 0$ which in our case is

$$a(FS)^2 + b(FS) + c = 0 \tag{13}$$

where

$$a = \left(W_A - N_A \cos\beta\right)\cos\left(\frac{\omega+\beta}{2}\right)$$

$$b = -\left[\left(W_A - N_A \cos\beta\right)\sin\left(\frac{\omega+\beta}{2}\right)\tan\phi + \left(N_A \tan\delta + C_a\right)\sin\beta\cos\left(\frac{\omega+\beta}{2}\right) + \sin\left(\frac{\omega+\beta}{2}\right)\left(C + W_P \tan\phi\right)\right]$$

$$c = \left(N_A \tan\delta + C_a\right)\sin\beta\sin\left(\frac{\omega+\beta}{2}\right)\tan\phi \tag{51}$$

As usual, the resulting FS-value can then be obtained using Eq. 15. To illustrate the use of the above developed equations, the design curves of Figure 21 are offered. They show that the FS-value increases in proportion to greater cover soil thicknesses at the toe of the slope with respect to the thickness at the crest. This is evidenced by a shallower surface slope angle than that of the slope of the geomembrane and the soil beneath, i.e., the value of "ω" being less than "β". Note that the curves are developed specifically for the variables stated in the legend. Example 6 illustrates the use of the curves.

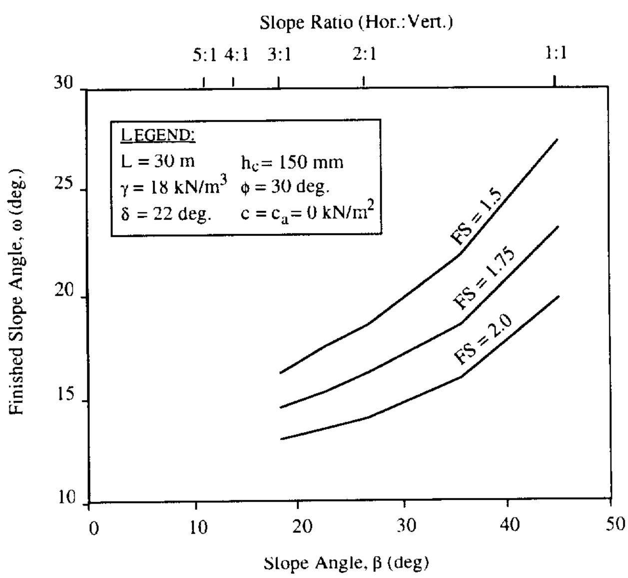

Figure 21. Design curves for FS-values of tapered cover soil thickness.

Example 6:
Given a 30 m long slope with a tapered thickness cover soil of 150 mm at the crest extending at an angle "ω" of 16 deg. to the intersection of the cover soil at the toe. The unit weight of the cover soil is 18 kN/m^3. The soil has a friction angle of 30 deg. and zero cohesion, i.e., it is a sand. The interface friction angle with the underlying geomembrane is 22 deg. with zero adhesion. What is the FS-value at an underlying soil slope angle "β" of 3(H)-to-1(V), i.e., 18.4 deg.?

Solution:
Using Eqs. 51, substituted into Eq. 15 yields the following:

$$\left.\begin{aligned} a &= 37.0\,\text{kN/m} \\ b &= -63.6\,\text{kN/m} \\ c &= 8.6\,\text{kN/m} \end{aligned}\right\} \quad FS = 1.57$$

Comment:
The result of this problem (with tapered thickness cover soil) is FS = 1.57, versus Example 1 (with a uniform thickness cover soil) which was FS = 1.25. Thus the increase in FS-value is 24%. Note, however, that at ω = 16 deg. the thickness of the cover soil normal to the slope at the toe is approximately 1.4 m. Thus the increase in cover soil volume used over Example 1 is from 8.9 to 24.1 m^3/m (≈170%) and the increase in necessary toe space distance is from 1.0 to 4.8 m (≈380%). The trade-offs between these issues should be considered when using the strategy of tapered cover soil thickness to increase the FS-value of a particular cover soil slope.

4.3 Veneer Reinforcement - Intentional

A fundamentally different way of increasing a given slope's factor of safety is to reinforce it with a geosynthetic material. Such reinforcement can be either intentional or non-intentional. By *intentional*, we mean to include a geogrid or high strength geotextile within the cover soil to purposely reinforce the system against instability, see Figure 22. Depending on the type and amount of reinforcement, the majority, or even all, of the driving, or mobilizing, stresses can be supported resulting in major increase in FS-value. By *non-intentional,* we refer to multi-component liner systems where a low shear strength interface is located beneath an overlying geosynthetic(s). In this case, the overlying geosynthetic(s) is inadvertently acting as veneer reinforcement to the composite system. In some cases, the designer may not realize that such geosynthetic(s) are being stressed in an identical manner as a geogrid or high strength geotextile, but they are. The situation where a relatively low strength protection geotextile is placed over a smooth geomembrane and beneath the cover soil is a case in point. Intentional, or non-intentional, the stability analysis is identical. The difference is that the geogrids and/or high strength geotextiles give a major increase in the FS-value, while a protection geotextile (or other lower strength geosynthetics) only nominally increases the FS-value.

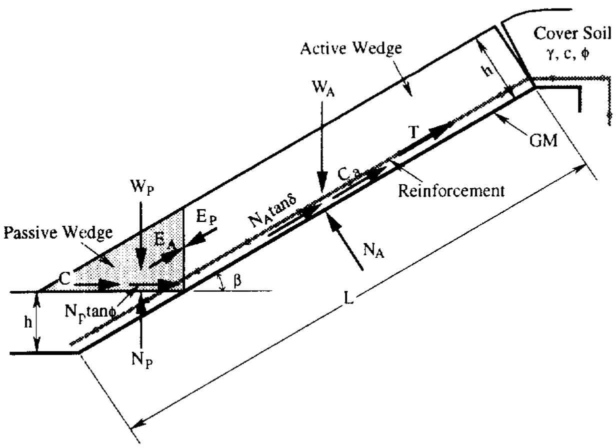

Figure 22. Limit equilibrium forces involved in a finite length slope analysis for a uniformly thick cover soil including the use of veneer reinforcement.

Seen in Figure 22 is that the analysis follows Section 3.1, but a force from the reinforcement "T", acting parallel to the slope, provides additional stability. This force "T", acts only within the active wedge. By taking free body force diagrams of the active and passive wedges, the following formulation for the factor of safety results. All symbols used in Figure 22 were previously defined (see Section 3.1) except the following:

T = T_{allow}, the allowable (long-term) strength of the geosynthetic reinforcement inclusion

Consider the active wedge and by balancing the forces in the vertical direction, the following formulation results:

$$E_A \sin\beta = W_A - N_A \cos\beta - \left(\frac{N_A \tan\delta + C_a}{FS} + T\right)\sin\beta \qquad (52)$$

Hence the interwedge force acting on the active wedge is:

$$E_A = \frac{(FS)(W_A - N_A\cos\beta - T\sin\beta)}{\sin\beta(FS)} - \frac{(N_A\tan\delta + C_a)\sin\beta}{\sin\beta(FS)} \qquad (53)$$

Again, by setting $E_A = E_P$ (see Eq. 12 for the expression of E_P), the following equation can be arranged in the usual form in which the "a", "b" and "c" terms are defined as follows:

$$a = (W_A - N_A\cos\beta - T\sin\beta)\cos\beta$$

$$b = -\left[(W_A - N_A\cos\beta - T\sin\beta)\sin\beta\tan\phi + (N_A\tan\delta + C_A)\sin\beta\cos\beta + \sin\beta(C + W_P\tan\phi)\right]$$

$$c = (N_A\tan\delta + C_a)\sin^2\beta\tan\phi \qquad (54)$$

Again, the resulting FS-value can be obtained using Eq. 15.

As noted, the value of T in the design formulation is T_{allow} which is invariably less than the as-manufactured strength of the geosynthetic reinforcement material. Considering the as-manufactured strength as being T_{ult}, the value should be reduced by such factors as installation damage, creep and long-term degradation. Note that if seams are involved in the reinforcement, a reduction factor should be added accordingly. See Koerner, 1998 (among others), for recommended numeric values.

$$T_{allow} = T_{ult}\left(\frac{1}{RF_{ID} \times RF_{CR} \times RF_{CBD}}\right) \qquad (55)$$

where

T_{allow} = allowable value of reinforcement strength
T_{ult} = ultimate (as-manufactured) value of reinforcement strength
RF_{ID} = reduction factor for installation damage
RF_{CR} = reduction factor for creep
RF_{CBD} = reduction factor for long term chemical/biological degradation

To illustrate the use of the above developed equations, the design curves of Figure 23 have been developed. The reinforcement strength can come from either geogrids or high strength geotextiles. If geogrids are used, the friction angle is the cover soil to the underlying geomembrane, under the assumption that the apertures are large enough to allow for cover soil strike-through. If geotextiles are used, this is not the case and the friction angle is the geotextile to the geomembrane. Also note that this value under discussion is the required reinforcement strength which is essentially T_{allow} in Eq. 55. The curves of Figure 23 clearly show the improvement of FS-values with increasing strength of the reinforcement. Note that the curves are developed specifically for the variables stated in the legend. Example 7 illustrates the use of the design curves.

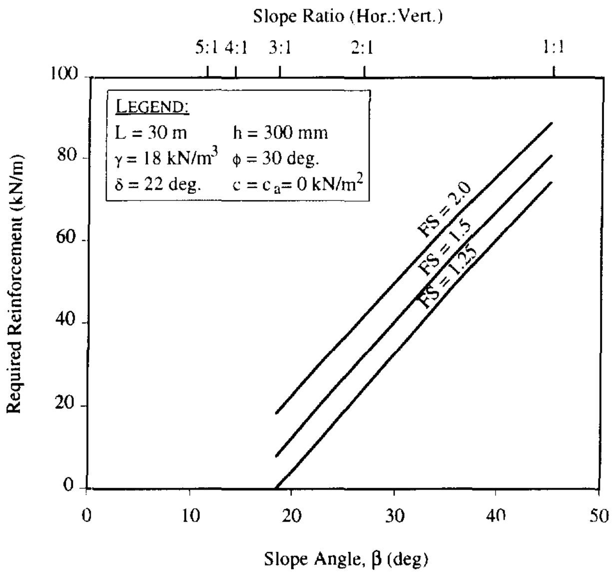

Figure 23. Design curves for FS-values for different slope angles and veneer reinforcement strengths for uniform thickness cohesionless cover soils.

Example 7:

Given a 30 m long slope with a uniform thickness cover soil of 300 mm and a unit weight of 18 kN/m^3. The soil has a friction angle of 30 deg. and zero cohesion, i.e., it is a sand. The proposed reinforcement is a geogrid with an allowable wide width tensile strength of 10 kN/m. Thus reduction factors in Eq. 55 have already been included. The geogrid apertures are large enough that the cover soil will strike-through and provide an interface friction angle with the underlying geomembrane of 22 deg. with zero adhesion. What is the FS-value at a slope angle of 3(H)-to-1(V), i.e., 18.4 deg.?

Solution:

Solving Eqs. 54 and substituting into Eq. 15 produces the following:

$$\left.\begin{array}{l} a = 11.8\,\text{kN}/\text{m} \\ b = -20.7\,\text{kN}/\text{m} \\ c = 3.5\,\text{kN}/\text{m} \end{array}\right\} \quad FS = 1.57$$

Comments:

Note that the use of T_{allow} = 10 kN/m in the analysis will require a significantly higher T_{ult} value of the geogrid per Eq. 55. For example, if the summation of the reduction factors in Eq. 55 were 4.0, the ultimate (as-manufactured) strength of the geogrid would have to be 40 kN/m. Also, note that this same type of analysis could also be used for high strength geotextile reinforcement. The analysis follows along the same general lines as presented here.

4.4 Veneer Reinforcement - Nonintentional

It should be emphasized that the preceding analysis is focused on intentionally improving the FS-value by the inclusion of geosynthetic reinforcement. This is provided by geogrids or high strength geotextiles being placed above the upper surface of the low strength interface material. The reinforcement is usually placed directly above the geomembrane or other geosynthetic material.

Interestingly, some amount of veneer reinforcement is often nonintentionally provided by a geosynthetic(s) material placed over an interface with a lower shear strength. Several situations are possible in this regard.

- Geotextile protection layer placed over a geomembrane
- Geomembrane placed over an underlying geotextile protection layer
- Geotextile/geomembrane placed over a compacted clay liner or geosynthetic clay liner
- Multilayered geosynthetics placed over a compacted clay liner or a geosynthetic clay liner

Each of these four situations are illustrated in Figure 24. They represent precisely the formulation of Section 4.3 which is based on Figure 22. On the condition that the geosynthetics above the weakest interface are held in their respective anchor trenches, the overlying geosynthetics provide veneer reinforcement, albeit of a nonintentional type. In the general case, such designs are not recommended although they can indeed provide increased resistance to slope instability of the weakest interface.

In performing calculations of the situations shown in Figure 24, the issue of strain compatibility must be considered. For the slopes shown in Figure 24 a and b, the issue is not important and the full wide width strength of the geotextile and geomembrane, respectively, can be used in the analysis. For the slopes shown in Figure 24 c and d, however, the complete stress vs. strain curves of each geosynthetic layer over the weak interface are necessary. The lowest value of failure strain of any one material dictates the strain at which the other geosynthetics will act. This will invariably be less than the full strength of the other geosynthetics. At this value of strain, however, the allowable strengths are additive and can be used in the analysis. Some detail on this issue is available in Corcoran and McKelvey (1995).

To illustrate the use of the above concepts, examples are given for the four situations shown in Figure 24.

Example 8:

Given four 3(H)-to-1(V), i.e., 18.4 deg. slopes with cover soils as shown in Figures 24 a to d. In each case, the slope is 30 m long with 300 mm of uniformly thick cover soil at a unit weight of 18 kN/m^3. The soil has a friction angle of 30 deg. and zero cohesion, i.e., it is a sand. The friction angle of the critical interface is 10 deg. What are the FS-values using the geosynthetic tensile strength data provided in the following table?

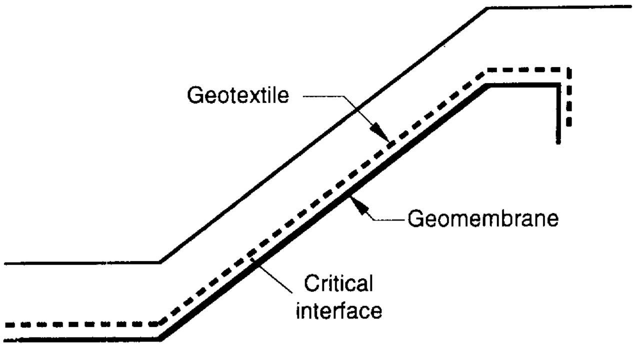

(a) Geotextile sliding on geomembrane

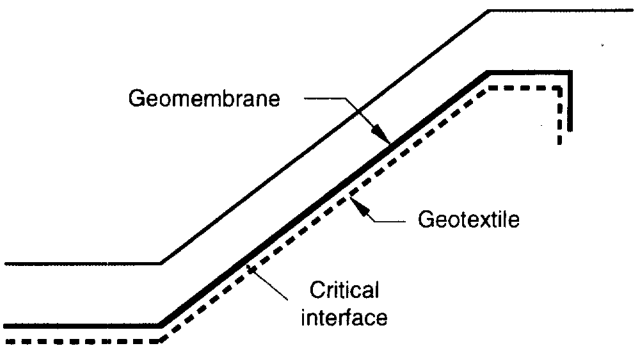

(b) Geomembrane sliding on geotextile

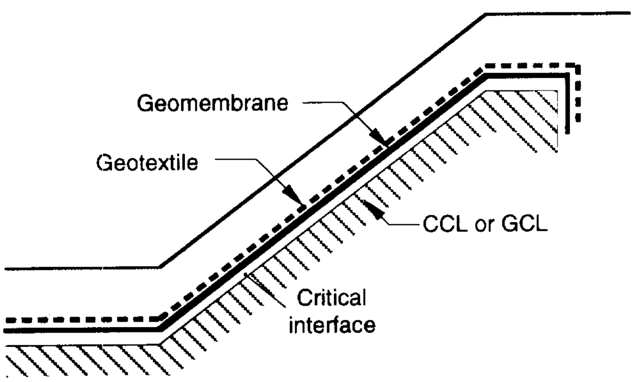

(c) Geotextile and geomembrane sliding on CCL or GCL

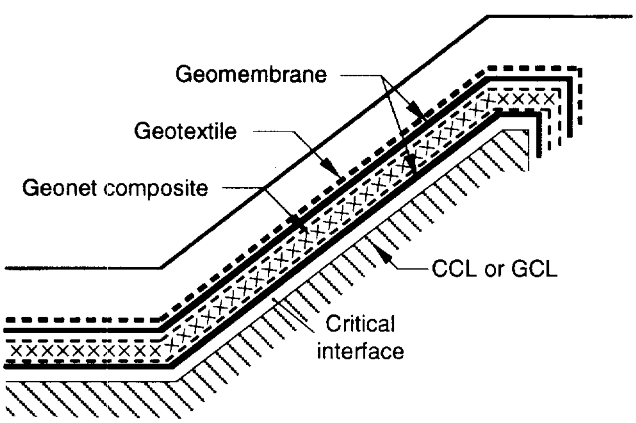

(d) Double liner system sliding on CCL or GCL

Figure 24. Various situations illustrating veneer reinforcement, albeit of an nonintentional type.

Values used for numeric examples of nonintentional veneer reinforcement.[1]

Slope type (figure)	GT strength[2] (kN/m)	GM strength[3] (kN/m)	GC strength[4] (kN/m)
24a	25	n/a	n/a
24b	n/a	15	n/a
24c	25	13	n/a
24d	25	13+13	36

Notes:
1. Strengths are product-specific and have been adjusted for strain compatibility.
2. Nonwoven needle punched geotextile of 540 g/m^2
3. Very flexible polyethylene geomembrane 1.0 mm thick
4. Biaxial geonet with two 200 g/m^2 nonwoven needle punched geotextiles thermally bonded to each side

Solution:

Substituting Eqs. 54 into Eq. 15 results in the following data and respective FS-values.

Slope type (figure)	a (kN/m)	b (kN/m)	c (kN/m)	FS-value
24a	7.3	-9.7	1.5	1.15
24b	10.3	-10.3	1.5	0.82
24c	3.4	-9.0	1.5	2.45
24d	-11.0	-6.2	1.5	>10.0

Comments:
While the practice illustrated in these examples of using the overlying geosynthetics as nonintentional veneer reinforcement is not recommended, it is seen to be quite effective when a number of geosynthetics overlying the weak interface are present. On a cumulative basis, they can represent a substantial force as shown in Figure 24d. If one were to rely on such strength, however, it would be prudent to apply suitable reduction factors to each material, and to inform the parties involved of the design situation.

5 SUMMARY

This paper has focused on the mechanics of analyzing slopes as part of final cover systems on engineered landfills, abandoned dumps and remediated waste piles. It also applies to drainage soils placed on geomembrane lined slopes beneath the waste, at least until solid waste is placed against the slope. Numeric examples in all of the sections have resulted in global FS-values. Each section was presented from a designer's perspective in transitioning from the simplest to the most advanced. It should be clearly recognized that there are other approaches to the analyses illustrated in the various examples. References available in the literature by Giroud and Beech (1989), McKelvey and Deutsch (1991), Koerner and Hwu (1991), Giroud et al (1995a), Giroud et al (1995b), Liu et al (1997), and Ling and Leshchinsky (1997) are relevant in this regard. All are based on the concept of limit equilibrium with different assumptions involving particular details, e.g.,

- Existence of a tension crack at the top of slope (filled or unfilled with water)
- Orientation of the failure plane beneath the passive wedge (horizontal or inclined)
- Specific details of construction equipment movement on the slopes in placing the cover soil, particularly the acceleration or deceleration, and the type of equipment itself (e.g., tracked versus wheel equipment)
- Specific details on seepage forces within the drainage layer, including the amount and its orientation
- Specific details on seismic forces, particularly the magnitude and the selection of interface strengths
- Specific details on the geometry of the toe berms or tapered cover soils
- Specific details on the strength and reduction factors used for intentional veneer reinforcement
- Specific details on the strain compatibility issues used with nonintentional veneer reinforcement.

When considering all of these site-specific details, it is readily seen that veneer cover soil analysis and design is a daunting, yet quite tractable, task. For example, one of the reviewers of this paper reanalyzed one of the examples presented herein and another reviewer reanalyzed all of the examples. Both used the analyses of Giroud et al (1995a) and (1995b). They found good agreement in all cases except the nonintentional veneer reinforcement with multiple geosynthetic layers, i.e., the last example presented. It is likely in this regard that different values of mobilized composite strength were being used.

Table 1 summarizes the FS-values of the similarly framed numeric examples presented herein so that insight can be gained from each of the conditions analyzed. Throughout the paper, however, the inherent danger of building a relatively steep slope on a potentially weak interface material, oriented in the exact direction of a potential slide, should have been apparent.

The standard example was purposely made to have a relatively low factor of safety, i.e., FS = 1.25. This FS-value was seen to moderately decrease for construction equipment moving up the slope, but seriously decrease with equipment moving down the slope, i.e., 1.24 to 1.03. It should be noted, however, that the example problems were hypothetical , particularly the equipment examples in the selection of acceleration /deceleration factors. There are an innumerable number of choices to select from, and we have selected values to make the point of proper construction practice. Also, drastically decreasing the FS-value were the influences of seepage and seismicity. The former is felt to be most serious in light of a number of slides occurring after heavy precipitation. The latter is known to be a concern at one landfill in an area of active seismicity.

The sequence of design situations shifted to scenarios where the FS-values were increased over the standard example. Adding soil either in the form of a toe berm or tapered cover soil both increase the FS-value depending on the mass of soil involved. The tapered situation was seen to be more efficient and preferred over the toe berm. Both designs, however, require physical space at the toe of the slope which is often not available. Thus the use of geosynthetic reinforcement was illustrated. By intentional veneer reinforcement it is meant that geogrids or high strength geotextiles are included to resist some, or all, of the driving forces that are involved. The numeric example illustrated an increase in FS-value from 1.25 to 1.57, but this is completely dependent on the type and amount of reinforcement. It was also shown that whenever the weakest interface is located beneath overlying geosynthetics they also act as veneer reinforcement albeit nonintentionally in most cases. The overlying geosynthetic layers must physical fail (or pull out of their respective anchor trenches, see Hullings, 1996) in order for the slope to mobilize the weakest interface strength layer and slide. While this is not a recommended design situation, it does have the effect of increasing the FS-value. The extent of increase varies from a flexible geomembrane to a nonwoven needle punched protection geotextile (both with relatively low strengths) to a multilayered geosynthetic system with 2 to 8 layers of geosynthetics (with very high cumulative strengths).

Table 1. Summary of numeric examples given in this paper for different slope stability scenarios.

Example No.	Situation or condition	Control FS-value	Scenarios decreasing FS-values	Scenarios increasing FS-values
1	standard example*	1.25		
2a	equipment up-slope		1.24	
2b	equipment down-slope		1.03	
3	seepage forces		0.93	
4	seismic forces		0.94	
5	toe (buttress) berm			1.35-1.40
6	tapered cover soil			1.57
7	veneer reinforcement (intentional)			1.57
8	veneer reinforcement (non intentional)			varies

* 30 m long slope at a slope angle of 18.4 deg. with sandy cover soil of 18.4 kN/m^3 dry unit weight with ϕ = 30 deg. and thickness 300 mm placed on an underlying geosynthetic with a friction angle δ =22 deg.

6 CONCLUSION

We conclude with a discussion on factor of safety (FS) values for cover soil situations. Note that we are referring to the global FS-value, not reduction factors which necessarily must be placed on geosynthetic reinforcement materials when they are present. In general, one can consider global FS-values to vary in accordance with the site specific issue of required service time (i.e., the anticipated lifetime) and the implication of a slope failure (i.e., the concern). Table 2 gives the general concept in qualitative terms.

Table 2. Qualitative rankings for global factor-of-safety values in performing stability analysis of final cover systems, after Bonaparte and Berg (1987).

Duration→ ↓Concern	Temporary	Permanent
Noncritical	Low	Moderate
Critical	Moderate	High

Using the above as a conceptual guide, the authors recommend the use of the minimum global factor-of-safety values listed in Table 3, as a function of the type of underlying waste for *static* conditions.

Table 3. Recommended global factor-of-safety values for static conditions in performing stability analyses of final cover systems.

Type of Waste→ ↓Ranking	Hazard-ous waste	Non-hazardous waste	Aban-donded dumps	Waste piles and leach pads
Low	1.4	1.3	1.4	1.2
Moderate	1.5	1.4	1.5	1.3
High	1.6	1.5	1.6	1.4

It is hoped that the above values give reasonable guidance in final cover slope stability decisions, but it should be emphasized that engineering judgment and (oftentimes) regulatory agreement is needed in many, if not all, situations.

ACKNOWLEDGMENTS

The opportunity of writing and presenting this paper on behalf of IGS and its Nominating Committee as the 1998 Giroud Lecture is sincerely appreciated. Financial assistance in its preparation by the consortium of Geosynthetic Institute members is gratefully acknowledged.

REFERENCES

Algermissen, S.T. (1991) "Seismic Risk Studies in the United States," *Proc. 4th World Conference on Earthquake Engineering,* Vol. 1, Santiago, Chile, pp. A1-14 to 27.

Bonaparte, R. and Berg, R. (1987) "Long-Term Allowable Tension for Geosynthetic Reinforcement," *Proc. Geosynthetics '87,* IFAI, St. Paul, MN, USA, pp. 181-192.

Cancelli, A and Rimoldi, P. (1989) "Design Criteria for Geosynthetic Drainage Systems in Waste Disposal," *Proc. of Sardinia '89,* 2nd Intl. Landfill Symposium, porto Conte, Sassari, Italy.

Corcoran, G.T. and McKelvey, J.A. (1995) "Stability of Soil Layers on Compound Geosynthetic Slopes," *Proc. Waste Tech '95,* New Orleans, LA, USA: Environ Industry Assoc., pp. 301-304.

Daniel, D.E., Shan, H.-Y. and Anderson, J.D. (1993) "Effects of Partial Wetting on the Performance of the Bentonite Component of a Geosynthetic Clay Liner," *Proc. Geosynthetics '93,* IFAI, St. Paul, MN, USA, pp. 1483-1496.

Giroud, J.P. and Beech, J.F. (1989) Stability of Soil Layers on Geosynthetic Lining Systems," *Proc.Geosynthetics '89,* IFAI, St. Paul, MN, USA, pp. 35-46.

Giroud, J.P., Williams, N.D., Pelte, T and Beech, J.F. (1995a) "Stability of Geosynthetic-Soil Layered Systems on Slopes," *Geosynthetic International,* Vol. 2, No. 6, pp. 1115-1148.

Giroud, J.P., Bachus, R.C. and Bonaparte, R (1995b) "Influence of Water Flow on the Stability of Geosynthetic-Soil Layered Systems on Slopes," *Geosynthetic International,* Vol. 2, No. 6, pp. 1149-1180.

Hullings, D.E. and Sansone, L.J. (1996) "Design Concerns and Performance of Geomembrane Anchor Trenches," *Proc. GRI-10 Conference on Field Performance of Geosynthetics,* GII, Philadelphia, PA, USA, pp. 245-259.

Idriss, I.M. (1990) "Response of Soft Soil Sites During Earthquake," *Proc. Symposium to Honor Professor H. B. Seed,* Berkeley, CA, USA.

Koerner, R.M. (1998) *Designing with Geosynthetics,* 4th Ed., Prentice Hill Book Co., Englewood Cliffs, NJ, USA, 761 pgs.

Koerner, R.M. and Hwu, B.-L. (1991) "Stability and Tension Considerations Regarding Cover Soils on Geomembrane Lined Slopes," *Jour. of Geotextiles and Geomembranes,* Vol. 10, No. 4, pp. 335-355.

Ling, H.I. and Leshchinsky, D. (1997) "Seismic Stability and Permanent Displacement of Landfill Cover Systems," *Jour. of Geotechnical and Geoenvironmental Engrg.,* ASCE, Vol. 123, No. 2, pp. 113-122.

Liu, C.N., Gilbert, R.B., Thiel, R.S. and Wright, S.G. (1997) "What is an Appropriate Factor of Safety for Landfill Cover Slopes?" *Proc. Geosynthetics '97,* IFAI, St, Paul, MN, USA, pp. 481-496.

Makdisi, F.I. and Seed, H.B. (1978) " Simplified Procedure for Estimating Dam and Embankment Earthquake-Induced Deformations," *J. of Geotechnical Engrg.,* ASCE Vol. 104, No. GT7, pp. 849-867

Matasovic, N., Kavazanjian E. Jr. and Yan, L. (1997) "Newmark Deformation Analysis with Degrading Yield Acceleration," *Proc. Geosynthetics '97,* IFAI, St. Paul, MN, USA, pp. 989-1000.

McKelvey, J.A. and Deutsch, W.L. (1991) "The Effect of Equipment Loading and Tapered Cover Soil Layers on Geosynthetic Lined Landfill Slopes, "*Proceedings of the 14th Annual Madison Avenue Conference,* Madison, WI, USA, University of Wisconsin, pp. 395-411.

McKelvey, J.A. (1994) "Consideration of Equipment Loadings in Geosynthetic Lined Slope Design," *Proc. 8th Intl. Conf. of the Intl. Asso. for Computer Methods and Advancements in Geomechanics*, Morgantown, WV: Balkema, pp. 1371-1377.

Poulos, H.G. and Davis, E.H. (1974) *Elastic Solutions for Soil and Rock Mechanics*, J. Wiley & Sons, Inc., New York, NY, USA, 411 pgs.

Richardson, G.N., Kavazanjian, E. Jr. and Matasovic, N. (1995) "RCRA Subtitle D (258) Seismic Design Guidance for Municipal Solid Waste landfill Facilities", EPA/600/R-95/051, U.S. Environmental Protection Agency, Cincinnati, Ohio, USA, 143 pgs.

Schnabel, P.B., Lysmer, J. and Seed, H.B. (1972) "SHAKE: A Computer Program for Earthquake Response Analysis of Horizontally Layered sites," Report No EERC 72-12, Earthquake Engineering Research Center, University of California, Berkeley, CA, USA.

Seed, H.B. and Idriss, I.M. (1982) "Ground Motions and Soil Liquefaction During Earthquakes," Monographs No. 5, Earthquake Engineering Research Center, University of California, Berkeley, CA, USA, 134 pgs.

Soong, T.-Y. and Koerner, R.M. (1996) "Seepage Induced Slope Instability," *Jour. of Geotextiles and Geomembranes*, Vol. 14, No. 7/8, pp. 425-445.

Stark, T.D. and Poeppel, A.R. (1994) "Landfill Liner Interface Strengths from Torsional Ring Stress Tests," *Jour. of Geotechnical Engineering,* ASCE, Vol. 120, No. 3, pp. 597-617.

Thiel, R.S. and Stewart, M.G. (1993), "Geosynthetic Landfill Cover Design Methodology and Construction Experience in the Pacific Northwest," Proc. Geosynthetics '93, IFAI, St. Paul, MN, USA, pp. 1131-1144.

Attachment 2

The Design of Drainage Systems Over

Geosythetically Lined Slopes

DREXEL
UNIVERSITY

Geosynthetic Research Institute
33rd & Lancaster Walk
Rush Building - West Wing
Philadelphia, PA 19104
TEL 215 895-2343
FAX 215 895-1437

FOR GSI/GRI MEMBER ORGANIZATIONS ONLY!

THE DESIGN OF DRAINAGE SYSTEMS OVER GEOSYNTHETICALLY LINED SLOPES

by

Te-Yang Soong, Ph.D.
Research Engineer

and

Robert M. Koerner, Ph.D.
Director and Professor

Geosynthetic Research Institute
Drexel University
West Wing - Rush Building
Philadelphia, PA 19104

GRI Report #19

JUNE 17, 1997

The Design of Drainage Systems Over Geosynthetically Lined Slopes

Table of Contents

Abstract

Upon investigating eight recent seepage induced slides of leachate collection and final cover systems, it was felt that many designs underestimate the site-specific required flux (lateral flow rate) value. Rather than rely on the HELP model, an hourly-interval procedure for calculating the required flux is presented. It is based on a severe storm event and subsequent water balance analysis over a 6 hour period. The various types of natural and geosynthetic drainage materials are presented and assessed in light of the 25 to 40 times higher required flux-values from such storm events.

The design methodology used to incorporate the site-specific required flux and the material specific allowable flux-values into a slope stability analysis is developed and illustrated. Example problems and a parametric study are presented. Based on the results, the recommendations of the report are as follows:

- The site-specific precipitation rate should be based on a severe storm event basis, particularly for the final covers of landfills.
- Permeability of natural soils and geosynthetic drains must be significantly increased over those currently used in practice.
- Well graded and poorly graded gravels, and possibly sandy gravels, are the obvious choice for natural soils.
- Higher flow rate geosynthetic drains than are currently used, e.g., triaxial geonets and composite sheet drains, are necessary to meet the higher flux requirements.
- The length of slope should probably be limited to 30 m, unless the site is in an arid region. The cumulative effect of long slopes was seen to be a major cause of seepage induced slope instability.
- The drainage outlet at the toe of the slope must have the greatest capacity of any part of the drainage system. Some design scenarios are offered.

Using the method proposed herein, the eight seepage induced slides were back calculated to estimate the site specific precipitation values. They were quite high for leachate collection layers, 14 to 44 mm/hour, except for one with very low permeability soil. For the final cover system slides, the precipitation values were remarkably low, i.e., 0.38 to 1.34 mm/hour. Clearly, the permeability of the drainage layer soil was far too low, i.e., 0.01 cm/sec. Interestingly, this is the regulatory minimum value in federal and many state regulations.

It is hoped that the report stimulates an increased awareness in the possibility of seepage induced slope instability. While instability of the leachate collection layer before waste is placed is often not a critical issue (the slope can often be repaired by on-site personnel), instability of final covers is a serious issue. Such instability could occur many years after closure of a facility, when the expense of repair is a very contentious issue. Such seepage induced instability situations can be avoided by the type of conservative drainage design presented herein.

Acknowledgments

This study was funded through general membership fees of the organizations in the Geosynthetic Institute consortium. We are grateful for their generosity and support. The organizations are as follows; along with the primary contact person within that organization or company. Members of the GSI Board of Directors (BOD) are identified accordingly.

GSE Lining Systems, Inc.
(William W. Walling)

RUST Environmental and Infrastructure, Inc.
(John Rohr/Anthony W. Eith)

U.S. Environmental Protection Agency
(David A. Carson)

Polyfelt GmbH
(Gernot Mannsbart/Gerhard Werner)

Browning-Ferris Industries
(Charles Rivette/Dan Spikula [BOD])

Monsanto Company
(Roy L. Hood)

E. I. duPont de Nemours & Co., Inc.
(John L. Guglielmetti/Ronald J. Winkler)

Federal Highway Administration
(Albert F. DiMillio/Jerry A. DiMaggio)

Golder Associates, Inc.
(Leo K. Overmann [BOD]/Mark E. Case)

Tensar Earth Technologies, Inc.
(Peter J. Vanderzee/Donald G. Bright/Mark H. Wayne)

National Seal Co.
(Gary Kolbasuk [BOD]/George Zagorski)

Poly-Flex, Inc.
(James Nobert/George Yazdani)

Akzo Nobel Geosynthetics Co.
(Wim Voskamp/Joseph Luna)

Phillips Petroleum Co.
(Rex L. Bobsein)

GeoSyntec Consultants Inc.
(Jean-Pierre Giroud)

NOVA Chemicals Ltd.
(Nolan Edmunds)

Tenax, S.p.A.
(Pietro Rimoldi [BOD]/Aigen Zhao)

Amoco Fabrics and Fibers Co.
(Gary Willibey)

U.S. Bureau of Reclamation
(Alice I. Comer)

EMCON
(Donald E. Hullings/Mark A. Swyka)

Montell USA, Inc.
(B. Alam Shah)

TC Mirafi, Inc.
(Thomas Stephens/Dean Sandri)

CETCO
(Richard W. Carriker)

Huesker, Inc.
(Thomas G. Collins)

Solvay Polymers
(Philip M. Dunaway)

Naue-Fasertechnik GmbH
(Georg Heerten/Kent von Maubeuge)

Synthetic Industries, Inc.
(Marc S. Theisen/Deron N. Austin)

STS Consultants Ltd.
(Cynthia Bonczkiewicz/Mark D. Sieracke)

Mobil Chemical Co.
(Frank A. Nagy)

BBA Nonwovens, Inc.
(William M. Hawkins/Ian R. Clough)

NTH Consultants, Ltd.
(Jerome C. Neyer/Robert Sabanas)

Netlon, Ltd.
(Richard A. Austin)

TRI/Environmental, Inc.
(Sam R. Allen [BOD]/Richard Thomas)

GeoSystems Consultants
(Craig R. Calabria)

U.S. Army Corps of Engineers
(David L. Jaros [BOD])

Chevron Chemical Co.
(Pamela L. Maeger [BOD])

Serrot Corp.
(Robert A. Otto/Bill Torres BOD])

Lockheed Martin Energy Systems
(Syed B. Ahmed/Sidney B. Garland)

Union Chemical Lab (ITRI)
(Yen-Jung Hu)

Haley and Aldrich, Inc.
(Richard P. Stulgis)

Westinghouse-Savannah River
(Michael Hasek)

Woodward-Clyde Consultants
(Pedro C. Repetto/John C. Volk)

S. D. Enterprise Co., Ltd.
(David Eakin)

PPG Industries, Inc.
(N. (Raghu) Raghupathi)

Solmax Géosynthétiques
(Robert (Bob) Denis)

EnviroSource Treatment & Disposal Services, Inc.
(Patrick M. McNamara)

Strata Systems, Inc.
(John N. Paulson[BOD])

CARPI, Inc.
(Alberto M. Scuero)

Rumpke Waste Service, Inc.
(Bruce Schmucker)

Civil & Environmental Consultants, Inc.
(Richard J. Kenter)

Agru Americas, Inc.
(Paul W. Barker/Peter Riegl)

THE DESIGN OF DRAINAGE SYSTEMS OVER GEOSYNTHETICALLY LINED SLOPES

The previous report in this series, GRI Report #18 dated December 9, 1996, presented numerous *analyses* involving the stability of cover soils overlying geomembrane lined slopes. In so doing, the report highlighted the precarious nature of several situations. For example, equipment loads and seismic forces can be critical, as can be multi-geosynthetic lined slopes. Nowhere, however, was stability more adversely effected than when seepage forces were involved. Paradoxically, this is one situation that can be completely avoided by use of proper drainage materials, either natural drainage soils or geosynthetic drains. Yet, slopes continue to fail due to seepage induced slope instability. This report focuses completely on the issue of proper drainage layer ***design*** and the subsequent analysis of the slope's factor of safety for soils located above geosynthetically lined slopes with the hope that seepage-related slides can be avoided in the future.

1.0 INTRODUCTION

For most geosynthetically lined slope applications like landfill liners and the final covers of closed landfills and waste piles, a geomembrane (*GM*), geosynthetic clay liner (*GCL*), or compacted clay liner (*CCL*) is used as a hydraulic barrier. Furthermore, the liner is directly oriented in the direction of the critical potential sliding plane. While this is unfortunate from a stability perspective, it does allow for a tractable solution of the problem in a relatively straightforward manner. The solution used by numerous researchers is a linear failure plane oriented along the direction of the slope angle, of finite length and of constant thickness e.g., Giroud and Beech (1989), Koerner and Hwu (1991), McKelvey and Deutsch (1991), Thiel and Stewart (1993), Bordeau, et al (1993), Soong and Koerner (1996), and others. In each case, the analysis uses limit equilibrium concepts where the destabilizing actions involved (gravity, live loads, etc.) create driving forces, and the shearing resistance of the materials at the critical interface provides the resisting force. This assumes that the shearing resistance of the critical interface is less than the shearing resistance of the soil itself, which is usually the case with geosynthetically lined slopes. In terms of a factor of safety (*FS*), this concept is expressed as follows:

$$FS = \frac{Resisting\ Force}{Driving\ Forces} \tag{1}$$

When the *FS* is less than 1.0, the slope fails by sliding along the critical interface. When the *FS* is greater than 1.0, stability is suggested with the higher the value, the greater the stability. For temporary slopes, *FS*-values are typically 1.2 to 1.4. For permanent slopes, the *FS*-value should be at least equal to 1.5. Liu, et al (1997) give greater insight in this regard.

A critical issue, and one which has not seen much attention [the exceptions being Thiel and Stewart (1993), Soong and Koerner (1996) and Richardson (1997)] is the negative influence of seepage forces within the drainage layer and/or cover soil above the geosynthetically lined interface. The tacit assumption of most designers appears to be that the cover soil can readily handle the required drainage, or that a drainage layer (often regulatory suggested insofar as thickness and permeability) will be adequate. Unfortunately, neither assumption is accurate and seepage-mobilized slope instability has all too frequently occurred.

This report focuses completely on the issue of the *design of adequate drainage systems* so as to prevent seepage-mobilized slope instability. The report will present background information, water balance analyses, drainage layer considerations (using both natural soils and geosynthetic drainage materials), slope stability analysis, behavior of selected cross-sections, parametric evaluations, related discussion, summary and recommendations.

2.0 BACKGROUND

This section of the report describes eight recent seepage induced slides known to the writers. It also presents the possible magnitude of heavy rainstorm events and the idiosyncrasies of various drainage systems.

2.1 Seepage Induced Slides

The occurrence of seepage induced instability was originally daylighted by Boschuk (1991) and actually challenged in a field trial reported by Giroud, et al. (1990). Yet, such incidents still occur and appear to have occurred more frequently in the intervening years. Figure 1 illustrates four case histories of slides occurring in the leachate collection soils above a geomembrane liner before waste was placed in the respective landfills. Figure 2 illustrates an additional four case histories of slides occurring in the drainage and cover soils above barrier layers after waste was placed in the respective landfills, i.e., final cover situations. While all four cases in the latter category involved compacted clay liners, the situations would probably have been similar with geosynthetic liners. A brief description of each slide follows, and then all eight are compared and contrasted in Table 1.

Case #1 occurred in 1992 with a 25 mm average diameter leachate collection stone underlain by a needle punched nonwoven protection geotextile sliding on a stationary smooth HDPE geomembrane. The geotextile failed at the top of the slope carrying it and the stone above into the base of the landfill. The slope was 3(H)-to-1(V) and a number of successive slides occurred during several heavy rainfalls. The stone was AASHTO #57 quarried limestone.

Case #2 occurred in 1993 with a 37 mm average diameter leachate collection stone placed directly on a smooth HDPE geomembrane. The stone slid on the surface of the stationary geomembrane down to the toe of the landfill. The slope was approximately 3(H)-to-1(V) and the slide occurred immediately after a heavy rainfall. The stone was a very coarse AASHTO #3 quarried material.

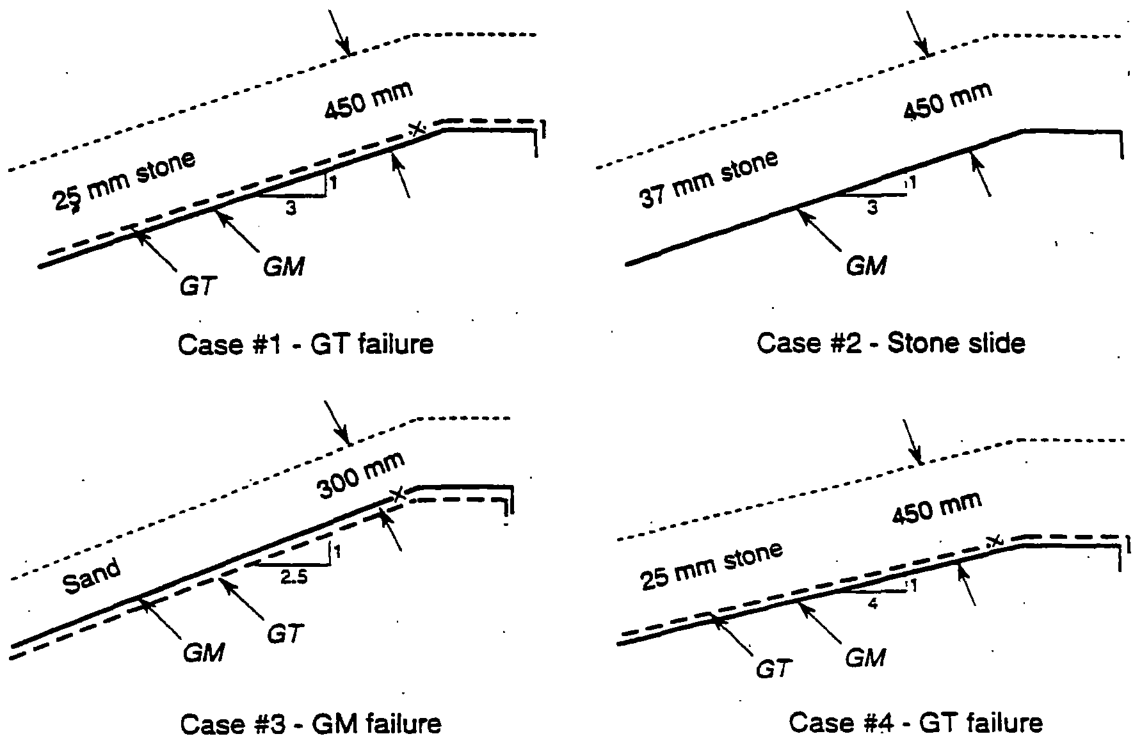

Figure 1 - Various seepage involved slides of leachate collection systems in landfill liner systems

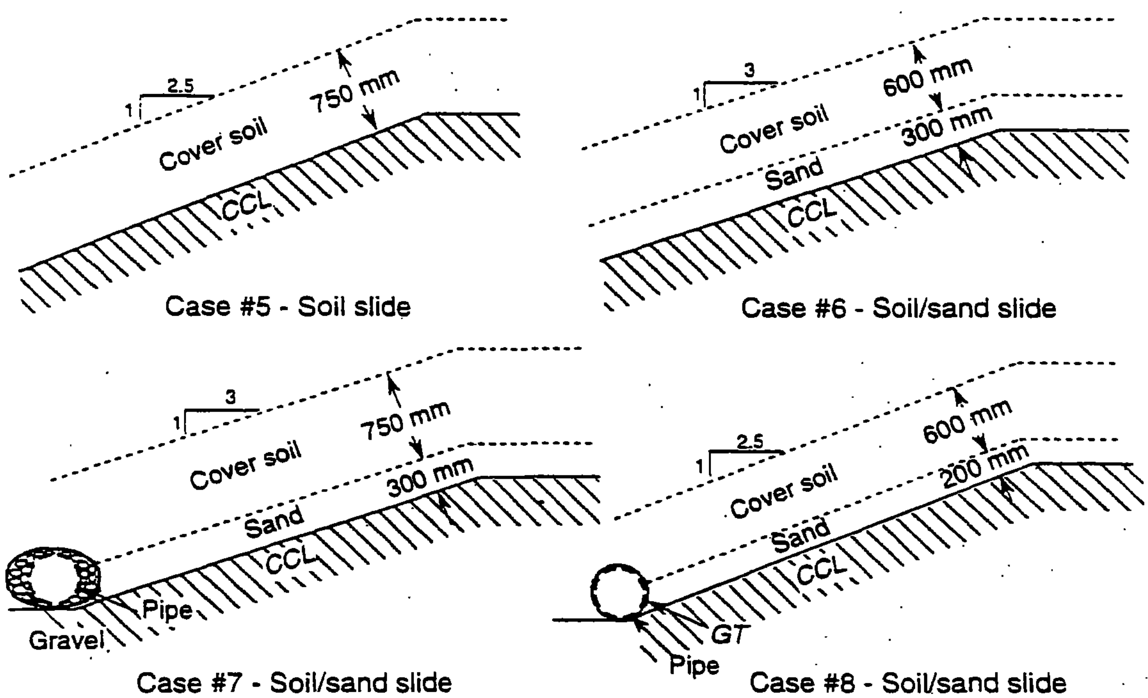

Figure 2 - Various seepage involved slides of final cover systems above solid waste landfills

Table 1 - Recent Slope Instability Case Histories Involving Seepage Forces

No.	Upper Interface	Lower Interface	Slope Inclination (Hor. : Vert.)	Cover Soil Thickness, (mm)	Approx. Slope Length, (m)	Approx. Time after Construction, (yr)	Cause of Seepage Force
(a) Slides of leachate collection layers before waste placement							
1	NW-NP-GT	HDPE-GM	3 : 1	450	45	1 - 2	fines in stone
2	Stone	HDPE-GM	3 : 1	450	30	3 - 4	fines in stone
3	VFPE-GM	NW-NP-GT	2.5 : 1	300	20	0.2 - 0.5	low initial permeability
4	NW-NP-GT	PVC-GM	4 : 1	450	90 (3 benches of 30 m each)	1 - 2	ice wedge at toe of slope
(b) Slide of final cover/drainage layers after waste placement							
5	Silty sand	CCL	2.5 : 1	750	40	2 - 3	no drainage layer
6	Sand	CCL	3 : 1	600 + 300	50	5 - 6	low initial sand permeability
7	Sand	CCL	3 : 1	750 + 300	45	5 - 6	fines clogging gravel around pipe
8	Sand	CCL	2.5 : 1	600 + 200	90 (2 benches of 45 m each)	4 - 5	fines clogging GT around pipe

Notes:
GT = Geotextile
GM = Geomembrane
CCL = compacted clay liner
NW-NP = Nonwoven needle punched
HDPE = High density polyethylene
VFPE = Very flexible polyethylene
PVC = Polyvinyl chloride

Case #3 occurred in 1994 with a sand leachate collection material and VFPE geomembrane sliding on a stationary needle punched nonwoven geotextile. The slope was approximately 2.5(H)-to-1(V) and the slide occurred during a relatively light rainfall. The geomembrane failed along the crest of the slope for a distance of approximately 30 m with its upper end remaining in the anchor trench.

Case #4 occurred in 1995 with a 25 mm average diameter quarried leachate collection stone underlain by a needle punched nonwoven protection geotextile sliding on a geomembrane. The difference between it and Case #1 was that the geomembrane was PVC, the slope was 4(H)-to-1(V) and the toe blockage was via a frozen ice wedge with sun-melted seepage forces being mobilized upslope. Approximately 3 ha of geomembrane was exposed after the geotextile and stone slid down to the toe of the landfill.

Case #5 occurred in 1995 with 750 mm of silty sand ($k \approx 0.001$ cm/s) cover soil sliding on a compacted clay liner (*CCL*) during a storm event. The slide was relatively small and localized. The slope was 2.5(H)-to-1(V).

Case #6 occurred in 1996 with 900 mm of sand drainage layer ($k \approx 0.01$ cm/s) and cover soil sliding on a CCL immediately after a storm event. At least four localized slides occurred. The slope was 3(H)-to-1(V).

Case #7 also occurred in 1996 under very similar circumstances to Case #6, except exhuming the gravel around the toe drain showed the gravel to be highly contaminated with fines which migrated through the cover soil and/or sand. A number of localized slides occurred at this site. The slope was 3(H)-to-1(V).

Case #8 also occurred in 1996 under very similar circumstances to Case #7 except the geotextile filter surrounding the prefabricated toe drain pipe was excessively clogged with fines from the cover soil and/or sand. There were a number of small localized slides at this site. This is the so-called "socked pipe" design which is known to be problematic in other situations, e.g., in leachate collection filters beneath the waste mass, Koerner G. R. et al (1993). The slope was 2.5(H)-to-1(V).

2.2 Storm Event Characteristics

In seven of the eight cases of seepage induced slides just described, the occurrence was during, or immediately after, rain storm events. Unfortunately, the exact storm magnitudes were not recorded. It is assumed, however, that localized short-term seepage forces created enough of an additional driving force to decrease the FS-value to less than 1.0 and thereby result in the slope's instability. The other case, Case #4, of an ice wedge at the toe of the slope and seepage forces due to thawing at the top of the slope is certainly a plausible situation depending on site specific climatic conditions. However, this case is somewhat unique and is somewhat outside of the main thrust of this report. Clearly its teaching, however, is that toe blockage of any type must be avoided in order to have a free up-gradient drainage system without mobilizing seepage forces.

It should be obvious that rain storms are not well-behaved, uniform events. Figure 3 illustrates just how random a short-term storm event can be. The peaks occur over extremely short time periods, i.e., minutes, and can reach dramatic rates. In light of this behavior, a slope will undoubtedly be most susceptible during periods of high rainfall and particularly during or immediately after the highest rainfall rate. In this regard, a seepage-related slope stability analyses should be analyzed as a severe storm event and the drainage system designed accordingly. This is not unlike all types of engineering design when considering live load circumstances, e.g., snow loads, seismic loads, equipment loads, etc.

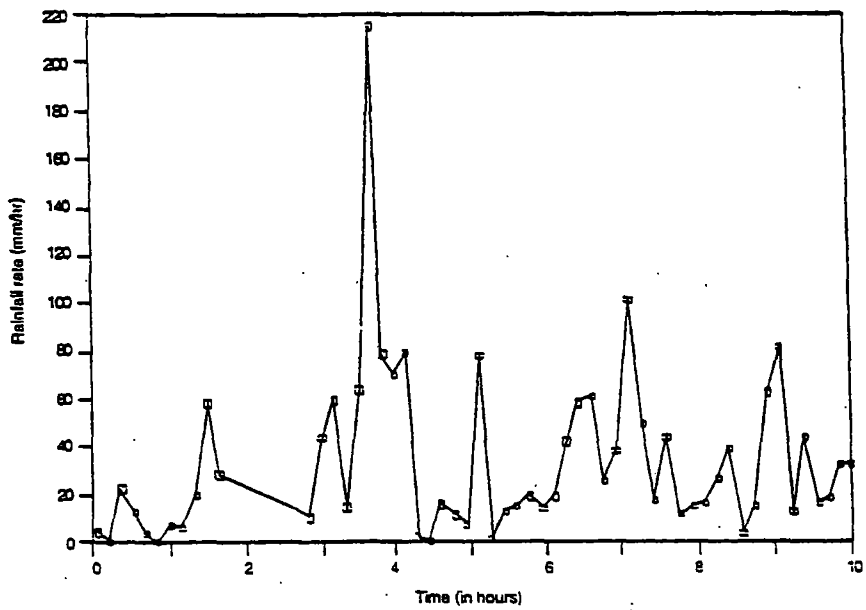

Figure 3 - Precipitation time-rate data for an extreme storm in Oklahoma on May 27, 1987, as measured by the National Storm Service Laboratory. Values are for a 2- by 2-km area, after Maidment (1993).

Ideally, one would like to select a design storm for which there is no risk of exceedance. This concept, however, is most troublesome and hydrologists even argue about the existence of an upper limit. More practical, and accepted in the design of spillways for dams, is the concept of the probable maximum precipitation (PMP). This term is defined by the World Meteorological Organization as:

> *"theoretically the greatest depth of precipitation for a given duration that is physically possible over a given size storm area at a particular geographical location at a certain time of the year."*

Four critical issues are related to the above definition: storm duration, storm intensity, orientation (slope) effects and infiltration into the cover soil. For the first two issues, Table 2 is available for the selected cases in the United States. It is seen that extremely high rates can occur over small, localized areas. For the second two issues, one must proceed on the basis of site specific material properties and an appropriate water balance analysis.

Table 2 - Maximum observed rainfall amount, area and duration data for selected locations in the United States

[Table values are for average rainfall in millimeters, after the World Meteorological Organization (1986).]

	Duration, hour						
Area	6	12	18	24	36	48	72
26 km²	627[a]	757[b]	922[e]	983[e]	1062[e]	1095[e]	1148[e]
260 km²	498[b]	668[e]	826[e]	894[e]	963[e]	988[e]	1031[e]
520 km²	455[b]	650[e]	798[e]	869[e]	932[e]	958[e]	996[e]
1300 km²	391[b]	625[e]	754[e]	831[e]	889[e]	914[e]	947[e]
2600 km²	340[b]	574[e]	696[e]	767[e]	836[e]	856[e]	886[e]
5200 km²	284[b]	450[e]	572[e]	630[e]	693[e]	721[e]	754[e]
13000 km²	206[h]	282[b]	358[b]	394[e]	475[i]	526[i]	620[i]
26000 km²	145[h]	201[j]	257[k]	307[k]	384[i]	442[i]	541[i]
52000 km²	102[h]	152[j]	201[k]	244[k]	295[i]	351[i]	447[i]
130000 km²	64[m]	107[n]	135[k]	160[k]	201[k]	251[r]	335[r]
260000 km²	43[m]	64[m]	89[k]	109[k]	152[p]	170[p]	226[q]

Storm	Date		Location of Center		Remark
a	July 17-18	1942	Smethport	PA	
b	Sept. 8-10	1921	Thrall	TX	
e	Sept. 3-7	1950	Yankeetown	FL	Hurricane
i	June 27-July 1	1899	Hearne	TX	
k	Mar. 13-15	1929	Elba	AL	
q	July 5-10	1916	Bonifay	FL	Hurricane
n	Apr. 15-18	1900	Eutaw	AL	
m	May 22-26	1908	Chattanooga	OK	
o	Nov. 19-22	1934	Millry	AL	
h	June 27-July 4	1936	Bebe	TX	
j	Apr. 12-16	1927	Jefferson Parish	LA	
r	Sept. 19-24	1967	Cibolo Ck.	TX	Hurricane
p	Sept. 29-Oct. 3	1929	Vernon	FL	Hurricane

For the cases of sliding of cover soils as described previously, it appears to the authors that a 6-hour duration storm event falls acceptably close to the concept of a *PMP* event, i.e., a 6-hour duration storm can be considered as a severe storm event and, arguably, a worst-case event. Local weather conditions would prevail and the nearest meteorological station would be the logical source of the hour-by-hour precipitation data. As far as the infiltration into the cover soil calculated via a water balance analysis, one is immediately drawn to the use of the U.S. EPA computer model entitled Hydrologic Evaluation of Landfill Performance (*HELP*). Clearly, the methodology of this model is beyond reproach. At issue, however, is the periodicity of monitoring the infiltration (hence drainage) quantity and some of the assumptions generally used by designers. The *HELP*-model proceeds on the basis of a daily monitoring of precipitation. As will be seen, this significantly underestimates the drainage quantities which must be efficiently removed in the site specific cross-section on the basis of hourly monitoring. Monthly, daily and hourly monitoring examples will be illustrated later in this report so as to illustrate the significance of this issue.

2.3 Types of Drainage Systems

The traditional material used for the drainage of liquids has been naturally occurring granular soils, e.g., sands and gravels. Beginning in the mid-1980's, geosynthetic drainage materials emerged. First geonets and later different types of drainage geocomposites. Each type, under the collective name "geosynthetic drains", will be described in this section.

2.3.1 Natural Soils

The drainage capacity of natural soils is usually analyzed using Darcy's formula:

$$q = kiA \tag{2}$$

where q = flow rate (through or within the soil),

k = coefficient of permeability (the term used herein but more properly, the hydraulic conductivity),

i = hydraulic gradient, and

A = cross sectional area perpendicular to flow.

Critical in the above formulation is the value of "k" for which many relationships exist. Formulas range from the empirical Hazen relationship;

$$k(\text{cm}/\text{sec}) = Cd_{10}^2 \tag{3}$$

where C = constant ranging from 0.4 to 1.2,

d_{10} = 10% finer particle size (mm).

to the more complex Kozeny-Carman equation:

$$k = \frac{1}{k_0 T^2 S_0^2}\left(\frac{e^3}{1+e}\right)\left(\frac{\gamma_p}{\mu}\right) \tag{4}$$

where k_0 = slope factor (≈2.5),

T = tortuosity (factor (≈1.4),

S_0 = wetted surface per unit volume of particles,

e = void ratio,

γ_p = unit weight of the permeating liquid,

μ = viscosity of the permeating liquid.

All formulas of this type indicate that particle size and gradation play the major role insofar as drainage of granular soils is concerned. Typical values of permeability for granular soils are provided in Table 3.

Table 3 - Typical values of permeability for granular soils.

Type of Soil	USCS* Classification	Range of "k"-values (cm/sec)
clean, poorly graded gravel	GP	5 - 20
clean, well graded gravel	GW	1 - 10
clean, poorly graded sand	SP	0.5 - 5
clean, well graded sand	SW	0.2 - 2
mixed, poorly graded sandy gravel	SP - GP	0.1 - 2
mixed, well graded sandy gravel	SW - GW	0.01 - 0.5
mixed, poorly graded gravely sand	GP - SP	0.005 - 0.05
mixed, well graded gravely sand	GW - SW	0.001 - 0.01
silty gravels	ML-GP, ML-GW,	0.0005 - 0.01
silty sands	ML-SP or ML-SW	0.0001 - 0.005

* Unified Soil Classification System

Of course, the use of estimated or typical values as presented in Table 3 is for illustrative purposes only and should never be used for final design. Testing by ASTM D2434 is necessary in this regard. Upon obtaining the value of "k" for the candidate drainage soil, it must be compared to the site-specific required value to arrive at a factor of safety. Alternatively, "k" can be used to calculate a flow rate, q, and used in a similar manner, for example:

$$FS = \frac{k_{allow}}{k_{req'd}} \tag{5}$$

or,

$$FS = \frac{q_{allow}}{q_{req'd}} \tag{6}$$

where FS = factor of safety,

k_{allow} = allowable permeability,

q_{allow} = allowable flow rate (using Darcy's formula),

$k_{req'd}$ = required permeability, and

$q_{req'd}$ = required flow rate (using Darcy's formula).

Depending on the drainage soil that is being used, a filter may also be necessary, e.g., when using GP or GW gravel in the final cover above the barrier layer, and perhaps with other coarse granular soils as well. Insofar as soil filters are concerned, the material will typically be a well-graded sand with particle sizes intermediate between the overlying protection or cover soil, and the underlying drainage soil. The following filtration criteria for sand filters are from the U.S. Army Corps of Engineers (1948).

To prevent piping:

$$\frac{d_{15}(\text{filter})}{d_{85}(\text{cover soil})} < 4 \text{ to } 5, \text{ and}$$

$$\frac{d_{15}(\text{drainage soil})}{d_{85}(\text{filter})} < 4 \text{ to } 5 \tag{7}$$

To maintain permeability:

$$\frac{d_{15}(\text{filter})}{d_{15}(\text{cover soil})} > 4 \text{ to } 5, \text{ and}$$

$$\frac{d_{15}(\text{drainage soil})}{d_{15}(\text{filter})} > 4 \text{ to } 5 \tag{8}$$

The d_{85}-values refer to the size of particle at which 85% by dry weight of the particles are smaller. Similarly, d_{15} refers to the size of particle below which 15% by dry weight is smaller.

2.3.2 Geosynthetics

Geosynthetic drains are always composites in that the drainage core transmitting the flow must be protected by a geotextile which acts as both a filter and a separator with respect to the overlying soil. There are many types of drainage cores that are available:

- Biaxial extruded geonets
- Triaxial extruded geonets
- Stiff 3-D entangled webs
- Vacuum formed cuspated sheets
- Extruded columns or nubbed sheets

The design of a geonet, or other type of drainage core is straightforward. It results in the quantification of a flow rate factor of safety as follows:

$$FS = \frac{q_{allow}}{q_{req'd}} \tag{9}$$

where FS = factor of safety,

q_{allow} = allowable flow rate as obtained from laboratory testing, and

$q_{req'd}$ = required flow rate as obtained from design requirements of the actual system.

The allowable flow rate comes from in-plane (transmissivity) laboratory testing of the geosynthetic drainage product under consideration. Options in this regard are ASTM D4716 and ISO/DIS 12958. The test setup must simulate the actual field system as closely as possible. If it does not model the field system accurately, then adjustments to the laboratory value must be made. This is generally the case. Thus, the laboratory generated flow rate is often an ultimate (or index) value which must be reduced before use in design; that is,

$$q_{allow} < q_{ult} \tag{10}$$

One way of doing this is to ascribe reduction factors* on each of the items not simulated in the laboratory test. This can be accommodated as follows:

$$q_{allow} = q_{ult}\left[\frac{1}{RF_{IN} \times RF_{CR} \times RF_{CC} \times RF_{BC}}\right] \tag{11}$$

Alternatively, if all of the reduction factors are grouped together:

$$q_{allow} = q_{ult}\left[\frac{1}{\Pi RF}\right] \tag{12}$$

where q_{allow} = allowable flow rate to be used for final design purposes,

q_{ult} = flow rate determined from a short-term transmissivity test between solid plates, e.g., see the index data of Figure 4 which was generated according to ASTM D4716,

*The term "reduction factor" is synonymous with the term "partial factor of safety" which has been used in past literature. This newer definition leaves the traditional term "factor-of-safety" to be uniquely associated with uncertainties in the design process.

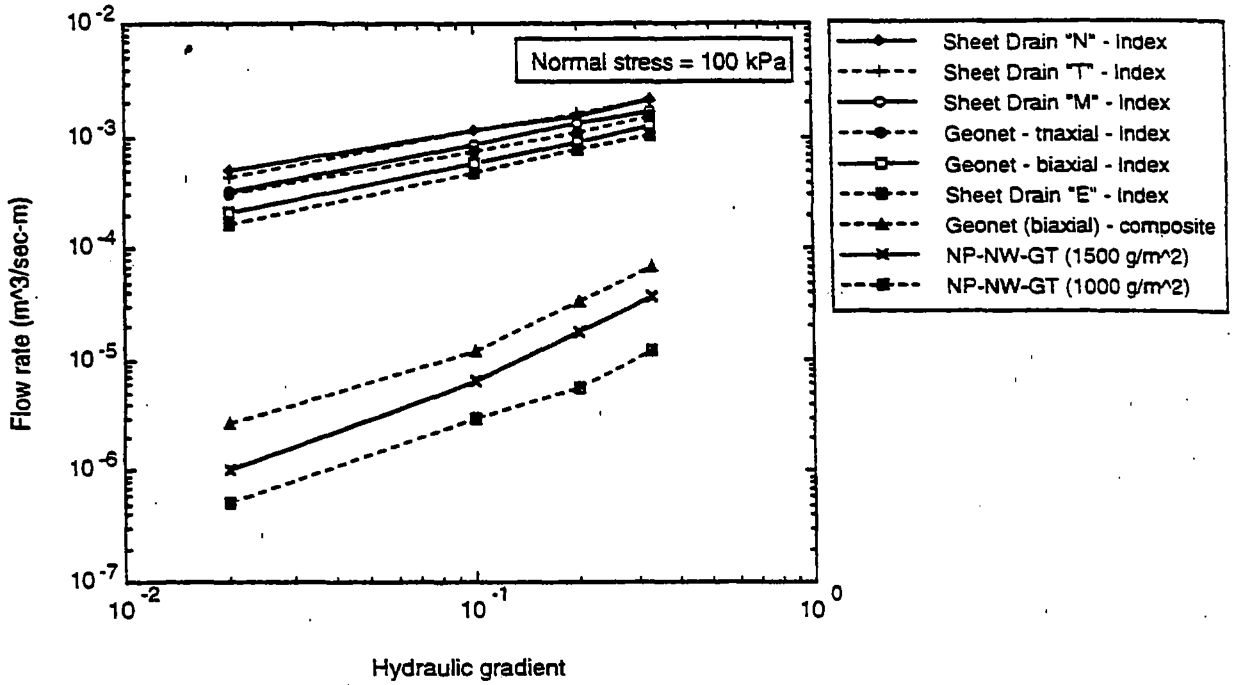

(a) Variation of hydraulic gradient with normal stress constant

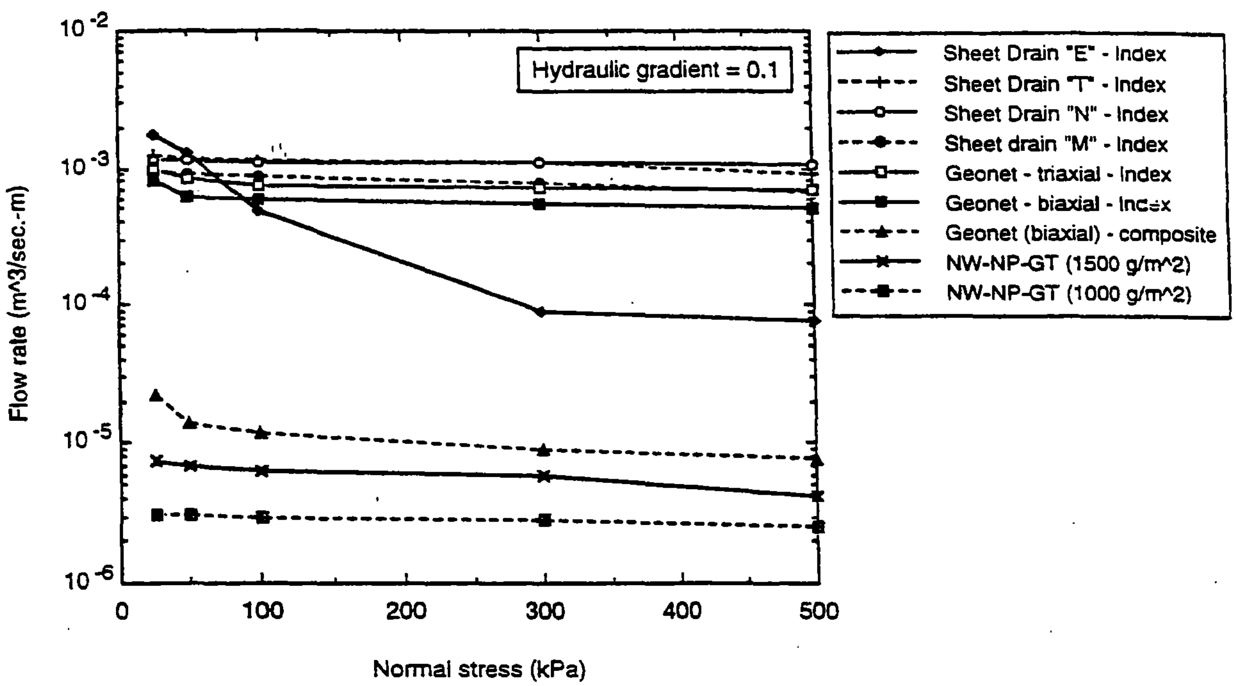

(b) Variation of normal stress with hydraulic gradient constant

Figure 4 - Flow rate behavior of various geosynthetic drainage materials and composites compared to the drainage capability of geotextiles and geonets.

RF_{IN} = reduction factor for elastic deformation, or intrusion, of the adjacent geotextile into the drainage core space,

RF_{CR} = reduction factor for creep deformation of the drainage core and/or adjacent geotextile into the drainage core space,

RF_{CC} = reduction factor for chemical clogging and/or precipitation of chemicals in the drainage core space,

RF_{BC} = reduction factor for biological clogging in the drainage core space, and

ΠRF = product of all relevant reduction factors for the site specific conditions.

Additional reduction factors, such as core overlap flow restriction, temperature effects and liquid turbidity, might also be considered. If needed, they can be included on a site-specific basis. On the other hand, if the test has included the particular item, the reduction factor would appear in the foregoing formulation as a value of unity. Details of the design and guidelines for the various reduction factors are given in Koerner (1997).

As noted previously, a geotextile must cover the geonet or drainage core and its primary function will be to serve as a filter. In so doing, the geotextile must allow the liquid to pass without mobilizing upstream pore water pressure and, simultaneously, must retain the upstream soil so that up-gradient piping and down-gradient clogging of the geonet or drainage core do not occur. Thus the design is a two-step process; first, openness for permeability (or permittivity) and second, tightness for soil retention (via the geotextile's apparent opening size).

Geotextile permeability is the first part of a geotextile filter design. A factor of safety is formulated using permittivity, which is the permeability divided by the geotextile's thickness, as follows:

$$FS = \frac{\psi_{allow}}{\psi_{req'd}} \tag{13}$$

$$\psi = \frac{k_n}{t} \tag{14}$$

where

ψ = permittivity

k_n = cross-plane permeability coefficient, and

t = thickness at a specified normal pressure.

The testing for geotextile permittivity follows similar lines as used for testing soil permeability. The method is standardized as ASTM D4491 and ISO/DIS 11058. Alternatively, some designers prefer to work directly with permeability and require the geotextile's permeability to be some multiple of the adjacent soil's permeability (e.g., 1.0 to 10.0, or higher).

The second part of a geotextile's filter design is focused on adequate upstream soil retention. There are many approaches toward a soil retention design, most of which use some characteristic of the upstream soil particle size and then compares it to the 95% opening size of the geotextile (i.e., defined as O_{95} of the geotextile). The test method used in the United States to determine this value is called the apparent opening size (*AOS*) test, designated as ASTM D4751. "*AOS*" is defined as the approximate largest soil particle that would effectively pass through the geotextile. In Canada and Europe, the test method is called filtration opening size (FOS) and is accomplished by hydrodynamic sieving. One variation is designated as ISO/DIS 12956. Wet sieving is felt by the writers to be the preferred method.

The simplest of the design methods examines the percentage of soil passing the No. 200 sieve, which has openings of 0.074 mm.

1. For soil with ≤ 50% passing the No. 200 sieve: $O_{95} < 0.59$ mm (i.e., *AOS* of the fabric ≥ No. 30 sieve)
2. For soil with > 50% passing the No. 200 sieve: $O_{95} < 0.30$ mm (i.e., *AOS* of the fabric ≥ No. 50 sieve)

Alternatively, a series of direct comparisons of geotextile opening size (O_{95}, O_{50}, or O_{15}) can be made to a specific soil particle size to be retained (d_{90}, d_{85}, d_{50}, or d_{15}). The numeric value depends on the geotextile type, soil type, flow regime, etc. For example, Carroll (1983) recommends the following widely used relationship.

$$O_{95} < (2 \; or \; 3)d_{85} \tag{15}$$

where O_{95} = the 95% opening size of the geotextile (in mm), and

d_{85} = soil particle size (in mm) for which 85% of the soil particle is finer.

More detailed procedures, for both static and dynamic flow are available, see Luettich, et al. (1992). Details of the design and example problems are given in Koerner (1997).

2.3.3 Long-Term Effects

All too often when designing natural soil or geosynthetic drainage systems the focus is on the as-received materials. While this may be appropriate for temporary slopes, it is not appropriate for permanent situations like the drainage layer of final covers above closed landfills.

The overriding long-term effect on drainage systems is the potential for fine particle migration and contamination of the drainage and/or filter materials. As seen in the case histories presented in Table 1, seepage induced slides have occurred in gravel soils having 25 to 38 mm average particle sizes. While these coarse drainage gravels may have appeared initially acceptable, it must be remembered that quarried stone always contains fines and furthermore with the weaker mineral types, e.g., limestone, many fracture surfaces exist to generate even more fines. Furthermore, the filter (if one is present) may allow fines from overlying soils to pass into the underlying drain. Over time and successive rain events, fines from various sources migrate down through the thickness of the drainage layer and can then further migrate downgradient. Obviously, the permeability of the stone (which always appears clean and porous on its surface) decreases over time. The potential clogging mechanisms can be modeled in the laboratory, but to the writers' knowledge long-term drainage tests of soils are rarely conducted and have never (?) been reported in the open literature.

In a similar manner, long-term clogging can also negatively influence geosynthetic drainage systems; both the drainage core and the geotextile filter. Focus in geosynthetic drainage systems has been on the geotextile due to its relatively small openings in comparison to the drainage core of geocomposites and geonets. Three candidate tests aimed at an assessment of long-term geotextile clogging are available. They are the following:

- Long-Term Flow (*LTF*) test via GRI GT-1.
- Gradient Ratio (*GR*) test via ASTM D 5101.
- Hydraulic Conductivity Ratio (*HCR*) test via ASTM D 5084.

Of these tests, the hydraulic conductivity ratio test is preferred by the authors since it can model the field situation under closely simulated conditions. The test is performed using a flexible wall soil permeameter of the type that is readily available in most soil testing laboratories, e.g., ASTM D5084.

As described in section 2.2, the precipitation (P) that we will focus upon is the hourly storm event over a 6-hour period. This will be seen to be very intense in comparison to daily or monthly monitoring of precipitation on the basis of the flux that is generated.

The infiltration (I) into the cover soil is minimized by increasing the surface runoff (R). For the cross sections we are considering, the runoff is relatively high since slope angles where instability occurs are usually greater than 14 deg. which is 4(H)-to-1(V). Of course, high surface runoff can easily lead to surface soil erosion but this consideration is not addressed in this report, see Koerner and Daniel (1997) for details in this regard. The infiltration is also influenced by the type of surface soil. For example, a coarse drainage gravel as shown in Figure 5a will accept significantly more infiltration and less runoff than will a fine grained soil as shown in Figure 5b.

Water that enters the cover soil as infiltration flows downward by gravitational forces. However, capillary action tends to retain water in the soil. Storage of water in soil, coupled with removal of water by evapotranspiration, are important mechanisms in limiting the percolation of water through the cover soils. Much of the water that falls on the soil surface infiltrates into the soil and is returned to the atmosphere over time by plants through evapotranspiration. Unfortunately, for very intense storms, the actual evapotranspiration (AET) is very limited due to the short time periods considered.

An important major retarding mechanism toward high percolation values is the water storage capacity of soils (WS). For dry, or partially saturated soils, infiltrating water will simply fill the available space in the soil voids. For sporadic and relatively mild rain events, the retardation of percolation by water storage is a major factor in limiting percolation through the system. When the voids in the cover soils are at field capacity or are fully saturated, however, there is no additional storage capacity and the infiltrating water all passes through the system as percolation in accordance with Darcy's formula. When the soils involved have high k-values the quantities can be quite large. Cover soils at field capacity, or fully saturated, are the likely case for the extreme storm events which are focused upon in this report.

The vertical percolation (*PERC*) value itself (in units of mm/hour) is based on a horizontal unit area, thus its units are mm/hour-m^2. It would continue downward except for the underlying hydraulic barrier. In this report we make the assumption that there is "zero leakage" through the hydraulic barrier layer (*GM, GCL* and/or *CCL*) beneath the drainage layer. This is done for the following reasons:

1. For slopes of 4(H)-to-1(V), and greater, the value will be quite small, e.g., roofs of homes at these angles (generally) do not leak.
2. The velocity of flow will be quite high for the short duration and intense storm events considered herein further minimizing leakage rates.
3. The no leakage assumption gives rise to conservative estimates of percolation.
4. We have no idea what value to assume for leakage and would much prefer to assume good CQC and CQA of the barrier system with no leakage.

Finally, whatever value of percolation arrives at the drainage layer, it translates completely into lateral drainage, or flux (*FLUX*). The flux accumulates as it flows on top of the hydraulic barrier to a maximum value at the toe of the slope. Thus, the flux is at a maximum at the toe of the slope and the drainage system is designed on the basis of this value. It is a worst case scenario assumption and is recommended for design so as to avoid seepage related slope instability problems.

3.2 Calculation Options

There are many possible calculation options for percolation and we have selected three of them; manually for peak *monthly* averages, computer modeling for peak *daily* averages, and manually for peak *hourly* averages. Each will be explained.

3.2.1 Manual Method for Monthly Averages

A water balance analysis can be performed on a monthly average basis. The procedure can be performed manually as proposed by Dr. D. E. Daniel of the University of Illinois-Urbana, however, it is highly amenable to use of a computer spread sheet to facilitate the actual computations. Three publications provide the basis of Daniel's procedure; Thornthwaite and Mather (1957), Fenn, et al. (1975), and Kmet (1982).

A table or spread sheet should be set up with twelve columns established for the twelve months of the year. In a progressive sequence of steps, an additional twelve rows (from A through P) are developed for each of the twelve months of the year. Table 4 gives an overview of the information needed and the respective calculations to eventually arrive at a percolation value (*PERC*) passing through the cross-section arriving at the drainage layer. The flow units are in "mm/month" over a square meter of horizontal surface. Table 5 gives an illustration of this procedure for a final cover system as shown in Figure 5b. Details of the procedure are found in Koerner and Daniel (1997). The target value in Table 5 is the maximum monthly value of "*PERC*", i.e., the required percolation value which is used to design the drainage system. Note that the value in this example is 8.54 mm/month in the month of January and thereafter the evapotranspiration has eliminated all of the infiltration resulting in zero percolation for the rest of the year.

3.2.2 Computer Method for Daily Averages

Nearly all water balance analyses performed in the United States are conducted using the computer program "*HELP*" (Hydraulic Evaluation of Landfill Performance). The HELP program was written by Dr. P. R. Schroeder of the U.S. Army Corps of Engineers, Waterways Experiment Station under sponsorship of the U.S. EPA. The program, which has been periodically updated, is available in the public domain. At the time of this writing, the latest version is Version 3.0 and is available by purchasing "The Hydraulic Evaluation of Landfill Performance Model, Engineering Documentation for Version 3", EPA/600/R-94/168b, from the National Technical Information Service in Springfield, Virginia. A user's manual is supplied with a diskette that contains the program, which is written in FORTRAN for use on a personal computer.

Table 4 - Manual Procedure for "PERC" Calculation, Based on Monthly Average Rainfall Values, see Table 5 for Example

Row	Value	Units	Comment or Calculation
A	average monthly temperature	°C	local weather station data
B	monthly heat index	—	calculated value needed to determine evapotranspiration
C	unadjusted daily potential evapotranspiration	mm/mo.	calculated value using data from Row A & Row B
D	monthly duration of sunlight	—	values taken from published tables
E	potential evapotranspiration	mm/mo.	multiply Row C by Row D
F	mean monthly precipitation	mm/mo.	local weather station data
G	runoff coefficient	—	estimated value, but guidance is available
H	runoff	mm/mo.	multiply Row F by Row G
I	infiltration	mm/mo.	subtract Row H from Row F
J	infiltration minus potential evapotranspiration	mm/mo.	subtract Row E from Row I
K	accumulated water loss	mm/mo.	sum of negative values in Row J
L	water stored	mm/mo.	calculated value having many details
M	change in water storage	mm/mo.	difference in monthly water storage from Row L data
N	actual evapotranspiration	mm/mo.	comparison to potential evapotranspiration
O	percolation (PERC)	mm/mo.	comparison to determine if percolation occurs (or not) and to what amount
P	check of calculations	mm/mo.	validation of water balance calculations

Table 5 - Illustration of the water balance analysis in a typical final cover system using the manual method for monthly averages.

Row	Parameter	January	Feburary	March	April	May	June	July	August	September	October	November	December	Total	%
A	Avg. monthly Temp., °C	9.5	11.8	15.8	20.4	23.9	27.6	29.3	29.2	26.2	21.0	14 8	11.2		
B	Monthly heat Index (H_a)	2.64	3.87	5.71	8 41	10.68	13.28	14.54	14.47	12.28	8.78	5.17	3.39	103.02	
C	Unadjusted daily potential evapotranspiration (UPET), mm/mo.	0 44	0.72	1.39	2.48	3 55	4.53	4.94	4 92	4.36	2.65	1.20	0.64		
D	Possible monthly duration of sunlight (N)	27	26.1	30.9	32.4	35.4	35.1	36	34.2	30.9	29.4	26.7	26.4		
E	Potential evapotranspiration (PET), mm/mo.	11.92	18.80	43.02	80.33	125.49	159.09	177.82	168 20	134.60	77.82	32.07	16.90		
F	Precipitation (P), mm/mo.	34.09	31.34	26.67	114.4	108.81	68.73	42.72	100.13	100.58	95.71	95.5	27.99	846.67	100%
G	Runoff Coefficient (RC)	0.40	0.40	0.40	0.40	0.40	0.40	0.40	0.40	0.40	0.40	0.40	0.40		
H	Runoff (R), mm/mo.	13 636	12.536	10.668	45.76	43.524	27.492	17.088	40.052	40.232	38.284	38.2	11.196	338.67	40%
I	Infiltration (IN), mm/mo.	20 45	18 80	16.00	68 64	65 29	41.24	25 63	60 08	60.35	57.43	57.30	16.79	508 00	
J	IN - PET, mm/mo.	8.64	0.01	-27.02	-11.69	-60.21	-117.85	-152.19	-108.12	-74.45	-20.40	25.23	-0.11		
K	Accumulated water loss (WL), mm/mo.	0.00	0 00	-27.02	-38 71	-98.92	-216 77	-368.96	-477.07	-551.53	-571.92	-571.92	-572.03		
L	Water stored (WS), mm/mo.	118.50	118.60	93.32	81.63	69 59	41.80	30.86	45.56	61.36	40 96	118.60	118 60		
M	Change in water storage (CWS), mm/mo.	0.00	0.00	-25.18	-11.69	-12.04	-27.79	-10 95	14.70	15.80	-20.40	77.54	0.00		
N	Actual evapotranspiration (AET), mm/mo.	11.92	18.80	41.18	80.33	77.33	69.02	36.58	45.38	44.55	77.82	32.07	16.78	551.77	65%
O	Percolation (PERC), mm/mo.	8.54	0.01	0.00	0.00	0.00	0.00	0.00	0 00	0.00	0.00	-52.31	0.00	-43.77	-5%
P	Check (CK), mm/mo.	34.09	31.34	26.67	114.40	108.81	68.73	42.72	100.13	100.58	95.71	95.50	27.99	846.67	100%

The computer program employs the same principles as the method of manual analysis described in section 3.2.1, but *HELP* uses a daily (rather than monthly) time internal and employs sophisticated algorithms for many of the computations. The model accepts weather, soil, and geometric data. It then uses solution techniques that account for the effects of surface storage, snowmelt, runoff, infiltration, evapotranspiration, vegetative growth, storage of soil moisture, lateral drainage of water in drainage layers, leachate recirculation, vertical percolation of soil water, and leakage through hydraulic barriers (*GM, GCL, CCL* or composite liners).

Engineering documentation of *HELP* is provided by Schroeder et al. (1994). We will not attempt to repeat the documentation here. Instead, we will provide an overview of *HELP*'s capability and discuss the key technical components of the model. The *HELP* program contains a number of default values for soil and other parameters, which can prove to be helpful even for manual analyses.

3.2.2.1 Design Profile

A schematic view of the profile that *HELP* was designed to simulate is shown in Figure 6. The profile is divided into three subprofiles (cover, waste and bottom liner system) to simulate a landfill. For purposes of this report, attention is focused on the cover.

The layers that are analyzed with *HELP* are categorized by the hydraulic function that they perform. Four types of layers are available, as summarized in Table 6.

(a) <u>Vertical Percolation Layer</u>

A vertical percolation layer is any layer permitting vertical movement of water (downward due to gravity or upward due to evapotranspiration) within it, and not serving as a lateral drainage layer. Examples of layers that are treated as a vertical percolation layers are top soil, protection soil, gas collection layer, foundation soil, and waste.

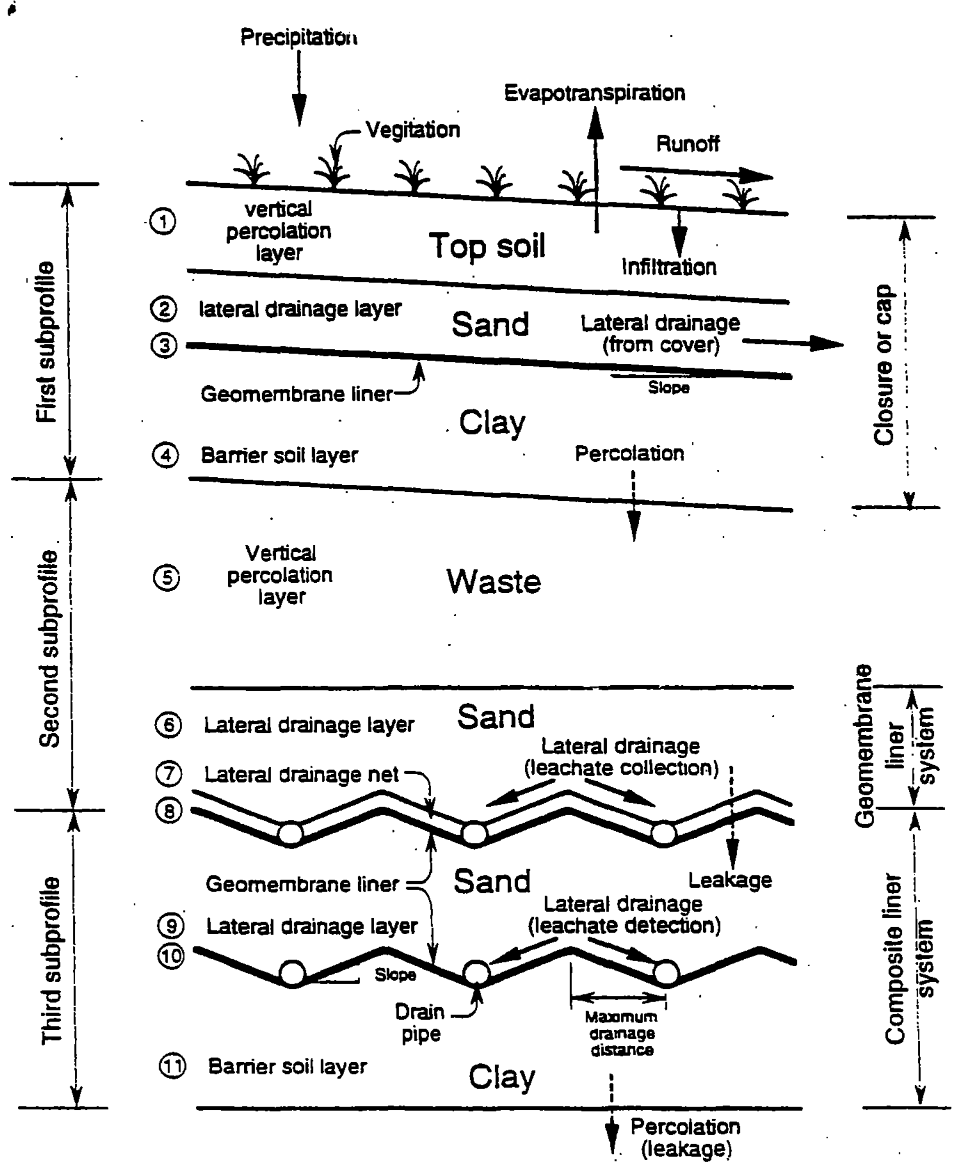

Figure 6 - Elevation view of a typical solid waste landfill

Table 6 - Four Types of Layers Allowed in the HELP Program

Type of Layer	Hydraulic Characteristics
Vertical Percolation Layer	Flow in this layer is strictly vertical (downward due to gravity or upward due to evapotranspiration). Hydraulic conductivity (permeability) at saturation is typically in the range of 10^{-3} to 10^{-6} cm/sec.
Lateral Drainage Layer	This layer promotes lateral drainage to collection systems, e.g., drains at the perimeter of the cover. Hydraulic conductivity (permeability) can vary greatly. (This layer is the focus of the present report). The underlying layer is normally a barrier consisting of some type of liner.
Barrier Soil Liner	Barrier soil liners are low-permeability soils; a compacted clay liner (*CCL*) with a permeability of 10^{-6} to 10^{-7} cm/sec or a geosynthetic clay liner (*GCL*) with a permeability of 10^{-8} to 10^{-9} cm/sec.
Geomembrane	Geomembranes can be of many types. In the HELP program, they are assumed to permit leakage via vapor diffusion, manufacturing flaws (pinholes), and installation defects (e.g., flaws).

The method of calculating the downward movement of water in the unsaturated vertical percolation layer is approximate. More rigorous analytic techniques are available that more carefully compute hydraulic gradients and consider vapor and thermal transport mechanisms. However, computer codes that account for unsaturated flow more rigorously tend to be difficult to use because of their complexity and, therefore, are rarely employed for water balance analyses. Nevertheless, *HELP* is not considered a particularly accurate simulation program for covers that are located in arid areas, where the subtleties of unsaturated moisture movement can dominate the water balance.

(b) <u>Lateral Drainage Layer</u>

Lateral drainage layers may consist of granular soils or geosynthetic materials. Vertical drainage in a lateral drainage layer is modeled in the same manner as a vertical percolation layer. However, lateral flow in the saturated zone at the base of the lateral drainage layer is allowed.

Unconfined lateral flow in the drainage layer is modeled using Darcy's formula, assuming continuity and employing the Depuit-Forcheimer assumptions (seepage parallel to the slope of the layer and hydraulic gradient proportional to the slope of the underlying barrier layer). The algorithm used by *HELP* is reasonably rigorous and accurate. The accuracy with which the permeability value of the lateral drainage is determined, not the method of analysis, limits the overall accuracy of the calculations.

(c) Low-Permeability Soil Barrier Layer

Compacted clay liners (*CCLs*) and geosynthetic clay liners (*GCLs*) are frequently used as hydraulic barrier layers. The soil is assumed to be saturated, i.e., to have no capacity to store water without drainage occurring. Leakage through the *CCL* or *GCL* is assumed to occur whenever there is a head of water on top of the barrier.

When the soil liner is located near to the surface of the cover and there is no geomembrane overlying the clay, the low-permeability soil layer will probably desiccate at times, invalidating the assumption of continuous saturation. To model this process, the low-permeability soil layer can be treated as a vertical percolation layer. Also, clay liners are not completely saturated with water at the time of construction, so the liners must first absorb some nominal amount of water before drainage is initiated.

(d) Geomembrane Layer

Geomembranes are widely and routinely used in well engineered covers and liners beneath the waste. Geomembranes can be extremely effective hydraulic barriers and can withstand many of the forces (e.g., differential settlement and freeze/thaw or wet/dry cycles) that are destructive to clay liners.

The *HELP* program assumes that liquids can leak through geomembranes by three mechanisms: (1) vapor diffusion through the intact geomembrane; (2) leakage through manufacturing defects (pinholes); and (3) leakage through construction defects (mainly flaws in seams). The equations are complex and involve a number of possible cases. The reader is referred to Schroeder, et al. (1994) for details.

3.2.2.2 Default Properties

One of the useful aspects of the *HELP* model is that it contains default parameters for various soil and waste properties based upon data available for more than a thousand soils. Default properties are available for low-density, moderate-density and high-density soils. Information is also available on default waste characteristics, on saturated hydraulic conductivity (permeability) of wastes, and on default material characteristics for various geosynthetic materials. In addition to the manual which documents the HELP program, these default tables are reproduced in Koerner and Daniel (1997).

3.2.2.3 Method of Solution

The *HELP* program models both surface processes and subsurface processes. The surface processes include snowmelt, interception of rainfall by vegetation, surface runoff, and evaporation of water. The subsurface processes modeled are evaporation of water from the soil, transpiration of water by plants, vertical percolation of water through unsaturated soil, lateral drainage in drainage layers, and leakage of water through clay barrier soils, geomembranes, or composite liners. Daily infiltration of water into the surface of the cover is determined indirectly from a surface water balance. Each day, infiltration is assumed to equal the sum of rainfall and snowmelt, minus the sum of runoff, surface storage (e.g., on the surfaces of plants), and surface evaporation (e.g., evaporation of water stored on the surfaces of plants).

The daily surface water accounting procedure used in *HELP* is as follows. Snowfall and rainfall are added to the surface snow storage, if present, and then snowmelt plus excess storage of rainfall is computed. The total outflow from the snow cover is then treated as rainfall in the absence of a snow cover for the purpose of computing runoff. A rainfall-runoff relationship is used to calculate runoff. Surface evaporation is then computed, but surface evaporation is not allowed to exceed the sum of surface snow storage and intercepted rainfall. The snowmelt and rainfall that does not run off or evaporate is assumed to infiltrate into the landfill. Computed infiltration in excess of the storage and drainage capacity of the soil is routed back to the surface and is added to the runoff or held as surface storage.

The subsurface processes modeled by *HELP* are as follows. The first subsurface process considered is evaporation of water from the soil. Next, transpiration of water from the evaporative zone by plants is computed. Other processes are modeled using a time step varying from 30 minutes to 6 hours. For vertical percolation layers, a water balance is performed on each layer to determine the water content of the material. Hydraulic conductivity is computed from the water content, and then the amount of gravity drainage (if any) is determined. For lateral drainage layers, a water balance is used to determine whether the drainage layer is saturated at any point, and if so, lateral drainage is computed for that portion of the layer that is saturated. Vertical percolation is assumed to occur in the lateral drainage layer above the zone of saturation. The same equations employed for analyzing gravity drainage in vertical percolation layers are used to analyze vertical flow above the saturated zone in lateral drainage layers. Soil barrier layers are assumed to be continuously saturated and, therefore, no water balance is performed for them. Leakage is computed from the hydraulic properties of the drainage layer and the amount of head acting on the barrier layer. Leakage through geomembranes is computed from vapor diffusion, leakage through pinholes, and leakage through installation defects.

The *HELP* program allows the user to select the number of years to simulate as well as the output frequency. The user may use a maximum of 100 years of simulation provided the weather are available for that many years. The user may also select any, all or none of the available output options - namely, daily, monthly or annual output. Note that daily output is the shortest time-interval available using the *HELP* program. Of the resulting output information, the peak daily percolation ($PERC_{peak\ daily}$, in units of mm/day) into the drainage layer within the cover soil system is the target value for this report. This value will be used to calculate the value of flux which is then used to design the drainage system.

3.2.3 Manual Method for Hourly Averages

Under the hypothesis that seepage induced slope instability occurs in periods consisting of hourly intervals, and recognition that the minimum time-internal from *HELP* is days, a manual method to calculate hourly averages is presented. Obviously, it requires hourly precipitation data. Based on the basic concepts of water balance analysis shown in Figure 5, the following relationships hold:

$$P = I + SR \tag{16}$$

and

$$I = PERC + AET + \Delta WS \tag{17}$$

where P = probable maximum (hourly) precipitation

I = infiltration

SR = surface runoff

$PERC$ = percolation

AET = actual evapotranspiration

ΔWS = change in water stored in cover soil
= (field capacity) - (actual water content)

Under the assumptions that the immediate time before the PMP event has been a period of regular rainfall, the actual evapotranspiration is negligible for a intense rainfall over a short period of time (e.g., a few hours), and the cover soil is at *field capacity* before the storm reaches its highest intensity (i.e., there is only nominal excess water storage capacity available at the time), the infiltration results directly in percolation, i.e., $I = PERC$. Therefore, the following relationships result:

$$P = PERC + SR \tag{18}$$

or $PERC = P - SR$

but $SR = P(RC)$ (19)

where "RC" equals the runoff coefficient

thus $PERC = P\,(1 - RC)$ (20)

Note that Equation (20) is valid only when the cover soil is sufficiently permeable so that the amount of water which does not runoff [i.e., $P(1 - RC)$] can percolate through the cover soil into the drainage layer. When the cover soil is not permeable enough to handle such amount of water, the difference will occur as sheet flow over the ground surface. The amount is governed by the permeability of the cover soil ($k_{cover\ soil}$). Thiel and Stewart (1993) showed that the percolation into the drainage layer, under such a situation, should be determined as:

$$PERC = k_{cover\ soil}; \quad \text{when } P(1 - RC) > k_{cover\ soil} \tag{21a}$$

otherwise:

$$PERC = \text{as calculated}; \quad \text{when } P(1 - RC) \leq k_{cover\ soil} \tag{21b}$$

3.3 Comparison of Results

The following example is used to demonstrate the dramatic differences between the three calculation options just presented; namely, *monthly, daily and hourly* averages.

<u>Example</u>: A landfill is to be built in Thrall, Texas (60 kilometers northeast of Austin). The site is a 200 m by 200 m square, i.e., it is 4 hectares. The side slopes of the leachate collection layer in the liner system, as well as the final cover, have slope inclinations of 3(H)-to-1(V). The runoff coefficients for the leachate collection layer is 0.18 and for the cover soil is 0.4. Calculate the percolation (*PERC*) and flux (*FLUX*) values of the leachate collection layer in the side slope liner system (figure "a" following) and the final cover system (figure b" following) for slope lengths of 10, 30, 60 and 100 m on the basis of monthly precipitation (per Section 3.2.1), daily precipitation (per section 3.2.2), and hourly precipitation (per section 3.2.3). The soil permeability values are default values suggested in the HELP manual.

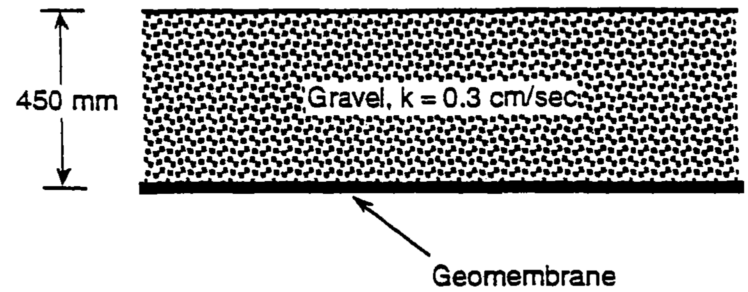

(a) Leachate collection system

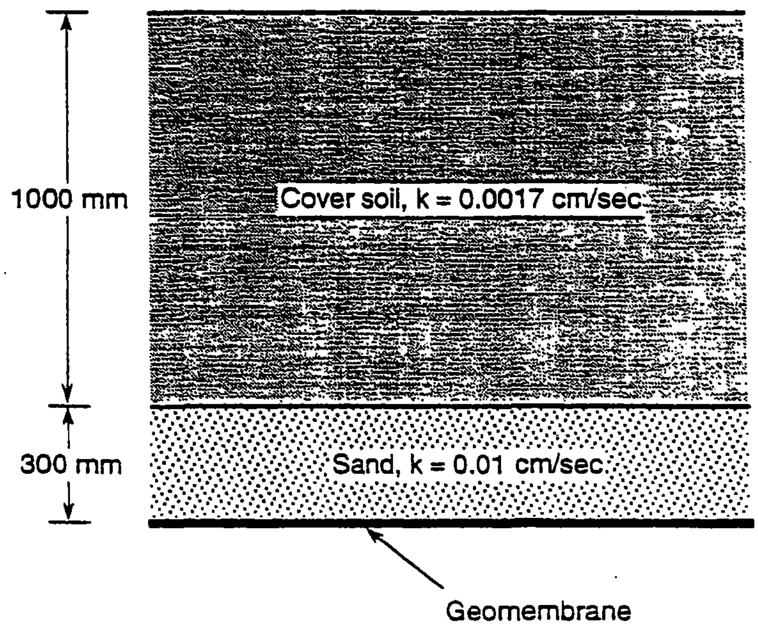

(b) Final cover system

<u>Solution</u>: Each of the three calculation options presented in the previous section were used to obtain the percolation (i.e., "*PERC*") and the results were multiplied by the respective slope lengths using a unit width to obtain the respective values of flow rates (i.e., "FLUX"). The results are summarized in Table 7.

Table 7 - Results of the example problem using various time interval options of water balance analyses to obtain PERC and varying slope lengths to obtain FLUX.

Type	Time Internal for Calculations	PERC (mm/hr)	FLUX (m^3/hr)			
			L = 10 m	L = 30 m	L = 60 m	L = 100 m
(a) leachate collection system	monthly	0.046 [1]	4.4×10^{-4}	1.3×10^{-3}	2.6×10^{-3}	4.4×10^{-3}
	daily	varies [2]	0.025	0.079	0.16	0.28
	hourly	68.1 [3]	0.65	1.9	3.9	6.5
(b) final cover system	monthly	0.011 [1]	1.1×10^{-4}	3.3×10^{-4}	6.6×10^{-4}	1.1×10^{-3}
	daily	varies [2]	0.013	0.041	0.088	0.14
	hourly	49.9 [3]	0.50	1.5	3.0	5.0

Note: 1. Via spread sheets as shown in Table 5, using the average monthly temperature, duration of sunlight and precipitation data from Austin, Texas.
2. Via the *HELP* model using evapotranspiration , synthetic temperature and solar radiation data from Austin, Texas and historical precipitation data (1974-1978) from San Antonio, Texas. The PERC and FLUX-values vary since the *HELP* model takes the slope length into consideration when calculating the amount of runoff.
3. Using the 6-hour rainfall data recorded at Thrall, Texas over an area of 260 km^2 (see Table-2) and Equations 20 and 21.

For the above example, the values of *FLUX* for the various slope lengths can be put into a comparison format by assuming that the *HELP* model gives the conventionally used values for design purposes. Thus the *HELP* generated *FLUX*-values will be assigned a value of 100% (or 1.0), and the monthly and hourly values compared accordingly. As seen in Table 8, it is readily apparent that the precipitation time interval plays a dominate role in the calculations. Using monthly intervals, the *FLUX*-values vastly underestimate the *HELP* generated values (≈ 60 to 120 times), whereas the hourly interval *FLUX*-values vastly overpredict the *HELP* generated values (≈ 25 to 40 times). *In the writers' opinion, it is the hourly interval calculations that result in flux-values which create seepage induced slope instability and calculations using this time interval should be used in the design of drainage layers for applications as described in this report.* This will be the approach taken in the remainder of the report. At the outset, however, it should be stated that drainage systems designed as just noted (i.e., on an hourly interval basis with the worst case assumptions stated in section 3.2.3) will require significantly greater hydraulic capacity than the comparable drainage systems designed using the *HELP* model.

Table 8 - Comparison of *FLUX*-values for different calculation options normalized to the conventionally used HELP generated values.

Type	Calculation option	Slope length (m)			
		10	30	60	100
(a) leachate collection system	monthly	0.018	0.016	0.016	0.016
	daily (HELP)	1.0	1.0	1.0	1.0
	hourly	26.0	24.0	24.4	23.2
(b) final cover system	monthly	0.008	0.008	0.008	0.008
	daily (HELP)	1.0	1.0	1.0	1.0
	hourly	38.5	36.6	34.1	35.7

4.0 DRAINAGE LAYER CONSIDERATIONS

As long as there is percolation into the drainage layer beyond its field capacity, there will be water flowing within the slope's drainage system. When the drainage layer is capable of handling this flow rate, which is generally the assumption made in the design stage, seepage will occur in the drainage layer only. Giroud and Houlihan (1995) describe the situation for both steady state and transient flow conditions. They caution that the drainage layer must be able to accommodate the required flow rate. However, when the flow rate is too large to be handled by the drainage layer and/or its toe drain, seepage will buildup above the drainage layer into the overlying cover soil or even flow above grade as an addition to runoff. Such seepage in the drainage layer or overlying cover soil could build up in a horizontal or a parallel manner, or as a combination of both. Since water tends to uplift soil particles due to a buoyancy effects and seepage tends to drag particles in the direction of flow, such seepage forces lead to a decrease in the slope's factor of safety and can easily result in seepage induced sliding.

From the above discussion, two issues are significant in conducting the design of the drainage layer above a lined slope: the flow (phreatic surface) orientation and the depth of submergence. Both issues are discussed in this section.

4.1 Patterns of Seepage Buildup in Cover Soils

Consider a cover soil of uniform thickness placed directly above a geomembrane or other barrier material at a slope angle of "β" as shown in Figure 7. Two discrete zones are illustrated; a small passive wedge at the toe of the slope resisting a long, thin active wedge extending the length of the slope. Only one type of soil is placed directly against the geomembrane and it is cohesionless, i.e., typical of a leachate collection layer or a drainage layer in a final cover. For the case of a drainage layer in a final cover, the profile can also consist of different soil materials placed in parallel layers. In this case, the drainage soil would be granular and placed directly above the geomembrane and then a locally available finer grained soil (including topsoil) would be placed above the drainage layer. Other soil properties, soil-to-geomembrane friction angle and the dimensions of the considered profile are shown in Figure 7.

Note should be made in Figure 7 of two possible phreatic surface orientations. This is necessary because seepage can be built-up in two different ways: horizontal or parallel to the slope. Thus, orientation is quantified as a horizontal submergence ratio (*HSR*), or a parallel submergence ratio (*PSR*). As to the depth of submergence, it is a function of the amount of infiltration, the permeability of the drainage layer and the drainage layer capacity. The dimensional definitions of both ratios are given in Figure 7.

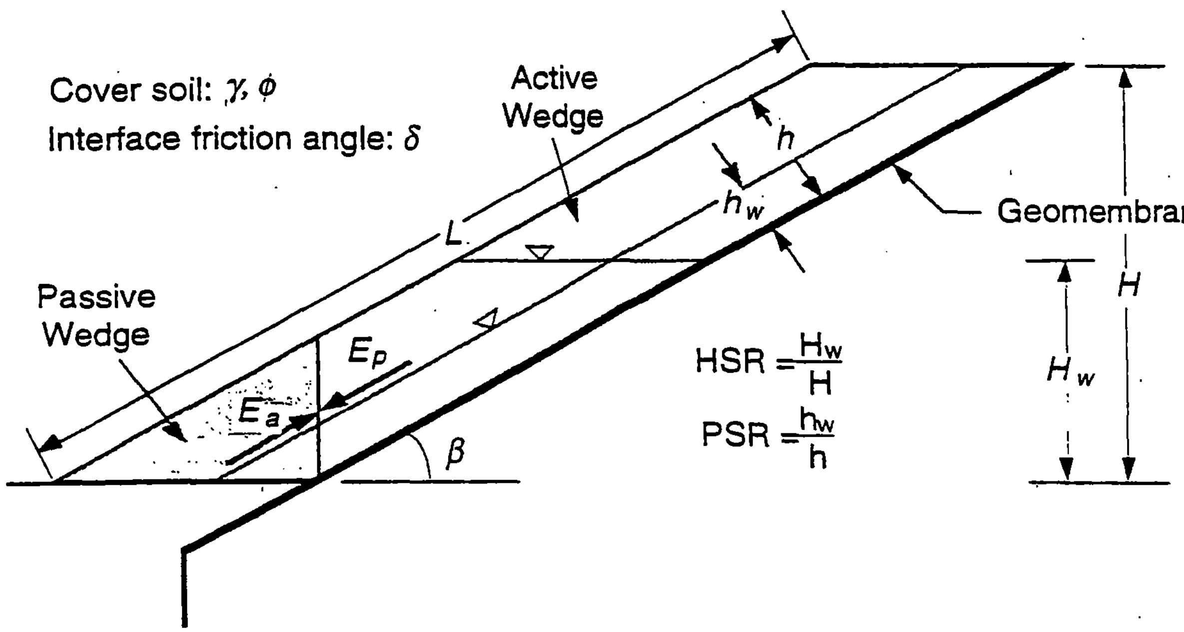

Figure 7 - Cross-section of cover soil on a geomembrane with different seepage buildup patterns.

Of the two seepage orientation possibilities shown in Figure 7, it is felt that extremely low permeabilities at the toe of slope will result in a horizontal seepage buildup, Soong and Koerner (1996). This would typify cases where toe blockage occurs due to fines migrating downgradient over time, or due to ice buildup at the toe of the slope as the up-gradient drainage layer thaws producing seepage pressure. However, in most steady-state situations, it is generally assumed that water flows parallel to the slope, e.g., Giroud et al. (1995), Thiel and Stewart

(1993). This would likely occur when the drainage system is underdesigned from the outset. In a separate study, however, it has been shown that different seepage orientations, under the same submergence ratio, make little difference in the resulting slope stability factor of safety values, Soong and Koerner (1996). Furthermore, a specific amount of percolation results in a unique submergence ratio regardless of the seepage orientation assumption, i.e., $HSR = PSR$, since the total submerged volume of soil remains the same. Based on the above reasons, only the parallel seepage orientation will be considered in this report.

4.2 Drainage Layer Capacity (*DLC*)

The rate of percolation per unit area (in units of m^3/hour) coming through a given cross section, assuming no leakage through the underlying hydraulic barrier layer (which is a conservative assumption), is determined as follows:

$$\boxed{FLUX_{reqd} = \frac{PERC}{1000} \times L(cos\beta) \times w} \qquad (22)$$

where $PERC$ = the rate of percolation in units of mm/hr [see Equations 20 and 21],

L = length of drainage slope, m

β = slope angle,

w = 1.0 = unit width of drainage slope, m

When designing the drainage layer in a soil covered slope, the following concept of drainage layer capacity should be evaluated:

$$\boxed{DLC = \frac{FLUX_{allow}}{FLUX_{reqd}}} \qquad (23)$$

where DLC = drainage layer capacity

$FLUX_{allow}$ = allowable flow rate of the drainage layer per unit width of slope,

$FLUX_{req'd}$ = actual flow rate per unit width of slope.

It is good design practice and is generally required by regulatory agencies that the drainage layer capacity cannot be exceeded, i.e., $DLC \geq 1.0$. That is, complete saturation of the drainage layer should not be allowed at any time.

4.3 Parallel Submergence Ratio (*PSR*)

In a cover soil slope stability analysis, it is necessary to determine the depth of submergence in the cross section so as to quantify the value of parallel submergence ratio (*PSR*). The value of *PSR* can then be used in the slope stability analysis and ultimately results in a factor of safety (*FS*) regarding slope stability. The following procedure can be used to calculate the parallel submergence ratio (*PSR*). The typical cover system configuration of Figure 5b and dimensions are illustrated in Figure 8. Note that the analysis also applies for full thickness drainage layers typical of leachate collection layers beneath the waste material as shown in Figure 5a.

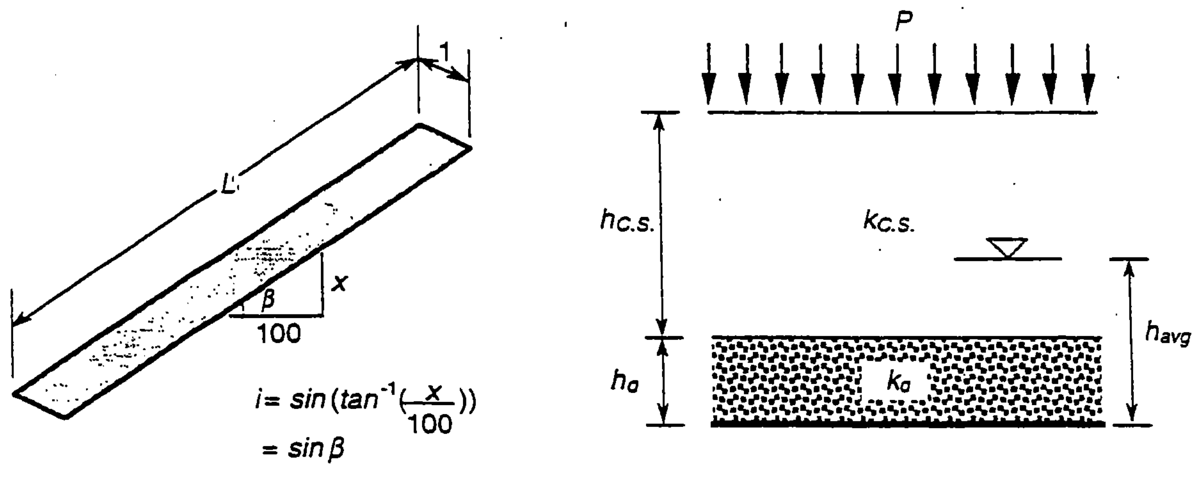

Figure 8 - Typical cover system configuration and dimensions used to calculate parallel submergence ratio

The average head buildup (h_{avg}) above the barrier layer can then be determined as follows:

When $h_{avg} \leq h_d$, i.e., $DLC \geq 1.0$ (and the average phreatic surface level is within the drainage layer).

$$\boxed{h_{avg} = \frac{(FLUX_{reqd} / 3600)}{k_d \times i}} \qquad (24)$$

When $h_{avg} > h_d$, i.e., $DLC < 1.0$ (the average phreatic surface level is within the cover soil layer),.

$$FLUX_{reqd} / 3600 = i \times [\, k_{C.S.} \, (h_{avg} - h_d) + k_d h_d \,] \qquad (25)$$

where $FLUX_{reqd}$ = required flux, m^3/hr

$k_{C.S.}$ = permeability of cover soil, m/sec

k_d = permeability of drainage soil, m/sec

$h_{avg.}$ = average head buildup above the geomembrane, m, and

h_d = thickness of the drainage layer, m.

$$\boxed{h_{avg} = \frac{\left(\dfrac{FLUX_{reqd}}{3600 \times i}\right) - [\, h_d (k_d - k_{C.S.}) \,]}{k_{C.S.}}} \qquad (26)$$

Finally, the parallel submergence ratio, "*PSR*", can be calculated as follows:

$$\boxed{PSR = \frac{h_{avg}}{h_{c.s} + h_d}} \qquad (27)$$

The parallel submergence ratio is then used in the slope stability analysis as the mechanism to incorporate seepage forces into the calculation. Note that the above discussion has been focused on natural drainage materials. However, the procedure is also applicable to geosynthetic drainage composites, providing the thickness and the equivalent permeability of the drainage geocomposite under the site specific normal pressure and hydraulic gradient is known.

5.0 SLOPE STABILITY ANALYSIS INCORPORATING SEEPAGE FORCES

Figure 9 shows the free body diagrams of both the active and passive wedges assuming parallel seepage buildup resulting in a parallel submergence ratio (PSR). As noted previously, it follows the same concept as does horizontal seepage buildup. The symbols used are defined below.

W_A	=	total weight of the active wedge
W_P	=	total weight of the passive wedge
$(Area)'_A$	=	area of the active wedge below the free water surface
$(Area)''_A$	=	area of the active wedge above the free water surface
$(Area)_P$	=	area of the passive wedge
$\gamma_{sat'd}$	=	saturated unit weight of the cover soil
γ_{dry}	=	dry unit weight of the cover soil
γ_W	=	unit weight of water
h	=	thickness of the cover soil
H	=	vertical height of the slope measured from the toe
h_W	=	$(PSR)\ (h)$ = height of the free water surface measured from the geomembrane
PSR	=	parallel submergence ratio
β	=	slope angle
U_h	=	resultant of the pore pressures acting on the interwedge surfaces
U_n	=	resultant of the pore pressures acting perpendicular to the slope
U_v	=	resultant of the vertical pore pressures acting on the passive wedge
N_A	=	effective force normal to the failure plane of the active wedge
N_P	=	effective force normal to the failure plane of the passive wedge
ϕ	=	cover soil friction angle
δ	=	interface friction angle between cover soil and geomembrane
E_A	=	interwedge force acting on the active wedge from the passive wedge
E_P	=	interwedge force acting on the passive wedge from the active wedge

Cover Soil Stability Analysis Worksheet Incorporating Seepage Forces with Parallel-to-Slope Seepage Buildup

Calculation of DLC and PSR

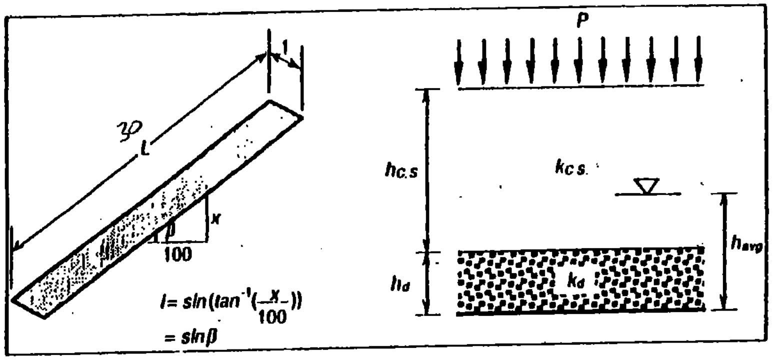

L =	30.0	m
β =	14.0	deg.
h_{cs} =	1000	mm
h_d or t_{ds} =	300.0	mm
k_{cs} =	1.00E-03	cm/s
k_d or k_{ds} =	1.00E-01	cm/s
P =	10.00	mm/hr
RC =	0.4	

I = 0.2419
$L(\cos\beta)$ = 29.11 m
x = 7.26 m
h_{cs} = 1.0 m
h_d or t_{ds} = 0.30 m
$h_{cs} + h_d$ = 1.30 m

k_{cs} = 1.0E-05 m/s
k_d or k_{ds} = 1.0E-03 m/s

$P(RC)$ = 4.0 mm/hr
Actual runoff = 4.00 mm/hr
PERC = 6.00 mm/hr
$FLUX_{reqd}$ = 0.175 m³/hr
$FLUX_{allow}$ = 0.26128 m³/hr

DLC	1.496
PSR	0.154
FS	1.661

* Note: If only one soil layer above GM, treat it as the drainage layer.

DLC = 1.4960

$FLUX_{reqd}$ = 4.85E-05 m³/sec

h_{avg} = 0.20 m

PSR = 0.154

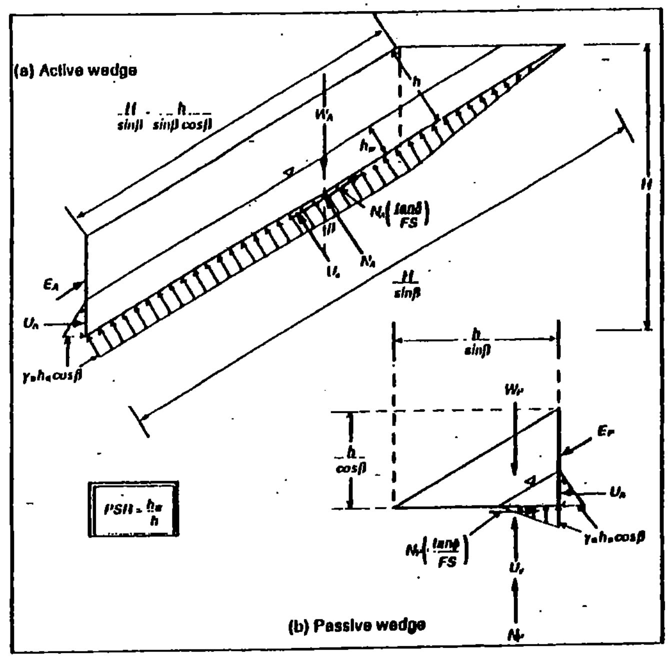

thickness of cover soil = h = 1.30 m
length of slope measured along the geomembrane = L = 30 m
soil slope angle beneath the geomembrane = β = 14.0 deg. = 0.24 (rad.)
vertical height of the slope measured from the toe = H = 7.3 m
parallel submergence ratio = PSR = 0.154
depth of the water surface measured from the geomembrane = h_w = 0.20 m

dry unit weight of the cover soil = γ_{dry} = 18.0 kN/m³
saturated unit weight of the cover soil = γ_{satd} = 21.0 kN/m³
unit weight of water = γ_w = 9.81 kN/m³
friction angle of the cover soil = ϕ = 30.0 ° = 0.52 (rad.)
interface friction angle between cover soil and geomembrane = δ = 22.0 ° = 0.38 (rad.)

Calculation of FS

Active Wedge:

W_A = 655 kN
U_n = 56.45 kN
U_h = 0.1973 kN
N_A = 579.04 kN

Passive Wedge:

W_P = 65.053 kN
U_v = 0.7912 kN

$$FS = \frac{-b \pm \sqrt{b^2 - 4ac}}{2a}$$

where a = 153.8
b = -275.1
c = 32.7

FS = 1.661

Note: numbers in boxes are required input data
numbers in italics are calculated values

Constructed by Te-Yang Soong

Figure 10 - Cover soil stability analysis worksheet incorporating seepage forces with parallel seepage buildup

6.0 BEHAVIOR OF SELECTED CROSS SECTIONS

In this section, several cross sections typical of leachate collection systems and final cover systems will be analyzed. These were the two general categories of the different failures described in Table 1 and illustrated in Figure 2.

6.1 General Slope Configurations and Dimensions

So as to minimize the large number of variables that are possible, the general configuration shown in Figure 11a will be used. It consists of a geomembrane lined slope which is either 30 m long at a 3(H)-to-1(V) slope, or 100 m long at a 4(H)-to-1(V) slope. These are commonly seen geometric choices by designers of both leachate collection systems and final cover soil systems. To keep the number of variables at a minimum, a single type of cover soil is used having the following properties:

γ_{dry} = 18 kN/m^3

$\gamma_{sat'd}$ = 21 kN/m^3

ϕ = 30 deg. (soil-to-soil)

c = 0

δ = 22 deg. (soil-to-geosynthetics)

In order to typify a leachate collection system which will eventually be covered by waste, the drainage soil will be constant in its thickness and uncovered; see Figure 11b. For final cover systems, a drainage layer will be incorporated between the underlying geomembrane and the overlying cover soil. The drainage layer will be considered as being either natural soil (Figure 11c) or a geocomposite drain (Figure 11d). Thus, three separate cases will be analyzed; each having two geometric lengths and slope angles. Note that in all cases the precipitation is calculated on an hourly basis as described in Chapter 3 and uses the assumptions stated therein.

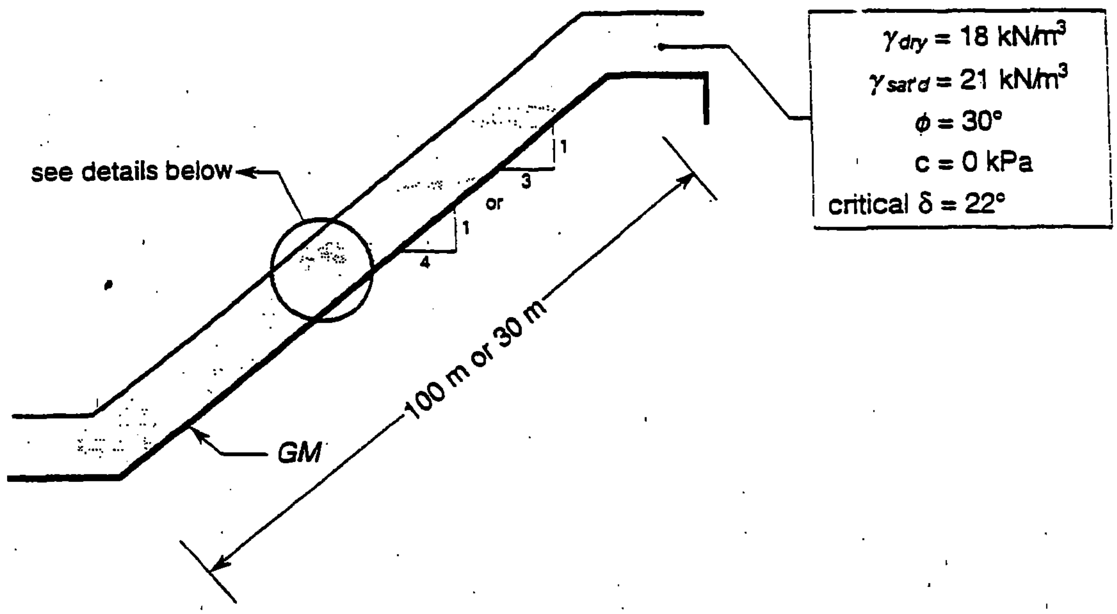

(a) General configuration and dimensions

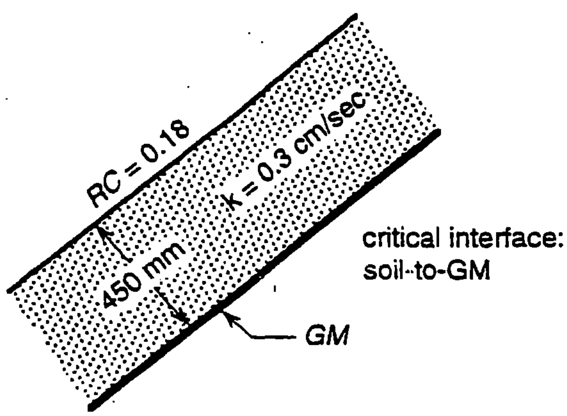

(b) Leachate collection system

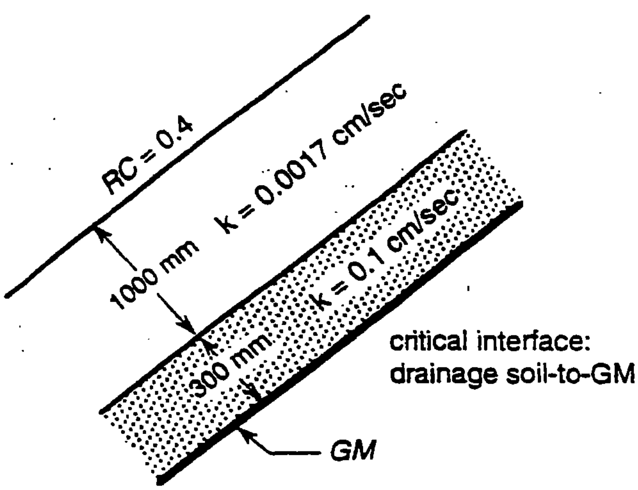

(c) Cover system over drainage soil

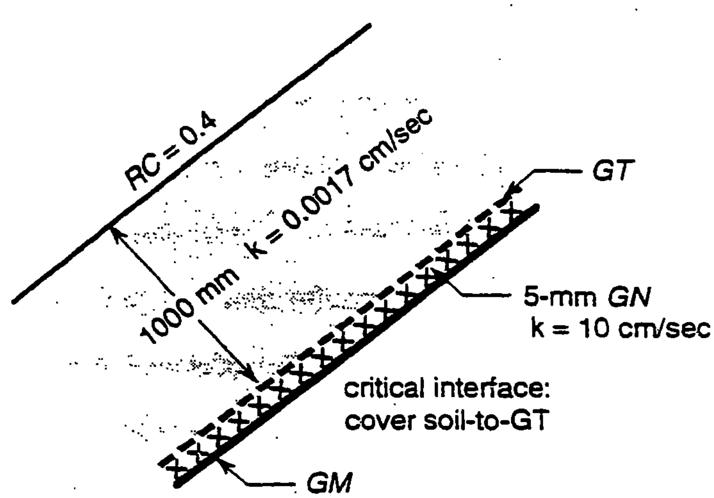

(d) Cover system over geosynthetic drain

Figure 11 - General configuration and specific dimensions of slopes to be analyzed.

6.2 Leachate Collection Systems

Using the general slope configuration shown in Figure 11a, along with the details shown in Figure 11b, an analysis for leachate collection soil stability was undertaken per the concepts developed in Chapters 3, 4 and 5. The homogeneous drainage layer is 450 mm thick and has a permeability of 0.3 cm/sec. This permeability was selected because it is the default value suggested in the HELP manual. A relatively low runoff coefficient of 0.18 is used since the soil is granular (sand or gravel) and will accept a large portion of the precipitation. The stability analysis has been performed for two separate geometric slopes:

- 100 m long slope at 4(H)-to-1(V)
- 30 m long slope at 3(H)-to-1(V)

The precipitation has been systematically varied between 5 mm/hr and 100 mm/hr. The results are presented in Figure 12 for drainage layer capacity (*DLC*), the resulting parallel submergence ratio (*PSR*), and the resulting slope's factor of safety (*FS*) against instability. The following trends can be observed.

- Only for relatively low values of precipitation, e.g., less than 5 mm/hr, is the *DLC* high, giving a low *PSR* and a *FS*-value greater than 1.2 for both slopes evaluated. Note that this relatively low value of factor of safety may be acceptable since the situation is temporary and stability will be established when waste is placed in the landfill.
- For precipitation values between approximately 15 and 65 mm/hr for the two slopes analyzed, the *DLC* drops below 1.0, the PSR is rapidly increasing and the FS-value is less than 1.0.
- The above trends, in *PSR* and *FS* values are very abrupt and they result in a discontinuity in the *PSR* and *FS* response curves when the *DLC* values drop lower than 1.0.

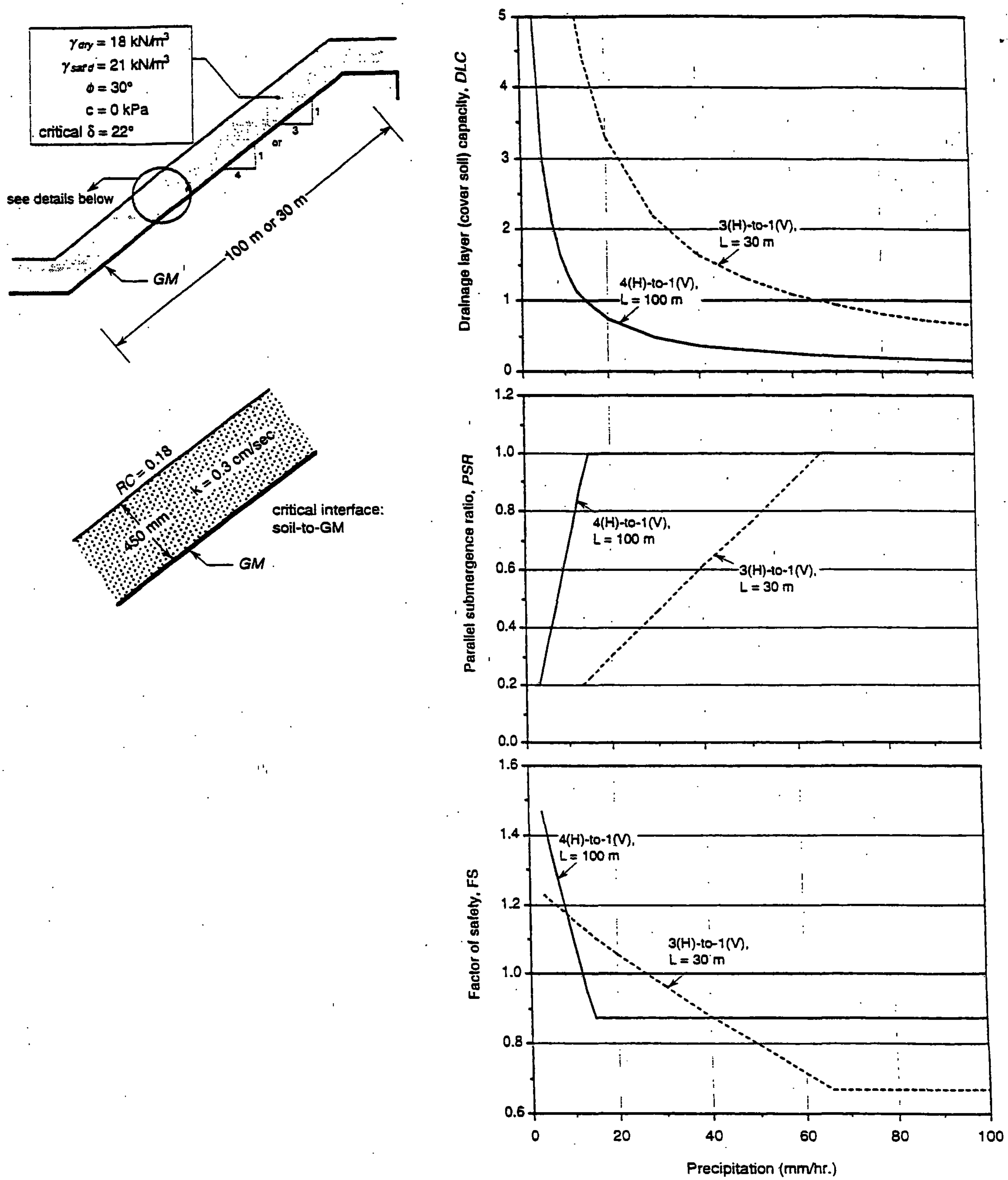

Figure 12 - Results of leachate collection system example problem

- The physical significance of the *DLC* decreasing to a value of 1.0, and continuing to values less than 1.0, is that water has filled the layer and will begin to flow on the surface of the leachate collection layer and add to the naturally occurring runoff.
- For the two geometric cross sections analyzed, the 100 m long 4(H)-to-1(V) slope reaches full drainage capacity sooner than the 30 m long 3(H)-to-1(V) slope, thus the FS-value is less than 1.0 at lower intensity precipitation storms.
- The reason for the above is more related to the length of slope than to its slope angle, since the require flux is cumulative over the length of slope. Long slope lengths will be seen to be very challenging in this regard.

6.3 Final Cover Systems Over Drainage Soils

Using the general slope configuration shown in Figure 11a, along with the details shown in Figure 11c, an analysis for stability was undertaken per the concepts developed in Chapters 3, 4 and 5. The cover soil is 1000 mm thick and has a permeability of 0.0017 cm/sec. This permeability is the default value of "SM" soils (commonly used for cover soils) suggested in the HELP manual. A relatively high runoff coefficient of 0.40 is used since the soil is fine grained and is probably somewhat cohesive. The underlying soil drainage layer is 300 mm thick and has a permeability of 0.1 cm/sec. This value of permeability is 10-times greater than the HELP manual's default value of "SP" soils and is used because the default value of 0.01 cm/sec *always results in FS-values less than 1.0.* The stability analysis has been performed for two separate geometric cases:

- 100 m long slope at 4(H)-to-1(V)
- 30 m long slope at 3(H)-to-1(V)

The precipitation has been systematically varied between 5 mm/hr and 100 mm/hr. The results are presented in Figure 13 for drainage layer capacity (*DLC*), the resulting parallel submergence ratio (*PSR*), and the resulting slope's factor of safety (*FS*) against instability. The following trends can be observed:

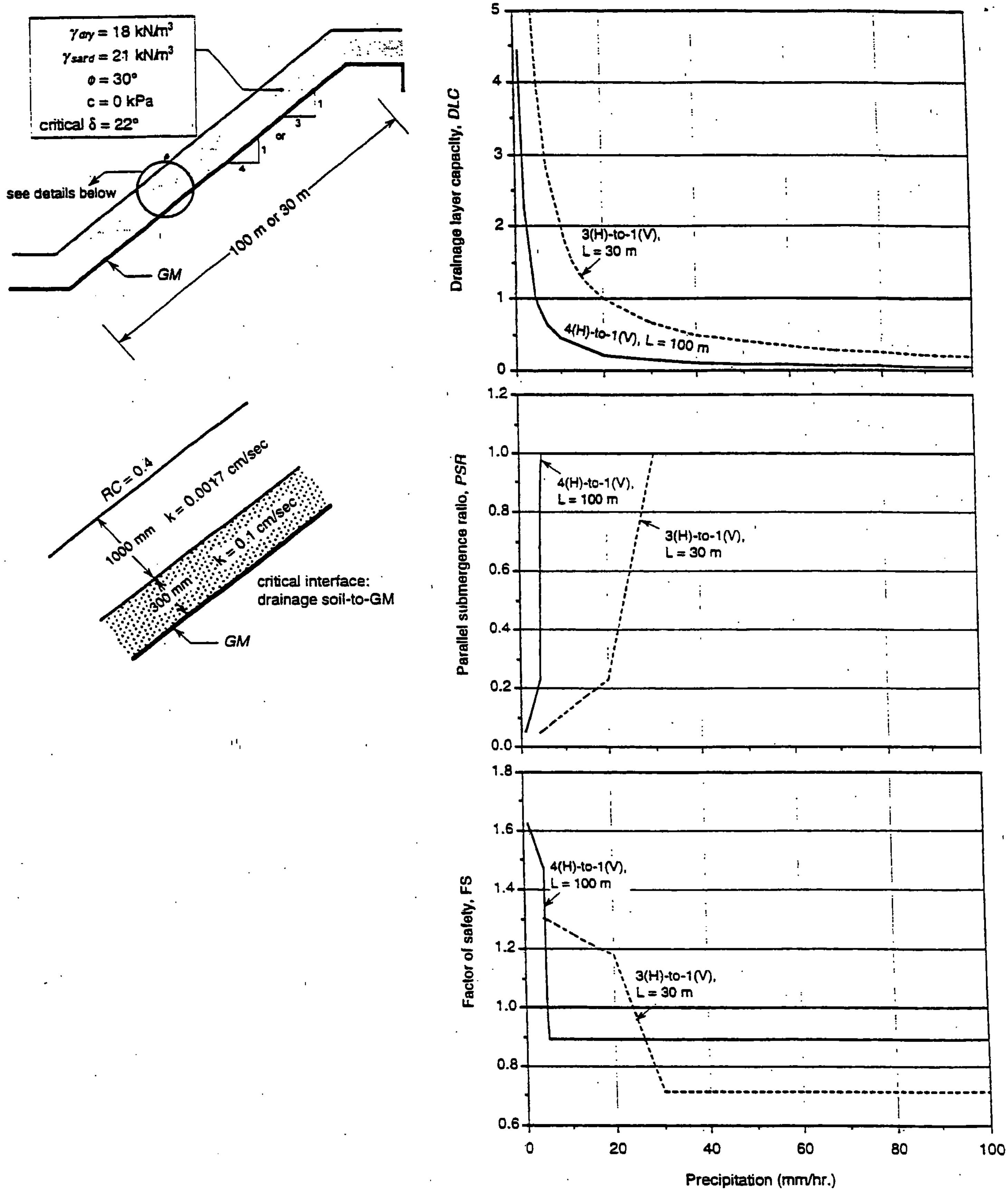

Figure 13 - Results of cover system over drainage soil example problem

- Only for relatively low values of precipitation, i.e., less than 5 mm/hr for the 100 m long 4(H)-to-1(V) slope and less than 20 mm/hr for the 30 m long 3(H)-to-1(V) slope. is the *DLC* high, giving low *PSR* values and *FS* values greater than 1.0.
- Furthermore, a *FS* greater than 1.5, which is recommended for permanent slopes, only occurs for the 100 m long 4(H)-to-1(V) slope at a precipitation value of less than 5 mm/hr.
- Water abruptly fills the drainage layer beyond this precipitation value rapidly decreasing the FS-value to less than 1.0.
- For the 30 m long 3(H)-to-1(V) slope between precipitation values of 5 and 20 mm/hr. the *DLC* falls to a value of 1.0. This increases the *PSR* and decreases the *FS* -value to 1.2. Water has completely filled the drainage layer at this point.
- As precipitation increases beyond 20 mm/hr for the 30 m long 3(H)-to-1(V) slope, the *DLC* becomes less than 1.0, the *PSR* increases rapidly to a value of 1.0 and the *FS*-values becomes less than 1.0.
- The above trends in *PSR* and *FS* values are very abrupt and result in discontinuities in the *PSR* and *FS* response curves when the *DLC* values drop lower than 1.0.
- When the *DLC* is less than 1.0, which occurs for both geometric slopes above 20 mm/hr, the phreatic surface rises above the drainage layer into the cover soil. This is clearly unacceptable insofar as slope stability is concerned. [Had the drainage layer permeability been used as 0.01 cm/sec, which is the U.S. EPA minimum technology guidance value and also the HELP default value, the FS-value would never have been acceptable.]
- For these two geometric considerations, the 100 m long 4(H)-to-1(V) slope is more sensitive to intense rain storms than is the 30 m long 3(H)-to-1(V) slope due to the cumulative nature of required flux value over the longer length of slope.

6.4 Final Cover Systems Over Geosynthetic Drains

Using the general slope configuration shown in Figure 11a, along with the details shown in Figure 11d, an analysis for stability was undertaken per the concepts developed in Chapters 3, 4 and 5. The cover soil is 1000 mm thick and has a permeability of 0.0017 cm/sec. This permeability is the default value suggested in the HELP manual for "SM" soils, which are commonly used for cover soils. A relatively high runoff coefficient of 0.40 is used since the soil is fine grained and probably somewhat cohesive. The underlying geosynthetic drainage layer is 5.0 mm thick and has a permeability of 10 cm/sec. This value is not available as a default value in the HELP manual and must be evaluated for the candidate geosynthetic drainage material as illustrated in Figure 4. The stability analysis has been performed for two separate cases:

- 100 m long slope at 4(H)-to-1(V)
- 30 m long slope at 3(H)-to-1(V)

The precipitation has been systematically varied between 5 mm/hr and 100 mm/hr. The results are presented in Figure 14 for drainage layer capacity (*DLC*), the resulting parallel submergence ratio (*PSR*), and the resulting slope's factor of safety (*FS*) against instability. The following trends can be observed:

- Only for relatively low values of precipitation, i.e., less than 10 mm/hr for the 100 m long 4(H)-to-1(V) slope and 30 mm/hr for the 30 m long 3(H)-to-1(V) slope, is the *DLC* high, giving a near zero *PSR* value and *FS* -values of 1.6 and 1.3, respectively.
- At the above precipitation limits the *PSR* response curves go from near zero to 1.0 very quickly because the geosynthetic drains are quite thin with respect to soil drainage layers and they fill very rapidly.
- At the above precipitation limits, the *FS*-values drop rapidly to values less than 1.0.
- When the *DLC* is less than 1.0, the phreatic surface rises above the geocomposite drainage layer into the cover soil. This is clearly unacceptable insofar as slope stability is concerned.

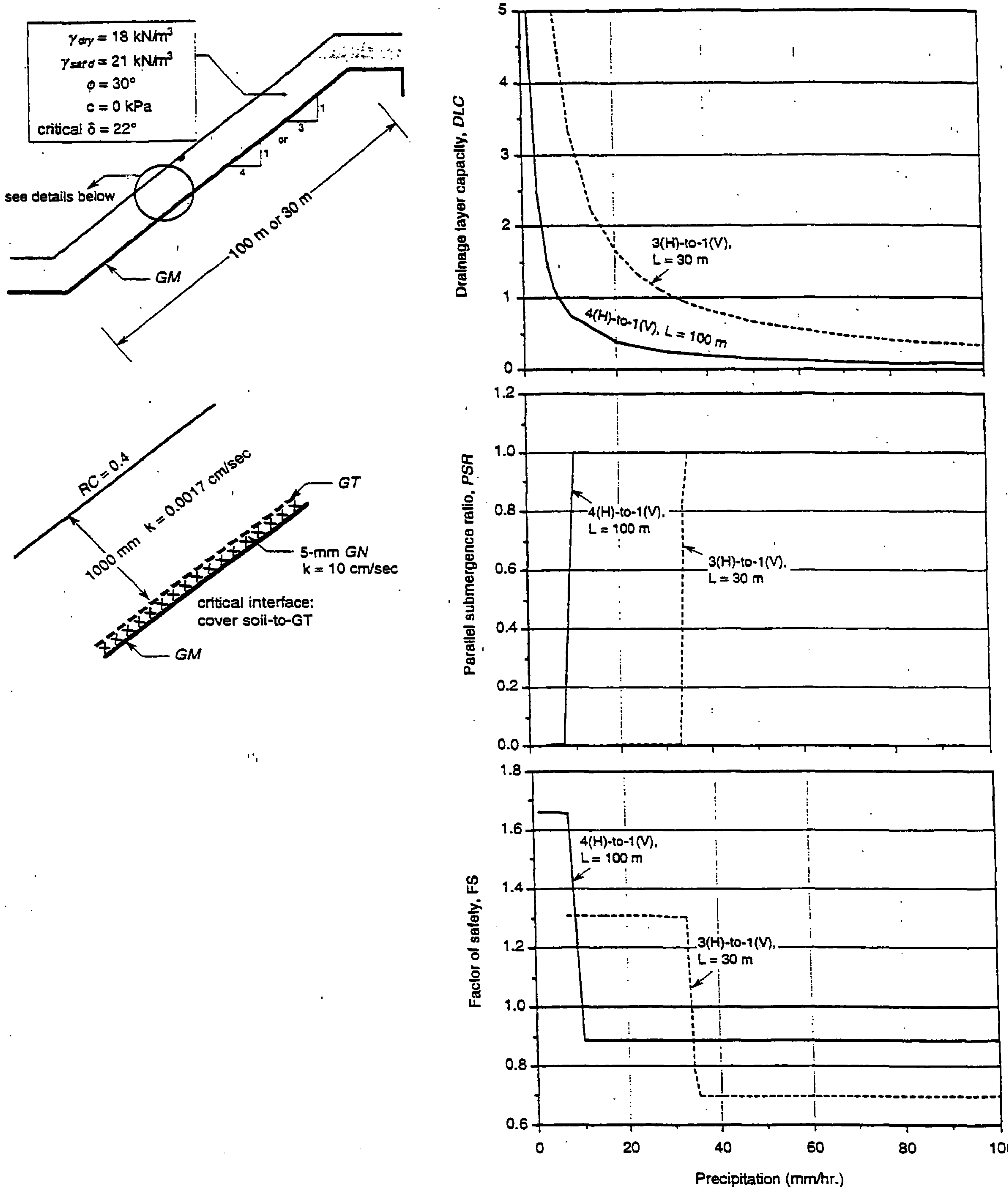

Figure 14 - Results of cover system over geosynthetic drain example problem

- For these two slopes, the 100 m long 4(H)-to-1(V) slope is somewhat more sensitive to intense rain storms than is the 30 m long 3(H)-to-1(V) slope since the required flux is cumulative over the relatively long slope length.

7.0 PARAMETRIC EVALUATIONS

Based on discontinuous trends in drainage layer capacity (*DLC*), parallel submergence ratio (*PSR*) and factor of safety (*FS*) in the previous section for only two slope conditions, it should be obvious that the selection of variables for illustrative purposes is very sensitive and quite subjective. Rather than select specific conditions, it is perhaps instructive to conduct a parametric evaluation on a range of variables. This section presents this type of parametric variation for the three profiles shown in Figures 11b, c and d. It includes variation of precipitation between 5 and 100 mm/hr, as well as variation in other selected variables.

7.1 Leachate Collection Systems

Using the general slope configuration shown in Figure 11a, along with details shown in Figure 11b, a parametric evaluation of leachate collection systems was undertaken per Table 16.

Table 16 - Conditions Evaluated for Leachate Collection Systems

Parameter Evaluated (in addition to precipitation)	Conditions				
	P (mm/hr.)	$k_{d.s.}$ (cm/sec)	$h_{d.s.}$ (mm)	L (m)	β (deg.)
Permeability of drainage soil, $k_{d.s.}$	5-100	**10^{-3}-10^{1}**	1000	100	14.0
Thickness of drainage soil, $h_{d.s}$	5-100	10^{-1}	**300-2000**	100	14.0
Length of slope, *L*	5-100	10^{-1}	1000	**10-300**	14.0
Slope angle, β	5-100	10^{-1}	1000	100	**2.9-40.0**

Values held constant for all iterations are as follows:

γ_{dry} = 18 kN/m³

$\gamma_{sat'd}$ = 21 kN/m³

ϕ = 30 deg. (soil-to-soil)

δ = 22 deg. (soil-to-geomembrane)

RC = 0.18

The response for the first variation in permeability of leachate collection soil between 0.001 and 10 cm/sec is given in Figure 15. The results are striking.

- With a permeability of leachate collection drainage soil equal, or less, than 0.05 cm/sec, the FS-values for all precipitation values, even as low as 5 mm/hr, are always less than one, signifying instability.
- Paradoxically, a permeability of 0.01 cm/sec drainage soil is the value noted in U.S. EPA regulations as being minimum technology guidance. As expected, this value is used widely. Here it is seen that such low permeability drainage soil will always lead to seepage induced slope instability under the conditions assumed herein.
- Depending on the precipitation intensity, *FS*-values of 1.5 require drainage soil *k*-values of 0.3 to 6.0 cm/sec.
- Referring back to Table 3, this value of permeability can only be achieved using "GP" or "GW" gravels, and possibly "SP" sand. However, the poorly graded gravels and sands are often unstable, leaving only well graded gravel as being the candidate material for leachate collection layers of the type being analyzed.
- The above gravel is typical of AASHTO #1, #3 or #5. In general, AASHTO #57 must be screened of its fines to meet such a permeability requirement.
- Of course, with such coarse sized gravel the underlying geomembrane must be protected using a thick needle punched nonwoven geotextile, or equivalent, see Koerner, et al. (1996).
- Furthermore, the issue of placing waste directly on the surface of the gravel versus using a geotextile filter, must be carefully considered, see Koerner, G. R. et al. (1993).

The second variation in the leachate collection system profile varied the thickness of the drainage layer between 300 and 2000 mm. The response curves are given in Figure 16. At a constant drainage layer permeability value of 0.1 cm/sec, essentially all of the resulting *FS*-values are less than 1.5. It should be noted that the minimum technology guidance of the U.S.

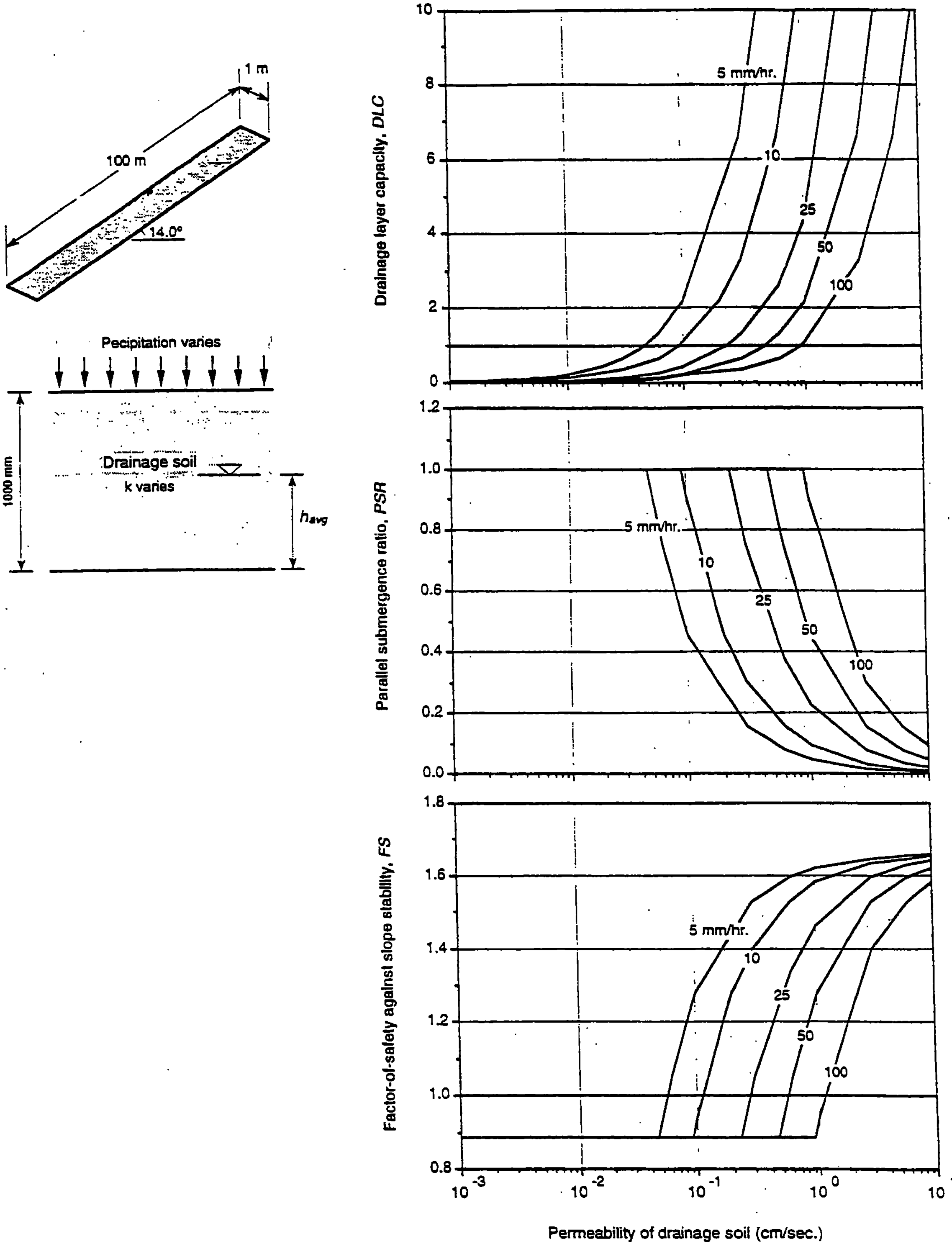

Figure 15 - Parametric study of leachate collection system: permeability variation

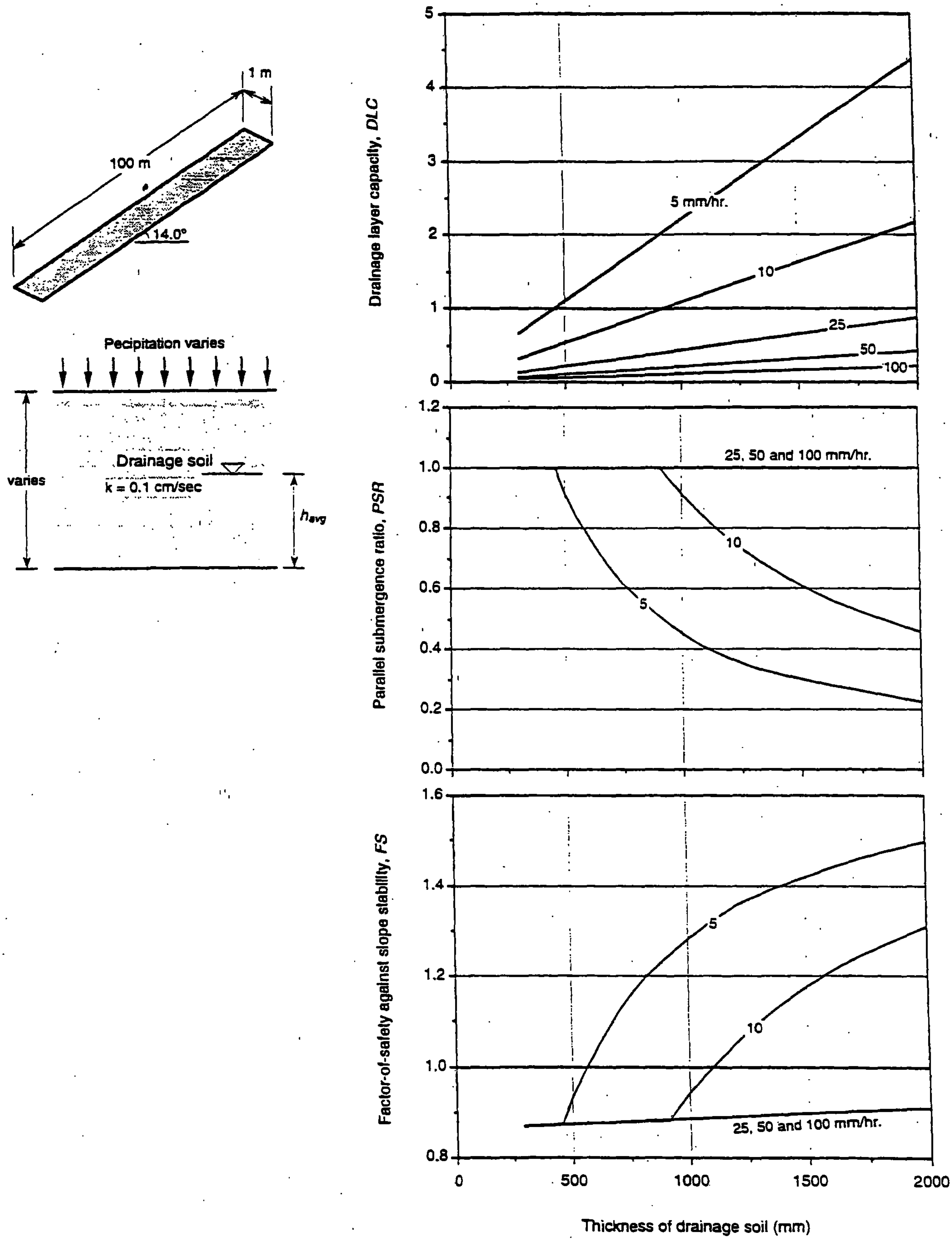

Figure 16 - Parametric study of leachate collection system: thickness variation

EPA regulations is an order of magnitude lower, i.e., 0.01 cm/sec, which (if analyzed) would produce proportionally even lower *FS*-values.

The third variation in the leachate collection system profile varied the slope length between 10 and 300 m. The response curves are given in Figure 17. With a constant drainage layer permeability value of 0.1 cm/sec, the *FS*-values are only acceptable for slope lengths between 10 and 50 m, for precipitation values between 100 and 5 mm/hr, respectively. In such cases, the storm intensity is a significant factor and therefore, careful selection of the design storm is necessary.

As discussed a number of times in Section 6.0 for the two example slopes of 30 m and 100m lengths, the longer slopes with cumulatively increasing required flux values are generally troublesome. If long slope lengths are necessary, it is suggested that they be segmented by berms and that the drainage be removed at each berm level. An illustration will be given later.

The fourth variation in the leachate collection system profile varied the slope angle between 2.9 and 40 deg. The response curves are given in Figure 18. With a constant permeability 0.1 cm/sec, it is seen that only relatively flat slopes are stable, e.g., less than approximately 10 deg. which is approximately 5(H)-to-1(V). The storm intensity is only nominally a factor, the major constituent being the permeability of the drainage layer as noted earlier in this section.

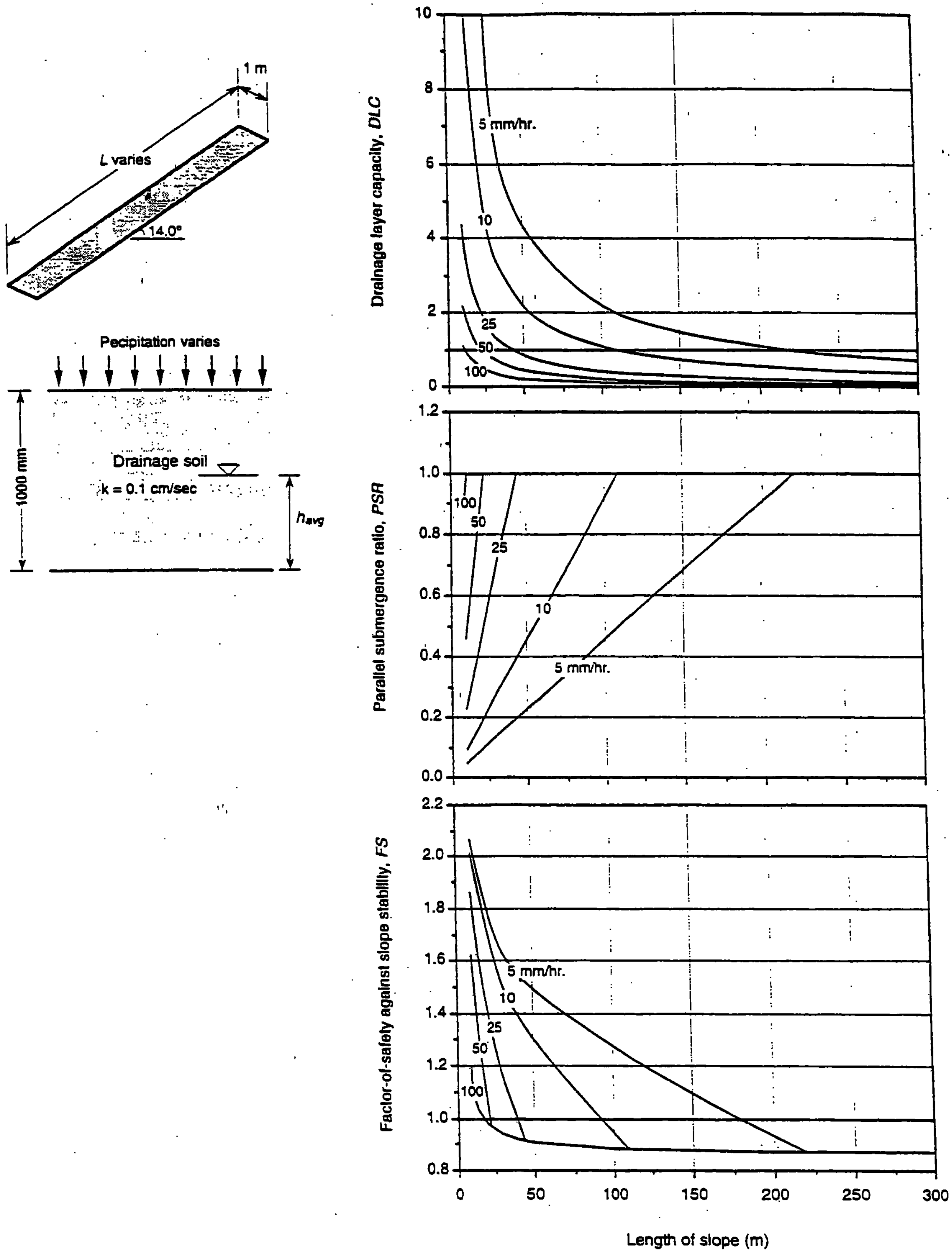

Figure 17 - Parametric study of leachate collection system: slope length variation

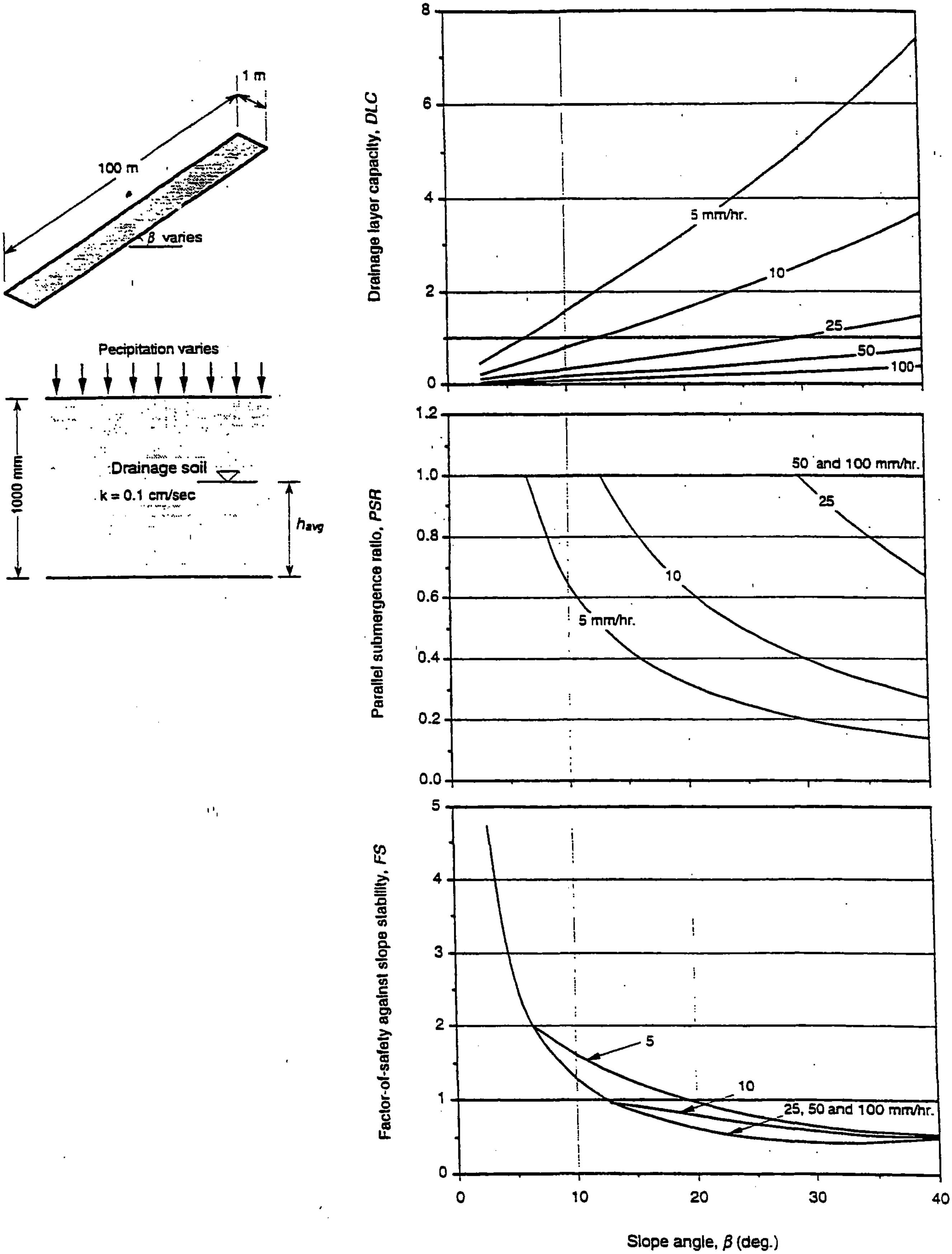

Figure 18 - Parametric study of leachate collection system: slope angle variation

7.2 Final Cover Systems Over Drainage Soils

Using the general slope configuration shown in Figure 11a, along with details shown in Figure 11c, a parametric evaluation of cover systems over drainage soils was undertaken per Table 17.

Table 17 - Conditions Evaluated for Cover Systems Over Drainage Soils

Parameter Evaluated (in addition to precipitation)	Conditions				
	P (mm/hr.)	$k_{d.s.}$ (cm/sec)	$k_{c.s}$ (cm/sec)	L (m)	β (deg.)
Permeability of drainage soil, $k_{d.s.}$	5-100	**10^{-2}-10^{1}**	10^{-3}	100	14.0
Permeability of cover soil, $k_{c.s.}$	5-100	10^{-1}	**10^{-5}-10^{-1}**	100	14.0
Length of slope, *L*	5-100	10^{-1}	10^{-3}	**10-300**	14.0
Slope angle, β	5-100	10^{-1}	10^{-3}	100	**2.9-40.0**

Values held constant for all iterations are as follows:

γ_{dry} = 18 kN/m^3

$\gamma_{sat'd}$ = 21 kN/m^3

ϕ = 30 deg. (soil-to-soil)

δ = 22 deg. (soil-to-geomembrane)

RC = 0.4

$t_{cover\ soil}$ = 1000 mm

$t_{drainage\ soil}$ = 300 mm

The response for the first variation of drainage soil permeability between 0.01 and 10 cm/sec is given in Figure 19. As with the leachate collection system described in section 7.1, the results are striking.

- Drainage soil permeabilities less than 0.1 cm/sec result in *DLC*-values less than 1.0 (i.e., the drainage layer is at full capacity), producing *PSR*-values equal to 1.0 and the *FS*-values are always less than 1.0.

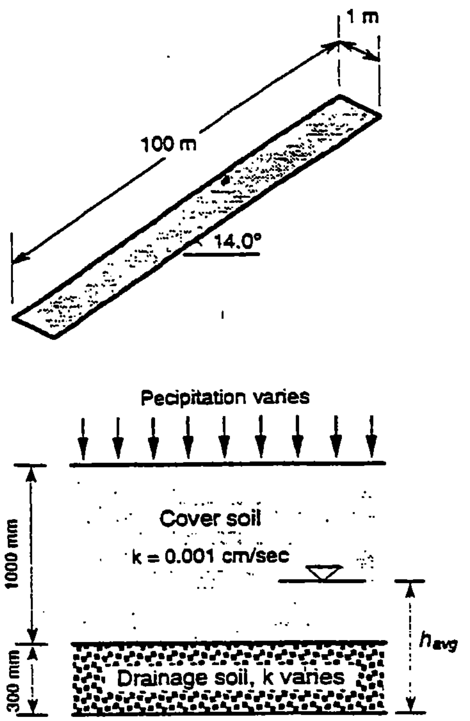

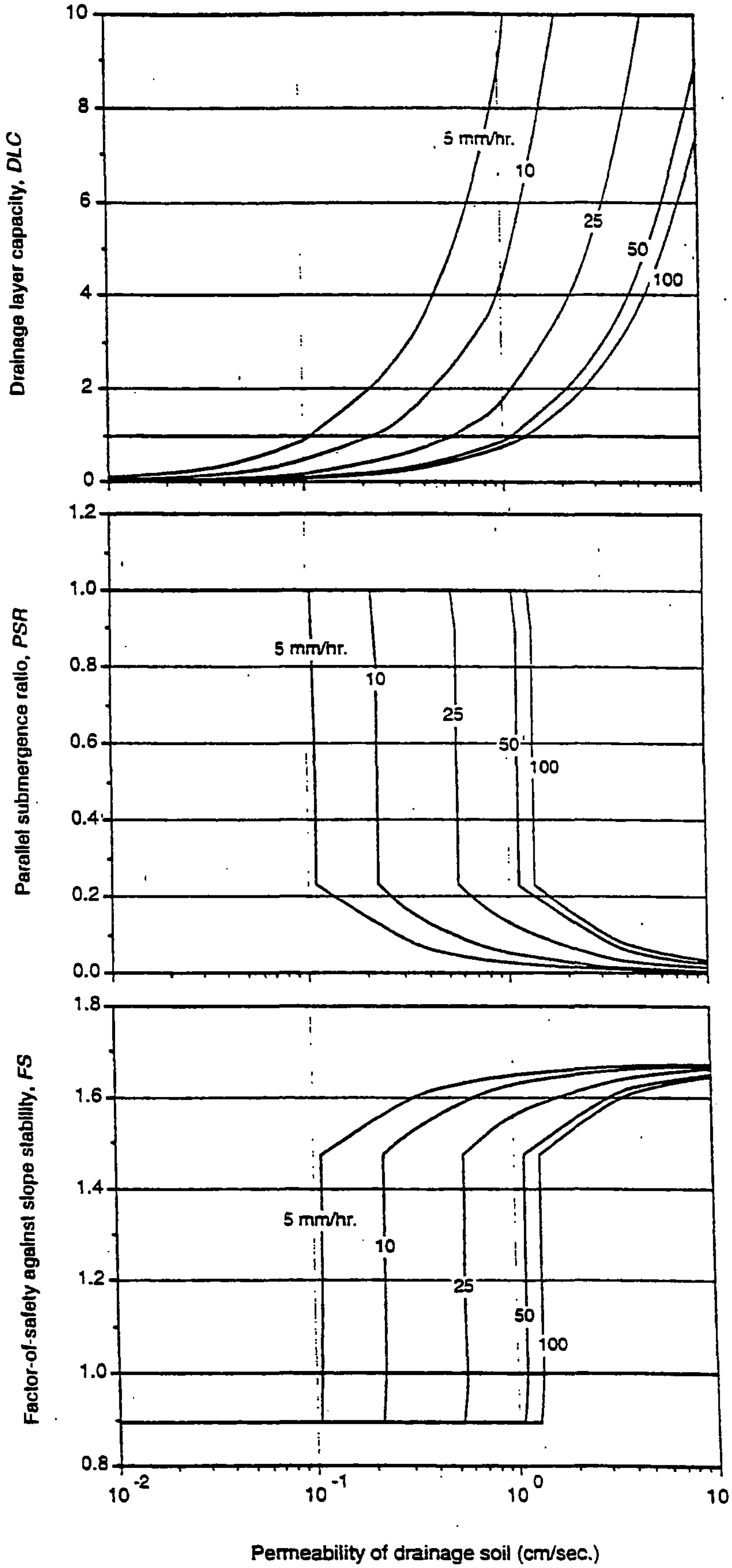

Figure 19 - Parametric study of cover system over drainage soil: permeability (drainage soil) variation

- The FS-values are less than 1.0 even for the 5 mm/hr precipitation, which is the lowest value analyzed.
- As precipitation increases, the permeability of the drainage layer must also increase for suitable FS-values. For example, for a factor of safety of 1.5:
  - A 5 mm/hr precipitation storm requires $k \geq 0.12$ cm/sec
  - A 10 mm/hr precipitation storm requires $k \geq 0.22$ cm/sec
  - A 25 mm/hr precipitation storm requires $k \geq 0.55$ cm/sec
  - A 50 mm/hr precipitation storm requires $k \geq 1.3$ cm/sec
  - A 100 mm/hr precipitation storm requires $k \geq 1.5$ cm/sec
- The implication of the above is that coarse sand or gravel must be used as discussed in section 7.1.
- Alternatively, the permeability of the cover soil could be reduced thereby allowing less percolation through this layer. (This alternative is treated in the next section.) Of course, this strategy will add to the runoff value and potentially create erosion of the cover soil, but this issue not treated in this report.

The second variation in the cover soil over drainage soil profile varied the permeability of the cover soil between 10^{-5} and 10^{-1} cm/sec. The response curves are given in Figure 20. The curves are somewhat challenging to interpret.

At cover soil permeability values less than 7×10^{-5} cm/sec, the FS-values can be quite reasonable. This permeability is sufficiently low that the underlying drainage layer ($k = 0.1$ cm/sec) can handle the relatively low percolation and its subsequent flux requirement. Similarly, at very high cover soil permeability values of greater than 0.05 cm/sec, the FS-values can also be acceptable but only for light precipitation, i.e., less than 5 mm/hr. In this case there is drainage within the cover soil which adds to the capability of the drainage layer. When the permeability of cover soil increases to 0.1 cm/sec, the entire profile becomes a homogeneous drainage layer. For cover soil permeability ranges between 7×10^{-5} and 5×10^{-2} cm/sec, however, unacceptable FS-values result under all precipitation conditions. Unfortunately, this is a very common

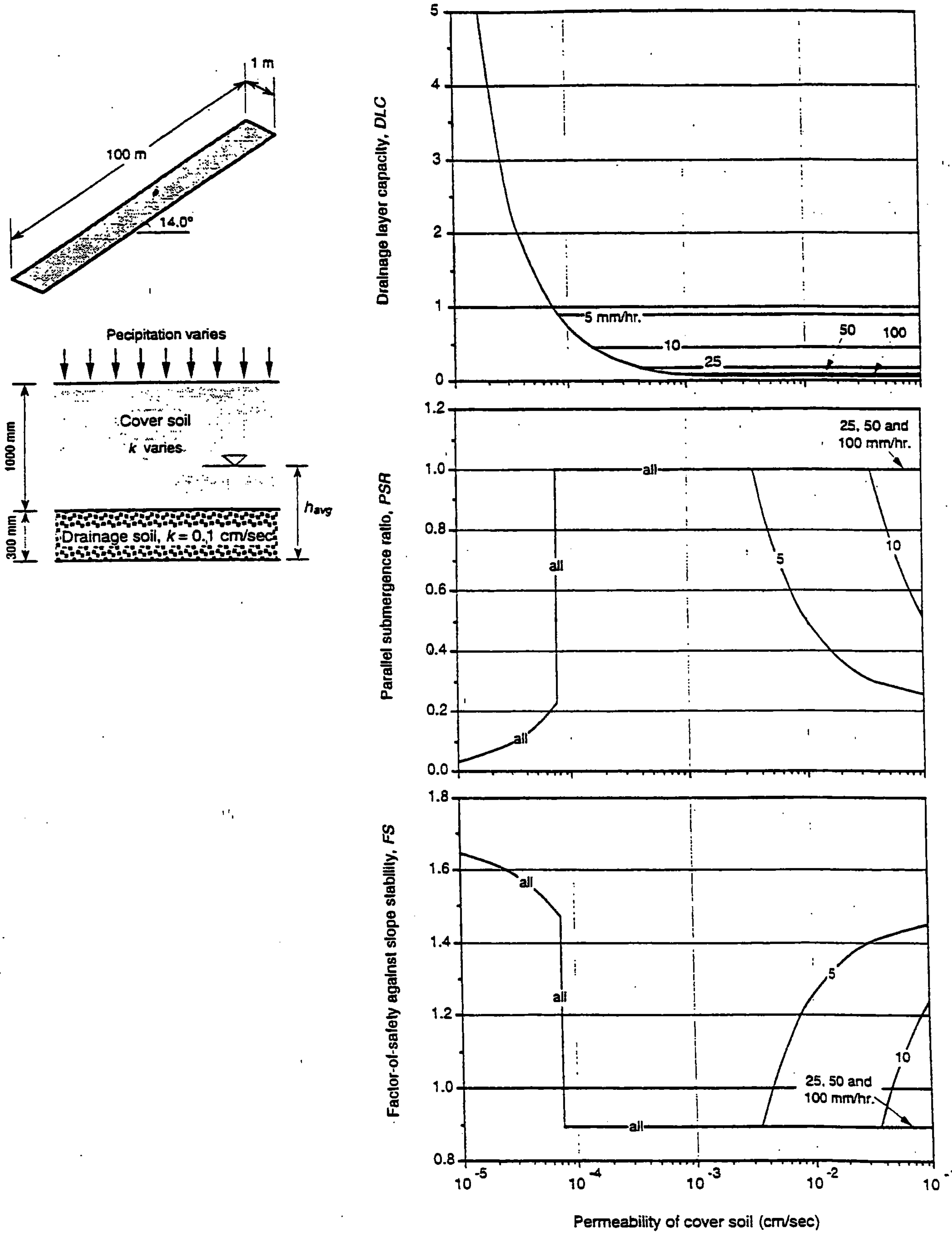

Figure 20 - Parametric study of cover system over drainage soil: permeability (cover soil) variation

permeability range for cover soil materials which are usually on-site borrow soils. If only such cover soils were available, the design strategy would be to increase the drainage layer capacity or shorten the slope length with benches.

The third variation in the cover soil drainage soil profile varied the length of slope from 10 to 300 m. The response curves are given in Figure 21. Here it is seen that slope lengths of less than 80 m can be acceptable depending on the magnitude of precipitation. The higher the precipitation, the shorter the slope must be in order to result in an acceptable *FS*-value, for example:

- For 5 mm/hr precipitation, the slope can be up to 80 m in length.
- For 10 mm/hr precipitation, the slope can be up to 45 m in length.
- For 25 mm/hr precipitation, the slope can be up to 20 m in length.
- For greater than 25 mm/hr precipitation, the slope must be less than 20 m in length.

The fourth variation in the cover soil over drainage soil profile varied the slope angle from 2.9 to 40 degrees. The response curves are given in Figure 22. Note that the *FS*-values are unacceptable for all cases except very shallow slope angles, e.g., less than 10 degrees (i.e., less than 5(H)-to-1(V)). The reason for this response is (a) the poorly selected permeability value of cover soil (held constant at 0.001 cm/sec) which is in the unacceptable mid-range in Figure 20, and (b) the unacceptably low value of drainage soil permeability (held constant at 0.1 cm/sec), recall Figure 19.

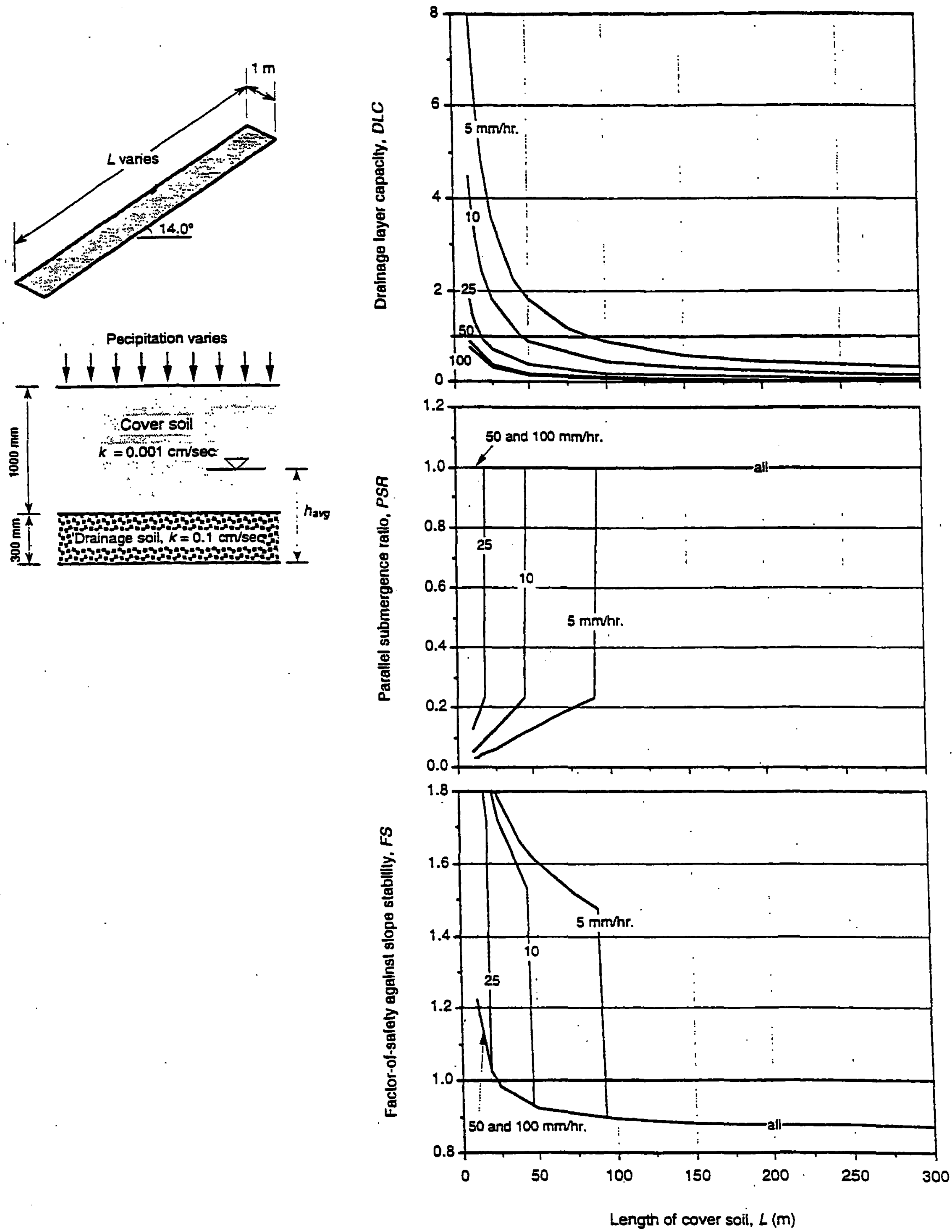

Figure 21 - Parametric study of cover system over drainage soil: slope length variation

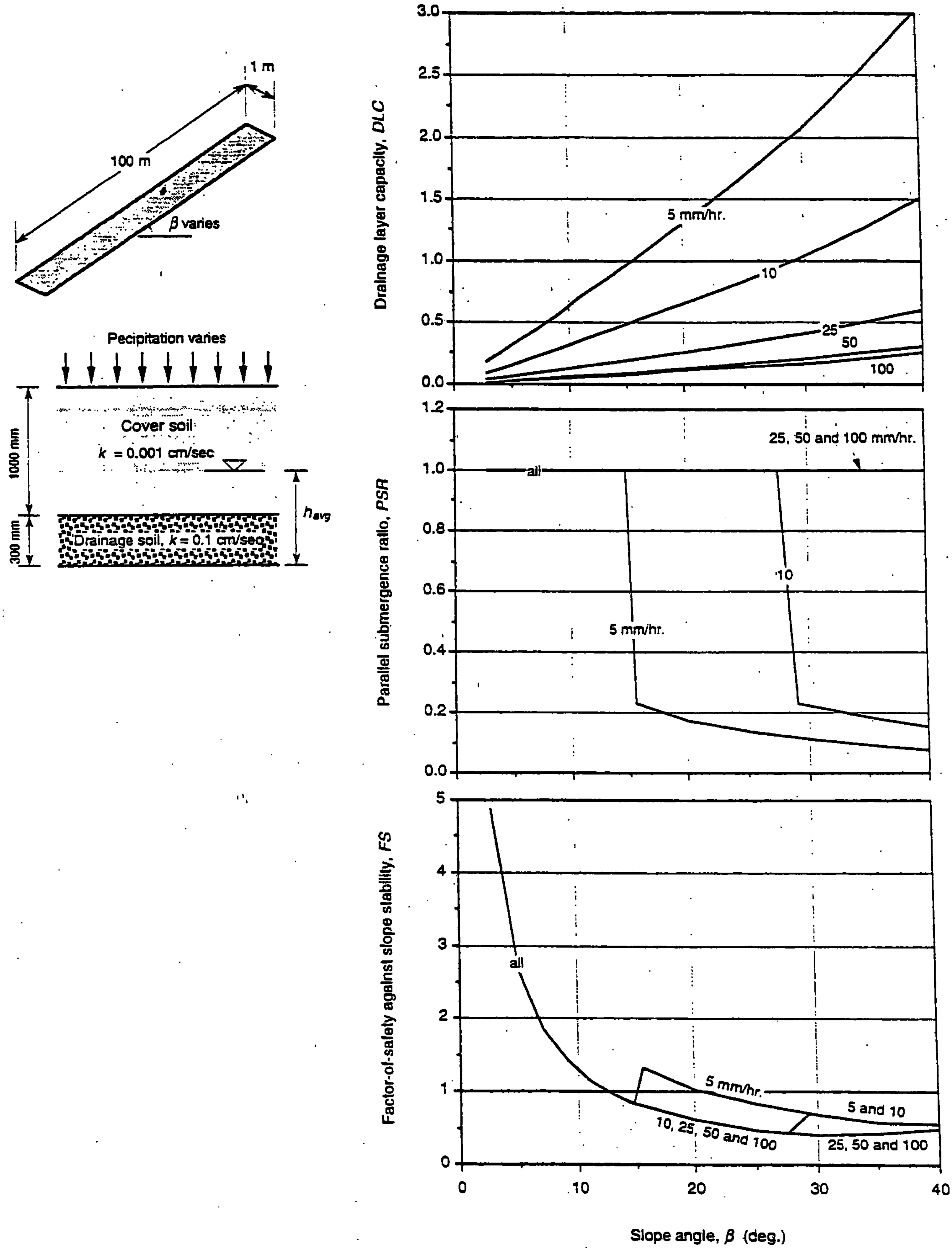

Figure 22 - Parametric study of cover system over drainage soil: slope angle variation

7.3 Final Cover Systems Over Geosynthetic Drains

Using the slope configuration shown in Figure 11a, along with details shown in Figure 11d, a parametric evaluation of cover systems over geosynthetic drains was undertaken per Table 18.

Table 18 - Conditions Evaluated for Cover Soil Systems Over Geosynthetic Drains

Parameter Evaluated (in addition to precipitation)	Conditions						
	P (mm/hr.)	k_{GS} (cm/sec)	$k_{c.s}$ (cm/sec)	L (m)	β (deg)	$h_{c.s}$ (mm)	t_{GS} (mm)
Rainfall intensity, P	1-100	0.6^{GS1}	10^{-3}	100	14.0	1000	5.5^{GS1}
Permeability of cover soil, $k_{c.s.}$	60	10^{GS2}	**10^{-5}-10^{-1}**	100	14.0	1000	5.5^{GS2}
Length of slope, *L*	60	12^{GS3}	10^{-3}	**10-300**	14.0	1000	14.0^{GS3}
Slope angle, β	60		10^{-3}	100	**2.9-40.0**	1000	

Values held constant for all iterations are as follows:

γ_{dry} = 18 kN/m^3

$\gamma_{sat'd}$ = 21 kN/m^3

ϕ = 30 deg. (soil-to-soil)

δ = 22 deg. (soil-to-geocomposite)

RC = 0.4

$t_{cover\ soil}$ = 1000 mm

$k_{cover\ soil}$ = 0.001 cm/sec

GS1 = GT/GN/GT composite*

GS2 = plate/GN/plate*

GS3 = sheet drain geocomposite*

*All geosynthetic drains were evaluated at 25 kPa normal stress and reduced by a cumulative reduction factor of 5.0.

The response for the first variation of precipitation intensity between 1 and 100 mm/hr is given in Figure 23. The response shows that only storm events of less than approximately 30 mm/hr can be handled by the *GS3* drain and approximately 8 mm/hr for the *GS2* drain. The *GS1* drain is unacceptable under all conditions.

The second variation in the cover soil over geosynthetic drain profile varied the permeability of the cover soil from 10^{-5} to 10^{-1} cm/sec. The rainfall intensity was held constant at 60 mm/hr. The response curves are given in Figure 24. Here it is seen that both *GS2* and *GS3* geocomposite drains result in acceptable *FS*-values when the permeability of the cover soil is less than 1.5×10^{-4} cm/sec and 4.5×10^{-4} cm/sec, respectively. At these relatively low values of cover soil permeability the percolation values are sufficiently low that the required flux can be handled. The *GS1* geocomposite is not acceptable at any cover soil permeability value.

The third variation in the cover soil over geosynthetic drain profile varied the length of slope from 10 to 300 m. The rainfall intensity was held constant at 60 mm/hr. The response curves are given in Figure 25. The cover soil permeability was held constant at 0.001 cm/sec. The curves indicate that the *FS*-values are only acceptable for the *GS2* and *GS3* geocomposites at slope lengths of 15 m and 40 m, respectively. Again, the *GS1* drain is never acceptable under these conditions.

The fourth variation in the cover soil over geosynthetic drain profile varied the slope angle between 2.9 and 40 degrees. The rainfall intensity was held constant at 60 mm/hr. The response curves are given in Figure 26. Again, the cover soil permeability was held at 0.001 cm/sec. The resulting *FS*-values are only acceptable at relative shallow slope angles, e.g., less than 9 deg., i.e., approximately 5(H)-to-1(V). All three geosynthetic drains give similar response up to this slope angle. The behavior is dominated by the slope angle, but steeper slopes could be accommodated by cover soil permeability values lower than 0.001 cm/sec (allowing for less percolation) or higher capacity geosynthetic drains (allowing for greater flux capacity).

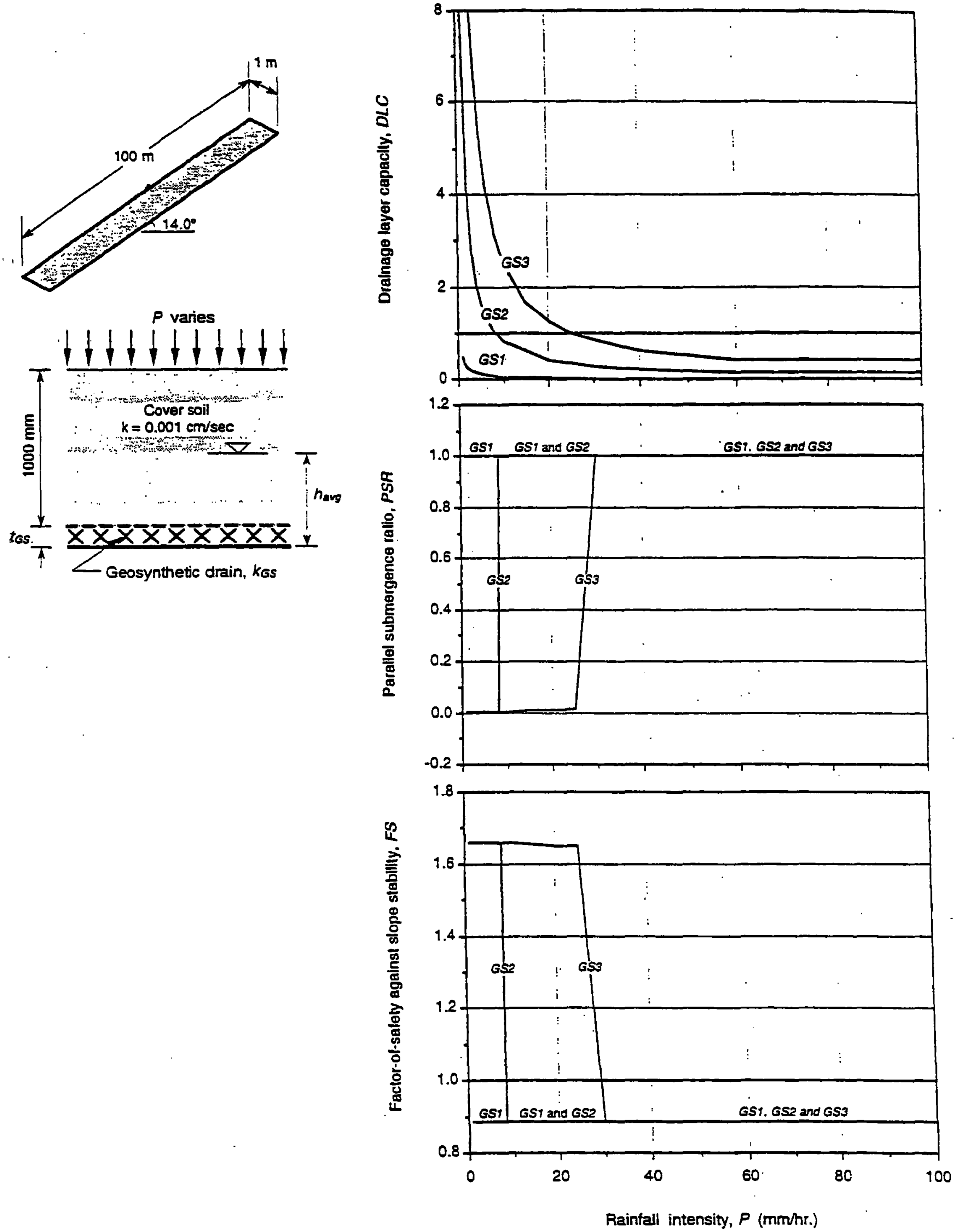

Figure 23 - Parametric study of cover system over geosynthetic drain: rainfall intensity variation

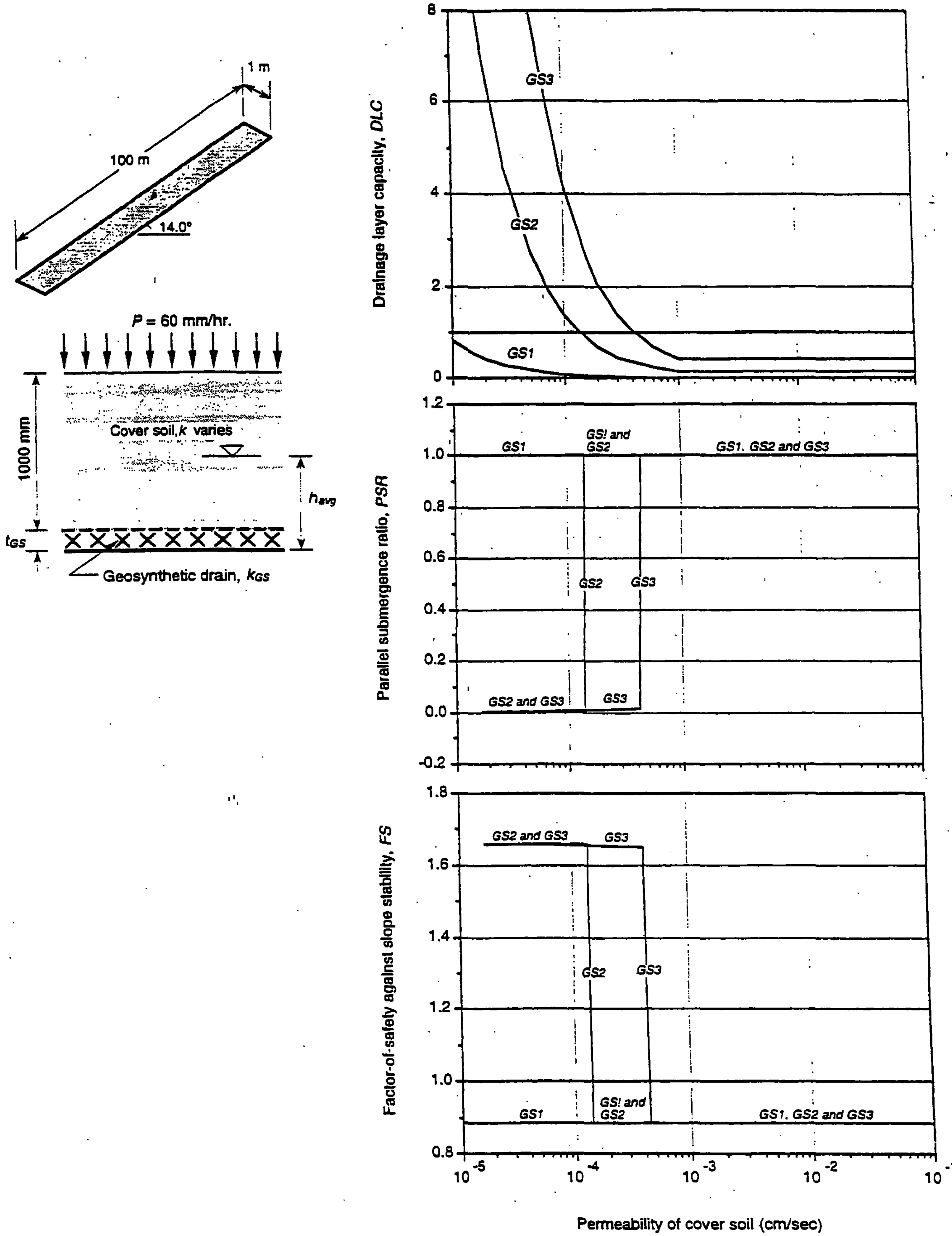

Figure 24 - Parametric study of cover system over geosynthetic drain: permeability (cover soil) variation

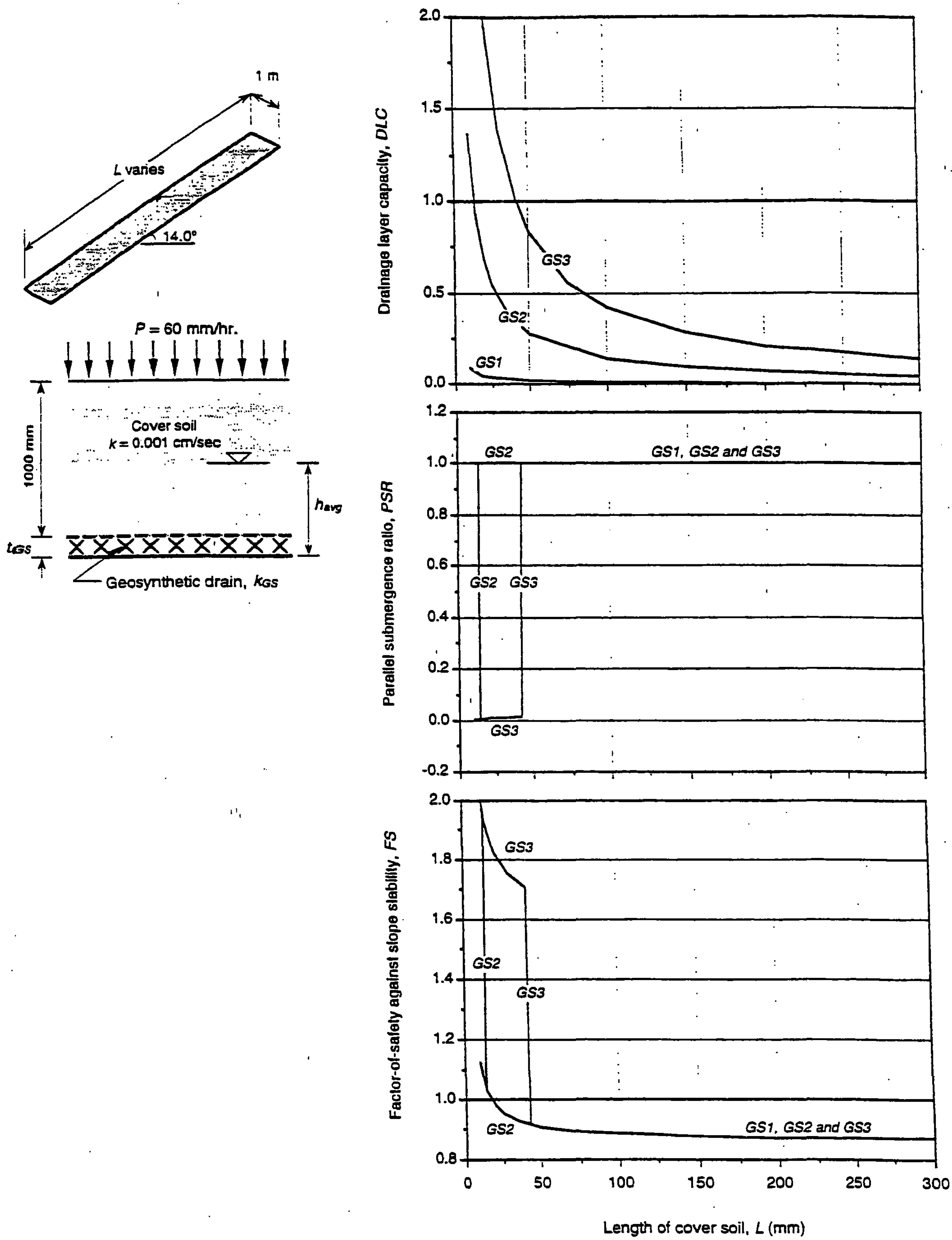

Figure 25 - Parametric study of cover system over geosynthetic drain: slope length variation

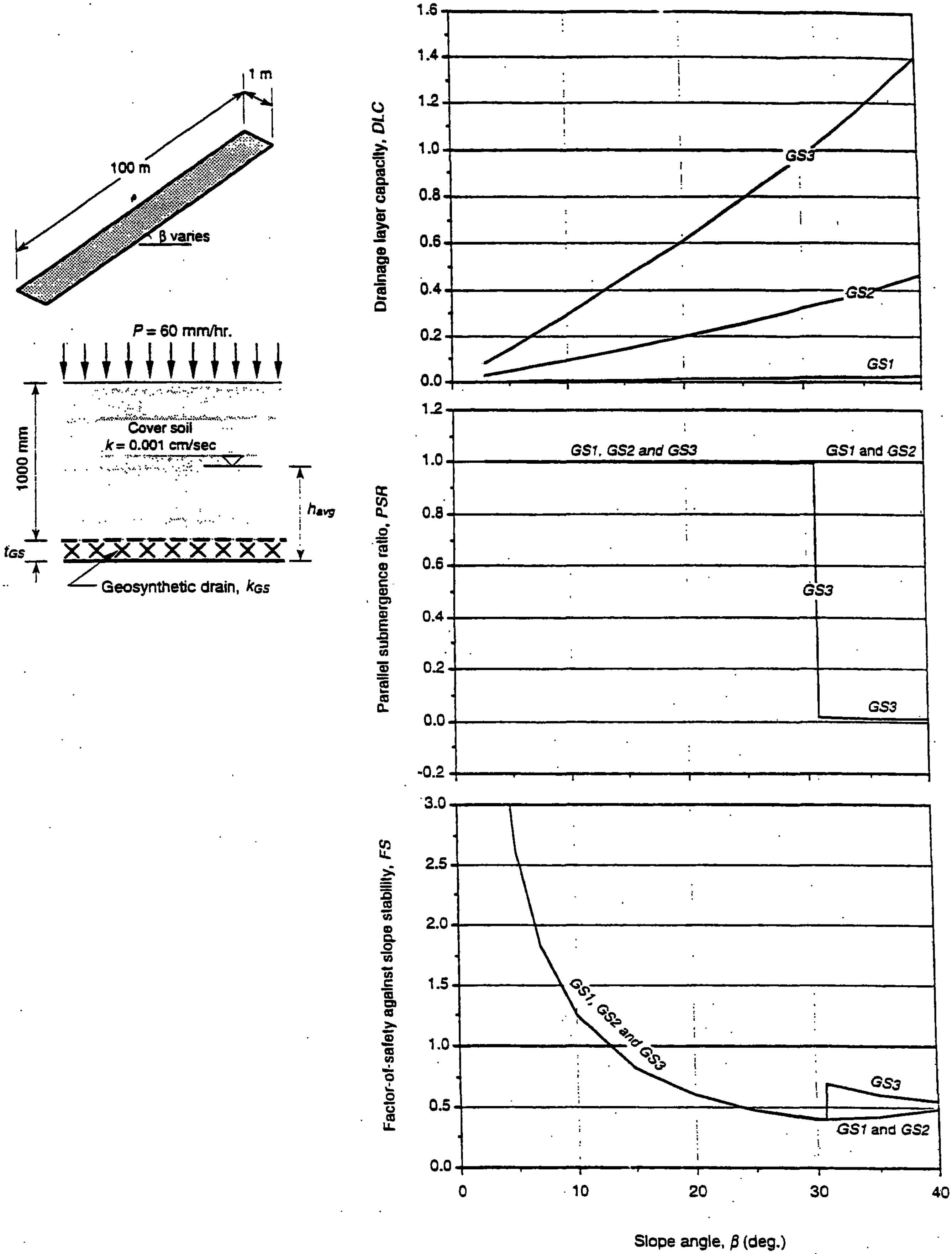

Figure 26 - Parametric study of cover system over geosynthetic drain: slope angle variation

8.0 SUMMARY

Presented in section 2.1 was information on the recent occurrence of four seepage induced slides of leachate collection systems and an additional four seepage induced slides of final cover systems. All occurred during, or immediately after, relatively large storm events (the one exception was by rapid thawing of frozen drainage soil above a still-frozen outlet drain at the toe of the slope). While the exact nature of these storm events are unknown, an idea of their magnitude can be gained by back calculating the various situations. Knowing the dimensions of the slopes and an approximation of the permeability of the soil(s) involved, the design methodology used herein (using an incipient failure FS-value of 1.0) has been followed resulting in the data of Table 19. Here it is seen that the precipitation values for the leachate collection systems was probably quite high, i.e., up to 44 mm/hour. Conversely, precipitation values for the final cover systems were apparently quite low, i.e., between 0.38 and 1.34 mm/hour. The latter are far from extraordinary events and the very low values of drainage soil permeability played strongly into the cause of the instability.

Table 19 - Back Calculated Precipitation Rates to Achieve Slope Instability for the Case Histories Presented in Table 1.

No.	Assumed permeability of cover soil, $k_{c.s.}$ (cm/sec)	Assumed permeability of drainage soil, k_d (cm/sec)	Precipitation at incipient sliding (i.e., FS = 1.0), $P_{critical}$ (mm/hr)
(a) Slides of leachate collection layers before waste placement			
1	none	0.25	14
2	none	0.50	44
3	none	0.05	1.0
4	none	0.25	35
(b) Slides of final cover/drainage layers after waste placement			
5	0.01	0.01	0.42
6	0.0001	0.01	1.20
7	0.0001	0.01	1.34
8	0.0001	0.01	0.38

Note: Values are calculated based on the following assumed constants:

Dry unit weight of soils, γ_{dry} = 18.0 kN/m^3
Saturated unit weight of soils, $\gamma_{sat'd}$ = 21.0 kN/m^3
Friction angle of soils, ϕ = 30 deg.
Critical interface friction angle, δ = 22 deg.
Runoff coefficient, RC = 0.18 for Type (a) slides and 0.40 for Type (b) slides

To the writers, the occurrence of such a large number of recent slides is an unacceptable situation. It appears that seepage forces are being considerably underestimated by the design community in view of the very low permeability drainage soils used in "conventional" design. Both required flux quantities (lateral flow rates) and drainage system capacities are involved.

8.1 Water Balance Analysis Critique

The occurrence of eight seepage induced cover soil slides (there are probably others not known to the writers) lead directly toward mounting a challenge to the manner in which required drainage quantities are calculated. Agreed upon is the necessity of using a water balance analysis to obtain a required value of percolation through the cover soil and into the drainage layer. This value of percolation over an unit area, is then used to calculate a flux-value (lateral flow rate) which accumulates within the drainage layer reaching a maximum value at the toe of the slope. The maximum flux-value is the required value to use in designing the drainage layer capacity. Not agreed upon is the customary manner of obtaining the percolation-value, hence the required flux is effected accordingly. Typically used in this regard is the computer program entitled Hydrologic Evaluation of Landfill Performance (*HELP*).

It is felt that HELP model is an excellent program for its originally intended use; namely, to estimate the leachate quantities at the base of a landfill. The gravitational flow process through the landfilled waste material is long and slow. The daily monitoring used in the program is an excellent model. HELP should continue to be used to estimate leachate quantities, as well as the hydraulic head on the liner system. However, for short time period intense storms, through relatively thin and often high permeability soils, HELP monitoring on a daily interval is not recommended. The resulting percolation values are too low, resulting in very low required flux values and an underdesigned drainage system capacity.

Recommended and illustrated in this report is to obtain the required percolation and flux values from an hourly monitoring of a short time intensive storm, e.g., a six-hour storm event. Using this type of design scenario for leachate collection layers (before waste is placed) or final cover soil systems (after waste is placed), the following assumptions regarding the mechanisms of the water balance process are felt to be appropriate:

- Evapotranspiration is negligible during such a short time interval.
- The soils are at field capacity before the most intense part of the storm arrives, thus water storage is negligible.
- The barrier system (GM, CCL, GCL) beneath the drainage layer has no appreciable leakage, at least at the slope angles focused upon in dealing with slope stability issues.

Using the above assumptions, the local site-specific precipitation falling on the leachate collection layer or final cover soil system will be initially bifurcated into runoff and infiltration. The runoff is controlled by the surface soil (or vegetation) and the slope angle. The remainder of the precipitation results in water infiltration into the soil. The value of infiltration results directly in the percolation coming to the drainage layer. It is controlled by Darcian flow according to the soil's permeability. This value of vertical flow, in turn, produces the flux-value in the drain which accumulates over the slope length and is the required design value for selecting the drainage material's type, permeability and thickness.

Design in the manner just described results in flux-values that are 25 to 40 times greater than do designs based on HELP modeling. Furthermore, it appears that minimum technology guidance in many federal and state regulations are based on, or substantiated by, HELP modeling. Such a process results in values of required permeability of 0.01 cm/sec, and even as low as 0.001 cm/sec by some state regulatory agencies, which are orders of magnitude lower than values suggested in this report. *It is felt by the authors that this situation is the fundamental reason that seepage induced slides are frequently occurring.*

8.2 Slope Stability Analysis Comments

Once the phreatic surface is established within the specific cross section (i.e., its flow orientation and its depth of submergence), the mechanisms of the calculation procedure are quite straightforward. [The details were not presented completely in this report since the full

9.0 RECOMMENDATIONS

It is hoped the results of this study change some long-standing assumptions and perspectives regarding seepage design in assessing slope instability.

First, and foremost, is the recognition that seepage induced slope instability has occurred often and that its timing is during, or immediately after, intense storm events. This suggests that hourly-interval tracking of precipitation is necessary for use in the water balance analysis used to obtain the required flux (or drainage rate) value. The HELP program, based on daily-intervals is not appropriate as it is currently configured. Furthermore, and related to any type of water balance analysis whatever is its time interval, is that worst case assumptions should be made. For example, evapotranspiration, soil water storage and leakage through barrier layers are all negligible (if not zero) for short interval, high intensity storms, on relatively steep slopes with soils having high drainage rates. There are precisely the conditions where seepage induced slope instability occurs.

Second, (and certainly related to the high values of required flux), is that allowable flux values of the drainage system must be increased over current practice. The federal and state minimum permeability values for drainage soils (often taken and used directly in design) of 0.01 cm/sec and 0.001 cm/sec are too low by a factor of 10, and in some cases 100. However, the use of higher permeability requirements has profound implications. <u>Natural soil drainage materials</u> can only be gravel and even then the fines can be troublesome. The use of coarse clean gravel requires the underlying geomembrane to be suitably protected against puncture. Further, serious consideration must be given to filter design with respect to overlying fine-grained soils or solid waste. Both are serious design considerations. <u>Geosynthetic drainage materials</u> (geonets and geocomposites) may not be capable of conducting such high required flux-values. Depending on site-specific conditions higher flow rate geosynthetics, or traditional geocomposites augmented by natural drainage soil may be needed.

Third, is that most of the focus of this report has been on the drainage layer but, in reality, the drainage layer is part of the larger drainage system. In this regard, too little attention has been paid to the drainage layer outlet at the toe of the slope. It must be free of excess blockage by fines, as well as physical blockage by ice formations, equipment ramps, access roads, etc. Each toe situation is unique, but the sketches of Figure 28 give some schemes which might be considered. Each shows a gradually increasing drainage layer permeability as the required flux becomes greater in moving from the crest to the toe of slope. Alternatively, a natural soil drainage layer can be augmented by a geosynthetic drainage layer as greater capacity is needed towards the toe of the slope. At the toe, the drainage capability must be at its maximum. Geotextile filters should be placed as far away from the drainage pipes as possible. The pipe itself may have to be increased in diameter as it conveys water to the ultimate off-site outlet.

Increasing the drainage capacity of the toe, as with the upgradient drainage layer is clearly within the design community's capability. It remains to see if we are up to the challenge (and the expenses involved to the owner community) to accomplish the task.

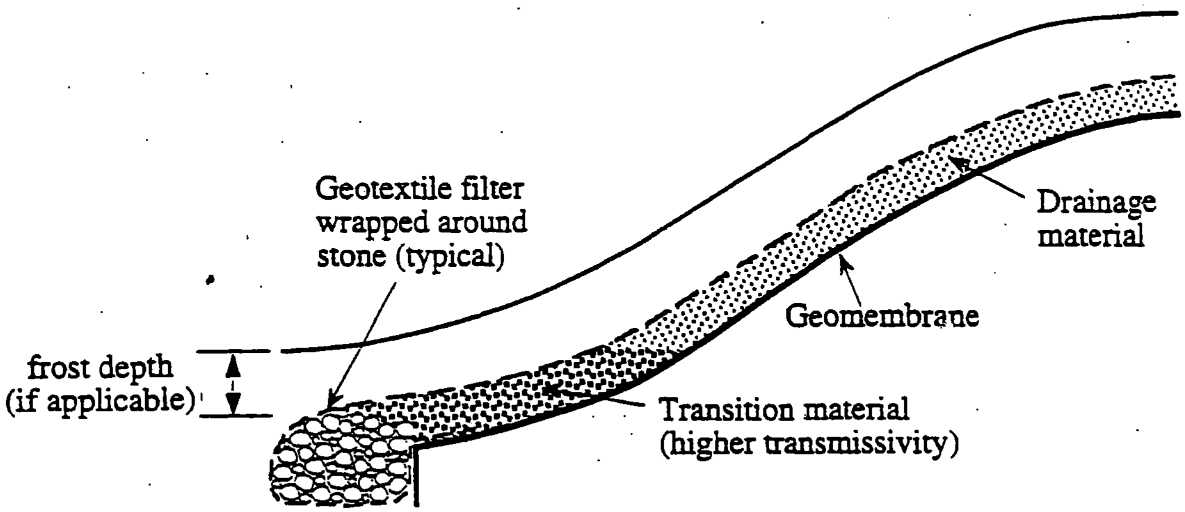

(a) Extremely large stone toe drain

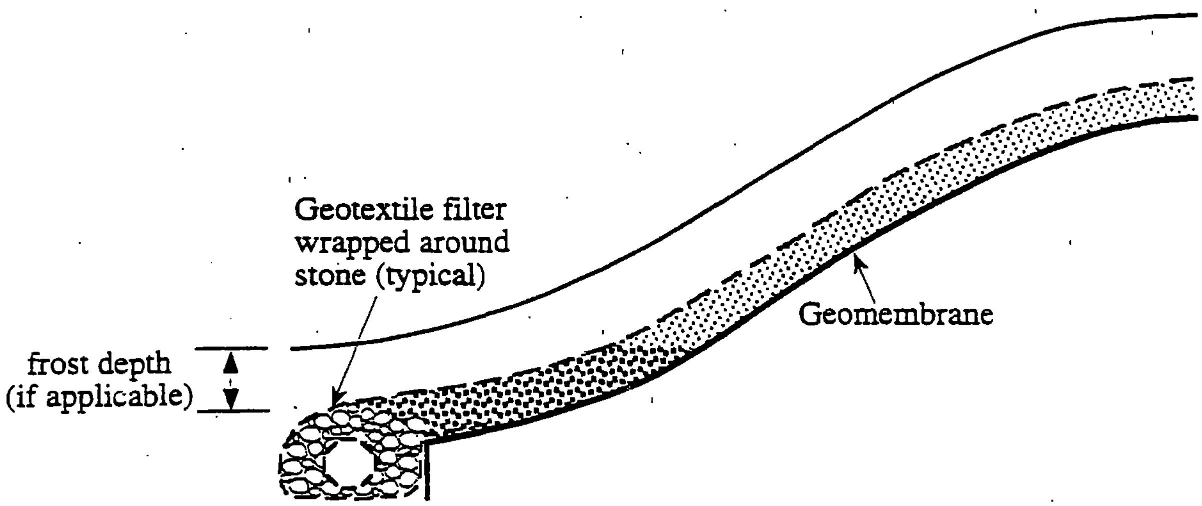

(b) Large perforated pipes surrounded by large stones

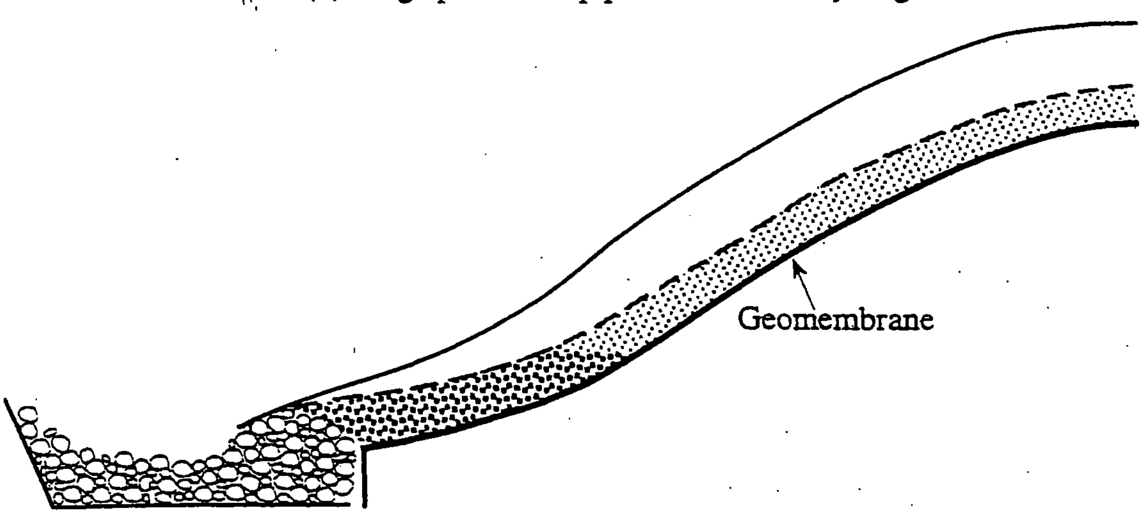

(c) Daylighting of drainage stone into a drainage channel in non-freezing climates

(Note: only feasible if sediments that run off the surface of the cover do not excessively clog the toe drainage material.)

Figure 28 - Various designs allowing for free drainage at the toe of slopes, after Soong and Koerner (1996).

Attachment 3

Rainfall Data

NOAA Atlas 14, Volume 9, Version 2
Location name: Lithia, Florida, USA*
Latitude: 27.79°, Longitude: -82.14°
Elevation: 113.84 ft**
* source: ESRI Maps
** source: USGS

POINT PRECIPITATION FREQUENCY ESTIMATES

Sanja Perica, Deborah Martin, Sandra Pavlovic, Ishani Roy, Michael St. Laurent, Carl Trypaluk, Dale Unruh, Michael Yekta, Geoffery Bonnin

NOAA, National Weather Service, Silver Spring, Maryland

PF_tabular | PF_graphical | Maps_&_aerials

PF tabular

PDS-based point precipitation frequency estimates with 90% confidence intervals (in inches/hour)[1]

Duration	Average recurrence interval (years)									
	1	2	5	10	25	50	100	200	500	1000
5-min	**6.52** (5.39-7.82)	**7.33** (6.05-8.81)	**8.60** (7.08-10.4)	**9.61** (7.85-11.6)	**10.9** (8.56-13.5)	**11.9** (9.08-14.9)	**12.7** (9.41-16.5)	**13.6** (9.59-18.1)	**14.6** (9.89-20.0)	**15.3** (10.1-21.5)
10-min	**4.77** (3.94-5.72)	**5.37** (4.43-6.44)	**6.30** (5.18-7.59)	**7.04** (5.75-8.51)	**7.99** (6.26-9.88)	**8.68** (6.65-10.9)	**9.32** (6.89-12.0)	**9.94** (7.02-13.2)	**10.7** (7.24-14.7)	**11.2** (7.41-15.7)
15-min	**3.88** (3.20-4.66)	**4.36** (3.60-5.24)	**5.12** (4.21-6.17)	**5.72** (4.67-6.92)	**6.50** (5.09-8.04)	**7.06** (5.40-8.88)	**7.58** (5.60-9.80)	**8.08** (5.70-10.8)	**8.69** (5.89-11.9)	**9.12** (6.02-12.8)
30-min	**2.98** (2.46-3.57)	**3.36** (2.77-4.03)	**3.95** (3.25-4.75)	**4.41** (3.61-5.34)	**5.02** (3.93-6.20)	**5.45** (4.17-6.86)	**5.86** (4.32-7.56)	**6.24** (4.40-8.30)	**6.71** (4.54-9.20)	**7.03** (4.65-9.87)
60-min	**1.93** (1.59-2.31)	**2.18** (1.80-2.61)	**2.58** (2.12-3.11)	**2.90** (2.37-3.51)	**3.34** (2.62-4.15)	**3.67** (2.81-4.63)	**3.99** (2.95-5.17)	**4.30** (3.04-5.74)	**4.71** (3.19-6.47)	**5.00** (3.31-7.03)
2-hr	**1.18** (0.984-1.41)	**1.34** (1.11-1.60)	**1.59** (1.32-1.90)	**1.80** (1.48-2.16)	**2.09** (1.65-2.58)	**2.31** (1.78-2.90)	**2.52** (1.88-3.26)	**2.74** (1.95-3.64)	**3.03** (2.07-4.15)	**3.24** (2.16-4.53)
3-hr	**0.853** (0.714-1.01)	**0.966** (0.807-1.15)	**1.16** (0.961-1.38)	**1.32** (1.09-1.57)	**1.55** (1.24-1.92)	**1.73** (1.35-2.17)	**1.92** (1.44-2.47)	**2.11** (1.51-2.80)	**2.38** (1.63-3.25)	**2.58** (1.72-3.59)
6-hr	**0.489** (0.413-0.576)	**0.552** (0.465-0.650)	**0.664** (0.557-0.785)	**0.767** (0.640-0.911)	**0.923** (0.749-1.15)	**1.05** (0.831-1.33)	**1.20** (0.907-1.55)	**1.35** (0.978-1.79)	**1.57** (1.09-2.14)	**1.74** (1.17-2.41)
12-hr	**0.281** (0.239-0.328)	**0.314** (0.267-0.368)	**0.380** (0.321-0.445)	**0.444** (0.373-0.523)	**0.546** (0.450-0.682)	**0.636** (0.508-0.803)	**0.737** (0.566-0.953)	**0.849** (0.622-1.13)	**1.01** (0.710-1.38)	**1.15** (0.776-1.58)
24-hr	**0.163** (0.139-0.189)	**0.182** (0.156-0.212)	**0.222** (0.190-0.259)	**0.263** (0.223-0.307)	**0.329** (0.274-0.410)	**0.388** (0.313-0.488)	**0.454** (0.352-0.586)	**0.529** (0.391-0.701)	**0.640** (0.452-0.870)	**0.732** (0.498-0.997)
2-day	**0.094** (0.081-0.108)	**0.106** (0.092-0.123)	**0.131** (0.113-0.152)	**0.156** (0.134-0.182)	**0.197** (0.165-0.243)	**0.232** (0.189-0.290)	**0.272** (0.213-0.349)	**0.317** (0.236-0.417)	**0.383** (0.273-0.518)	**0.438** (0.300-0.593)
3-day	**0.069** (0.060-0.079)	**0.078** (0.068-0.090)	**0.097** (0.084-0.111)	**0.115** (0.099-0.133)	**0.143** (0.121-0.176)	**0.169** (0.138-0.210)	**0.197** (0.154-0.251)	**0.229** (0.171-0.299)	**0.275** (0.197-0.370)	**0.314** (0.216-0.423)
4-day	**0.056** (0.049-0.064)	**0.064** (0.055-0.073)	**0.078** (0.068-0.090)	**0.092** (0.079-0.106)	**0.114** (0.097-0.140)	**0.134** (0.109-0.165)	**0.156** (0.122-0.197)	**0.180** (0.135-0.234)	**0.215** (0.154-0.288)	**0.244** (0.168-0.328)
7-day	**0.039** (0.034-0.044)	**0.044** (0.038-0.050)	**0.053** (0.046-0.060)	**0.061** (0.053-0.070)	**0.074** (0.063-0.090)	**0.086** (0.070-0.104)	**0.098** (0.077-0.123)	**0.111** (0.084-0.144)	**0.131** (0.094-0.174)	**0.147** (0.102-0.196)
10-day	**0.031** (0.028-0.036)	**0.035** (0.031-0.040)	**0.042** (0.037-0.048)	**0.048** (0.042-0.055)	**0.057** (0.049-0.069)	**0.065** (0.054-0.079)	**0.074** (0.058-0.092)	**0.083** (0.062-0.106)	**0.096** (0.069-0.126)	**0.106** (0.074-0.142)
20-day	**0.022** (0.020-0.025)	**0.024** (0.022-0.027)	**0.028** (0.025-0.032)	**0.032** (0.028-0.036)	**0.037** (0.031-0.043)	**0.041** (0.034-0.048)	**0.045** (0.036-0.055)	**0.049** (0.037-0.062)	**0.055** (0.040-0.072)	**0.060** (0.042-0.079)
30-day	**0.018** (0.016-0.020)	**0.020** (0.018-0.023)	**0.023** (0.021-0.026)	**0.026** (0.023-0.029)	**0.029** (0.025-0.034)	**0.032** (0.027-0.038)	**0.035** (0.028-0.043)	**0.038** (0.029-0.048)	**0.042** (0.030-0.054)	**0.045** (0.031-0.059)
45-day	**0.015** (0.014-0.017)	**0.017** (0.015-0.019)	**0.020** (0.017-0.022)	**0.022** (0.019-0.024)	**0.024** (0.021-0.028)	**0.026** (0.022-0.031)	**0.028** (0.023-0.034)	**0.030** (0.023-0.038)	**0.033** (0.024-0.042)	**0.035** (0.025-0.046)
60-day	**0.013** (0.012-0.015)	**0.015** (0.013-0.017)	**0.017** (0.016-0.019)	**0.019** (0.017-0.021)	**0.022** (0.018-0.025)	**0.023** (0.019-0.027)	**0.025** (0.020-0.030)	**0.027** (0.020-0.033)	**0.028** (0.021-0.036)	**0.030** (0.021-0.039)

[1] Precipitation frequency (PF) estimates in this table are based on frequency analysis of partial duration series (PDS).

Numbers in parenthesis are PF estimates at lower and upper bounds of the 90% confidence interval. The probability that precipitation frequency estimates (for a given duration and average recurrence interval) will be greater than the upper bound (or less than the lower bound) is 5%. Estimates at upper bounds are not checked against probable maximum precipitation (PMP) estimates and may be higher than currently valid PMP values.

Please refer to NOAA Atlas 14 document for more information.

Back to Top

PF graphical

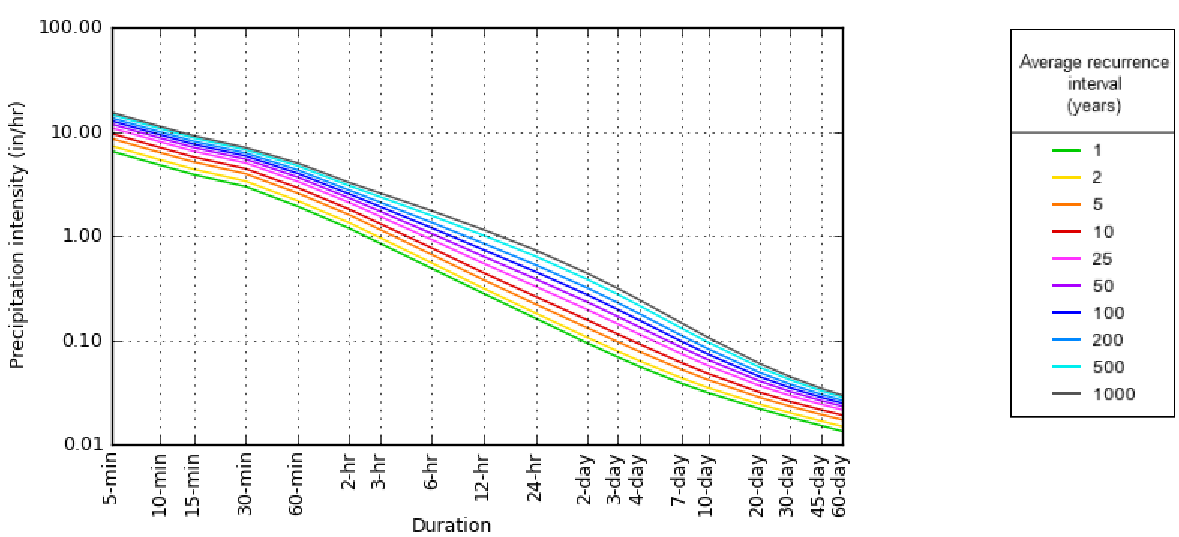

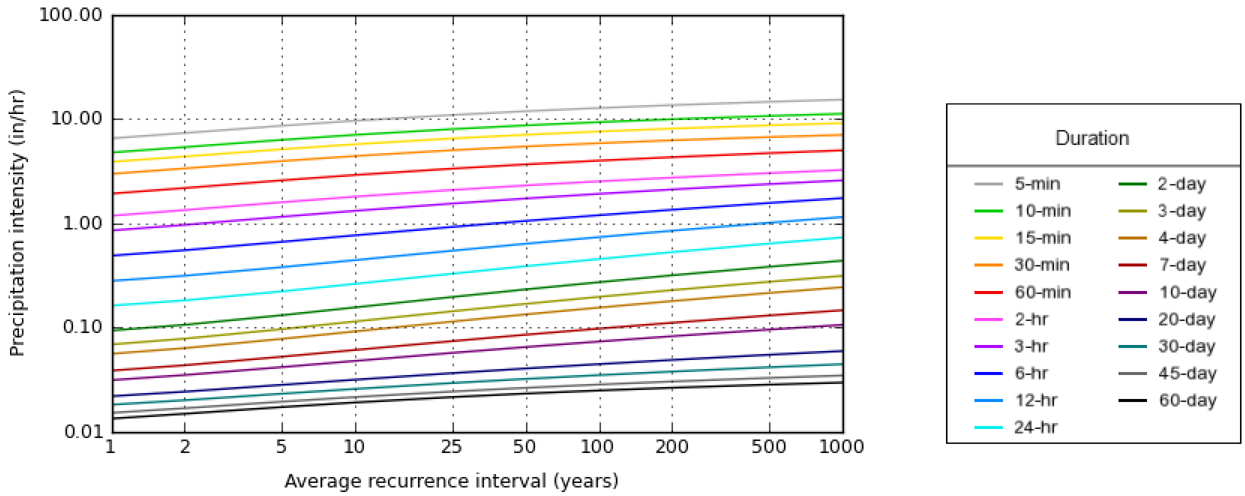

NOAA Atlas 14, Volume 9, Version 2

Created (GMT): Wed Sep 22 17:31:14 2021

Back to Top

Maps & aerials

Small scale terrain

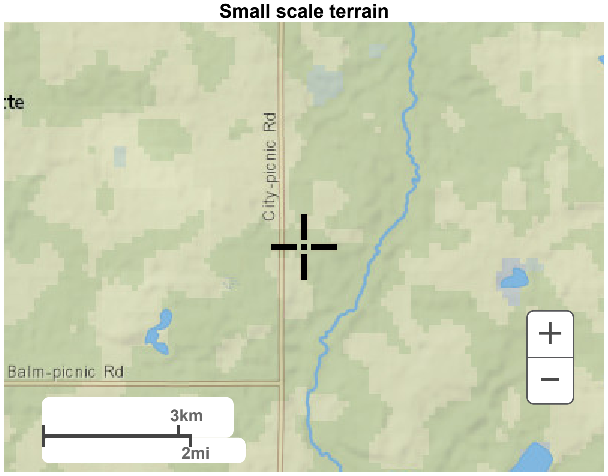

Large scale terrain

Large scale map

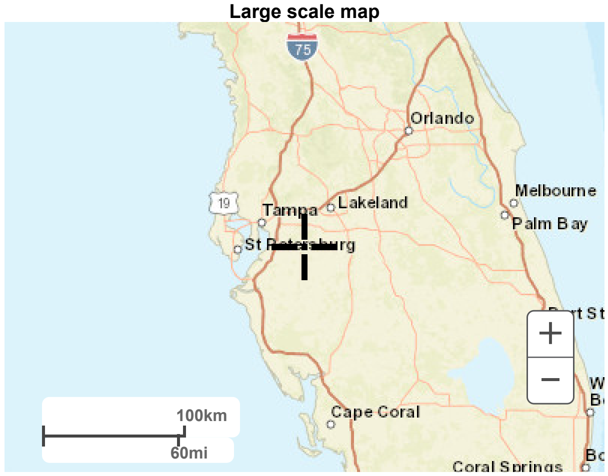

Large scale aerial

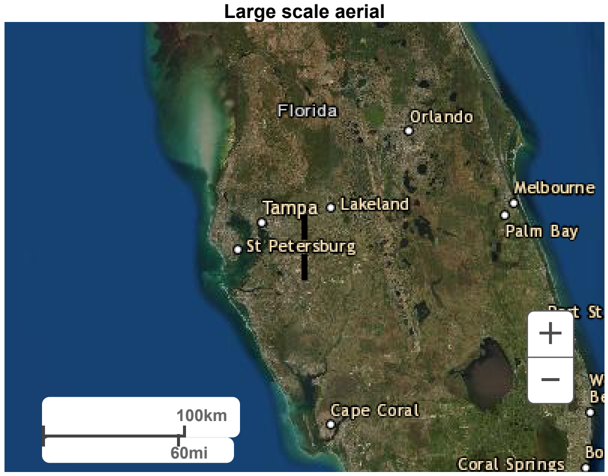

[Back to Top](#)

[US Department of Commerce](#)
[National Oceanic and Atmospheric Administration](#)
[National Weather Service](#)
[National Water Center](#)
1325 East West Highway
Silver Spring, MD 20910
Questions?: HDSC.Questions@noaa.gov

[Disclaimer](#)

Attachment 4

Soil Properties

Soil Mechanics

T. William Lambe • Robert V. Whitman

Massachusetts Institute of Technology

1969

JOHN WILEY & SONS, New York • Chichester • Brisbane • Toronto • Singapore

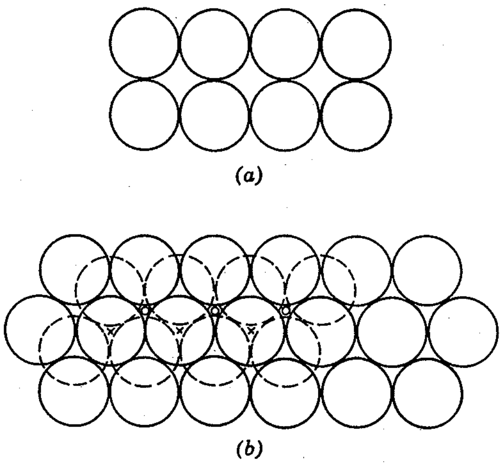

Fig. 3.2 Arrangements of uniform spheres. (*a*) Plan and elevation view: simple cubic packing. (*b*) Plan view: dense packing. Solid circles, first layer; dashed circles, second layer; ∘, location of sphere centers in third layer: face-centered cubic array; ×, location of sphere centers in third layer: close-packed hexagonal array. (From Deresiewicz, 1958.)

these simple packings can be computed from the geometry of the packings, and the results are given in Table 3.2.

This table also gives densities for some typical granular soils in both the "dense" and "loose" states. A variety of tests have been proposed to measure the maximum and

Table 3.2 Maximum and Minimum Densities for Granular Soils

Description	Void Ratio		Porosity (%)		Dry Unit Weight (pcf)	
	e_{max}	e_{min}	n_{max}	n_{min}	$\gamma_{d\,min}$	$\gamma_{d\,max}$
Uniform spheres	0.92	0.35	47.6	26.0	—	—
Standard Ottawa sand	0.80	0.50	44	33	92	110
Clean uniform sand	1.0	0.40	50	29	83	118
Uniform inorganic silt	1.1	0.40	52	29	80	118
Silty sand	0.90	0.30	47	23	87	127
Fine to coarse sand	0.95	0.20	49	17	85	138
Micaceous sand	1.2	0.40	55	29	76	120
Silty sand and gravel	0.85	0.14	46	12	89	146

138 pcf

B. K. Hough, *Basic Soils Engineering*. Copyright © 1957, The Ronald Press Company, New York.

minimum void ratios (Kolbuszewski, 1948). The test to determine the maximum density usually involves some form of vibration. The test to determine minimum density usually involves pouring oven-dried soil into a container. Unfortunately, the details of these tests have not been entirely standardized, and values of the maximum density and minimum density for a given granular soil depend on the procedure used to determine them. By using special measures, one can obtain densities greater than the so-called maximum density. Densities considerably less than the so-called minimum density can be obtained, especially with very fine sands and silts, by slowly sedimenting the soil into water or by fluffing the soil with just a little moisture present.

The smaller the range of particle sizes present (i.e., the more nearly uniform the soil), the smaller the particles, and the more angular the particles, the smaller the minimum density (i.e., the greater the opportunity for building a loose arrangement of particles). The greater the range of particle sizes present, the greater the maximum density (i.e., the voids among the larger particles can be filled with smaller particles).

A useful way to characterize the density of a natural granular soil is with *relative density* D_r, defined as

$$D_r = \frac{e_{max} - e}{e_{max} - e_{min}} \times 100\%$$
$$= \frac{\gamma_{d\,max}}{\gamma_d} \times \frac{\gamma_d - \gamma_{d\,min}}{\gamma_{d\,max} - \gamma_{d\,min}} \times 100\% \qquad (3.1)$$

where

e_{min} = void ratio of soil in densest condition
e_{max} = void ratio of soil in loosest condition
e = in-place void ratio
$\gamma_{d\,max}$ = dry unit weight of soil in densest condition
$\gamma_{d\,min}$ = dry unit weight of soil in loosest condition
γ_d = in-place dry unit weight

Table 3.3 characterizes the density of granular soils on the basis of relative density.

Table 3.3 Density Description

Relative Density (%)	Descriptive Term
0–15	Very loose
15–35	Loose
35–65	Medium
65–85	Dense
85–100	Very dense

Values of water content for natural granular soils vary from less than 0.1% for air-dry sands to more than 40% for saturated, loose sand.

Typical Values of Phase Relationships for Cohesive Soils

The range of values of phase relationships for cohesive soils is much larger than for granular soils. Saturated sodium montmorillonite at low confining pressure can exist at a void ratio of more than 25; saturated clays

Attachment 5

Soil Friction Angle

into the direct shear box. The box has a top half and a bottom half that can slide laterally with respect to each other. A normal stress, σ_n, is applied vertically, and then one half of the box is moved laterally relative to the other at a constant rate. Measurements of vertical and horizontal displacement, δ, and horizontal shear load, P_h, are taken. The test is usually repeated at three different vertical normal stresses.

Because of the box configuration, failure is forced to occur on a horizontal plane. Results from each test are plotted as horizontal displacement versus horizontal stress, τ_h (horizontal force divided by the nominal area). *Failure* is determined as the maximum value of horizontal stress achieved. The vertical normal stress and failure stress from each test are then plotted in Mohr's circle space of normal stress versus shear stress.

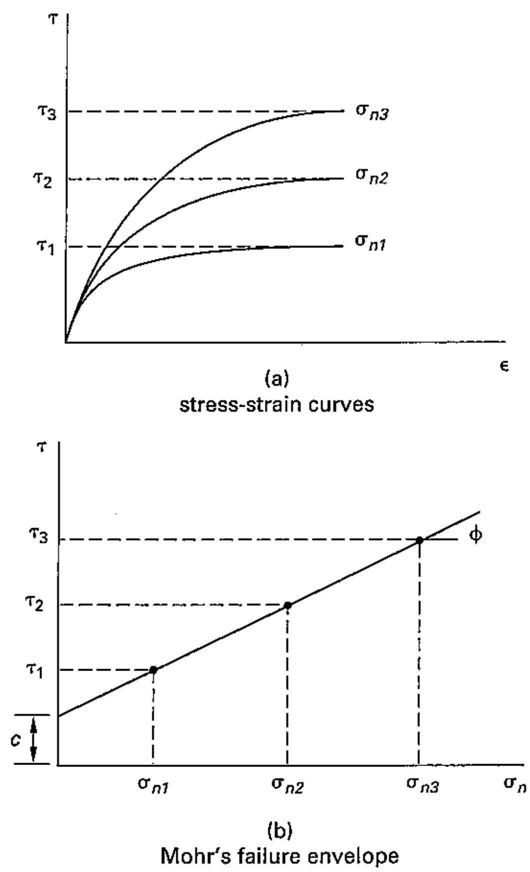

Figure 35.13 *Graphing Direct-Shear Test Results*

A line drawn through all of the test values is called the *failure envelope* (*failure line* or *rupture line*). The equation for the failure envelope is given by *Coulomb's equation*, which relates the strength of the soil, S, to the normal stress on the failure plane.[10,11,12]

$$S = \tau = c + \sigma \tan \phi \qquad 35.37$$

[10]Equation 35.37 is also known as the Mohr-Coulomb equation.
[11]The ultimate shear strength may be given the symbol S in some soils books.
[12]τ and σ in Coulomb's equation are the shear stress and normal stress, respectively, on the failure plane at failure.

ϕ is known as the *angle of internal friction*.[13] c is the *cohesion intercept*, a characteristic of cohesive soils. Representative values of ϕ and c are given in Table 35.12.

Table 35.12 *Typical Strength Characteristics*

group symbol	cohesion (as compacted) c lbf/ft^2 (kPa)	cohesion (saturated) c_{sat} lbf/ft^2 (kPa)	effective stress friction angle ϕ
GW	0	0	> 38°
GP	0	0	> 37°
GM	–	–	> 34°
GC	–	–	> 31°
SW	0	0	38°
SP	0	0	37°
SM	1050 (50)	420 (20)	34°
SM-SC	1050 (50)	300 (14)	33°
SC	1550 (74)	230 (11)	31°
ML	1400 (67)	190 (9)	32°
ML-CL	1350 (65)	460 (22)	32°
CL	1800 (86)	270 (13)	28°
OL	–	–	–
MH	1500 (72)	420 (20)	25°
CH	2150 (100)	230 (11)	19°
OH	–	–	–

(Multiply lbf/ft^2 by 0.04788 to obtain kPa.)

Geotechnical

18. TRIAXIAL STRESS TEST

The *triaxial test* is a more sophisticated method than the direct shear test for determining the strength of soils. In the triaxial test apparatus, a cylindrical sample is stressed completely around its peripheral surface by pressurizing the sample chamber. This pressure is referred to as the *confining stress*. Then, the soil is loaded vertically to failure through a top piston. The confining stress is kept constant while the axial stress is varied. The radial component of the confining stress is called the *radial stress*, σ_R, and represents the minor principal stress, σ_3. The combined stresses at the ends of the sample (confining stress plus applied vertical stress) are called the *axial stress*, σ_A, and represent the major principal stress, σ_1.[14]

Results of a triaxial test at a given chamber pressure are plotted as a stress-strain curve. Two such examples are illustrated in Fig. 35.14. The axial component of

[13]In a physical sense, the angle of internal friction for cohesionless soils is the angle from the horizontal naturally formed by a pile. For example, a uniform fine sand makes a pile with a slope of approximately 30°. For most soils, the natural angle of repose will not be the same as the angle of internal friction, due to the effects of cohesion.
[14]In reality, the triaxial test apparatus is a "biaxial" device because it controls stresses in only two directions: radial and axial.

Attachment 6

GRI GM13

Geosynthetic Research Institute
475 Kedron Avenue
Folsom, PA 19033-1208 USA
TEL (610) 522-8440
FAX (610) 522-8441

Direct Shear Database of Geosynthetic-to-Geosynthetic and Geosynthetic-to-Soil Interfaces

by

George R. Koerner, Ph.D., P.E.
Geosynthetic Research Institute
Folsom, PA 19033-1208
gkoerner@dca.net

and

Dhani Narejo, Ph.D.
GSE Lining Technology, Inc.
Houston, TX 77073
dnarejo@gseworld.com

GRI Report #30

June 14, 2005

- Residual adhesion values are zero in all cases.

Table 3. HDPE geomembranes against various interface materials.

Interface No. 1	Interface No. 2	Peak Friction (deg)	Residual Friction (deg)	Peak Adhesion (kPa)	Residual Adhesion (kPa)
HDPE-S	Granular Soil	21	17	0	0
HDPE-S	Cohesive Soil				
	Saturated	11	11	7	0
	Unsaturated	22	18	0	0
HDPE-S	NW-NP GT	11	9	0	0
HDPE-S	Geonet	11	9	9	9
HDPE-S	Geocomposite	15	12	0	0
HDPE-T	Granular Soil	34	31	0	0
HDPE-T	Cohesive Soil				
	Saturated	18	16	10	0
	Unsaturated	19	22	23	0
HDPE-T	NW-NP GT	25	17	8	0
HDPE-T	Geonet	13	10	0	0
HDPE-T	Geocomposite	26	15	0	0

4.3 LLDPE Data

In Appendix Figures 3a and 3b, for LLDPE smooth against granular soil it is seen that the peak and residual friction angles are 27° and 24°, respectively. This is 6° to 7° higher than the comparable surface for HDPE, perhaps due to the somewhat softer surface and more compliant characteristic of LLDPE. Caution is appropriate, however, since the number of points is extremely low. Against cohesive soil, as indicated in Appendix Figures 3c and 3d, the friction angels are similar to HDPE, however, the adhesion values are markedly greater, i.e., from 4 to 5 kPa.

The smooth LLDPE against NW-NP geotextiles in Appendix Figures 3e and 3f are remarkably similar to their HDPE counterparts. Again it is noted that the number of points is significantly less than with HDPE and the R^2-values are very low. This same trend of LLDPE